DISS. ETH NO. 28387

DEVELOPMENT AND CHARACTERIZATION OF PARENTERAL LIPID EMULSIONS FROM VEGETABLE OIL SOURCES TO REDUCE INFLAMMATORY RESPONSES

A thesis submitted to attain the degree of

DOCTOR OF SCIENCES of ETH ZURICH

(Dr. sc. ETH Zurich)

presented by

Gregory A. Holtzhauer

MSc MIPS, ETH Zurich

born on 27.06.1993
citizen of Glarus Süd GL

accepted on the recommendation of

Prof. Dr. Stefanie D. Krämer, examiner
Prof. Dr. Michael Zaugg, co-examiner
Prof. Dr. Laura Nyström, co-examiner
Dr. Eliana Lucchinetti Zaugg, co-examiner

2022

ACKNOWLEDGEMENT

Many people deserve credit for their invaluable contribution to the achievements we reached. I want to use this opportunity to thank the most important people involved:

First and foremost, I would like to express my deepest gratitude to my supervisor, Prof. Stefanie Krämer, for your continuous belief and trust in me and my decisions, but also sincere and honest support when it was needed. Stefanie, thank you very much for all your encouragement and assistance!

I am deeply indebted to Prof. Michael Zaugg and Dr. Eliana Lucchinetti for their scientific inputs and profound knowledge of the literature. You often had great ideas on how to tackle obstacles and overcome hurdles, but were also challenging me to reflect on my approaches. Michael and Eliana, thank you very much for being part of my committee and for providing constant guidance and scientific advice, your comments were of great help!

The meeting with Prof. Laura Nyström and Dr. Wei Chunyue finally provided us with a starting point for developing our assays for the quality control of the oils that we previously never got to work. Laura and Wei, my sincere thanks for your openness and collaborative mindset.

I very much appreciated the regular scientific exchange with all our project partners from the University Children's Hospital Zurich, the University Hospital Zurich and the University of Alberta: Nazek Noureddine, Dr. Paulina Wawrzyniak, Claudio Gemperle and Prof. Martin Hersberger, as well as Dr. Marcin Wawrzyniak and Prof. Gerhard Rogler. Thank you all for the fruitful collaboration, the mutual trust, conducting measurements and analyses for us, and sharing collected data. Collectively, we received funding from the Swiss National Science Foundation through a Sinergia team grant (#177225). We are grateful for this financial support as it not only allowed us to conduct this valuable research, but also gave us the financial freedom to acquire our own equipment, bringing the project a critical step forward.

This project would never have been possible without the support from Christina Liechti, Marco Comby and Bernhard Henes, at that time employees of Mibelle Biochemistry in Buchs. The unconditional access to the high-pressure homogenizer, when no other option was available yet, played a crucial role in the progress of this work. Christina, thank you very much for bringing us in contact with David Hunter from Dyhydromatics. We owe our gratitude to David together with Thomas and Maja Hunter from Dyhydromatics who made it possible for us to install our own high-pressure homogenizer at ETH. Thank you David, Thomas and Maja, although it was a long and demanding undertaking, we are glad about your openness for comments and suggestions from our side, particularly when it came to the modifications of the manufacturing setup, where you enabled uncomplicated assistance.

Throughout the course of my thesis, I was fortunate to share my passion from an early stage and supervise many Master students conducting thesis projects on my topic. Everyone brought in their own background and shaped the project with their individual touch. Thank you, Ramona, Simona, Thomas, Tino, Elin, Thuschi, Jonas, Jovana, Anja, Selina, Camilla and Ana for all your contributions!

From my colleagues at the Center for Radiopharmaceutical Sciences at ETH, special thanks are owed to Dr. Linjing Mu, Alexandre Bory, Bruno Mancosu and Dr. Yingfang He for all their efforts in the attempt to establish a method for the radiolabelling of triglycerides. Thank you all for the fruitful discussions and let's hope for the best that we have now made a breakthrough and finally get it to work!

I would like to thank Claudia Keller for her technical assistance with the injections during the animal studies. Stephan Handschin from the Scientific Center for Optical and Electron Microscopy, ScopeM at ETH Zurich, is acknowledged for capturing all scanning and transmission electron micrographs.

Besides the direct scientific input, of course, many more people supported me, whether intentionally by giving me advice, or rather unintentionally by supporting me emotionally, caring for me and my project, or showing interest in what I was doing. I would like to thank all these wonderful people that I was lucky to meet during my journey for being more than just colleagues, but truly amazing friends; accompanying me to sports, sharing beers on a sunny evening after work, motivating each other, and creating unforgettable memories. Thank you, Claudia, Marco, Nathalie, Hazem, Yingfang, Luisa, Giulia, Caitlin, Severin and Aro, I have greatly benefited from crossing your paths!

TABLE OF CONTENTS

SUMMARY

Lipid emulsions as an integral part of parenteral nutrition provide vital energy to prevent malnutrition when the intake or absorption of nutrients is impaired. Supply of essential fatty acids avoids deficiencies and ensures proper growth and neurological development, which is particularly important in pre-term infants. For many patients, parenteral nutrition is required for life. However, existing formulations suffer from substantial inflammatory adverse effects when used for an extended period. Adverse effects primarily affect the liver and impair its function with cholestasis, steatosis, and fibrosis with potential progression to cirrhosis.

Several underlying causes have been proposed, including the oil type and – associated with this – the ratio of *n*−6 polyunsaturated fatty acids (PUFA) to *n*−3 PUFA, a high phytosterol content and a low α-tocopherol content. Soybean oil, the most commonly used oil in lipid emulsions, is rich in *n*−6 PUFAs that are metabolized in the body to pro-inflammatory mediators. The tissue distribution with a high uptake into the liver is thought to further aggravate the observed adverse effects. Evidence has been published that oils rich in *n*−3 PUFAs cause less inflammatory adverse effects and even reverse inflammatory conditions. Available alternative formulations still come with drawbacks, including the non-sustainability due to overfishing of oceans and bear the risk of exposure to lipid-soluble environmental toxins accumulating in the food chain.

We aimed at developing intravenous lipid emulsions with a composite oil source rich in *n*−3 PUFAs achieving a more balanced tissue distribution, ultimately eliciting less adverse effects. Various formulations with different compositions were designed, manufactured and evaluated for improved *in vitro* and *in vivo* effects while maintaining compliance with regulatory requirements. Excipients interfering with steps of the lipid oxidation chain reaction were incorporated into the formulation to minimize the extent of oxidative degradation. α-Tocopherol as potent antioxidant also endogenously present in a wide variety of natural oils was added and helped reduce the degree of oxidation to similar levels found in commercially available formulations. Due to the lack of suitable assays for the quantification of degradation products from lipid oxidation and hydrolysis, in-house assays were developed. Three assays were developed or adapted for our needs to characterize the new emulsions with a focus on minimizing sample consumption and achieving rapid sample throughput.

Radioactively labelled triglyceride molecules were used to study the *in vivo* tissue distribution of lipid emulsions produced from different oil sources. Distinct tissue distributions were found based on the used oil type and the *n*−6 to *n*−3 balance. At 10 and 60 min after intravenous injection in mice, the highest uptake was seen in lung tissue, followed by the uptake in the liver and spleen. Clearance from blood and plasma was faster for the newly developed *n*−3 PUFA-rich emulsions than the soybean oil-based emulsions.

We also hypothesized that reducing the droplet size would further reduce the uptake in the liver. Several excipients were evaluated for the production of stable emulsions with smaller droplet size. However, reducing the droplet size increased the levels of lipid oxidation products. A compromise between droplet size reduction and oxidation product levels resulted in droplet sizes around 160-170 nm. The smaller droplet sizes did not substantially affect the distribution pattern *in vivo* as compared to the corresponding

emulsions with a droplet size of 280-300 nm, indicating that the oil type is the main driver governing the tissue distribution. Collectively, the feasibility of manufacturing lipid emulsions from a composite oil mixture rich in *n*−3 PUFA complying with the thresholds set by the United States Pharmacopoeia was demonstrated.

ZUSAMMENFASSUNG

Fettemulsionen als integraler Bestandteil von parenteraler Ernährung liefern lebenswichtige Energie, um Unterernährung zu verhindern, wenn die Nahrungsaufnahme oder Nährstoffabsorption im Verdauungssystem beeinträchtigt ist. Die Zufuhr essenzieller Fettsäuren beugt Mangelerscheinungen vor und gewährleistet ein normales Wachstum und eine ordnungsgemässe neurologische Entwicklung, was besonders bei der Anwendung bei Frühgeborenen wichtig ist. Bei vielen Patienten ist parenterale Ernährung lebenslang nötig. Die existierenden Formulierungen führen jedoch zu erheblichen entzündlichen Nebenwirkungen, wenn sie über einen längeren Zeitraum angewendet werden. Unerwünschte Nebenwirkungen betreffen hauptsächlich die Leber und beeinträchtigen die Funktion durch Cholestase, Steatose und Fibrose mit möglichem Fortschreiten bis hin zur Leberzirrhose.

Mehrere zugrundeliegende Ursachen wurden dafür vorgeschlagen, unter anderem die Art des Öls und – damit verbunden – das Verhältnis von *n*−6 mehrfach ungesättigten Fettsäuren (englisch "polyunsaturated fatty acids", PUFA) zu *n*−3 PUFA, ein hoher Phytosterolgehalt und ein niedriger α-Tocopherolgehalt. Sojabohnenöl als das am häufigsten in Fettemulsionen verwendete Öl, ist reich an *n*−6 PUFA, die im Körper zu entzündungsfördernden Mediatoren umgewandelt werden. Es wird vermutet, dass die Verteilung der Lipidemulsion im Gewebe mit einer hohen Aufnahme in der Leber die beobachteten schädlichen Auswirkungen noch verstärkt. Es gibt Belege dafür, dass Öle, die reich an *n*−3 PUFAs sind, geringere entzündliche Nebenwirkungen hervorrufen und im Gegenzug entzündliche Zustände mildern können. Die verfügbaren alternativen Formulierungen haben jedoch nach wie vor Nachteile, u.a. sind sie nicht ökologisch nachhaltig wegen Überfischung der Meere und bergen das Risiko einer Exposition gegenüber fettlöslichen Umweltgiften, die sich über die Nahrungskette anreichern.

Wir verfolgten das Ziel, intravenöse Fettemulsionen zu entwickeln mit einer aus verschiedenen Ölen zusammengesetzten Ölkomponente, die reich an *n*−3 PUFAs ist, um so eine ausgewogenere Verteilung im Gewebe zu erreichen und letztlich weniger unerwünschte Wirkungen hervorzurufen. Dazu wurden verschiedene Formulierungen mit unterschiedlichen Zusammensetzungen konzipiert, hergestellt und auf verbesserte *in vitro*- und *in vivo*-Wirkungen hin untersucht, unter gleichzeitiger Einhaltung der regulatorischen Anforderungen. Um das Ausmass des oxidativen Abbaus zu minimieren wurden Hilfsstoffe, die in die Lipidoxidationskettenreaktion eingreifen und diese hemmen, in die Formulierung eingebaut. α-Tocopherol als ein starkes Antioxidans, welches auch endogen in einer Vielzahl natürlicher Öle vorhanden ist, trug dazu bei, den Oxidationsgrad auf ein Niveau zu senken, das mit demjenigen in kommerziell erhältlichen Formulierungen vergleichbar ist. In Ermangelung geeigneter Methoden für die Quantifizierung von Abbauprodukten aus Lipidoxidation und -hydrolyse wurden in unseren Laboren drei Assays entwickelt. Diese wurden so entwickelt bzw. auf unsere Bedürfnisse angepasst, um die neuen Emulsionen effizient zu charakterisieren, wobei der Schwerpunkt auf der Minimierung des Substanzverbrauchs und dem Erreichen eines hohen Probendurchsatzes lag.

Radioaktiv markierte Triglyceridmoleküle wurden verwendet um die *in vivo*-Gewebeverteilung von aus verschiedenen Ölquellen hergestellten Lipidemulsionen zu untersuchen. Je nach verwendeter Ölquelle und dem Verhältnis von *n*−6 zu *n*−3 PUFA wurden unterschiedliche Gewebeverteilungen festgestellt. Sowohl nach 10 als auch 60 Minuten nach der intravenösen Verabreichung in Mäusen wurde die höchste Aufnahme im Lungengewebe beobachtet, gefolgt von der Aufnahme in der Leber und Milz. Die neu entwickelten *n*−3 PUFA-reichen Emulsionen wurden schneller aus dem Blut und Plasma aufgenommen als die Emulsionen auf Sojabohnenölbasis.

Wir vermuteten, dass eine Verringerung der Tröpfchengrösse die Aufnahme in die Leber weiter reduzieren würde. Es wurden mehrere Hilfsstoffe für die Herstellung stabiler Emulsionen mit kleinerer Tröpfchengrösse untersucht. Die Verringerung der Tröpfchengrösse führte jedoch zu einem Anstieg der Lipidoxidationsprodukte. Ein Kompromiss zwischen der Verringerung der Tröpfchengrösse und der Bildung von Oxidationsprodukten ergab Formulierungen mit einer Tröpfchengrösse von etwa 160-170 nm. Die kleineren Tröpfchengrössen hatten keinen wesentlichen Einfluss auf das Verteilungsmuster *in vivo* im Vergleich zu den entsprechenden Emulsionen mit einer Grösse von 280-300 nm. Dies deutete darauf hin, dass der Öltyp der Haupteinflussfaktor für die Gewebeverteilung ist. Insgesamt konnte die Machbarkeit der Herstellung von Lipidemulsionen aus einer zusammengesetzten Ölmischung, die reich an *n*−3 PUFA ist, unter Einhaltung der vom amerikanischen Arzneibuch festgelegten Grenzwerte gezeigt werden.

LIST OF ABBREVIATIONS

AA, C20:4 *n*−6	arachidonic acid
ABTS	2,2′-azinobis-(3-ethylbenzothiazoline-6-sulphonic acid)
ALA, C18:3 *n*−3	α-linolenic acid
AOCS	American Oil Chemists' Society
BAT	brown adipose tissue
BSA	bovine serum albumin
C10:0	capric acid (decanoic acid)
C12:0	lauric acid
C13:0	tridecanoic acid
C14:0	myristic acid
C15:0	pentadecanoic acid
C17:0	heptadecanoic acid
C18:0	stearic acid
C18:1	oleic acid
C18:3 *n*−6	γ-linolenic acid
C18:4 *n*−3	stearidonic acid
C8:0	caprylic acid (octanoic acid)
CD	conjugated diene
CoA	certificate of analysis
DBD-PZ	4-(N,N-dimethylaminosulfonyl)-7-piperazino-2,1,3-benzoxadiazole
DCF	2,7-dichlorofluorescein
DCFH	2,7-dichlorodihydrofluorescein
DHA, C22:6 *n*−3	docosahexaenoic acid
DLS	dynamic light scattering
DMSO	dimethyl sulfoxide
DMT-MM	4-(4,6-dimethoxy-1,3,5-triazin-2-yl)-4-methylmorpholinium chloride
DPPG	1,2-dipalmitoyl-sn-glycero-3-phospho-rac-glycerol sodium salt
DPPH	2,2-diphenyl-1-picrylhydrazyl
DPPP	diphenyl-1-pyrenylphosphine
DSPG	1,2-distearoyl-sn-glycero-3-phospho-rac-glycerol sodium salt
EDTA	ethylenediaminetetraacetic acid
EPA, C20:5 *n*−3	eicosapentaenoic acid
FA	fatty acid
FFA	free fatty acid
FO	fish oil
Formula #3, F#3	oil mixture consisting of 50% Ahiflower oil, 25% coconut oil and 25% olive oil
GC	gas chromatography
GMP	good manufacturing practice
HLB	hydrophilic-lipophilic balance

HPH	high-pressure homogenizer
HPLC	high-performance liquid chromatography
HPN	home parenteral nutrition
IFALD	intestinal-failure associated liver disease
ILE	intravenous lipid emulsion
LA, C18:2 *n*−6	linoleic acid
LOOH	lipid hydroperoxide
MCT	medium chain triglyceride
MDA	malonaldehyde bis(dimethyl acetal); 1,1,3,3-tetramethoxypropane
mFOX	modified ferrous oxidation-xylenol orange
MS	mass spectrometry
MUFA	monounsaturated fatty acid
o/w	oil-in-water
PA, C16:0	palmitic acid
pAV	*para*-anisidine value
PBS	phosphate buffered saline
PC	phosphatidylcholine
PDI	polydispersity index
PFAT5	percentage of fat particles above 5 μm
Ph Eur	European Pharmacopoeia
PN	parenteral nutrition
PUFA	polyunsaturated fatty acid
PV	peroxide value
RES	reticuloendothelial system
rt	retention time
SEM	scanning electron microscopy
SFA	saturated fatty acid
SO	soybean oil
SUV	standardized uptake value
TBA	thiobarbituric acid; 4,6-dihydroxy-2-mercaptopyrimidine
TBARS	thiobarbituric acid reactive substance
TCA	trichloroacetic acid
TEM	transmission electron microscopy
TO	triolein
TOTOX	total oxidation value, TOTOX = pAV + 2 x PV
TPN	total parenteral nutrition
USP	United States Pharmacopoeia
w/o	water-in-oil
WAT	white adipose tissue

1 General Introduction

1.1 Parenteral nutrition

Adequate provision with nutrients is crucial for survival to prevent malnourishment or starvation. If supply with nutrients is inadequate, nutritional support may be needed.[1] Malnourishment can rapidly lead to severe consequences up to lethal starvation. Life relies on sufficient provision with external nutrients, as the human body is unable to self-sustainably generate energy on its own. In certain medical conditions, this nutritional support cannot be delivered via the oral route to the stomach and digestive system, but needs to be delivered into the circulatory system directly.[2] This is then termed parenteral nutrition (PN); parenteral from Latin, "circumventing the enteral way".

Inability to swallow alone does not justify use of PN as enteral feeding via a nasogastric tube can still be provided.[3] However, if the uptake of nutrients is impaired, either through chronic inflammatory conditions such as ulcerative colitis[4], Morbus Crohn, insufficient intestinal length after surgical resection[5] or short bowl syndrome, or destruction of intestinal mucosa following cancer therapy[6,7], provision of nutrients directly into the blood stream may be necessary. In these cases, duration of use can be persistent over longer times, but there are also other transient indications. Premature infants do not tolerate enteral nutrition yet and therefore need nutritional support to ensure adequate supply of essential nutrients for growth and proper, especially neurological, development to bridge the first few days of life.[8] Prolonged use of PN is associated with adverse effects and therefore timely change over to enteral nutrition is sought.[8–10]

Most indications that require long-term use of PN do not require hospital stay. Thus the number of PN usage is highest in a home parenteral nutrition (HPN) setup. HPN prevalence varies among countries in western Europe with 5 users per million inhabitants at the lower end in Spain[11] to 25.6 per million in Italy (data from 2005)[12] and 26 per million in France[13] to 53.26 per million in Poland[14] up to 80 per million in Denmark.[2] In Switzerland numbers of 45 per million inhabitants[15] are reported (with regional differences), hence, usage of artificial nutrition support lies at the upper end in Europe[16], but still lower than the number in the US at 79 per million (data from 2013, with a decline from 157 per million in 1995).[17,18] The prevalence in children is lower and ranges from 9.6 per million in the Netherlands to 13.7 per million in the UK.[19] Use of artificial nutrition support caused costs of CHF 13'000 per patient and year in Switzerland[15] and € 10'015 in Poland.[14] In a recent report from Switzerland, 16.5% of hospitalized patients were identified to be at risk for the development of malnutrition and thus requiring (short-term) nutritional support, either by parenteral or enteral route.[20]

Energy can be provided in different forms.[21] The most common energy source for nutritional support is glucose, readily available energy that can easily be prepared and administered, and allows the immediate control over the body's energy balance. However, the body cannot survive in a healthy state solely on glucose, also other essential nutrients need to be supplied. These include lipids and essential fatty acids, amino acids as well as vitamins and trace elements.[22] Amino acids are important building blocks for protein synthesis, tissue build-up and regeneration as well as muscle growth. They need to be supplied externally as the body is unable to synthesize all required amino acids on its own.

When all nutrients are provided parenterally, this is termed total parenteral nutrition (TPN)[23] whereas PN support in combination with enteral nutrition is referred to as partial PN. TPN admixtures consist of

all the essential components for a sustainable diet, including sugar, lipids, amino acids, vitamins and trace elements.

For potential interactions between glucose and amino acids (Maillard reaction), combinations for TPN are either prepared immediately before use or are provided as 2- or 3-chamber bag system where the individual components remain separated until mixing in the infusion line.[24–26] Many studies have been conducted on the use of different forms of sugar and their metabolic effects, comparing insulin signaling. This work focusses exclusively on the lipid constituents in PN.

1.2 Lipids and their metabolic effects

Lipids are important constituents of PN admixtures as they possess a high energy density and provide long-lasting energy.[27] Especially essential fatty acids need to be supplied externally to the body, either via oral enteral nutrition or by TPN infusion. Essential fatty acids are important constituents, as the body is unable to synthesize them by itself. The necessary enzymes for generating them are present in plants.[28] Lipids act as important building blocks for hormones and cell membranes, transport fat-soluble vitamins and also possess functions in cell signaling.[27,29,30] Essential fatty acids are crucially important for proper neurological development in preterm infants.[31,32]

Due to negligible water solubility, lipids are formulated as oil-in-water emulsions for parenteral application. Upon administration, intravenous lipid emulsions (ILE) are recognized similarly to endogenous chylomicrons, whose droplet sizes ILEs mimic.[33] Triglycerides contained in ILEs are metabolized in a comparable manner to those stemming from enteric digestion and packaged as chylomicrons.[34,35] Lipid droplets during their passage in the vasculature acquire apolipoproteins, primarily apolipoprotein E (apoE).[36,37] Subsequently, the triglycerides are hydrolyzed by lipoprotein lipase to yield free fatty acids and 2-monoaclyglycerol.[29,38] The remaining cholesterol-rich chylomicron remnants are taken up via the LDL receptor.[28] Intracellularly, medium-chain fatty acids can passively diffuse into mitochondria and are readily available for oxidation to generate energy. Long-chain fatty acids on the other hand first need to be transformed into acyl carnitines for crossing the mitochondrial wall, before transformation into long chain acyl-CoA finally also ready for energy-generation by oxidation.

Lipids – commonly referred to as oils, fats or waxes, depending on the aggregation state – exist in different forms. Typical chemical structures of lipids include triglycerides, phospholipids, fatty acids (FA), sterols and ceramides to name a few.[39] Triglycerides consist of a glycerol backbone esterified with three FA chains.[29] Naturally occurring triglycerides in general consist of FA chains with an even number of carbon atoms. The carbohydrate chains can either be fully saturated or partially unsaturated. The term unsaturated FA is further subdivided into monounsaturated and polyunsaturated FAs (PUFA).[40] Naturally occurring double bonds are chiefly *cis*-oriented, *trans*-fatty acids are mainly of synthetic origin or a degradation product from industrial processing.[41] Unsaturated FAs with chain lengths below 19 carbon atoms are classified as short chain FAs and unsaturated FAs with chain lengths above 19 carbon atoms are termed long chain fatty acids.[42] In the common case of more than one double bond, they are classified as long chain polyunsaturated fatty acids.[43,44] Most essential fatty acids contain more than 18 carbon atoms. They cannot be synthesized by human enzymes and thus need to be provided through the diet. Saturated FAs with chain length of 8 to 13 carbon atoms are referred to as medium-chain FAs[45] while saturated FAs with more than 14 carbon atoms are already classified as long-chain FAs. Medium-chain FAs are metabolically important for rapid delivery of energy. Shorter FA chains are less important for providing energy, but rather as second messenger for signaling. Unsaturated FAs are further classified according to the position of the double bond(s).[40] The nomenclature of the double bonds originates from

counting from the methyl carbon end of the FA tail, called the *n*-end (or ω-end).[42] Depending on the position of the first double bond when counting from the *n*-end, if it starts at the *n*−3-position or *n*−6-position, the FA is termed *n*−3 PUFA or *n*−6 PUFA, respectively. This difference is illustrated in Fig. 1.1.[46]

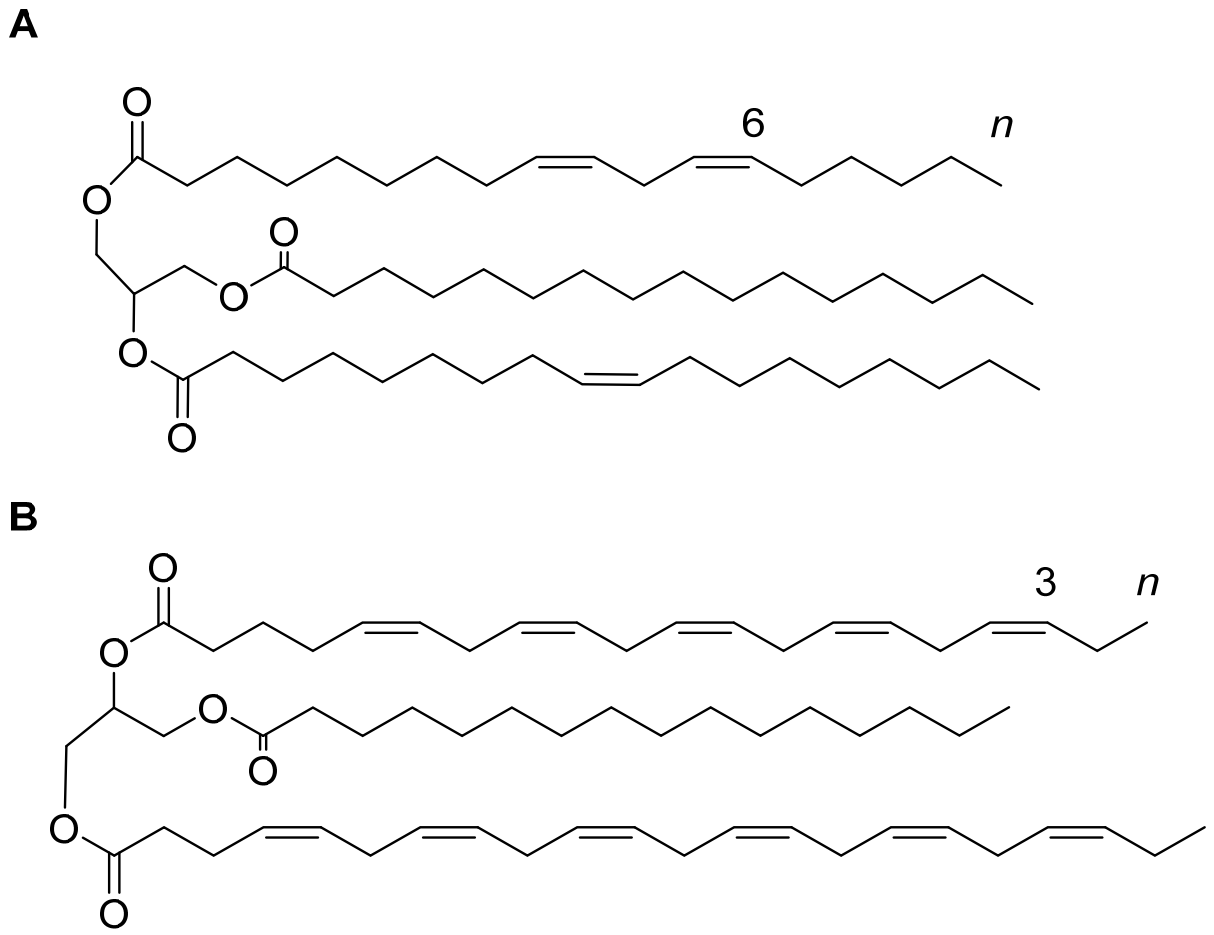

Fig. 1.1: Structural formula of triglycerides consisting of three fatty acids (FA) esterified to a glycerol head group. Esterified FAs from top to bottom: A) Linoleic acid (C18:2), palmitic acid (C16:0) and oleic acid (C18:1). The n-position as well as the position of the first double bond are indicated. Typical triglyceride present in soybean oil. B) Typical n−3 PUFA triglyceride prevalent in fish oil. FAs from top to bottom: Eicosapentaenoic acid (C20:5), palmitic acid (C16:0) and docosahexaenoic acid (C22:6). The beginning of the first double bond at the n−3-position of the eicosapentaenoic acid is indicated.

The physiological functions differ between *n*−3 and *n*−6 PUFAs.[44] The position of the first double bond (seen from the *n*-end) also influences the physiological response. This distinction is depicted in Fig. 1.2: *n*−6 PUFAs such as linoleic acid (LA, C18:2) are converted by three different enzymes to arachidonic acid (AA, C20:4). *n*−3 PUFAs, such as α-linolenic acid (ALA, C18:3 *n*−3) get converted by the same series of enzymes to eicosapentaenoic acid (EPA, C20:5).[46] EPA can be further converted to docosahexaenoic acid (DHA, C22:6), all while maintaining the position of the first double bond when counting from the *n*−end. The change from the *n*−6 to the *n*−3 pathway is possible via the enzyme Δ15-desaturase. Since this enzyme is only present in plants, dietary intake of either *n*−6 or *n*−3 PUFAs automatically determines the metabolic end products in humans.

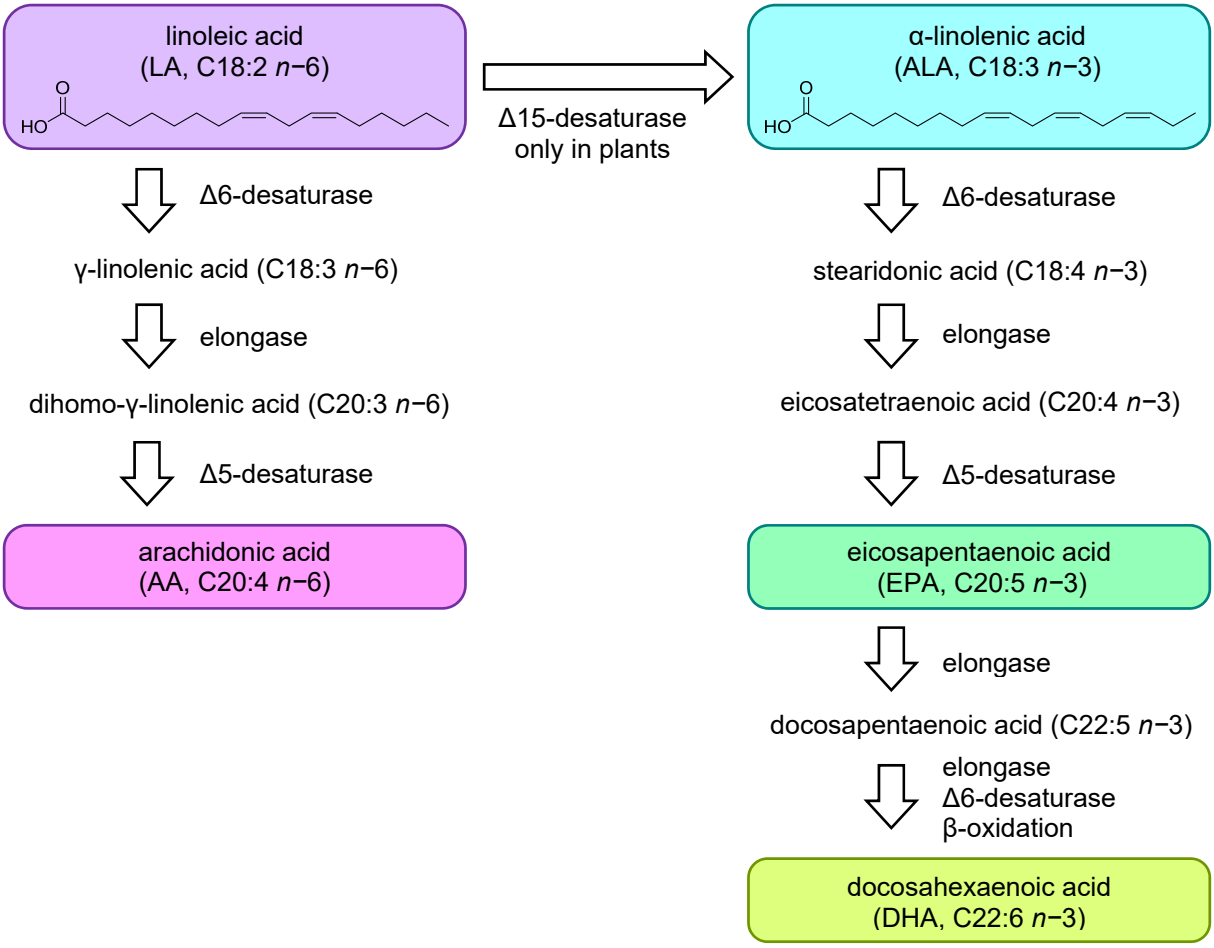

Fig. 1.2: Schematic overview of the metabolic pathways of fatty acids. n−6 PUFAs such as linoleic acid (LA, C18:2) are converted by a series of enzymes to arachidonic acid (AA, C20:4). α-linolenic acid (ALA, C18:3 n−3) on the other hand is converted by the same enzymes first to eicosapentaenoic acid (EPA, C20:5) and further to docosahexaenoic acid (DHA, C22:6). Since the converting enzyme between n−6 and n−3 FAs, Δ15-desaturase, is only present in plants, the intake of either n−6 or n−3 PUFAs determines the metabolic pathway. The resulting AA, EPA and DHA further elicit different physiological responses.

As illustrated in Fig. 1.3, AA, EPA and DHA elicit different responses in the body.[44] AA mainly triggers the production of pro-inflammatory markers such as prostaglandins, thromboxanes and leukotrienes and only to a lesser extent also anti-inflammatory lipoxins.[28,47–51] EPA and DHA on the other hand predominantly lead to the generation of anti-inflammatory resolvins, protectins and maresins.[52–55] From the two key *n*−3 intermediates, only EPA can be further metabolized to pro-inflammatory prostaglandins, thromboxanes and leukotrienes, but to a much lesser extent. In summary, intake of high quantities of *n*−6 PUFAs leads to a pro-inflammatory reaction in the body, while provision of *n*−3 PUFAs from a balanced *n*−6 to *n*−3 ratio[56,57] can counteract existing inflammations in the body. Through the metabolism described above, also oils originally not rich in AA, but only *n*−6 PUFAs, can elicit a pro-inflammatory response. Of course, the picture is not all black-and-white and we do not want to ban all *n*−6 PUFAs from the diet.[28] Also some *n*−6 PUFAs such as γ-linolenic acid (C18:3 *n*−6) belong to the essential fatty acids required for a healthy development.[58] *n*−3 PUFAs on the other hand fulfil essential functions in neurodevelopment, especially important when administering ILEs to preterm infants.[31,32] Generally, by fine-tuning the ratio of *n*−6 and *n*−3 PUFAs in our diet we can influence the effect on the body.[59,60] In case of normal oral nutrition this usually does not pose a problem as oils from a natural source usually consist of a broad mixture of FAs of all kinds, long-chained, medium-chained and short-chained; saturated, monounsaturated and polyunsaturated; *n*−6 and *n*−3 PUFAs. However, when relying

on PN the picture shifts. For facilitating regulatory acceptance, parenteral lipid emulsions usually consist of only one or two, in rare cases up to four oil sources.[61] The precondition of a broad balance from an oral diet is then not fulfilled anymore. *n*−6 PUFAs are most prevalent in soybean oil[22,62] while *n*−3 PUFAs are common in oils of marine origin, either fish, krill or marine algal oil.[30,63–68]

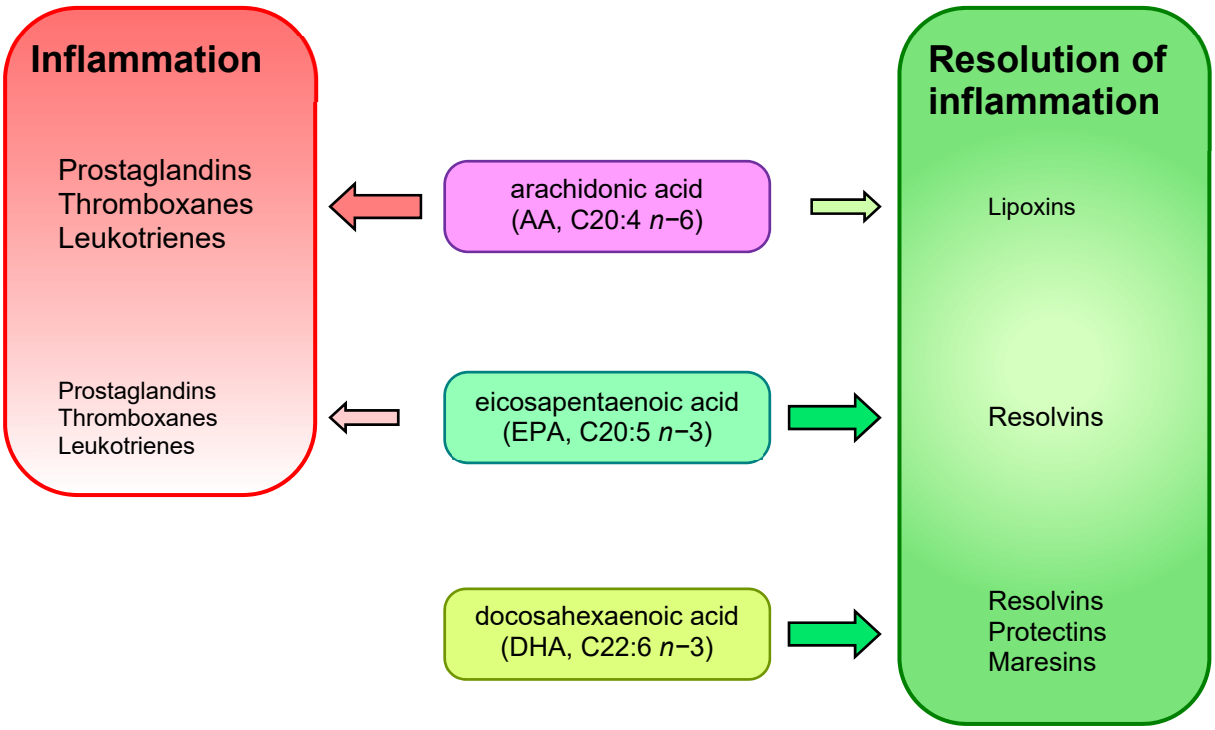

Fig. 1.3: Graphical illustration of the physiological response triggered by different intermediates from fatty acid metabolism. While arachidonic acid (AA, C20:4 n−6) mainly leads to pro-inflammatory prostaglandins, thromboxanes or leukotrienes and only to a lower extent to anti-inflammatory lipoxins, eicosapentaenoic acid (EPA, C20:5 n−3) and docosahexaenoic acid (DHA, C22:6 n−3) rather lead to the production of anti-inflammatory markers such as resolvins, protectins and maresins and only EPA to a much smaller extent also to pro-inflammatory mediators.

1.3 Parenteral lipid emulsions available for clinical use

Most important currently marketed formulations include Intralipid (20% soybean oil), Omegaven (10% fish oil) and SMOFlipid (6% soybean oil, 6% medium-chain triglycerides, 5% olive oil and 3% fish oil), all from Fresenius Kabi.[61,69] Intralipid, based on soybean oil, was the first intravenous lipid emulsion to be marketed in 1961 in Europe[45,70] and in the US in 1975.[61,71] First experiments with parenteral lipid emulsions date back to the early 1960s with a patent[72] and early reports.[73] In the initial patent, the application was not specified for PN yet, but only as drug delivery vehicle. Already from the very beginning on also the paediatric population as a field of application was kept in mind.[74,75] More than 50 years ago, in 1971, first evidence of potential benefits of *n*−3 PUFAs over use of classical *n*−6 rich oil sources emerged.[76] About 10 years later, also the reports about adverse effects of parenteral lipid emulsions started to accumulate and the clinical manifestation was summarized under the general term "intestinal failure".[77]

In the meantime, more formulations entered the marked, also based on different oil sources (safflower, olive oil, in combination with soybean oil), but were again withdrawn and by 2010, only Intralipid was approved in the US.[61] In the late 1980s, the use of high-pressure homogenization to produce lipid

emulsions was described[78] but then not much innovation followed until recent years. In 2004, the mixed-oil formulation SMOFlipid, containing soybean, olive, fish oil and medium-chain triglycerides, was approved by the European Medicines Agency EMA, but only received US approval in 2016. In 2018 finally, the fully fish oil-based Omegaven gained US approval.[69] The development of Omegaven was initially driven to have an alternative in case of patients with severe soy allergy.

The ILEs most commonly used nowadays in the clinics with their respective oil source are listed in Tab. 1.1.[28,62,79] Intralipid, SMOFlipid, and Omegaven are manufactured by Fresenius Kabi (Bad Homburg, Germany); Lipofundin by B. Braun (Melsungen, Germany) and ClinOleic by Baxter Healthcare Corporation (Deerfield IL, USA).

Tab. 1.1: Composition and fatty acid characteristics of the most frequently used commercially available ILEs.[28,62,79] Abbreviations: saturated fatty acids (SFA), monounsaturated fatty acids (MUFA), polyunsaturated fatty acids (PUFA). Amounts in gram per 100 ml, with relative contribution to the oil phase in % (in brackets). FAs, % of total FAs.

	Intralipid	Omegaven	SMOFlipid	ClinOleic	Lipofundin
Soybean oil	20 g (100%)		6 g (30%)	4 g (20%)	10 g (50 %)
Olive oil			5 g (25%)	16 g (80%)	
Coconut oil			6 g (30%)		10 g (50%)
Fish oil		10 g (100%)	3 g (15%)		
PUFA	60%	58%	29%	20%	30%
MUFA	24%	26%	30%	63%	12%
SFA	16%	16%	41%	17%	58%
n−6 FA	53%	6-7%	20%	19%	26%
n−3 FA	7.8%	52%	8%	2%	4%
n−6 to *n*−3 ratio	7/1	1/8	2.5/1	9/1	7/1

It is striking how – with the exception of Omegaven – all formulations are highly rich in *n*−6 PUFAs and *n*−3 PUFAs are negligible. When refraining from oil of marine origin, it is indeed challenging to achieve a balanced *n*−6 to *n*−3 distribution. Excessive use of fish oil is associated with the risk of administering lipid-soluble environmental toxins that accumulated through the food chain, to already weakened patients.[30,64,80,81] This is less an issue for plant oil, although there toxins from the soil can end up in the purified oil as well. Moreover, the use of fish oil is also debated because of potential overfishing and low yield while using up valuable resources in the fight to feed the global population. The challenge is thus to find a sustainable, most likely plant-based to also fulfill the need of the growing population relying on vegan nutrition, oil source rich in *n*−3 PUFAs. Potential candidates – along with the established soybean and fish oil – are listed in Tab. 1.2. Owing to their FA composition, vegetable oils and fish oil display a distinct pattern of SFA, MUFA and PUFAs.

In our work, we aimed at developing an ILE which combines all the requirements for a healthy (anti-inflammatory) and environmentally sustainable lipid composition. No single oil source was found to fulfill all the necessary requirements and therefore a mixture of three oil sources was composed. Half of the lipid dose consists of Ahiflower oil, the *n*−3 PUFA-rich oil of *Buglossoides arvensis* (corn gromwell). This plant is native in moderate to north temperate regions in Europe (Sweden, Czech Republic, UK, Switzerland), Asia (India), New Zealand and Canada.[82,83] Along high contents of ALA (C18:3 *n*−3, 46%) and of stearidonic acid (C18:4 *n*−3, 20%), it also contains the anti-inflammatory γ-linolenic acid (C18:3 *n*−6, 5.8%).[58,65,84–86] Although so far not used in parenteral applications yet, Ahiflower oil was

shown to be safe for humans and provided a beneficial effect on inflammatory responses after oral supplementation.[82,87] It is inherently low in phytosterols and should thus pose less risk for the development of intestinal failure associated liver disease (see below).[82] Coconut oil with > 80% of C14 and shorter FAs was added at one quarter to provide short and medium chain triglycerides (MCT)[22,40,88] for rapidly available energy. To provide *n*−9 PUFAs, the remaining quarter consists of olive oil. The composite oil mixture now contains plant-based oils with a beneficially low *n*−6 to *n*−3 PUFA ratio and all essential FAs.

Tab. 1.2: Natural oils most frequently used in ILE manufacturing and their relative FA composition in %, alongside with Ahiflower oil used in this work.[22,33,62,84,86,89] *The composition of fish oil from menhaden fish is shown.*

Fatty acid	Soybean oil	Flaxseed oil	Coconut oil	Olive oil	Fish oil	Ahiflower oil
Caproic acid (C6:0)			0.5%			
Caprylic acid (C8:0)			8%			
Capric acid (C10:0)			6%			
Lauric acid (C12:0)			48%			
Myristic acid (C14:0)			18%		7.3%	
Palmitic acid (C16:0)	11%	5.5%	8.5%	13%	16.1%	5.2%
Palmitoleic acid (C16:1 *n*−7)				0.5%	8.0%	0.1%
Stearic acid (C18:0)	4%	3.5%	2.5%	1%	3.1%	1.9%
Oleic acid (C18:1 *n*−9)	23%	17%	7%	70%	8.2%	7.5%
Linoleic acid (C18:2 *n*−6)	54%	15%	1.5%	15%	1.4%	11.8%
α-Linolenic acid (C18:3 *n*−3)	7.5%	58%		0.5%	0.7%	46.1%
Stearidonic acid (C18:4 *n*−3)					2.6%	20.1%
Arachidonic acid (C20:4 *n*−6)	0.4%	1%			1.1%	
Eicosapentaenoic acid (C20:5 *n*−3)					18.0%	
Docosapentaenoic acid (C22:5 *n*−3)					2.0%	
Docosahexaenoic acid (C22:6 *n*−3)					12.8%	
Others					18.7%	7.3%
SFA	15%	9%	91.5%	14%	26.5%	7.3%
MUFA	23%	17%	7%	70.5%	22.0%	8.6%
PUFA	62%	74%	1.5%	15.5%	51.5%	84.1%
n−6 FA	54.4%	16%	1.5%	15%	5.0%	17.6%
n−3 FA	7.5%	58%		0.5%	39.9%	66.2%
n−6 to *n*−3 ratio	7.25/1	1/3.6		30/1	1/8	1/3.76

Prolonged use of ILEs is associated with inflammatory adverse effects. They not only mean an additional harm to already suffering patients, but also further increase overall mortality.[90] These adverse effects, collectively termed intestinal-failure associated liver disease (IFALD), present as conditions of the liver and associated gall bladder/bile duct when PN is used and other causes can be ruled out. IFALD manifests as cholestasis progressing to cholelithiasis, hepatic steatosis inducing hepatic fibrosis, with the potential of ultimately developing liver cirrhosis.[9,18,28,91] Signs of IFALD during TPN therapy are reported to range from 5% up to 40%[9,18] and even up to 72% if PN had been used for longer than 56 days.[92]

In pediatric patients, the incidence is further increased and ranges between 40% to 60%.[9,18] The etiology of IFALD is still unknown to date. A genetic susceptibility has been identified as risk factor.[91,93,94] Risk was increased in case of high infusion rates at > 1.5 g lipids/kg body weight and day.[95–98] The strongest link has been identified with the used oil type[18,45,49,51,99]: Intralipid is the most prevalently used ILE in the clinic. It consists of 100% soybean oil and is rich in *n*−6 PUFAs (Tab. 1.1). Oil sources rich in *n*−6 PUFAs (according to the mechanisms shown above and illustrated in Fig. 1.2 and Fig. 1.3)[9,45,100] and phytosterols[91,100–102], but low α-tocopherol content[9,22,100] have been shown to promote the development of IFALD.

Apart from IFALD, unknown effects on the intestinal microbiome can occur, when the gut is abstained from nutrients and dietary fibers for longer times.[103–111] The fish oil-based – and thus *n*−3 PUFA rich – commercially available Omegaven and SMOFlipid were shown to elicit less inflammatory adverse effects.[48,112–118] Many clinical studies have been conducted to compare Intralipid and Omegaven with diverse outcomes. In larger meta-analyses, a slight benefit of using Omegaven has been found.[45,50,119] Use of *n*−3 PUFA containing ILEs instead of the traditional *n*−6 PUFA formulations in acute settings shortened the length of hospital stay and thereby also the costs.[120–123] This demonstrates the importance of reducing the harm to these patients and also the healthcare costs by developing improved formulations for PN.

Broad use of Omegaven however also comes with issues; on the one hand the oil source is not sustainable (see above), on the other hand this formulation only contains 10% oil. This becomes a problem in a setting where the patient relies on TPN, since to fully administer the required amount of oil calories and essential fatty acids, the required volume of ILE must be doubled. In a TPN setting, when fluid overload is already an issue, this makes the situation even worse.[124] Developing an ILE for PN based on plant-derived oil sources rich in *n*−3 PUFAs eliciting less inflammatory adverse effects posed the starting point of this project.

1.4 Principles of lipid emulsions

Parenteral delivery of lipids to patients is associated with some challenges. Lipids are not soluble in the aqueous environment of the blood.[125,126] Instead, direct injection of oil into the blood stream would lead to fatal clogging of the vasculature and lipid embolisms.[70,127,128] To mediate the delivery of lipids and essential fatty acids they need to be formulated as an emulsion with the help of surfactant molecules, as depicted in Fig. 1.4.[28] Surfactants lower the surface tension and allow then miscibility with an aqueous outer phase.[127,129] The stability of the formulation depends on the dosing of the surfactant relative to the inner lipid and outer aqueous phase, but also the input energy.[125,130–132] Emulsions can be manufactured by different means, simple shaking as in the example of French salad dressing, the simplest lipid emulsion commonly known from household. For improved stability, a higher energy input is needed and thus methods such as high-shear mixing, ultrasonication or high-pressure homogenization are favored.[133–135]

For this project, mainly high-pressure homogenization was employed. Emulsions are subjected to high pressures and resulting shear forces lead to a reduction in droplet size. Typical values range from around 800 bar up to 2000 bar (10’000-30’000 psi).[78,136] When preparing emulsions by high-pressure homogenization, the stability of the produced emulsions depends on the composition and the energy input. The higher the content of surfactant or surfactant-to-lipid phase ratio, the more stable the resulting formulation.[137,138] On the energy side, the stability is improved by increasing the process pressure or by subjecting the emulsion to the shearing for several passes.[78,139–141] For efficient manufacturing, the typical number of passes ranges between three to twelve passes. Above this, over-processing is possible, so that the

balance of the system is destroyed and the phases separate.[126] Over-processing is irreversible, once a stable formulation has been processed too much, it is impossible to achieve a stable formulation again. It is thus crucial to determine an adequate number of passes in pilot experiments.

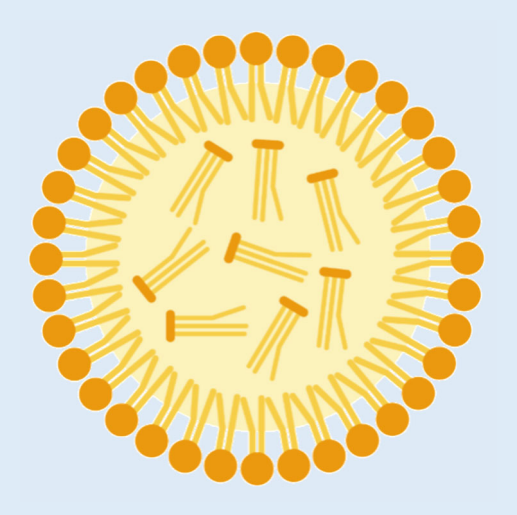

Fig. 1.4: Graphical representation of a lipid droplet in an aqueous continuous phase. Surfactant molecules (in the drawing phospholipid molecules) engulfing the lipid core with triglyceride molecules for illustration. Cross-section of a spherical lipid droplet, not drawn to scale; the number of triglyceride molecules exceeds the number of phospholipid molecules.

The process pressure is generated by pressure-multiplication of input air at a pressure of 7-10 bar. This input air is directed at a T-shaped plate so that the input pressure acting on a large surface is multiplied on a much smaller area and thus multiplied manifold. Depending on the ratio between the diameter of the input area and the output area, multiplication factors between 150 up to 300 are possible. Once the maximum pressure on the product side has been reached, the plunger moves backwards.[142] Afterwards, the processed emulsion is fed forward and the pressure is released. Then again incoming air on the input side builds up the pressure for the next stroke. This process is repeated as required. The input air flow determines the stroke frequency and in turn also the sample throughput within a given time. The input air pressure can either be generated externally, the machine is then powered by centrally generated high-pressure air from the building air supply (or central compressor), or the machine can generate the input air pressure by itself using a built-in compressor.[143] This comparison is summarized in Tab. 1.3. In the first case, the operation principle of the machine is termed pneumatically-driven, while in the second case it relies on a power supply and is thus electrically-driven. For a pneumatically-driven machine, the maximally available input air pressure and flow are the limiting factors determining the process pressure and sample throughput, while for the electrically-driven machine it is the output specifications of the compressor. While both types of machines were evaluated in the course of this project, due to insufficient high-pressure air supply in our laboratories, we decided to acquire an electrically-driven machine for our purposes.

The high process pressure is used to accelerate the coarse emulsion. The emulsion is fed into a reaction chamber (also termed interaction chamber, IXC, for different suppliers) where the emulsion is exposed to shear forces leading to a size reduction.[129,133,144,145] Again, two main principles exist. For Y-type reaction chambers the liquid flow is split up into two paths that are then directed at each other can, thereby effectively doubling the shear forces. Later, the combined fine emulsion is fed through an optional cooling unit to account for the formed heat of compression to the outlet. The principle is illustrated in Fig.

1.5. The process can be repeated for a next pass if necessary. Different lengths of cooling coils exist where the product is chilled for varying durations, but the cooling can also be completely omitted if the product is not heat-sensitive. By changing the temperature of the cooling medium, the cooling efficiency can further be influenced. The Y-type is preferentially used in the manufacturing of emulsions. For other applications such as cell disruption, Z-type reaction chambers are used (Fig. 1.5).[146]

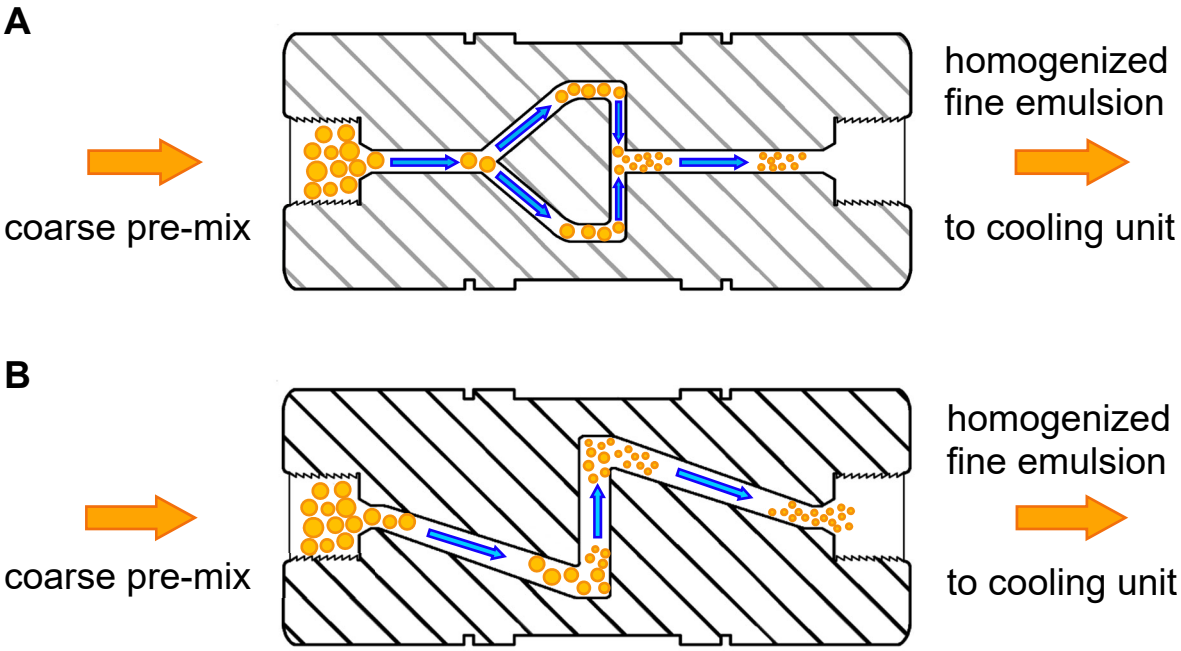

Fig. 1.5: Graphical representation of the two most frequently used mechanisms in the reaction chamber of the high-pressure homogenizer. A: Working principle of a Y-type reaction chamber. The coarse emulsion is fed in from the left side (orange arrow). The liquid flow is split up and re-directed towards each other. The resulting shear forces lead to a droplet size reduction. The resulting fine emulsion is guided to a cooling unit (orange arrow on the right) before a potential second pass. B: Working principle of Z-type reaction chamber. The coarse emulsion is fed in from the left side and encounters a first impact at the first right-angle turn, followed by a second impact after a short acceleration distance. The homogenized fine product is then guided to the cooling unit.

Here, the product is accelerated and shot against the wall, before taking a right-angle turn and a second impact. Afterwards, also an optional cooling unit can follow before a potential repetitive cycle. The sudden drop from the process pressure of up to 2000 bar back to atmospheric pressure can be quite abruptly and some products might be sensitive to this stress. When using a longer cooling coil, the pressure drop is alleviated through the length of the cooling coil. To further account for this, in some setups a backpressure module is inserted between the reaction chamber and the cooling unit to apply a certain pressure from the back and further modulate the pressure drop.[147,148] A backpressure module is built relatively easy, it just consists of narrow paths for the product so that parts of the high process pressure are preserved instead of being released immediately. The models Microfluidizer M-110Y (Ceramic Auxiliary Processing Module; Microfluidics, Westwood MA, USA) and ShearJet PL300 (200.2 L; Dyhydromatics, Maynard MA, USA) are by default equipped with a backpressure module.

Tab. 1.3: Comparison of pneumatically- and electrically-driven high-pressure homogenizer working principles (A) and side-by-side comparison of Y-type and Z-type reaction chamber types (B).[143,145]

A Working principle	Pneumatically-driven	Electrically-driven
Relies on	Input air (800-1200 l/min at 7-10 bar)	Electrical power supply
Generation of process pressure	Pressure-multiplication of input air from central building air supply or air compressor	Generated by built-in compressor
Commercial examples evaluated in this project	Microfluidizer M-110Y, LM10 Dyhydromatics ShearJet PL60, ShearJet PL300	Microfluidizer LM20 Dyhydromatics ShearJet HL60
B Reaction chamber type	Y-type	Z-type
Working principle	Flow is split up inside the reaction chamber and shot against each other, thereby effectively doubling the resulting shear forces	The product is shot against the wall of the reaction chamber two times
Commercial examples evaluated in this project	Microfluidics F20Y, F12Y Dyhydromatics 75.1 T	Microfluidics H30Z Dyhydromatics 75.3 T

In the early phase of this project, a third supplier of high-pressure homogenizers with a slightly different working principle was evaluated. Avestin Emulsiflex C5 works with a static homogenizing valve.[129,139,146] The machine is pneumatically-driven and the coarse emulsion is accelerated by the same principle as above. The mechanism of the size reduction is different from those presented in Fig. 1.5 and Tab. 1.3 and illustrated in Fig. 1.6. A valve creates a small slit where the coarse emulsion is pressed through. This also leads to a size reduction, although less energy is introduced than in the above described systems, and the size reduction thus is less sustainable. Since droplets are only compressed, subsequent particle maturation is likely. By applying varying pressure from the product outlet side, the width of the slit and thus the size reduction can be regulated. A too narrow slit on the other hand easily leads to a clogging of the machine. In the standard setup, no cooling option is implemented for the Emulsiflex C5.

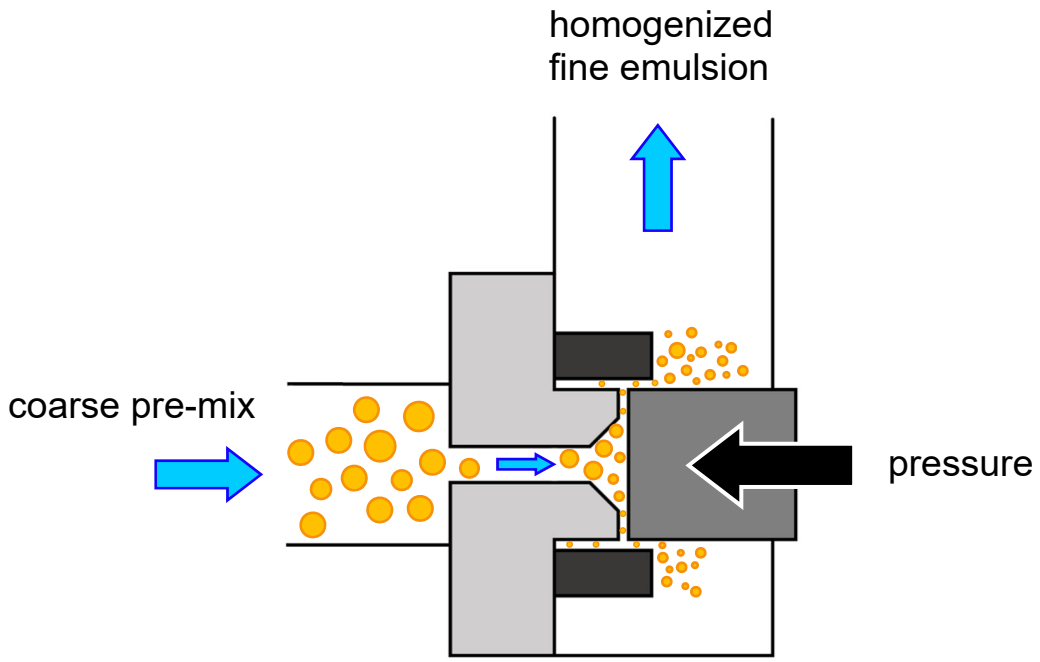

Fig. 1.6: Cross-section through a static homogenization valve to illustrate the working principle. The coarse pre-mix is fed in from the left and by applying a pressure pushed through a narrow slit, leading to a reduction of the droplet size. The width of the slit is regulated by applying varying pressure from the opposite side on a valve (depicted in dark grey). The resulting fine emulsion is guided to the outlet for a second pass.

1.5 Surfactants in lipid emulsions

Water and lipids inherently do not mix. It is energetically more favourable for the two phases to stay separated and form hydrogen bonds and Van-der-Vaal's interactions respectively among themselves. To mediate a mixture of these two immiscible phases surfactants are needed.[127] Surfactants are surface-active substances lowering the interfacial tension. With the help of surfactants, it becomes energetically possible for the two phases to mix. Surfactants for the manufacturing of emulsions are amphiphilic molecules that are miscible with both phases and can thus act as spacer in between.[149,150] They thus consist of a hydrophilic part that often is also able to be charged, depending on the pH of the aqueous environment, and a longer apolar chain. Commonly used substances are sucrose esters[151,152] or phospholipids.[153,154] When used synergistically in combination, they are referred to as co-surfactants. Also proteins can be used as emulsifiers to form an emulsion, as for example casein stabilizing the lipid droplets in cow milk.[155–157] The nature of the produced emulsion can be influenced through the choice of the nature of the surfactants and the volume-ratio between aqueous and lipid phase. Surfactants are classified according to the hydrophilic-lipophilic balance (HLB-value), a measure for the likelihood how well the surfactant distributes into either the aqueous of lipidic phase.[158–161] It is a dimensionless number between 0 and 20 and reflects the ratio of hydrophilic to total molecular weight (to be precise, 1 minus fraction of molecular mass of lipophilic parts and total molecular mass). Choosing surfactant(s) with HLB-values above 8 and using more water than oil in general yields oil-in-water (o/w) emulsions where lipid droplets are dispersed in a continuous aqueous phase. Lipid emulsions with an aqueous outer phase (o/w-emulsions) are relevant in the context of intravenous application, as only these fulfil the criteria of an outer phase that is compatible with the circulatory system. Choosing surfactants with HLB-values of 4-6 and more oil than water yields the opposite case, that water droplets are dispersed in a continuous lipid phase (water-in-oil, w/o-emulsions).[162] These are more relevant for topical applications.

Sucrose esters consist of a sugar moiety that is esterified once (Tween and some Span variants) or several times (some Span variants) with fatty acids of different chain length via a hydroxyl group.[152,162] In the case of Tweens, the sugar moiety is further conjugated with chains of repeated units of polyethylene glycol of varying length. Phospholipids consist of two fatty acids that are esterified with a glycerol backbone.[154] Instead of the third fatty acid in case of a triglyceride, phospholipids contain a phosphate head group with different functionalities. The most common form naturally occurring in egg yolk is a choline moiety, but also ethanolamine, a serine residue and inositol are possible. Phosphatidylcholine contains two charges in the head group, a negative from the phosphate group and a positive from the quaternary nitrogen of the choline group, further facilitating miscibility with the aqueous continuous phase while remaining a net neutral molecule at physiological pH. In this project, phospholipids from various sources were studied, including phospholipids derived from egg yolk, or isolated from plant sources such as soybeans, sunflower and rapeseed.

1.6 Clinical aspects and pharmacopoeial requirements for parenteral lipid emulsions

TPN admixtures are administered via a central venous catheter directly to a central vein, for example the right subclavian vein.[5,40,163] Smaller doses of ILEs when used as drug vehicles can also be administered to peripheral veins. Still, for easier handling, also TPN administration occurs through a peripheral access point, but that is then connected to a peripherally inserted central catheter so that the administered TPN admixture only comes into contact with the blood in a large central vein.[2,13,164–166] As TPN admixtures are administered directly to the blood stream, stricter requirements for droplet size and pH-value apply than for *e.g.*, intramuscular injections. Moreover, also the continuously administered high dose of emulsion demands a strict evaluation of the ingredients and final formulation. In an acute setting, for the provision of adequate calories via TPN, up to 2500 ml total volume need to be administered daily for adult patients (350-875 ml ILE for a 70 kg adult patient).[5,167] This high volume means additional stress for the patients' vasculature and thus a high nutritional density is favoured to lower the volume. Chronic fluid overload when TPN is administered over longer periods can lead to chronic hypertension and damage the heart muscle.[124] Additionally, increasing infusion speed is further promoting inflammatory adverse effects and thus needs to be limited. Thus, often intermittent infusion – which would give conscious patients more freedom to regularly disconnect from the dosing unit for longer time periods – of TPN is not possible as otherwise the required caloric requirements cannot be met. Further requirements for ILEs are set by the different pharmacopoeial monographs.[168,169] The pH value is tolerated between 6.0 and 9.0, but for a large-volume infusion is preferred to be close to that of the blood around 7.4 to prevent irritations and promotion of inflammation. For improved stability of ILEs a higher pH above pH 8.5 would be favourable for a ζ-potential above |35| mV (in general below -35 mV).[136,170,171] The ζ-potential is pH-dependent as the pH value of the emulsion affects the charge of the head group of phospholipid molecules and potentially present free fatty acids (FFA) at the lipid droplet surface. When the pH drops below the pKa of the surfactants, in our case phosphatidylcholine, phosphatidylethanolamine and potentially FFAs, the stabilizing partial charge of the head group and in turn also the repulsive forces are lost.[172] This no longer prevents droplets from getting in close contact, ultimately leading to particle maturation and phase separation. The native pH of ILEs directly after manufacturing, depending on the used phospholipids, was between pH 4 and 5 in our preliminary studies. In particular at low infusion speed (typically around 1-2 ml/min)[173] compared to the large volume of the blood of around 5 liter (for a 70 kg adult), the blood possesses a certain buffering capacity. But once again, through the large volume this cannot be exploited infinitely. At the site of the infusion the local buffering capacity might be exhausted much earlier. Measuring the pH of lipid emulsions can be challenging. In the lipid

part, no pH is defined, as for energetic reasons no H^+ atoms will be present there, but all H^+ are in the aqueous continuous phase. In the outer phase, viscosity might be increased because of the emulsion's droplets. An increased viscosity in turn means a reduced ion mobility, so that a reliable pH measurement can be time-consuming.

Since ILEs and TPN admixtures are administered directly to the blood stream, it is crucial that these formulations are not immunogenic, are sterile and endotoxin-free to not cause sepsis.[168] In order to obtain sterile formulations, emulsions are steam-sterilized by autoclaving at elevated pressure.[133,141,149,170,174] This thermal stress leads to a drop in pH, most probably mediated through the generation of FFAs by triglyceride or phospholipid hydrolysis, and thus prior to autoclaving the pH is adjusted to pH 8.5, so that the final pH ends up around physiological pH of 7.4. Adjusting the pH with sodium hydroxide also ensures proper ζ-potential to prevent phase separation when the stabilizing effect is lost. Because of the average droplet size of standard lipid emulsions at around 300 nm, sterile filtration through a 0.2 µm filter is not possible. Alternative modes of sterilization without a thermal stress such as ethylene oxide gassing or γ-irradiation were not possible for our low batch sizes. Endotoxins cannot be inactivated by sterilization and would be challenging to remove. Thus, introduction of endotoxins needs to be prevented by proper processing ("Quality by design" approach). Similar to the sterility, it is better to prevent a high bioburden already in the beginning rather than needing to tackle the challenge afterwards. Sterility (membrane-filtration method, Ph Eur 2.6.1)[175] and absence of endotoxins (gel-cloth method, Ph Eur 2.6.14)[176] was tested at the FDA-approved lab Bioexam (Lucerne, Switzerland). Because of the cost for this analysis and no anticipated effects on other parameters (not affecting physical or chemical stability), this analysis was only performed for batches intended for *in vivo* application. For in-house determination of endotoxins, a commercial kit based on the gel-cloth method was utilized (GenScript ToxinSensor™ Single Test Kit, Cat. No. L00450). Although the gel-clot assay is not the gold-standard, the chromogenic assay is not possible due to the opacity of the emulsion.[177] This is a common issue in the quality control of lipid emulsions. Through the high lipid concentration (10-20%) and the droplet size > 100 nm, there is interference with the wavelength of natural sunlight, the light is diffracted at lipid droplets and the emulsion occurs white-opaque. This in turn renders all optical determination methods ineffective, as all light transmission is reduced, not just of a specific wavelength. Normally, absence of visible particles needs to be tested for all injections, but this is not possible here because of the opacity.[178] Dilution of samples is often not possible, as then also the concentration of the analyte of interest (in this case potential endotoxins) is diluted and may end up below the limit of detection of the assays when finally a sufficiently transparent sample compatible with a spectrophotometric determination method has been reached.

The next parameter to be considered is the osmolarity.[8,134,179] This is not specifically stated by the pharmacopoeia, but still is an important parameter when considering the high applied volume as well long-term continuous use. Iso-osmolarity with the blood at around 280 mOsm/kg is important to prevent haemolysis. To render ILEs iso-osmolar, glycerol is added.[8,179] For the preparation of ILEs in this project, the amount of glycerol needed to achieve iso-osmolar ILEs was calculated based on the sum of all low-molecular aqueous-soluble solutes[180,181] and added accordingly to the ILE. Compliance with iso-osmolarity with the blood was not tested for all ILE batches because they often are not administered alone, but mixed with other constituents (glucose, amino acids, electrolytes, vitamin solutions) prior to administration, changing the osmolarity again. The reason for the osmolarity not to be limited specifically in the pharmacopoeia is that the other constituents of TPN admixtures, 70% glucose and concentrated amino acid solutions are inherently hyperosmolar. Again because of avoiding fluid overload

syndrome, these preparations cannot be diluted further. So, prevention of haemolysis is another reason to limit the infusion speed to prevent local adverse reactions from happening. Haemolysis as a consequence of inadequate osmolarity or arising from toxic excipients was tested by incubating selected ILE batches intended for *in vivo* experiments with human blood from donors. This was not required from the pharmacopeia but as an effective mode of detecting adverse effects prior to administration.

Although not explicitly specified, the viscosity of the emulsion to be administered needs to be considered.[149,182–184] It needs to be possible to infuse the emulsion at the intended 1-2 ml/min through the corresponding needle diameter (18-20G for human application). The emulsion needs to rapidly disperse after getting in contact with the blood rather than clumping together.

The droplet size of emulsions intended for intravenous application needs to be carefully controlled to avoid lipid embolism. The USP limits the average droplet size at 500 nm and also limits the number of particles above a diameter of 5 µm at 0.05% (PFAT5).[130,169,185,186] In our case, the average particle size was determined by dynamic light scattering (DLS).[187,188] DLS is the method of choice for determining the size of droplets up to 1000 nm.[169] It is based on the diffraction of laser light on the individual droplets and from the movement of particles caused by Brownian motion. The software back-calculates the sedimentation coefficient and finally using Stokes-Einstein equation, the droplet diameter is calculated.[188] Lipid emulsions do not uniformly consist of droplets of a single size, but a distribution with a certain width. Sometimes, samples can be polydisperse (several size populations), that do or do not overlap. Based on the theory used for the evaluation of size measurements, an intensity, volume or number-weighted average is calculated.[189] For intensity-weighing (based on the intensity of the refracted light, according to Rayleigh theory proportional to size to the power of 6; used by default when reporting Z-average mean diameters from DLS) a few particles much larger than the rest can have a major influence on the reported value. Number-weighted results may better reflect the proportions of a certain size population. Volume-weighted results may be used when information on the mass percentage of the populations are needed to calculate appropriate dosing volumes. Besides the average droplet size, the polydispersity index (PDI) is reported. This is a dimensionless number between 0 and 1 and a measure for the broadness of the distribution (squared standard deviation divided by the corresponding squared mean size, assuming a normal (Gaussian) intensity distribution).[188] A value close to 0 means an almost uniform, homogenous monodisperse distribution, while values above 0.5 usually indicate a broad size distribution or the existence of several size populations. We aim at manufacturing emulsions with a PDI < 0.1 at the time of manufacturing. An elevated PDI can be an early sign for susceptibility towards particle maturation and phase separation. DLS assumes a spherical droplet shape and thus is not suited for rod-shaped particles. This however is more an issue for crystals rather than lipid droplets. For lipid droplets, a sphere is the energetically most favoured shape and thus usually adopted.[190] Sphericity can be confirmed by scanning electron microscopy (SEM).[191–194] SEM also allows to ensure the absence of particles with droplet sizes above the measuring range of DLS above 1000 nm. In contrast to DLS, for SEM the droplet size distribution needs to be manually evaluated and the sample preparation process is much more complicated. Samples need to be shock-frozen and cracked in order to be imaged. The costs are higher and the throughput is lower.

The droplet size not only needs to comply at the time of manufacturing, but throughout the whole shelf life. The physical stability, how long the droplet size stays within the compendial limits, is taken into consideration when defining the shelf life. Stability monitoring is carried out throughout a certain period until either onset of physical or chemical degradation is detected. A degradation mechanism occurring early is flocculation when droplets aggregate, but remain separated.[125,126,131,161,162] Following

flocculation, droplets in close proximity can fuse to single larger droplets in a process termed coalescence. Size-increase can also happen via a second process called Ostwald ripening when unequally sized particles, for example stemming from insufficient homogenizing during manufacturing, get in close contact and transfer some of the material. This results in a larger droplet and the originally smaller droplet further decreases in size. In contrast to coalescence, the two original droplets remain separated which further promotes the process. At some point, creaming happens, that larger lipid droplets migrate to the surface because of the lower density than the surrounding continuous aqueous phase. Through the missing repulsive forces from equally-sized, equally charged neighboring droplets, they are not kept in balance anymore, but float towards the surface. The density difference between the two media and the viscosity of the outer phase determine how fast this process occurs. Ultimately the emulsion breaks into a biphasic system, with the lipid and aqueous phase separated, and a monolayer of surfactants along the interface.

Next to the physical stability, the quantification of oxidation products is also an important quality parameter. These parameters are not set by the pharmacopoeia, only some general requirements are stated for raw oils mainly intended for the preparation of semi-solid dosage forms such as creams and ointments (Ph. Eur. 10.8 chapter 2.4.19-23, .29, .31, .32; respective monographs of raw oils). However, when lipid emulsions are intended to be given to weakened patients, precaution should be taken to avoid further harm from oxidation products. Oxidized lipids on the one hand cannot fulfil their intended function as essential fatty acids anymore, but also cause further harm to the vasculature and promote inflammatory side effects.[195,196]

Unsaturated lipids are susceptible to oxidative degradation. Double bonds can be attacked by radicals and atmospheric oxygen.[197] Via a chain reaction depicted in Fig. 1.7, primary, secondary and tertiary oxidation products result.[198–200] The process is described by three main phases, namely initiation, propagation and termination. Radicals generated via diverse other pathways, either by photolysis or high energy from the manufacturing process with susceptible components of the formulation, react with electropositive hydrogen atoms of unsaturated lipids, producing lipid radicals.[201,202] Transition metal ions either natively present in the oil or introduced from the processing (purification or emulsion manufacturing) may promote this process by acting as catalysts.[203] This initiates the oxidative degradation. These unstable species rapidly rearrange to conjugated dienes.[203] Conjugated dienes can be measured and quantified, but usually are transient and short-lived.[204–207] Lipid radicals can further attack remaining intact lipids and thereby promote the oxidative degradation (propagation of the chain reaction). Molecular oxygen species present from the atmosphere can attack the lipid radical, yielding the lipid peroxyl radical that in acidic environment (presence of free H^+ atoms) quickly associates to the primary oxidation product lipid hydroperoxide. This reaction occurs in the presence of free H^+ atoms, i.e. preferentially at the interface between the aqueous continuous and the lipidic phase.[202,208–211] For energetic reasons, charged atoms rarely occur inside the lipid phase. This explains another phenomenon: For a fast reaction, molecules need to get into contact. A smaller droplet size at equal lipid volume yields a largely increased surface with more potential for reactive interactions, further leading to the accelerated degradation of lipids at higher surface areas.[209,212–214] Loss of the radical position terminates the chain reaction and slows down the rate of the degradation reaction. Under continuous contact with free protons, but slower this time, the reactive hydroperoxide is reduced to the alcohol form. The resulting lipid hydroxide represent the secondary oxidation products that can be quantified. The degradation process is not finished there yet, but can carry on further to tertiary oxidation products. These are less well-defined and structurally more diverse.

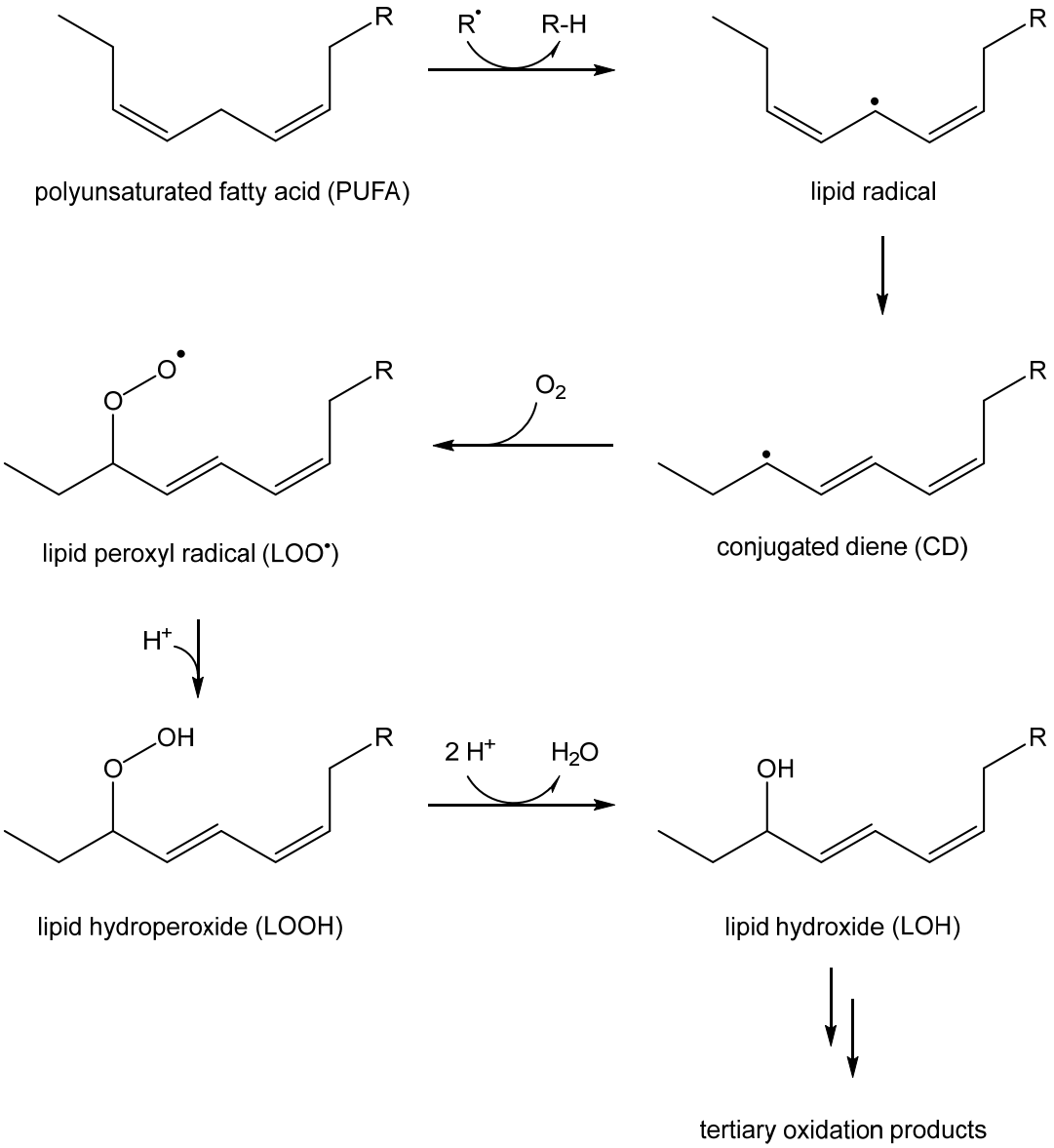

Fig. 1.7: Degradation pathway of polyunsaturated lipids. In the presence of radicals, a hydrogen atom gets abstracted, leading to a lipid radical that quickly rearranges to a conjugated diene. The radical position is instable and can be attacked by atmospheric molecular oxygen to form the lipid peroxyl radical that in acidic environment (presence of free H^+ atoms) quickly associates to the primary oxidation product lipid hydroperoxide. Over time and in aqueous environment, i.e. preferentially at the interface where lipids can get into contact with charged hydrogen atoms, the reactive hydroperoxide is reduced to the alcohol lipid hydroxide. Lipid hydroxides reflect the species secondary oxidation products. Degradation is not finished there but can go on to further tertiary oxidation products, more diverse in structure and less specific.[198–200]

The oxidative degradation can be reduced by either optimizing the manufacturing process or by adding suitable excipients to the formulation. Such excipients interfere with one step in the generation of lipid oxidation products and thereby help to lower the oxidation.[215] They can include chelator substances, *e.g.,* EDTA, to scavenge transition metal ions or antioxidants, for example α-tocopherol.

1.7 Aims of the project

Prolonged use of lipid emulsions in life-saving PN therapy is associated with considerable adverse effects, primarily of inflammatory nature. Several causes have been proposed, including the oil type and – associated with that – a high ratio of *n*−6 PUFA to *n*−3 PUFA, a high phytosterol content in plant-based lipids, a low α-tocopherol content, as well as an unfavourable tissue distribution with a high uptake in the liver. Available alternative formulations still come with drawbacks, including the non-sustainability and risk of exposure to lipid-soluble environmental toxins accumulated in fish oil. The overall goal of the present thesis is the development of sustainable lipid emulsions with less inflammatory adverse effects.

We were challenged with the lack of suitable assays for the quantification of lipid oxidation products in the lipid emulsions. A first aim was to adapt available methods to allow routine quantification of primary and secondary oxidation products in our own and reference emulsions. We aimed at low sample consumption, high sample throughput and good reproducibility. The adaptation of suitable methods to fit our needs is described in Chapter 2, "Quantification of Lipid Oxidation Products in Lipid Emulsions Requiring Minimal Sample Volume".

FFAs liberated by hydrolysis of triglycerides or phospholipids are limited by pharmacopoeial specifications. Compliance is especially crucial when using lipid emulsions in preterm infants. Excess FFAs bind to albumin and compete with the binding of bilirubin. Hyperbilirubinemia can lead to severe consequences from jaundice up to neurotoxicity. Chapter 3, "Determination of Free Fatty Acids in Lipid Emulsions by Fluorescence-Detection Based High Performance Liquid Chromatography" covers the development of a HPLC method based on fluorescence labelling for free fatty acids for quantification and thus ensuring compliance with pharmacopoeial standards.

We hypothesized that by exchanging the established soybean or fish oil in currently marketed lipid emulsions with a composite plant-based oil mixture rich in 18-carbon *n*−3 PUFAs and low in phytosterols, we could obtain formulations eliciting less inflammatory adverse effects. Chapter 4, "Excipient Screening for the Development of Lipid Emulsions based on Vegetable Oils Rich in *n*−3 Polyunsaturated Fatty Acids", is dedicated to the development of new lipid emulsion formulations based on *n*−3 PUFA rich oil sources. This includes the evaluation of excipients to limit the lipid degradation and the *in vivo* tissue distribution of radio-labelled lipids included in test emulsions.

Chapter 5, "Engineering of Lipid Nanoemulsions at Low Surfactant Concentrations Stabilized by High Contents of Glucose", covers the development of formulations with modified lipid droplet size and the effect of droplet size on the *in vivo* tissue distribution. Liver steatosis is a common adverse effect of ILEs resulting from lipid accumulation in the liver. We hypothesized that beside the oil type, the droplet size affects the lipid tissue distribution. We aimed at modifying the lipid droplet size of our *n*−3 PUFA rich formulation and studied the effect on tissue distribution *in vivo*.

The new *n*−3 PUFA rich oil source is highly susceptible to lipid oxidation. Apart from adding counteracting excipients (Chapter 3), we aimed to reduce the oxidation by optimizing the manufacturing process. Our efforts and the observed influences are described in Chapter 6, "Identification of Optimal Manufacturing Setup for the Production of Lipid Emulsions by High-Pressure Homogenization with Minimal Oxidation Products."

Together, all listed studies aimed at searching for an improved lipid emulsion eliciting less inflammatory adverse effects than commercially available formulations, with the potential to shift paradigms in clinical use of ILEs.

2 Quantification of Lipid Oxidation Products in Lipid Emulsions Requiring Minimal Sample Volume

Gregory Holtzhauer, Ana Curavić, Thushanthini Vilvalinkam, Selina Lehner, Jovana Radonjic, Jonas Bossart, Tino Delaloye and Stefanie D. Krämer

Biopharmacy / Center for Radiopharmaceutical Sciences, Institute of Pharmaceutical Sciences, ETH Zurich

Scientific contributions:

Gregory Holtzhauer (GH) planned, executed and analyzed experiments, and wrote the chapter. Several undergraduate students were involved in this project, all under the supervision of GH: Ana Curavić evaluated different reaction conditions for the TBARS and mFOX assay; Thushanthini Vilvalinkam performed titrations to determine the peroxide value and was involved in the initial development of the TBARS assay; Selina Lehner evaluated the ABTS assay, evaluated alternative calibrators for TBARS and mFOX assay and supported the evaluation of the pAV assay; Jovana Radonjic helped with the initial development of the mFOX assay; Jonas Bossart was involved in the initial evaluation of the pAV assay; Tino Delaloye performed experiments in relation to the luminescence assay. Stefanie D. Krämer supervised the work.

2.1 Introduction

Intravenous lipid emulsions are indicated in conditions or diseases where patients are already weakened and do not tolerate further harm to their health.[216–218] The regulatory bodies generally account for that by setting strict guidelines before approving medical products for clinical use and implementing quality parameters in the pharmacopoeias.[219] For lipid emulsions, only general requirements exist: The mean droplet size (< 500 nm) as well as the fraction of large particles (droplets larger > 5 µm must not exceed 0.05%) are limited.[169] Besides that, also the pH-value (6.0-9.0) and the amount of free fatty acids (< 0.07 mEq per gram oil) are restricted.[168] However, no requirements with regard to lipid oxidation products exist. Lipid emulsions contain a large fraction of unsaturated fatty acids to maintain the health of the patients and provide essential fatty acids. Intralipid and Omegaven, the two most prevalent lipid emulsions used in clinics, both contain 84% of either mono- or polyunsaturated fatty acids (PUFA, see Tab. 1.1 in the General Introduction). PUFAs in turn are prone to lipid oxidation.[202] Via a chain reaction, displayed in Fig. 1.7 in the General Introduction, lipid hydroperoxides and hydroxides are formed.[198]

Lipid oxidation products are harmful as they can impair membrane function and damage proteins and DNA.[220–224] For pure oils, the pharmacopoeias have set mandatory test for the quality control with specific limits, including the iodine value (determining the degree of unsaturation, Ph Eur 2.5.4[225]; USP ⟨401⟩ Fats and Fixed Oils[226]) and peroxide value (measure of lipid hydroperoxides, Ph Eur 2.5.5).[227] For processed oils in finished products such as emulsions, however, no corresponding limits are set. We found that the manufacturing process of emulsions has a major detrimental influence on the lipid oxidation (see Chapter 6, "Identification of Optimal Manufacturing Setup for the Production of Lipid Emulsions by High-Pressure Homogenization with Minimal Oxidation Products"), therefore, quality control of the pure oils prior to processing does not adequately reflect the condition one faces later in the finished product that is administered to the patient. For the quality control of oils in emulsions, different challenges are present than when testing pure oils alone where large quantities are available. When setting up the pharmacopoeial methods for the quality control of oils, primarily oils for topical large-volume preparations such as creams or ointments had been in mind. For the titrimetric determination of iodine value and peroxide value, larger quantities (5-10 g of oil for a single, destructive measurement) are requested, but also easier available from such preparations.

When keeping the chain reaction of the lipid oxidation in mind, it is apparent that it is not sufficient to quantify a single species of lipid oxidation product due to the degradation dynamics.[228] A single measurement is only able to reflect part of the situation. A low value of primary oxidation products can either imply acceptable product quality and that few lipids have been oxidized so far. On the other hand, it can also stem from all the formed primary oxidation products already being further reacted to secondary and subsequent oxidation products. It is thus impossible to draw the correct conclusions from a low primary oxidation value, unless also subsequent oxidation products are quantified.

Though various assays have been reported in literature, none of them fully satisfied our needs. The challenges involved in the development or adaptation of assays for the quality control of oils in lipid emulsions are described in this chapter along the steps we took to overcome the limitations. Our goal was the development of operator-independent measurements, yielding reliable/reproducible data from minimal sample amount (low sample consumption). In early stages of formulation development, the available sample volume is low and measurements need to be fast (high sample throughput) to incorporate the findings in the design of subsequent formulation to enable an efficient formulation development process. Apart from the lack of defined thresholds by the pharmacopoeias, in an academic setting limited

to preclinical *in vitro* and small animal *in vivo* trials, the offered design space is broader and more assumptions are tolerated compared to clinical application in patients. All values determined critically rely on the method with which they have been assessed. It is thus possible to develop our own assays and adapt them specifically for our needs, as long as we only compare them among ourselves and properly describe how the values were assessed. In the absence of specific threshold values set by the pharmacopoeia, benchmarking to commercially available lipid emulsions approved for clinical use was employed.

This chapter is limited to the development of assays for quantification of lipid oxidation products. The quantification of hydrolysis products (free fatty acids) is described separately in Chapter 3, "Determination of Free Fatty Acids in Lipid Emulsions by Fluorescence-Detection Based High Performance Liquid Chromatography". In the following, the most important established assays with their individual working principles and limitations are reviewed.

General limitations

Among the widely available technologies are spectrophotometric measuring techniques. However, they require a transparent solution to be tested, opaque emulsions absorb light and thus lead to inaccurate results. A key challenge is the generation of a transparent analyte solution to be measured. To achieve this the emulsion is either diluted, the emulsion is separated or the oxidation products are extracted. When diluting it is critical to ensure that the limit of quantification of the assay is still below the proposed concentration of analyte in the diluted solution. To separate the phases of an emulsion, it is possible to apply high gravitational forces (centrifugation), increase the ionic pressure so that it is energetically more favourable to dissolve salts in an isolated aqueous phase and have the lipid phase as isolated layer again. Further, organic solvents not miscible with water can be utilized to dissolve the lipid phase, also leading to two isolated phases. When separating emulsions, it is crucial to keep in mind in which phase the analyte of interest is located and thus which phase to follow or to discard respectively. In all these sample extraction steps, it remains crucial to ensure that no further degradation products are formed because of the sample preparation process. Lipid extraction usually consumes more emulsion sample, as the lipid emulsions are on average between 2-20% oil. Solvents used for the extraction need to be compatible with the rest of the assay. This includes the optical measurement, the containers (some organic solvents require glass plates, as they would dissolve the plastic surface and render them opaque), but also the used chromophores, where based on the pH or the medium the ability to form a quantifiable color reaction fades. Identifying a global solvent capable of dissolving the sample as well as the chromophore while maintaining its spectral properties remains a key challenge in the assay development.

Titration of peroxides with iodine

The pharmacopoeial methods[226,227], as well as the American Oil Chemists' Society (AOCS) Official Method Cd 8-53[229] for the determination of the peroxide value (PV) are based on titration. Iodide ions from potassium iodide react with lipid hydroperoxides under acidic conditions to form iodine. The amount of iodine is then determined by titration with sodium thiosulphate solution using a starch indicator to the end point, indicated as a loss of the color. To reliably detect the end point, an oil mass of 5-10 g (equivalent to 25-50 g of a 20% lipid emulsion) is required. Still, determination of the end point by eye is prone to subjective assessments by the respective operator. To reduce this source of error, the detection of the end point can be automated.[230] Apart from the high sample consumption, isolation of the oil phase from the emulsion without affecting the level of analyte is needed. A miniaturization down to 0.5 g oil (2.5 g 20% lipid emulsion) has been proposed[231] but gave unsatisfactory reproducibility in our analyses due to difficulties in detecting the endpoint.

Spectrophotometry for conjugated dienes

The measurement of the conjugated dienes (CD) is simple and straightforward. An oil or emulsion sample is diluted at a defined ratio in ethanol or isopropanol and the absorption is measured at 234 nm.[206] From the measured absorption and a published molar extinction coefficient, the concentration of CD is calculated.[204] CD represent an early species in the oxidation chain reaction (see Fig. 1.7 in General Introduction) and are thus only short-lived.[205] Though a very fast method requiring only minimal sample amount, its significance may be limited: A low value does not necessarily mean a low degree of oxidation. The absence of a proper calibrator lowers it even further. Measuring absorptions at a wavelength below 300 nm demands working with glass cuvettes due to possible interference from plastic cuvettes absorbing UV-light. Though used in the beginning of this work as an easy and rapid measurement, this method was later abandoned for limited predictability.

Fluorescence assay for peroxides after enzymatic activation of the dye

Measuring the fluorescence emitted from 2,7-dichlorofluorescein (DCF) first requires the enzymatic deacetylation of the stable precursor 2,7-dichlorodihydrofluorescein diacetate.[232] 2,7-Dichlorodihydrofluorescein (DCFH) is subsequently oxidized by peroxides to DCF with a characteristic fluorescence signal.[233] In the absence of cellular esterases, no fluorescence signal is measurable. Direct use of DCFH is not possible due to the instability of the molecule. While this assay has been used for emulsions, it was in combination with Caco-2 intestinal epithelial cells during *in vitro* digestion.[234,235] Due to the lack of cellular esterases in our experimental setting, this approach did not produce the desired signal.

Gas chromatography

Gas chromatography (GC)-based methods, most often coupled to mass spectrometry (GC-MS), have been described for the analysis of lipid peroxides[197,236–238], but were not evaluated in this work. Unless used for volatile secondary oxidation products (via headspace-sampling) where it can also be employed directly[239], samples need to be vaporized. For this process, it must be ensured that no additional lipid oxidation products are formed from the thermal stress.

High-pressure liquid chromatography

Due to lipid oxidation products – similar to the parent triglycerides – being insufficiently UV-active on their own, derivatization is needed to obtain a measurable UV-absorption or fluorescence. Under these circumstances, using high-performance liquid chromatography (HPLC) is often overpowered compared to direct reading on a spectrophotometer. A separation of individual species (the advantage of HPLC) is rarely needed at the cost of diminishing sample throughput. Direct measurement using advanced detectors and/or coupling to MS are further developments.[240]

Luminescence assays to quantify peroxides

Two closely related assays based on the measurement of chemiluminescence were studied, once based on luminol[241,242] and acridan[243,244]. Both probes emit a chemiluminescence signal after excitation from peroxide molecules. Both approaches did not produce reliable results. In the case of acridan, the highest signal was measured in the negative control without sample and led to the hypothesis that there is a negative correlation with signal quenching. However, higher amounts of oil lead to a higher signal, disproving the hypothesis. For luminol, high signals were also measured from the negative control, even higher than from the lipid samples. Hydrogen peroxide as positive control substantially increased the signals. This led to the assumption that the miscibility of the oil and aqueous reagents was the limiting factor. Neither adapting the setup according to literature by adding Triton X-100 as detergent and

potassium hexacyanoferrate(III)-solution in basic borate buffer (pH 10)[245] nor adding hemin[246] improved the situation and no linear relationship was observed for the standards.

Fluorescence assay for peroxides

The oxidation of diphenyl-1-pyrenylphosphine (DPPP) by hydroperoxides yields DPPP oxide, emitting a fluorescence signal.[247] The signal should not be affected from added colors[248] and compatibility with emulsion samples without the need of lipid extraction has been demonstrated previously.[247] However, in our experiments, no fluorescence signal could be measured using a fluorescence spectrometer. Using HPLC separation followed by fluorescence detection[249], a signal was measured, but the retention times were not reproducible and no calibration curve could be established using hydrogen peroxide as calibrator.

BODIPY 665/676

Use of an oxidation-selective fluorescent probe has been previously described.[80] It offered great advantages for qualitative (selective imaging of oxidized lipid droplets by confocal microscopy), but also quantitative (flow cytometry)[250] applications. Knowledge on the preferential oxidation in for example larger droplets would provide valuable additional knowledge to take preventive measures to reduce the oxidation process. No reasonable signal could be measured in our experiments, presumably due to limited resolution and/or sensitivity. The application in literature has been described for food emulsions with droplet sizes in the range of 1-10 µm[212,213] compared to our 250-300 nm droplet.

The issue seems not to be related to the oxidation of the dye not taking place, as also trials with the non-selective lipid dye BODIPY 493/503[251,252] failed to produce a measurable signal (by fluorescence microscopy).

mFOX assay to quantify lipid hydroperoxides

The modified ferrous oxidation-xylenol orange (mFOX) assay is a measure for lipid hydroperoxides (LOOH) as primary oxidation products.[253] Ferrous ions are oxidized by LOOH to ferric ions (Fig. 2.1).[254] The reaction also yields a lipid radical, that can further oxidize a second equivalent of ferrous ion under acidic conditions.[255] The two equivalents of ferric ions are complexed by xylenol orange to form a purple-colored complex with a characteristic absorption at a wavelength of 570 nm.[256] Calibration is achieved by replacing the ferrous ions with ferric ions directly. This assay was developed for the measurements of LOOH in oils[254], but was also shown to be compatible with measuring parenteral lipid emulsions.[257] Studies by *e.g.*, Shanta and Decker[253] comparing the mFOX method found good agreement of the determined values with the ones determined for the PV according to the AOCS method[229] based on the sample-consuming titration. Also, a miniaturization has been published already.[258]

There is a similar assay based on the same principle of the oxidation of ferrous ions by LOOH. Instead of xylenol orange, thiocyanate ions are used.[259] Experiments date back more than 75 years[260–262], to date this is still the officially recognized method by the International Dairy Federation for lipid oxidation products in milk and other dairy products.[263] A 3.94 M solution of ammonium thiocyanate is incubated with equal volume of 40-140 mM Fe(II) and the absorption is read at 510 nm.[264,265] In initial reports, the direct use of ferrous ions from iron sulphate was discouraged, instead, it should be purified from oxidized ferric ions by using in combination with barium chloride to precipitate barium sulphate and ensure the sole presence of ferrous chloride.[266]

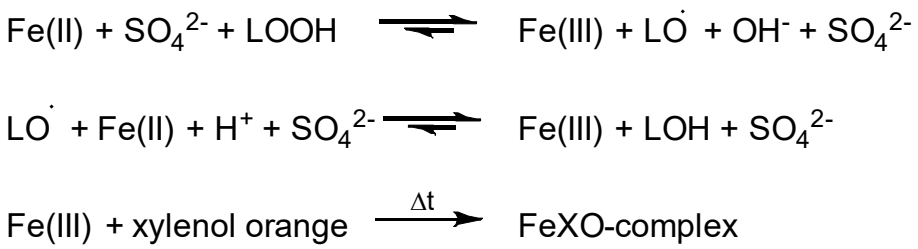

Fig. 2.1: Quantification of lipid hydroperoxides (LOOH) by the mFOX assay. Ferrous ions are oxidized by LOOH to ferric ions, the resulting lipid radical (LO•) can under acidic conditions oxidize a second equivalent of ferrous ions. The produced ferric ions are captured in a selective complex with xylenol orange (FeXO-complex) with a distinct absorption at a wavelength of 570 nm.[255]

para-Anisidine Value

The *para*-anisidine value (pAV) is the official AOCS method[267] for secondary oxidation products such as aldehydes.[207] First, the blank absorption of oil or emulsion in organic solvent is measured.[211,268] Afterwards, *para*-anisidine is added to the supernatant and reacts with the aldehydes to form a color adduct with a distinct spectral absorption at 350 nm.[269,270] Working with strong organic solvents required using glass cuvettes as plastic multiwell plates are not resistant enough. Reading an individual blank takes more time and further lowers sample throughput. The formation of two phases demands for a horizontal absorption measurement and thereby renders glass-coated multiwell plates ineffective. Relative standard deviations > 30% were measured and thus the method was abandoned.

In combination with the pAV, the introduction of the total oxidation value (TOTOX) has been proposed.[83] The TOTOX is defined as the sum of the pAV plus twice the PV, thus accounting once the weight of the present degradation (secondary oxidation products assessed by the pAV) plus double the past (primary oxidation products; assessing the PV now might underestimate the real value, as parts may have already been further oxidized to secondary oxidation products). Since we could not establish the pAV method, calculating the TOTOX was not possible.

TBARS assay to quantify malondialdehyde as secondary oxidation product

The thiobarbituric acid reactive substances (TBARS) assay is a rapid measure of secondary oxidation products.[271] The reaction scheme is depicted in Fig. 2.2.[197] Two equivalents of thiobarbituric acid (TBA) react with one equivalent of malondialdehyde (MDA) to form a strong pink-colored adduct with a characteristic absorbance at 532 nm.[272] The reaction requires prolonged incubation between 15 to 35 minutes[273] at elevated temperatures up to 100 °C.[274] Initial experiments have already been described in 1962 by Dahle, Hill and Holman[275] as a measure of MDA that has been formed through secondary oxidation reactions.[276] There is some controversy on the specificity of the TBARS assay whether it quantifies MDA only or also other products, and if these other products are secondary oxidation products as well (in which case TBARS would still be a valid measure of secondary oxidation products) or unrelated molecules leading to erroneous results.[199,272,277] In combination with samples containing proteins, there is the risk of underestimating the MDA content as MDA can react with amino acid side chains and is therefore not available for TBA reaction anymore.[242] Quantification is established from preparing a linear calibration curve of malondialdehyde bis(dimethyl acetal) (1,1,3,3-tetramethoxy propane) that in-situ forms MDA and is treated the same way as emulsion samples.[257] Because of its simplicity, it is still widely used for assessing emulsions[278] though originally developed for oil samples.[279] Also, the miniaturization down to as low as 50 µl emulsion has been demonstrated.[271]

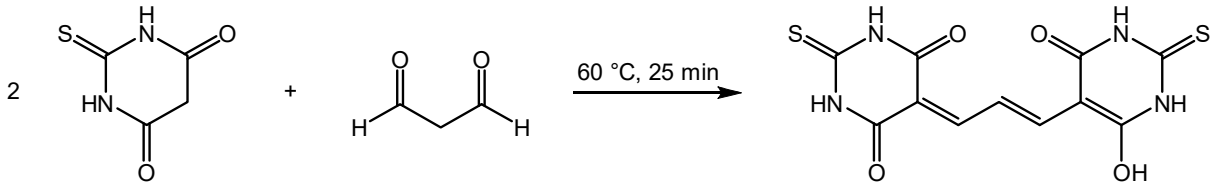

Fig. 2.2: Reaction scheme of the formation of a colored thiobarbituric acid (TBA)-malondialdehyde (MDA) adduct with a characteristic absorbance at 532 nm from the reaction of 2 TBA molecules with one equivalent of MDA at 60 °C over 25 minutes.[197]

ABTS assay to assess antioxidant capacity

The 2,2′-azinobis-(3-ethylbenzothiazoline-6-sulphonic acid) (ABTS) assay is a widely used measure for the radical scavenging activity to compare the antioxidant potential.[280] It was evaluated to test the remaining α-tocopherol capacity. The reaction requires preparation, first ABTS radicals are created by incubating ABTS with potassium persulfate for 12-16 hours.[281,282] Upon reaction with antioxidants, the color from the ABTS radical is lost and the signal disappears.[283] Trolox was used as calibrator standard.[284] After some initial troubles, finally the intended calibration curve with Trolox could be established. However, no reasonable signal was measured from lipid emulsion samples, even after spiking with additional α-tocopherol. The proposed addition of myoglobin did not bring any improvement.[285]

The 2,2-Diphenyl-1-picrylhydrazyl (DPPH)[285–288] assay is based on the same working principle. From the assumption that the ABTS assay failed because of insufficient antioxidant amounts in our samples, this approach was not evaluated yet.

Based on the evaluation of the described methods in preliminary experiments, we chose the mFOX assay to quantify primary oxidation products (peroxides) and the TBARS assay to quantify secondary oxidation products (malondialdehyde) as most promising approaches for the quality control in our project. The goal of this sub-project was to further optimize the two assays for their routine use in the development of our lipid emulsions for parenteral nutrition.

2.2 Methods

mFOX assay

Unless stated otherwise, chemicals were obtained from Sigma-Aldrich, Buchs, Switzerland. For the measurement of primary oxidation products according to the mFOX method, LOOH were extracted from lipid emulsion samples by diluting 1:80 (13 µl *ad* 1 ml) in DMSO (≥99.5%), vortexed and centrifuged at 15'000 g for 10 minutes (Beckman GS-15R, Beckman Coulter, Brea CA, USA). Later, 20 µl from the supernatant of the LOOH-extract in DMSO was pipetted together with 300 µl of a 0.15 mM xylenol orange solution[289] (xylenol orange disodium salt, for spectrophotometric determination of metal ions) in 25 mM H_2SO_4 onto a 96-well plastic microplate reader plate. The reaction was started by the addition of 20 µl of freshly prepared 40 mM iron(II) solution ($FeSO_4$ • 7 H_2O, ≥99.0%) in 3.5% HCl. The absorbance was monitored for 16 minutes[290] at room temperature at a wavelength of λ = 570 nm[256] on a Synergy HT microplate reader (BioTek Instruments GmbH, Sursee, Switzerland). Quantification was achieved with a calibration curve established with iron(III) solution ($FeCl_3$ • 6 H_2O, ≥99%) in the range of 0.05 – 0.5 g/L and using the equation given in [253], further taking the 1:80 dilution factor into account and standardizing to the oil content of the original emulsion.

To study the influence of reaction parameters, iron(II) concentrations in the range of 10-400 mM were tested. The emulsion volume was varied between 3 µl and 43 µl, but the total volume of the DMSO

solution was maintained at 1 ml (addition of 957-997 µl DMSO). Translation into a molarity-based quantification using either cumyl hydroperoxide[80] (80%; Acros Organics, New Jersey, USA) or *tert*-butyl hydroperoxide[258,291] (70% in water; Tokyo Chemical Industries, Tokyo, Japan) was attempted.

TBARS assay

Secondary oxidation products were quantified according to the TBARS assay. A 0.67% thiobarbituric acid solution[277] (4,6-dihydroxy-2-mercaptopyrimidine, 98%; abcr GmbH, Karlsruhe, Germany) in 10% DMSO (≥99.5%) and 0.03% HCl was prepared.[274] Of this 0.67% TBA solution, 60 µl were mixed with 300 µl lipid emulsion, vortexed, and incubated for 25 minutes at 60 °C in an Eppendorf Thermomixer 5436 (Eppendorf SE, Hamburg, Germany).[273] Afterwards, the reaction was quenched for at least 5 minutes on ice, and 400 µl of hexane (≥97.0%) were added to separate the phases. The mixture was vigorously vortexed and centrifuged for 15 minutes at 15'000 g (Beckman GS-15R, Beckman Coulter). Afterwards, 100 µl of the lower aqueous layer were added to 800 µl 1-butanol (99.9%; VWR International, Fontenay-sous-Bois, France), the reaction mixture was again vortex-mixed and centrifuged for 5 minutes at 15'000 g (Beckman GS-15R, Beckman Coulter). The absorption of 200 µl of the supernatant was measured at a wavelength of λ = 532 nm on a Synergy HT microplate reader (BioTek Instruments GmbH). Quantification was achieved with a calibration curve established by treating 300 µl of aqueous dilutions of 1,1,3,3-tetramethoxypropane (malonaldehyde bis(dimethyl acetal), 99+%; Acros Organics) in the range of 2.8 – 60 µM the same as samples followed by standardizing for the oil content of the original emulsion.

The possible interference of ethylenediaminetetraacetic acid (EDTA) and glucose was tested by adding 2.5 µM final concentration EDTA (disodium salt dihydrate, ≥99%; Carl Roth GmbH + Co. KG, Karlsruhe, Germany) or 63% glucose (D(+)-glucose anhydrous, pure, EP, USP; neoFroxx, Einhausen, Germany) to MDA standards. For studying the influence of reaction temperature and time, durations of 5-55 min[273] at 25-95 °C[274] were evaluated. Validation of the MDA calibration was attempted with two other aldehydes, 2,4-heptadienal (90%) and *trans,trans*-2,4-decadienal (95%; Acros Organics) and two isoforms of a dialdehyde, terephthalaldehyde (>98.0%; Tokyo Chemical Industries) and isophthalaldehyde (>97%; Apollo Scientific, Stockport, UK), dissolved either in ethanol, DMSO or ethanol:water 1:1 at a pH of 1.86 and 13.91 in the concentration range 9.6-74.5 µM.

2.3 Results

mFOX assay

In initial experiments using the tetrasodium salt of xylenol orange, we were not able to measure the expected signal at a wavelength of 570 nm and instead got a pH-dependent shift in absorption, independent of added ferric ions. By switching the salt form of xylenol orange to the disodium form, the expected UV maximum was measured with iron(III) and emulsion samples.

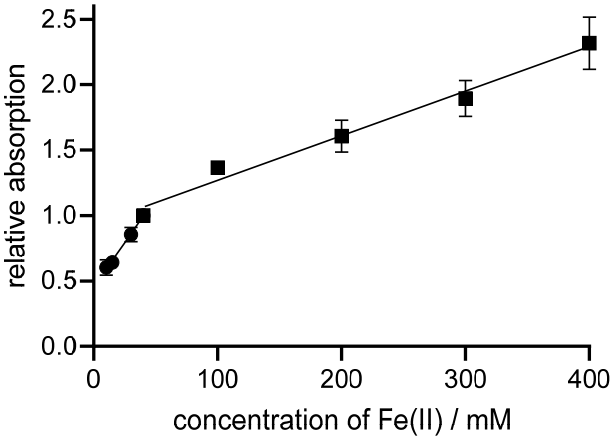

Fig. 2.3: Influence of iron(II) concentration on obtained absorption at 570 nm after a constant incubation time of 16 minutes. For relative comparison, the absorption obtained from 40 mM iron(II) is assumed as 1 and all other values are calculated relative to its absorption. Dots and squares represent averages from 4 and 3 emulsions, respectively (means ± standard deviation), along a linear fit in the range 10-40 mM and 40-400 nm, respectively.

The iron(II) concentration had a dose-dependent effect on the obtained absorption values after a constant incubation time and constant emulsion volume used in the assay (Fig. 2.3). For relative comparison across different emulsions, the absorption obtained from 40 mM iron(II) was arbitrarily set as 1 and all other values were calculated relative to the absorption at 40 mM ($A_{x\ mM}/A_{40\ mM}$). Two linear relationships with different slopes below as well as above 40 mM iron(II) concentration resulted. The variation of the used emulsion volume shown in Fig. 2.4 (A) revealed that with increasing emulsion volume, higher relative absorption values were measured. To allow reasonable comparison, values obtained from the default 13 µl were set as 1 and all other values were calculated relative to it. The correction for the individual emulsion volume in Fig. 2.4 (B) then showed an increased standard deviation for the minimal emulsion volume of 3 µl. At higher emulsion volumes, the trend levels off with low standard deviations. Choosing 13 µl over *e.g.*, 43 µl might overestimate the hydroperoxide content, but reduces sample consumption considerably.

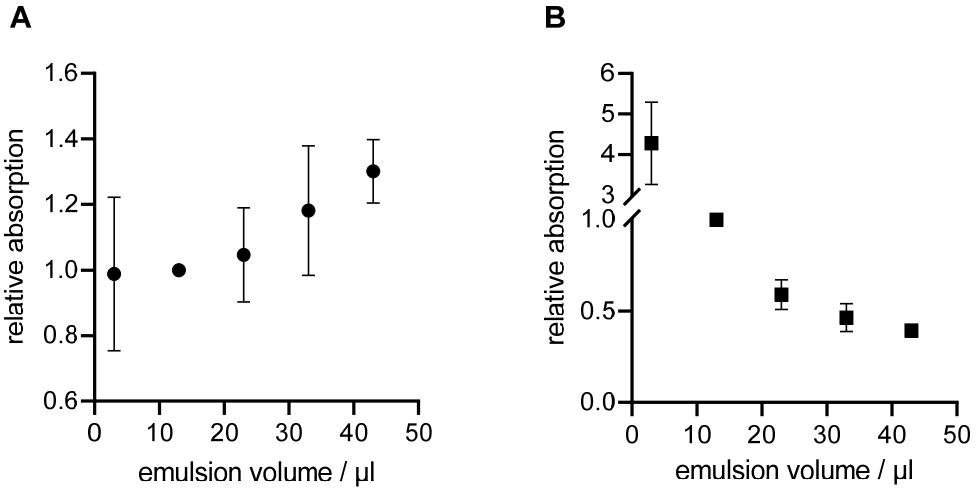

Fig. 2.4: Influence of emulsion volume on obtained absorption after 16 minutes incubation time. The absorption obtained from the default 13 µl of emulsion is set as 1 and all other absorptions are calculated relative to it (A). In (B), the same data as in (A) are normalized (divided) for the different emulsion volumes. Mean ± standard deviation (n=4).

In Fig. 2.5 the absorptions at a wavelength of 570 nm with increasing concentrations of *tert*-butyl hydroperoxide and cumyl hydroperoxide diluted in different solvents are shown. For comparison, the calibration curve obtained from using iron(III) directly is shown as well. Using water to dilute tert-butyl hydroperoxide led to a steeper slope, while using DMSO to dissolve both alternate standards led to a higher intercept at comparable slope. While with both synthetic hydroperoxides linear relationships were established, maintenance of the pH-value in the reaction mix was crucial to ensure a comparable signal. The absorption values obtained from iron(III) directly are lower at equimolar concentrations. Thus, no cross-calibration could be achieved to give the results of the mFOX assay as hydroperoxide concentrations in µM instead of milliequivalents of oxygen.

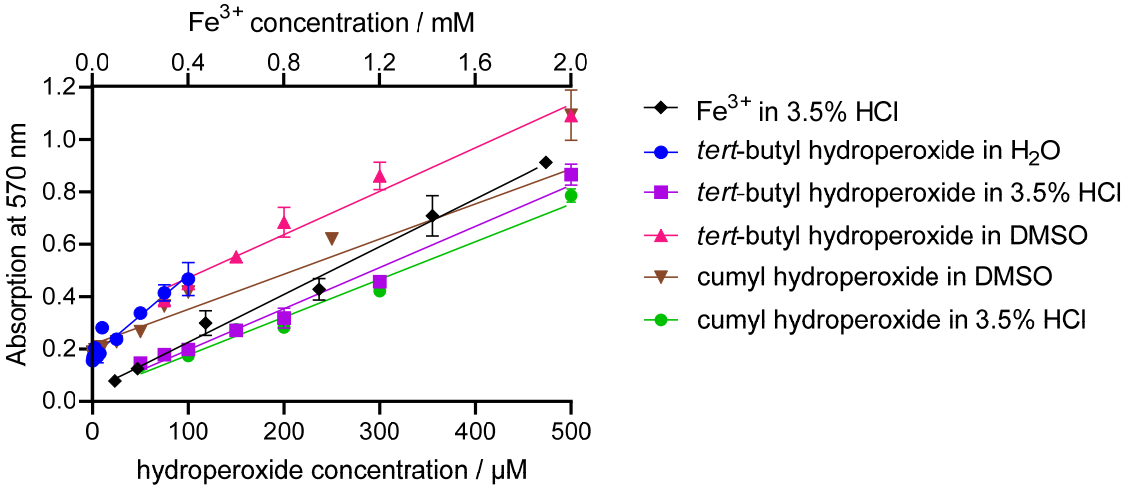

Fig. 2.5: Absorption at 570 nm after using increasing tert-butyl hydroperoxide or cumyl hydroperoxide dilutions in different solvents (bottom x-axis) in comparison to the calibration obtained from using iron(III) in 3.5% HCl (top x-axis). Colors as indicated, mean absorption measurements ± standard deviation (n=3).

Using the thiocyanate anion or xylenol orange for the complexation of ferric ions yielded similar absorption values (see Fig. 2.6). However, the cross-calibration with tert-butyl hydroperoxide and cumyl hydroperoxide was not possible for the ammonium thiocyanate assay and therefore the mFOX assay was given preference over the ammonium thiocyanate assay for future routine use.

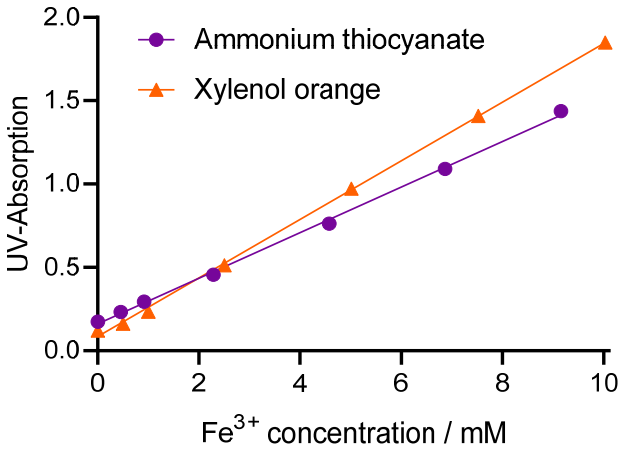

Fig. 2.6: Calibration curves obtained from incubating increasing iron(III) concentrations with either ammonium thiocyanate (purple curve) or xylenol orange (orange curve) and measuring the color complex formation by UV-absorption at 510 nm (ammonium thiocyanate) or 570 nm (xylenol orange), respectively.

TBARS assay

The color adduct formation requires elevated temperature. The influence of the reaction temperature is shown in Fig. 2.7 for oil and emulsion samples, respectively. For oil samples, above 60 °C comparable values were obtained, while for emulsion samples the values considerably increased above temperatures of 60 °C. Along with the increasing values, the standard deviation was also markedly increased. Cooling on ice slightly reduced the measurements, indicating that the reaction would still have continued otherwise. Cooling on ice as opposed to at room temperature thus allows to more precisely control the reaction duration and increase reproducibility.

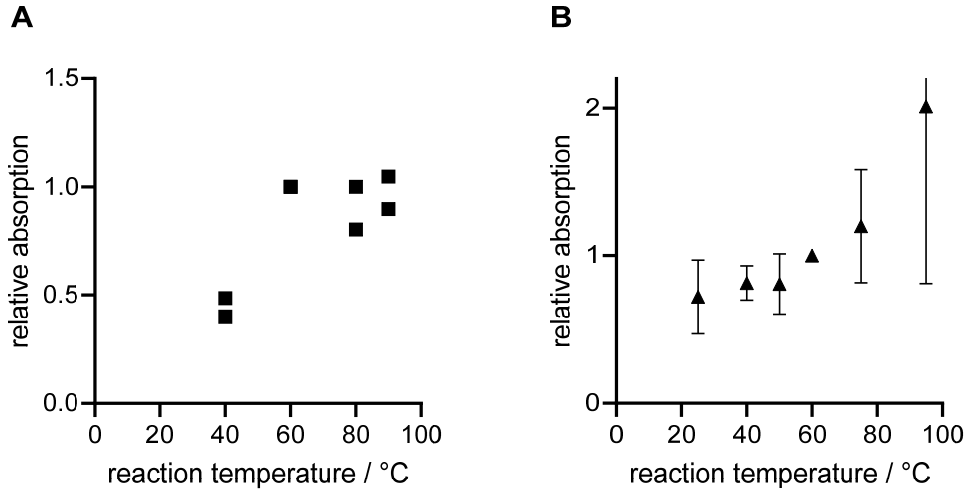

Fig. 2.7: Influence of the reaction temperature on the obtained absorption values after incubating oil samples (A, squares, individual values, n=2) and emulsion samples (B, triangles, mean ± standard deviation, n=4) for 25 minutes. For relative comparison, the absorption obtained from the default 60 °C was set as 1 and the other values were calculated relative to it.

For oil samples, the reaction time had little influence in preliminary studies, assuming the elevated value at 35 minutes resulting in a large standard deviation was an outlier. At 60 minutes and above, the standard deviations were also increased. For emulsion samples, incubation for longer than 25 minutes yielded increased relative values with larger standard deviations. Our finally chosen reaction time of 25 minutes lies in the range of published values in literature.[273]

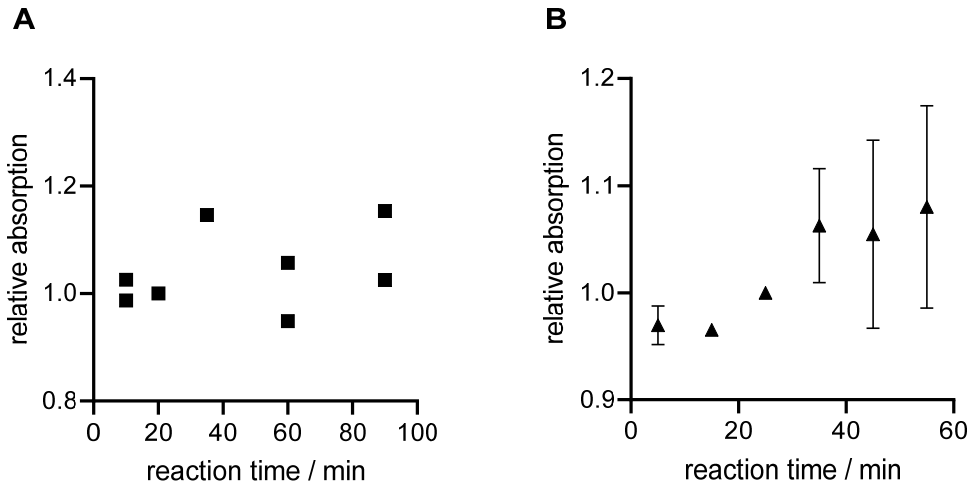

Fig. 2.8: Influence of the reaction time on relative absorption obtained after incubating oil samples (A, square symbols, individual values, n=2) at 90 °C and emulsion samples (B, triangles, mean ± standard deviation, n=4) at 60 °C. The absorption values are calculated relative to the absorption obtained after 20 min for oil samples and 25 min for emulsion samples.

Inclusion of trichloroacetic acid (TCA) in TBA solutions led to phase separation of the emulsion samples and considerably increased the obtained values. Incubation of TBA solution with the polyunsaturated mono-aldehydes 2,4-heptadienal and *trans,trans*-2,4-decadienal did not produce a measurable signal. Neither did the two benzene-dialdehydes isophthalaldehyde and terephthalaldehyde lead to the expected color adduct formation, irrespective of used solvent and pH-value. In the literature, TBA concentrations in the range of 0.375%-1% are described[292], usually at a volume ratio of around 5:1 for the TBA solution over the emulsion. For reduction of sample and solvent consumption, a more concentrated TBA solution was prepared and used in combination with the minimal emulsion amount for a reproducible result. Lastly, the whole reaction mixture was downscaled to still fit into 1.5 ml Eppendorf tubes after addition of sufficient amounts of hexane (or chloroform in initial experiments) to avoid the need for transferring the samples to a larger container between individual steps.

No signal difference was measured from MDA calibration curves, spiked with either 25 µM EDTA or 63% glucose and a corresponding unspiked MDA calibration curve alone (Fig. 2.9).

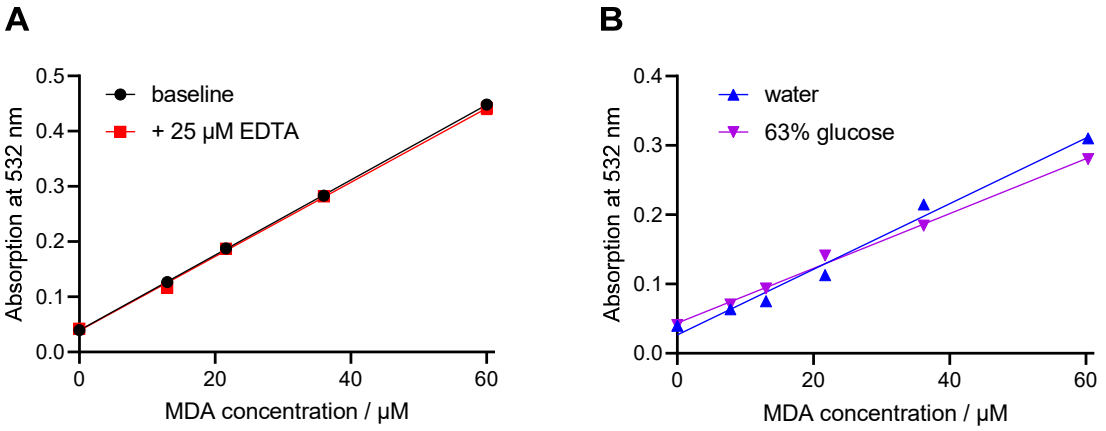

Fig. 2.9: Calibration curves obtained from increasing concentrations of malondialdehyde standard and measuring absorption at a wavelength of 532 nm. In (A), standards were spiked with 25 µM EDTA, in (B) with 63% glucose to study the influence of these two agents on the obtained absorption values.

2.4 Discussion

Two assays for the quantification of primary and secondary oxidation products in lipid emulsions showed promising results in our experiments. The mFOX and TBARS assays were further developed for the successful implementation in the routine quality control of lipid emulsions in our laboratories.

mFOX assay

In the literature, it is shown that the formation of the ferric-xylenol orange complex takes time to form.[258] While some sources show that a level-off is reached after 5 minutes already, other take up to 20 with maximal value after 60 minutes[293] We considered an incubation time of 15 min sufficient[290], despite not always already reaching the absolute maximum. As long as the incubation time was diligently kept constant for all assays, differences in the formation of the complex could be accounted for. By keeping the incubation short, the sample throughput was increased and the plate reader was not unnecessarily blocked. Instead of incubation outside, we considered it advantageous to incubate the plates inside the plate reader and monitor the complex formation. Measurements could in this case still be rescued from issues arising from precipitation/phase separation at later time points turning the solution turbid and interfering with a spectrophotometric measurement. As the reaction starts immediately after the addition

of the iron(II) solution, use of a multichannel pipet proved beneficial in our experiments to avoid a time delay between the first and last sample when measuring several samples at once on a 96-well microplate.

The concentration of xylenol orange was chosen according to examples from the literature.[289] Also the default concentration of 40 mM iron(II) for the reaction lay in the range of reported values. The linear increase found in our experiments when using larger concentrations is another hint that the equilibrium is not reached after 16 minutes incubation yet; under the assumption that the iron(II) concentration is not the rate limiting reactant (less than 100 mM hydroperoxides expected in out formulations) only the reaction rate, but not the maximal (equilibrium) signal should be affected. The iron(II) concentration for routine measurements was chosen to yield absorption values between 1.0 and 1.2 to avoid detector saturation. It has also been found by other researchers that increasing sample amount led to an increasing signal, until saturation of the reaction.[292] In our experiments, emulsion volumes were chosen as low as possible to reduce sample consumption and signal saturation was not reached. The total volume of the DMSO-extract was kept constant in our experiments. For future experiments to maintain low sample consumption, but avoid overestimation of the peroxide content, experiments at lower total DMSO volume (ad 500 µl or even 100 µl) could be evaluated. Thereby, the relative oil content in the 20 µl DMSO-extract used for the assay is greatly increased. Care needs to be taken to avoid saturation of the detector when the absolute oil content used in the assay is in fact suddenly increased up to 10-fold.

The external validation of the calibration failed, while at least a linear relationship could be established, no correlation to the calibration with iron(III) was possible (reasonably explainable factor, instead of calculated 0.29x conversion factor). When in the assay iron(II) is used, the calibration with iron(III) was considered more valid; the efficiency of ferrous oxidation may be different for various peroxide species. As long as the assay is always carried out in the same way, the information value is greater by giving the results as mEq of oxygen rather than transforming to a molar amount with the assumption of a specific oxidation efficiency of either cumyl hydroperoxide or *tert*-butyl hydroperoxide

The signal of the mFOX depends greatly on the pH-value of the medium where the reaction takes place.[293] When using the tetrasodium salt instead of the disodium salt of xylenol, instead of obtaining the expected complex formation, we got a pH-responsive signal. Through the choice of diluted sulfuric acid as solvent for our reaction, we ensured that the pH stayed constant over the course of the reaction.[255] Still, the influence of the dilution medium of the alternate standards that are only added at below 6% (20 µl of a total of 340 µl) was observed when studying the different dilution media. It has been reported that using sulfuric acid over methanol, also commonly used when working for the measurement of values in oils, resulted in faster establishment of the equilibrium.[255]

Chelator substances in emulsion samples could interfere with the mFOX assay. EDTA might capture iron and prevent it from complexing with xylenol orange and thereby lead to misleading low measured results not reflecting the hydroperoxide content.[255] However, in our case the relative ratio of EDTA to iron was negligible. In the assay, 20 µl 40 mM iron(II) is used compared to 20 µl of a DMSO-extract from 13 µl emulsion with 2.5 µM EDTA (the DMSO-extract has a final EDTA concentration of 32.5 nM) was negligible.

While the ammonium thiocyanate method produced comparable results (as also demonstrated by Shanta and Decker[253]), experiments showed a higher distinctability between samples compared to the FeSCN-assay. Moreover, it yielded better results in the cross-validation attempts with cumyl hydroperoxide and therefore preference was given to the mFOX assay for routine use over the ammonium thiocyanate assay.

TBARS assay

According to literature, the adduct formation of TBA and MDA in the TBARS assay requires elevated temperature. Increasing the temperature up to 95 °C should speed up the reaction, but our experiments showed that above 60 °C a level off with only minimal signal gain at higher temperatures was found for oil samples. Out of concern of promoting the formation of additional MDA and thereby influencing the measured result during the sample preparation process, we opted for a reaction temperature of 60 °C. Literature proposes the use of butylated hydroxytoluene (BHT), a strong synthetic antioxidant, to prevent further degradation from taking place.[294] We did not evaluate this over concerns of affecting the measured result as well when lowering the reaction temperature allowed equal results than in a boiling water bath.

Many protocols suggest the inclusion of TCA in the TBA solution with the aim to precipitate any proteins that could otherwise interfere with the assay.[242] Due to the absence of proteins in our lipid emulsion samples this was not a concern in our case. Introduction of TCA led to phase separation and considerably increased the obtained values. In contrast to the mFOX assay, for the TBARS assay, the color adduct formation takes place while the emulsion is still intact and only the formed adduct is later on extracted. It remains unclear by which mechanism TCA increased the obtained values.

The attempted validation with two polyunsaturated monoaldehydes did not produce a colored adduct. As expected, the two monoaldehydes were not able to link two TBA molecules. However, the confirmation with two alternative dialdehydes failed, indicating specificity for MDA over the other two dialdehydes. Interference from EDTA or glucose was excluded: Emulsions with elevated EDTA incorporated led to drastically reduced TBARS values (see Chapter 5, "Engineering of Lipid Nanoemulsions at Low Surfactant Concentrations Stabilized by High Contents of Glucose"). No difference was measured from MDA calibration curves spiked with either EDTA or glucose and compared to unspiked controls, excluding the interference of EDTA or glucose with the formation of the color adduct. Instead, a beneficial effect of the chelator on lowering the generation of secondary lipid oxidation products is more likely.[294]

2.5 Conclusion

PUFAs in lipid emulsions are highly susceptible to lipid oxidation and thus lipid oxidation products need to be quantified diligently before the use of any lipid emulsions in patients. A multitude of assays are reported in the literature with individual advantages but also considerable limitations. The obtained values highly depend on the assay with which they have been measured. We developed two assays for the quantification of lipid hydroperoxides as primary lipid oxidation products and TBARS assay for secondary oxidation products and adapted them for the measurement on a 96-well plate.

The chosen reaction parameters, including the reaction temperature, reactant concentration and incubation time, highly influence the obtained signal. We optimized the two assays to reduce emulsion consumption and optimized for high throughput by establishing a plate-reader compatible setup. In summary, we established two assays for practical use to quantify oxidation products in lipid emulsions.

3 Determination of Free Fatty Acids in Lipid Emulsions by Fluorescence-Detection Based High Performance Liquid Chromatography

Gregory Holtzhauer, Marco Taddio and Stefanie D. Krämer

Biopharmacy / Center for Radiopharmaceutical Sciences, Institute of Pharmaceutical Sciences, ETH Zurich

Scientific contributions:

Gregory Holtzhauer optimized the HPLC method, evaluated reaction conditions, established calibration curves for quantification, manufactured emulsions and quantified the FFAs, determined the limit of quantification, and wrote the chapter; Marco Taddio developed the initial HPLC method and introduced DMT-MM as coupling agent; Stefanie D. Krämer supervised the work.

3.1 Introduction

Triglycerides in close contact with an aqueous environment as for example in the form of lipid emulsions are prone to hydrolysis.[295] The resulting free fatty acids (FFA) can impair the patient's health by *e.g.*, damaging the vasculature.[296–298] The hydrolysis reaction is acid-catalyzed and thus accelerated by the produced FFA, further promoting degradation over time and reducing shelf-life.[299] Lipid emulsions are indicated in severe health conditions and patients should be spared from further harm by products of inferior quality.[218,300] Thus, also the United States Pharmacopoeia limits the level of free fatty acids to be administered in a lipid emulsion to 0.07 mEq of FFA per gram of oil.[168] The lipid profile of an emulsion is carefully compiled and selected to consist of all essential fatty acids. If some are lost due to degradation, the body becomes deficient and can develop adverse effects with time.[79,301]

Lipid emulsions are especially indicated in pre-term infants to bridge the first few days of life by providing essential nutrients until the digestive system is ready to tolerate enteral nutrition.[8,302] FFAs bind to albumin (as confirmed by our *in vitro* distribution studies described in Chapter 4, "Excipient Screening for the Development of Lipid Emulsions based on Vegetable Oils Rich in $n-3$ Polyunsaturated Fatty Acids"), competing with the albumin binding of bilirubin.[303,304] As bilirubin levels are frequently elevated in neonates, the liberation from the albumin binding may further increase the toxic effects of the increased bilirubin levels. Emulsions with excess FFAs increased free bilirubin in serum, potentially posing an increased risk for the development of jaundice and in severe cases even neurotoxicity.[305–309] It is thus even more critical in pre-term infants than in adults to diligently quantify the extent of free fatty acids prior to administering lipid emulsions.

The US pharmacopeia limits the level of total but not of individual free fatty acids.[168] However, knowledge on the extent of individual fatty acid (FA) species can show the triglycerides' susceptibility towards hydrolysis. Various methods are available for the quantification of FFAs, including titration, enzymatic color reactions, high-performance liquid chromatography (HPLC) or gas chromatography (GC). The ability to separate lipids and phospholipids and corresponding subclasses (phosphatidyl choline, ethanolamine, inositol) by solid phase extraction has been shown for quite some time.[310–314] As fatty acids alone are not sufficiently UV-active, especially the saturated fatty acids with no delocalized electron system, they need to be derivatized to get a measurable signal for spectrophotometric detection. This can be achieved with an UV-active dye or a fluorophore.[315–317] GC also does not work directly but needs the derivatization to fatty acid methyl esters.[318,319] In this process, all the triglycerides get hydrolysed, so no information on the FFA levels prior to the derivatization step is available. If chromatographic methods are coupled to mass spectroscopy, the labelling-step can be omitted, though this costly instrument requirement is not broadly available.[320] Clinically, for measuring FFA-levels in plasma samples, a method based on enzymatic conversion of FFAs to their corresponding enoyl-coenzyme A products is used.[321–323] This conversion generates hydrogen peroxide that can be quantified in a subsequent reaction. The challenge of using this approach for the measurement of FFAs in lipid emulsions is to bring the enzymes dissolved in aqueous solvents in contact with the FFAs in the lipid phase of emulsions. Titration has the drawback that it requires large sample volumes to reliably detect a faint color change.[324] Moreover, this determination is operator-dependent and prone to subjective assessment. A method especially used to quantify total FFAs released during *in vitro* gastric digestion is the pH-stat method where FFAs generated upon (enzymatic) lipolysis are constantly neutralized with sodium hydroxide in the presence of lipase and bile salts. From the consumption of base over time, the amount of released FFA can be quantified, but also requires similar sample volumes as titrimetric methods.[235,325–329] Published HPLC methods rely on toxic coupling agents and take a considerable analysis time.[315–317]

Our goal was to optimize sample throughput, limit sample consumption so that the method can be applied in early screening when still little substance is available and avoid or replace potentially toxic reagents. An improved HPLC method was thus developed to accurately quantify the total amount of FFA in oil-in-water emulsions for parenteral nutrition prior to administration and to identify the individual FFAs from their retention time.

3.2 Methods

Fluorescent labelling procedure

The method is based on activation of extracted FFAs with the triazine derivative 4-(4,6-dimethoxy-1,3,5-triazin-2-yl)-4-methylmorpholinium chloride (DMT-MM) as a coupling agent and subsequent conjugation with the fluorescent dye 4-(N,N-dimethylaminosulfonyl)-7-piperazino-2,1,3-benzoxadiazole (DBD-PZ). After incubation, aliquots were quenched with diluted acid to terminate the coupling reaction and separated and analyzed by high-performance liquid chromatography. The method was modified from previous work by Ueno *et al.*[317] Unless stated otherwise, chemicals were obtained from Sigma-Aldrich (Buchs, Switzerland). Briefly, 195 µl acetonitrile, 7.5 µl emulsion sample, 15 µl premixed 100 µM pentadecanoic acid (C15:0, 99%; Acros Organics, New Jersey, USA) and 100 µM heptadecanoic acid (C17:0, >98.0%; Tokyo Chemical Industries, Tokyo, Japan), both as internal standards, and 7.5 µl 200 µM DMT-MM (>98.0%; Tokyo Chemical Industries) in 80/20 acetonitrile/water were mixed by gentle vortexing and incubated for 5 minutes. Then, 75 µl 5 mM DBD-PZ (>98.0%; Tokyo Chemical Industries) in acetonitrile were added, the sample was gently vortexed and incubated for 2 hours at room temperature in the dark. The reaction scheme is depicted in Fig. 3.1.

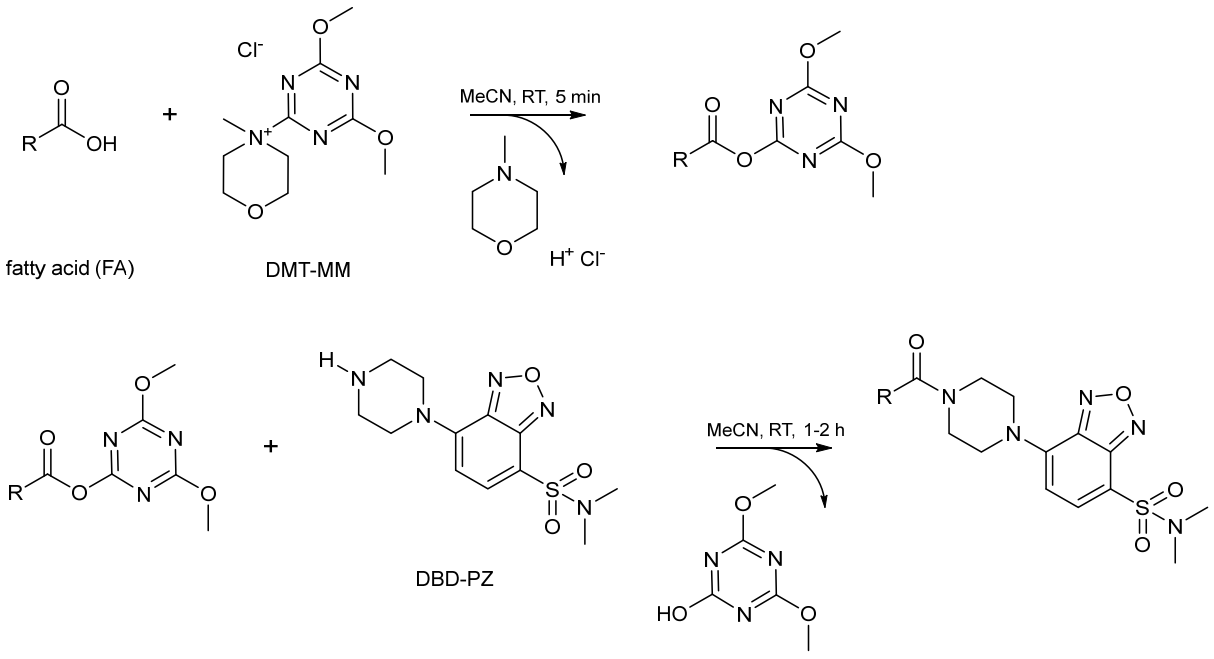

Fig. 3.1: Reaction scheme of the fluorescence-labelling of free fatty acids. First, the fatty acid is activated with the coupling agent DMT-MM to form an active ester. The introduced leaving group is then replaced by the fluorophore DBD-PZ.

Afterwards, an aliquot of 75 µl was quenched with 25 µl of 1% formic acid (98.0-100%) in acetonitrile and analysed by HPLC. Part of the sample (10 µl) was injected at a flow rate of 1 ml/min and separated on a Waters XBridge™ C18 5 µm, 4.6 x 150 mm (Waters, Antwerp, Belgium) column. Acetonitrile (≥99.9%) and 0.1% trifluoroacetic acid (≥99.9%) in water were used for the mobile phase. A visual

representation of the solvent gradient is shown in Fig. 3.2. The mobile phase was 15% aqueous from 0-3 minutes; from 3-12 min, the polarity was gradually decreased to 5% aqueous and maintained for 10 minutes; from 22 to 22.5 minutes, 15% aqueous was re-established and the column was equilibrated for 2.5 min (total run duration: 25 min).

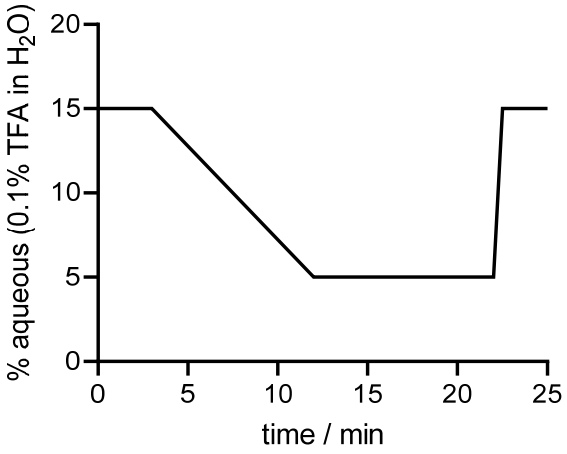

Fig. 3.2: Solvent gradient of the mobile phase used for the separation of fluorescently-labelled fatty acids. The percentage of 0.1% TFA in water as aqueous solvent was varied between 15% and 5% over a total run time of 25 minutes. The organic solvent was acetonitrile. Labelled FFAs were separated on a Waters XBridge™ C18 5 µm, 4.6 x 150 mm (Waters, Antwerp, Belgium) column.

Fluorescence was detected at an excitation wavelength of λ_{ex} = 444 nm and emission wavelength of λ_{em} = 557 nm. The system was equipped with a VWR Hitachi LaChrom Elite L-2200 autosampler, VWR Hitachi LaChrom Elite L-2130 pump and VWR Hitachi LaChrom Elite L-2480 Fluorescence detector (VWR Hitachi, Tokyo, Japan). Quantification was achieved by standardization the integrated peak areas to those of non-natural FFAs C15:0 and C17:0 as internal standards as well as comparison with calibration curves established from individual pure standards in the concentration range from 0.5-50 µM (concentration in injected solution) followed by standardization to the oil content of the original emulsion. Details on the used FA standards can be found in the Appendix in Tab. A1.

Influence of reactant concentrations

To test the influence of the reactant concentrations, runs with 5-50 µM final concentration of DMT-MM, 0.25-12.5 mM final concentration of DBD-PZ and emulsion volumes between 1.5-75 µl were conducted. Varied incubation periods between 1-24 h were evaluated. The labelling reactions were carried out at room temperature protected from light. In preliminary experiments temperatures of up to 60 °C were examined. To facilitate dissolution of concentrated FA standards, stock solutions were heated up to 60 °C to melt. Interference was tested by replacing the emulsion sample in the labelling reaction with 2% solutions of common co-surfactants Tween and Span (2% v/v in acetonitrile).

Quantification of FFA in lipid emulsions

Commercially available lipid emulsions Intralipid, Omegaven and SMOFlipid (all from Fresenius Kabi) and in-house manufactured mimics with 20% soybean oil, 10% fish oil or 20% soy-olive-coconut and fish oil mixture along with 20% Formula #3 (oil mixture consisting of 50% Ahiflower oil, 25% olive oil and 25% coconut oil, see detailed description in Chapter 4) lipid emulsion were characterized for the amount of FFA. In-house emulsions were manufactured according to the general procedure described in chapter 4. As oil source for in-house mimics of commercial emulsions, soybean oil (either purified soybean oil 700, Ph. Eur., USP; Lipoid GmbH, Ludwigshafen, Germany; super refined soybean oil,

USP; Croda, Mill Hall PA, USA; or refined soybean oil IV, Ph. Eur., USP; Société Industrielle des Oléagineux (SIO), St-Laurent Blangy, France) and fish oil (Bioriginal, Saskatoon SK, Canada) were used. For mimicking the SMOFlipid-based four-oil mixture additionally coconut 30% coconut oil (Bioriginal) and 25% olive oil (purified, Ph. Eur., USP; Lipoid) were used.

We found competition for the reagents when FA standards were mixed. Combining various FA standards in a single sample resulted in lower signal for the individual FAs than when analysed individually. Because of this, sample matrices aiming at a "typical" intermediary FFA level were used for the calibration samples. Commercially available lipid emulsions mentioned above were spiked with the indicated amounts of FA standards. An exemplary composition is shown in Tab. 3.1; Appendix Tab. A2 to Tab. A4 show all compositions. The control sample ("Ctrl" in Tab. 3.1) was spiked with the internal standards C15 and C17 alone.

Tab. 3.1: Composition of a spiking matrix for establishing calibration curves for quantification of FFA levels in lipid emulsions. Displayed below is the example for Formula #3 with its main contributing FA species, based on the certificates of analysis (CoA) of the three oils. Mix 1-3 describes the three calibration mixtures consisting of a combination of different concentrations of FA standards.

Fatty acid standard	Mix 1	Mix 2	Mix 3	Ctrl
C12:0	+2.5 µM	+10 µM	+5 µM	
C18:3 *n*−3	+10 µM	+2.5 µM	+5 µM	
C14:0	+10 µM	+5 µM	+2.5 µM	
C18:2	+2.5 µM	+10 µM	+5 µM	
C15:0	+10 µM	+10 µM	+10 µM	+10 µM
C17:0	+10 µM	+10 µM	+10 µM	+10 µM

After establishing the calibration curve, the relative fatty acid profile of Intralipid, Omegaven and Formula #3 emulsions was compared against the theoretical profile calculated from literature data and certificates of analysis (CoA) of the used oil sources.

Determination of limit of quantification

For the determination of the limit of quantification, dilutions of the pure FA standards from 2.5 µM to 0.1 µM in acetonitrile were measured accordingly. C15:0 and C17:0 were added as internal controls at 10 µM each.

Total hydrolysis of oil samples

We furthermore analyzed raw oil samples after hydrolysis to confirm the fatty acid composition provided in the CoAs, determined by gas chromatography by the supplier. Oil samples (600 µl) were incubated for 45 minutes to 2 hours at 37 °C with 40 mg lipase (from porcine pancreas, Type II, 100-500 units/mg protein) to hydrolyze the triglycerides. Subsequently, samples containing 1.5 µl hydrolyzed oil (mimicking the oil content in 7.5 µl 20% lipid emulsion) were analyzed as described above.

To further streamline the assay setup, preparation of diluted aliquots of FA standards, coupling agent and fluorophore and their respective stability upon storage in the freezer was studied.

3.3 Results

HPLC method development

A representative chromatogram after running a lipid emulsion sample is depicted in Fig. 3.3. Distinct fatty acid patterns were detected, based on the composition of the lipid emulsion and its oil source. The retention times listed in Tab. 3.2 were obtained from running pure standards. Excess unreacted fluorophore DBD-PZ had a retention time of 1.9 min, close to the dwell time of 1.7 min. The solvent gradient system was optimized in such a way that 13 individual FA species, including the two non-natural FAs used as internal standards (C15:0 and C17:0), were separated. When choosing flatter solvent gradients (prolonging the method) and more polar starting conditions (30% aqueous instead of 15% aqueous), it was also possible to detect C8:0 and C10:0 that were otherwise co-eluting with the fluorophore peak in the current method. Some retention times were closely together and may overlap at increased concentrations. However, FAs of concern were not naturally present together in the same oil sample and thus with knowledge about the used oil source in a given lipid emulsion sample, it was possible to assign the identity to all peaks found in the overlay of three commercially available lipid emulsions depicted in Fig. 3.4. The figure is scaled from 4-17 min to only show the peaks of the FAs of interest, excluding the unreacted fluorophore and the equilibration time at the end. The different FA compositions and extent of certain FA species based on the origin of the oil can nicely be appreciated. To allow reasonable comparison, all results are standardized to the two internal standards C15:0 (rt = 9.2 min) and C17:0 (rt = 13.5 min).

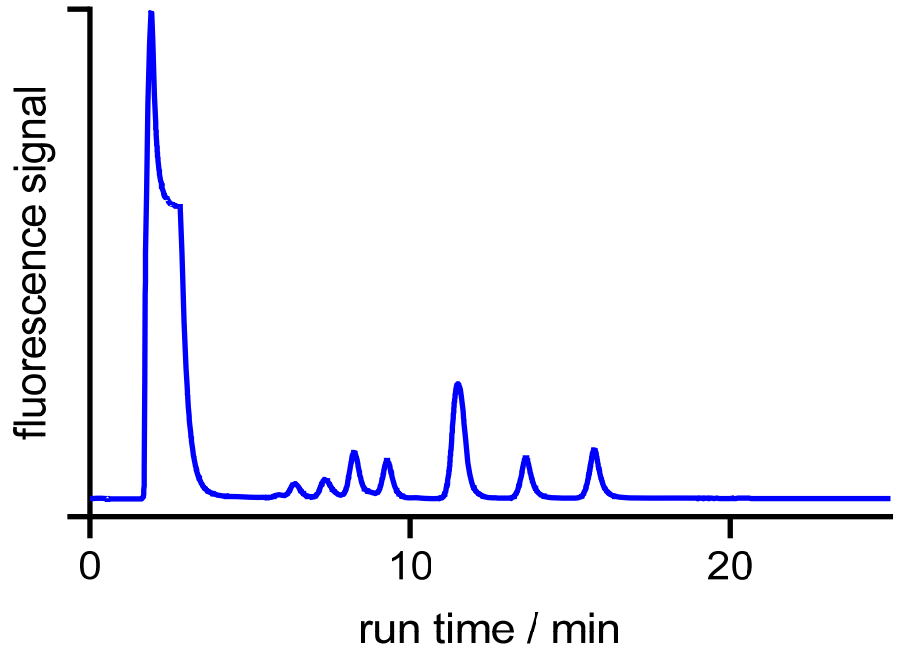

Fig. 3.3: Chromatogram of Intralipid after separation of fluorescently-labelled fatty acids by HPLC.

Besides C15:0 and C17:0, tridecanoic acid (C13:0) was evaluated as internal standard but it eluted close to eicosapentaenoic acid and α-linolenic acid, either of which is present in most lipid emulsion samples studied. Most excipients commonly present in lipid emulsions were not affected by the fluorescence labelling and did not result in a signal. The situation was different for Tween and Span co-surfactants that were readily hydrolysed (already prior to high-pressure treatment during homogenization) and

considerably contributed to the measured signal. A 2% solution of Span 20 (sucrose ester esterified with C12:0) contained > 45 µM of C12:0 and shorter fatty acids, Span 40 (esterified with C16:0), Span 60 (C18:0 esterified) and Span 65 (3 times esterified with C18:0) each contained > 260 µM C16- and C18-FFAs. Tween 40, Polysorbate 60 and Tween 65 (PEGylated version of Span 40, 60 and 65, respectively) also showed considerable amounts of C16- and C18-FFAs, although to a lesser extent than the corresponding Span equivalents (20-100 µM). Span 80 and Tween 80 (esterified with C18:1, Tween additionally PEGylated) contained amounts of 60 µM and 20 µM C18:1 FFAs, respectively. Tween 20 (C12:0-esterified) showed > 12 µM of C12:0 FFAs.

Tab. 3.2: Retention time of fatty acids obtained from individually running pure standards, sorted according to retention time. C15:0 and C17:0 were used as internal standards in the analysis of the emulsions and oils.

Fatty acid standard	Retention time ± 0.1 min
C12:0, lauric acid	4.6 min
C20:5, eicosapentaenoic acid, EPA	5.2 min
C13:0, tridecanoic acid	5.6 min
C18:3 *n*−3, α-linolenic acid, ALA	5.8 min
C18:3 *n*−6, γ-linolenic acid	6.3 min
C22:6, docosahexaenoic acid	6.4 min
C14:0, myristic acid	7.2 min
C20:4, arachidonic acid	7.3 min
C18:2 *n*−6, linoleic acid	8.2 min
C15:0, pentadecanoic acid	9.2 min
C16:0, palmitic acid	11.4 min
C18:1, oleic acid	12.8 min
C17:0, heptadecanoic acid	13.5 min
C18:0, stearic acid	15.7 min

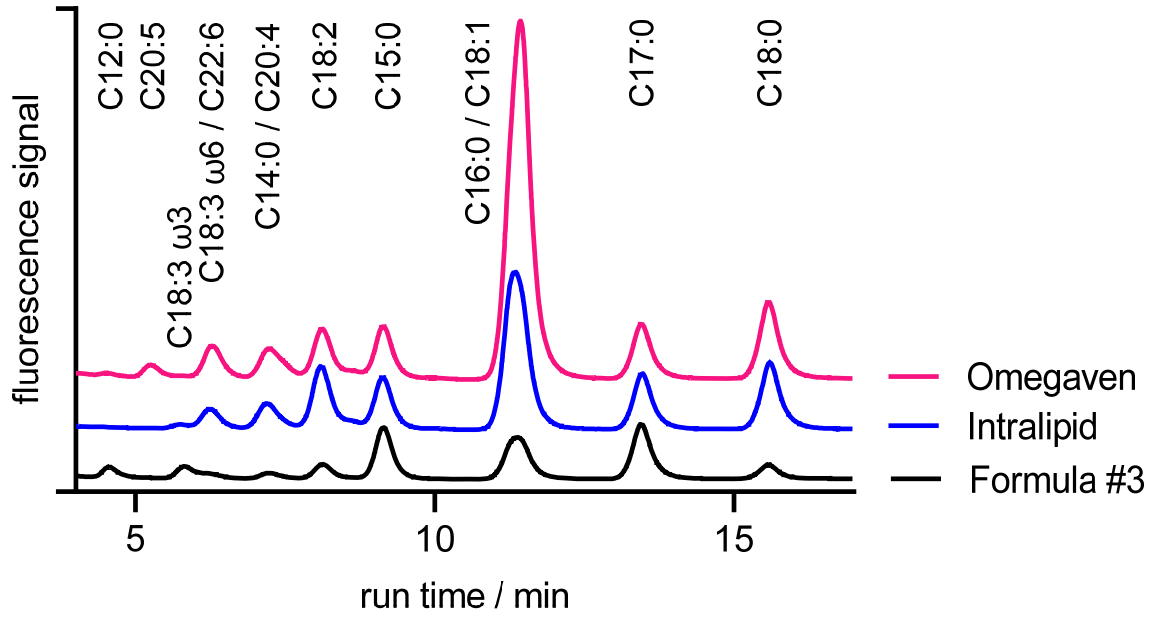

Fig. 3.4: Stacked FFA chromatograms of commercially available emulsions Omegaven and Intralipid as well as in-house manufactured Formula #3 oil-based lipid emulsion after HPLC-separation, scaled to the two internal standards C15:0 and C17:0, from 4 to 17 min. The peaks are annotated based on their retention time obtained from runs with pure standards alone.

Quantification of FFAs in lipid emulsions

Standardization to the two internal standards and comparison with calibration curves established from pure standards allowed the quantification of total FFAs in the tested lipid emulsion samples. A representative comparison of Formula #3 emulsion samples spiked with increasing amounts of FFA to establish the calibration curve for the individual FFAs is shown in Fig. A1 in the Appendix. Results of commercial references and in-house manufactured mimics with similar oil composition are shown in Tab. 3.3. Results are given as concentrations per emulsion volume as well as standardized to the oil mass of the respective emulsion to account for the lower oil content in fish oil-based emulsions. The limit for total FFA stipulated by the USP lies at 0.07 mmol per gram oil[168]; FFA levels of all in-house manufactured emulsions and Intralipid were below this limit. There is a notable difference between the commercial reference emulsions and the respective in-house mimics, though measured at different times within their life cycle. Total FFA concentrations were an order of magnitude higher in the older, but not yet expired commercial references. These measurements furthermore show a tendency that soybean oil-based emulsions had the lowest FFA content in both commercial and in-house emulsions.

Tab. 3.3: Measured FFA-levels in commercially available lipid emulsions and corresponding in-house manufactured emulsions mimicking their composition. Mean ± standard deviation from n=3 (for in-house 20% SO-emulsion), n=9 (for 20% F#3 emulsion), or quantifications from a single batch (n=1).

Emulsion	Total FFA	
Intralipid	3.12 mmol (L emulsion)$^{-1}$	0.016 mmol (g oil)$^{-1}$
Omegaven	7.04 mmol (L emulsion)$^{-1}$	0.070 mmol (g oil)$^{-1}$
SMOFlipid	14.6 mmol (L emulsion)$^{-1}$	0.073 mmol (g oil)$^{-1}$
20% Soybean oil (SO)-based emulsion	0.26 ± 0.09 mmol (L emulsion)$^{-1}$	0.0013 ± 0.0005 mmol (g oil)$^{-1}$
10% Fish-oil (FO)-based emulsion	0.47 mmol (L emulsion)$^{-1}$	0.0047 mmol (g oil)$^{-1}$
20% SO/FO/MCT-based emulsion	0.69 mmol (L emulsion)$^{-1}$	0.0035 mmol (g oil)$^{-1}$
20% Formula #3 oil mix-based emulsion	0.83 ± 0.11 mmol (L emulsion)$^{-1}$	0.0042 ± 0.0006 mmol (g oil)$^{-1}$

Apart from the total FFAs, also the individual FFA profile was analyzed. As shown in Tab. A5 in the Appendix, as a general trend the relative percentage of free PUFAs was lower than the theoretical expectation from gas chromatographic analyses taking into account all (esterified and free) FAs, and in turn the percentage of shorter and saturated FAs was higher than the reported percentage considering esterified and free saturated FAs. This trend was observed in all three studied formulations, independent of the oil type.

Determination of the limit of quantification

The extension of the calibration curves by serial dilution of stock solutions with known concentrations and taking the injection volume into account allowed the determination of the limit of quantification (Tab. 3.4). For all studied FA, the quantification limit was between 0.19 and 1.9 pmol and independent of the retention time.

Tab. 3.4: Limit of quantification for studied fatty acids as determined from pure standards. Sorted according to the degree of saturation and chain length as second criterion.

Fatty acid	Limit of quantification
lauric acid (C12:0)	1.9 pmol
myristic acid (C14:0)	0.94 pmol
palmitic acid (C16:0)	0.19 pmol
stearic acid (C18:0)	0.94 pmol
oleic acid (C18:1)	0.38 pmol
linoleic acid (C18:2)	0.38 pmol
α-linolenic acid (C18:3 *n*−3)	0.94 pmol
γ-linolenic acid (C18:3 *n*−6)	0.38 pmol
arachidonic acid (C20:4)	0.66 pmol
eicosapentaenoic acid (C20:5)	0.94 pmol
docosahexaenoic acid (C22:6)	0.38 pmol

Influence of reactant concentrations

Fig. 3.5 shows the influence of reactant concentration in the labelling reaction on the obtained chromatograms. The absolute measured signal in Fig. 3.5 A was reduced compared to a standard sample (1 x fluorophore, 1 x emulsion volume, 1 x coupling agent) when only half the fluorophore dose was employed. Increasing the emulsion dose also reduced the absolute measured signal (lowest dark green trace in A, particularly visible at rt of 9.2 min and 13.5 min), presumably due to competition between the increased FFA levels already seen in the establishing of the calibration curves (as described above). Increasing the coupling agent concentration on the other hand led to higher signal (dark blue trace, also visible at 9.2 min and 13.5 min). When the traces were normalized to the two internal standards, depicted in Fig. 3.5 B, no difference between the standard setup and the varied fluorophore- or coupling agent concentrations was visible anymore. The traces with the increased emulsion volume in turn showed the increased peak area from the increased total FFAs.

Increasing the concentration of the coupling agent allowed to reduce the incubation time from up to 24 hours in initial experiments down to 1 hour in the current setup. Prolonging the initial activation period of 5 min when only the emulsion and the coupling agent are mixed prior to the addition of the fluorophore did not change the signal. The stock solutions of FA standards for calibration or of the internal standards were stable when stored in the freezer. The fluorophore solution was stable at room temperature for longer than six weeks when protected from light. However, the coupling agent lost activity when in solution at room temperature for longer than 2 hours.

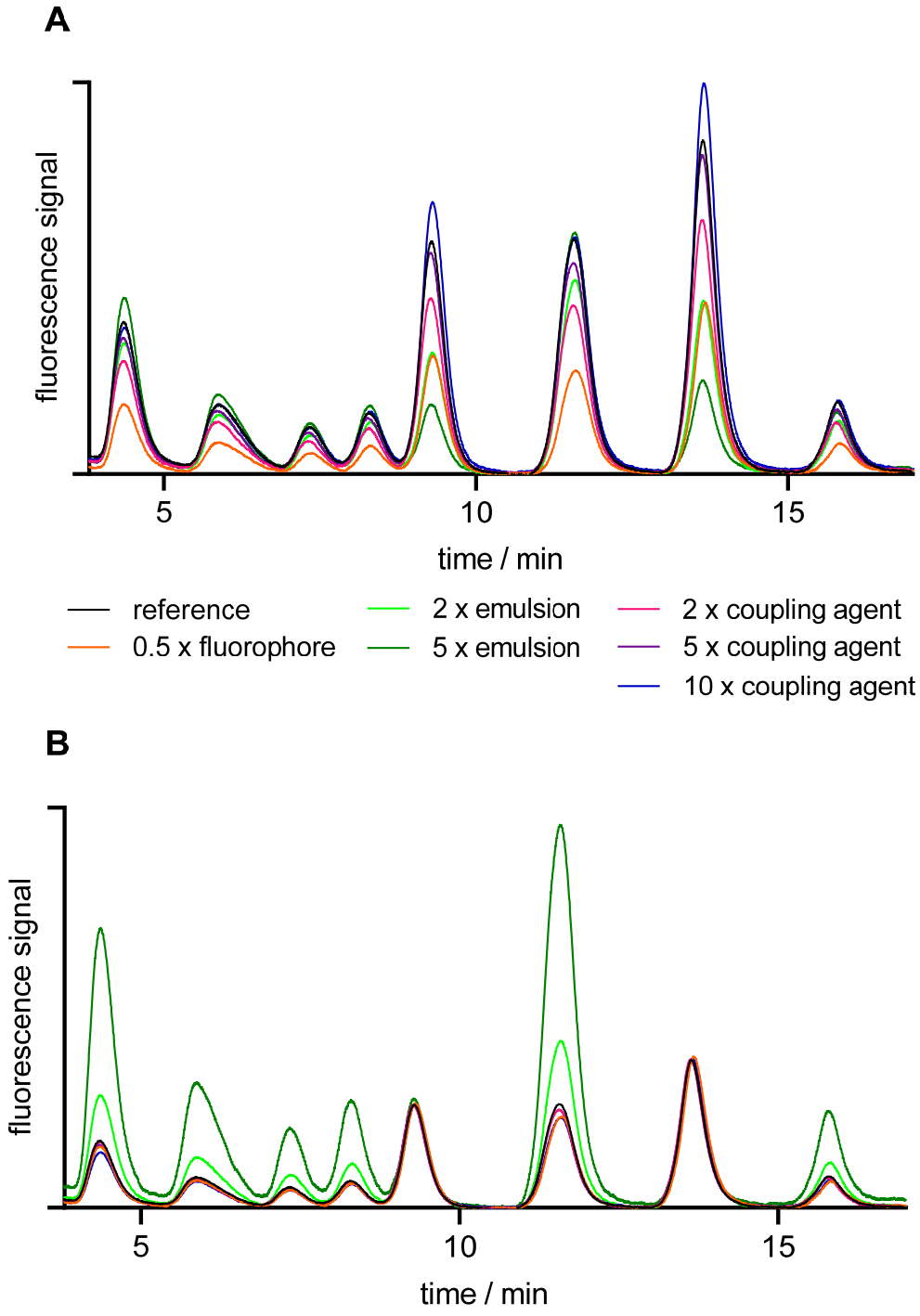

Fig. 3.5: Influence of reactant concentrations on the measured chromatograms of a model Formula #3 lipid emulsion. Absolute fluorescence signal (A) and same data normalized (B) to the two internal standards C15 (rt = 9.2 min) and C17 (rt = 13.5 min). Reaction conditions as indicated by color codes in (A).

Total hydrolysis of oil samples

The FFA determination after total hydrolysis revealed some discrepancies to the expectations from the CoAs (see Tab. 3.5), in particular for fish oil. Similar to the relative fraction of FAs found in emulsion samples (Tab. A5), percentages of PUFAs with longer chain length were reduced compared to the theoretical calculations based on published values[62] determined by gas chromatography. Saturated and

monounsaturated FAs with shorter chain length in turn were increased compared to the calculated values. This trend was observed for all three studied oils, though less pronounced for soybean oil and Formula #3 oil mix. Due to the high signal at a retention time of around 7.2 min, it was not possible to separately quantify C14:0 and C20:4 in fish oil.

Tab. 3.5: Relative FA composition of soybean, fish and Formula #3 oil mixture after total enzymatic lipolysis (45 minutes at 37 °C, 40 mg lipase added to 600 µl oil). List sorted for ascending FA chain length. Experimentally determined values in comparison with values calculated from literature and CoAs of used oils.

Soybean oil	experimental	literature / CoA
C14:0	-	0-0.1%
C16:0, C18:1	43.5%	32-35%
C18:0	8.2%	4%
C18:2	41.5%	53-56%
C18:3 *n*−6	6.8%	7.8-8.1%
Fish oil	experimental	literature / CoA
C12:0	1.1%	-
C14:0, C20:4	22.6%	4% + 2.5-2.8%
C16:0, C18:1	50%	32-35.4%
C18:0	12.7%	1.25-2.1%
C18:2	2%	3.4-4%
C18:3 *n*−3	-	4%
C20:5	6.6%	20.3-24%
C22:6	5%	17.5-24%
Others	-	7%
Formula #3 oil	experimental	literature / CoA
C12:0	15.1%	12%
C14:0	7.1%	4.5%
C16:0, C18:1	46.5%	32.3%
C18:0	5.9%	0.9%
C18:2	5.3%	9.1%
C18:3 *n*−3	20.1%	31.6%
others	-	9.6%

3.4 Discussion

The work of Ueno *et al.*[317] and Toyo'oka *et al.*[315] built the starting point for this investigation. These methods, published in 1999 and 1991, respectively, have several drawbacks and there has not been much improvement in the past 20 years in the development of a fast, reliable and broadly applicable method for the quantification of FFA in lipid emulsions. Both groups used the potentially toxic coupling agent diethyl phosphorocyanidate. Today, alternatives with lower toxicity are available. The fluorophore DBD-PZ has already successfully been used in combination with the coupling agent DMT-MM before[330], although this was for the detection of sialic acid derivatives in saliva and plasma samples.

While Toyo'oka *et al.* showed the separation of odd-numbered FA chains, they did not use them as internal standards. Use of non-naturally occurring synthetic FAs in our method allows the comparison and correction of samples measured at different times. The retention time of C13:0 overlapped with other FAs of interest and was thus unsuitable for this purpose. C15:0 and C17:0 on the other hand worked well and in combination gave further confidence to balance out deviations from the sample preparation process. Internal standards were used at a concentration of 10 µM each to avoid too broad peaks that could overlap with signals from FAs from the sample.

The retention time of palmitic acid (C16:0) and oleic acid (C18:1) are similar in the presented method. While it was possible to separate pure standards at low concentrations, typical quantities present in oil samples exceeded these low concentrations and it was not possible to individually quantify palmitic and oleic acid without either prolonging the method (at the cost of the sample throughput) or diluting the sample further (with the loss of sensitivity for all other FA species). As the calibration curves of C16:0 and C18:1 were similar, we combined both peaks for analysis and used the calibration curve of palmitic acid for quantification. Based on the fatty acid profiles of the used oil sources provided in the CoAs, the expected content of C8:0 and C10:0 was negligible and did not justify prolongation of the method, reducing sample throughput. Neglecting C8:0 and C10:0 results in an underestimation of the FFA levels by < 4 % (for Formula #3-based emulsions, stemming from coconut oil; none in other formulations without coconut oil; based on the CoAs, under the assumption that during the degradation only triglycerides are hydrolysed and no C2-units are lost).

The limit of total FFA stipulated by the United States Pharmacopoeia[168] is 0.07 mEq $(g \text{ of oil})^{-1}$. All of the in-house manufactured lipid emulsions were below this level. Values in commercially available emulsions are higher, presumably due to the addition of 0.3 g sodium oleate per liter of emulsion as stabilizer to Omegaven and SMOFlipid[128], thus accounting for 1 mmol $(L \text{ emulsion})^{-1}$ (equal to 0.005-0.01 mmol $(g \text{ oil})^{-1}$) already. In our analysis, soybean oil-based emulsions showed lower values than the other formulations based on a different oil source, though this needs to be confirmed as the sample number was low.

The final conditions of the labelling reaction, with incubations at room temperature and using acetonitrile as solvent, were considered mild enough to assume that no further hydrolysis occurred during the labelling reaction. It was challenging to find a solvent which was both miscible with the lipid emulsion and able to dissolve the apolar saturated fatty acids with long carbon chains such as stearic acid (C18:0). An additional challenge was to avoid precipitation on the column when eluting with high aqueous content. To overcome these issues, acetonitrile was chosen as apolar solvent.

Extraction of the lipid phase of the emulsions prior to the labelling reaction was not necessary; the method was sensitive enough and the required amount of lipid emulsion was sufficiently low to yield a transparent mixture with the reagents posing no issue for signal quenching due to the opacity of the emulsion. The determined limit of quantification was on average 200-fold higher than the values reported by Ueno *et al.*[317], but were still considered sufficient for our purposes.

The concentration of the coupling agent had the strongest influence on the measured absolute fluorescence signals. Introduction of two internal standards for normalization allowed to correct for changed labelling reaction conditions. The required emulsion volume was successfully lowered so that 7.5 µl of emulsion is sufficient for the quantification of FFAs present in the emulsion.

A suitable reference determination method for validation of the measured values (mass spectroscopy, gas chromatography) is still pending.

3.5 Conclusion

The presented method provides a valuable contribution for the quality control of lipid emulsions intended for parenteral nutrition. Especially for application in pre-term infants, it is crucial to keep FFA levels as low as possible, as competition for binding of bilirubin to albumin may aggravate the toxic effects arising from hyperbilirubinemia. The method utilizes minimal sample volumes of 7.5 µl lipid emulsion to reproducibly quantify individual FFA species after just 90 min analysis time. The limit of quantification is in the single-digit or sub-pmol range for the most commonly encountered natural FA species. Compared with previous reports on the labelling of FFAs or quantification by fluorescence detection after separation by HPLC, highly toxic reagents were replaced, sample consumption was reduced by a factor of 130 and the use of the costly fluorescent dye was lowered by a factor of 4. Increasing the concentration of the coupling reagent allowed to shorten the reaction time for labelling, and together with the accelerated HPLC method reduced total analysis time by a factor of 2.9 to increase sample throughput. Validation of the quantification by comparison with the official titrimetric method or a GC-MS method remains to be done.

3.6 Acknowledgment

Purified soybean oil 700 (Ph. Eur., USP) and purified olive oil (Ph. Eur., USP) were a kind gift of Lipoid GmbH, Ludwigshafen, Germany. Super refined soybean oil (USP) was kindly provided by Croda, Mill Hall PA, USA. Refined soybean oil IV (Ph. Eur., USP) and refined olive oil IV (Ph. Eur.) were donated by Société Industrielle des Oléagineux (SIO), St-Laurent Blangy, France.

4 Excipient Screening for the Development of Lipid Emulsions based on Vegetable Oils Rich in *n*−3 Polyunsaturated Fatty Acids

Gregory Holtzhauer[a], Elin Huwiler[a], Anja Herbst[a], Simona Tschopp[a], Ramona Grob[a], Jovana Radonjic[a], Jonas Bossart[a], Eliana Lucchinetti[b], Michael Zaugg[b,c], Nazek Noureddine[d], Paulina Wawrzyniak[d], Claudio Gemperle[d] and Stefanie D. Krämer[a]

[a] *Biopharmacy / Center for Radiopharmaceutical Sciences, Institute of Pharmaceutical Sciences, ETH Zurich*

[b] *Department of Anesthesiology and Pain Medicine and Cardiovascular Research Centre, University of Alberta, Edmonton*

[c] *Department of Pharmacology, University of Alberta, Edmonton*

[d] *Division of Clinical Chemistry and Biochemistry, University Children's Hospital Zurich*

Scientific contributions:

Gregory Holtzhauer (GH) established a manufacturing protocol, prepared emulsions with various compositions, performed *in vivo* tissue distribution studies, and wrote the chapter. GH acknowledges the work of several undergraduate students in this project: Elin Huwiler supported the evaluation of buffer salts, casein, and DSPG as excipients; Anja Herbst contributed to establish manufacturing on the in-house high-pressure homogenizer and evaluation of Tween co-surfactants; Simona Tschopp and Ramona Grob performed initial experiments with soybean, sunflower and rapeseed lecithin, sodium oleate and Kolliphor; Jovana Radonjic performed experiments with citrate buffer; Jonas Bossart was involved in antioxidant evaluation; all under the supervision of GH. Eliana Lucchinetti and Michael Zaugg conceptualized the Formula #3 oil mixture. Nazek Noureddine, Paulina Wawrzyniak and Claudio Gemperle measured cell viability and haemolysis. Stefanie D. Krämer supervised the work.

4.1 Introduction

Currently available lipid emulsions for parenteral nutrition are associated with considerable adverse effects in prolonged use.[96,97,100] Parenteral nutrition is indicated in conditions where uptake of nutrients is impaired such as short bowel syndrome[5] or when enteral nutrition is not tolerated yet in pre-term infants.[8] These patients are already severely weakened and do not tolerate further harm from adverse therapy effects. We thus aim at developing novel lipid emulsions with reduced adverse effects.

The most commonly observed adverse effects, collectively termed intestinal-failure associated liver disease (IFALD), manifest as cholestasis progressing to cholelithiasis, hepatic steatosis inducing hepatic fibrosis, with the potential of ultimately developing liver cirrhosis.[9,18,28,91] The term IFALD is used for diseases of the liver and gall bladder/bile duct when parenteral nutrition is used and other causes can be excluded. The etiology for the development of IFALD is not fully elucidated. A certain genetic susceptibility[91,93,94] is proposed, but there is also strong evidence that it is based on the nature of the administered oil[18,45,49,51,99]: While oils rich in *n*−6 polyunsaturated fatty acids (PUFA) elicit pro-inflammatory effects, oils rich in *n*−3 PUFA rather resolve inflammatory states. This has been explained through the production of either pro-inflammatory (upon administration of *n*−6 PUFAs) or anti-inflammatory (*n*−3 PUFAs) mediators in the body, as elaborated in detail in the General Introduction.[9,45,100] Since the human body lacks the converting enzyme Δ15-desaturase, there is no switch between the two metabolic pathways possible and the choice of the supplementation of the respective oil source directly determines the immune response.[27,29] Moreover, a strong link between the development of IFALD and high phytosterol levels[91,100–102] as well as low α-tocopherol levels[9,22,100] – stemming from the used oil type – has been found. The most commonly used parenteral lipid emulsion in clinics is Intralipid, derived from soybean oil.[331] Soybean oil in turn is especially rich in phytosterols and *n*−6 PUFA. With emulsions based on fish oil rich in *n*−3 PUFA, rather anti-inflammatory effects are found clinically. However, the use of large quantities of fish oil is not sustainable[30,64,80], bears the risk of exposure to lipid-soluble toxins accumulated via the food-chain and we thus sought to develop lipid emulsions based on plant-derived oil sources rich in *n*−3 PUFA, but low in phytosterols.

Based on literature search, a composite mixture of three oil types was designed (Dr. Eliana Lucchinetti) in the framework of an interdisciplinary Sinergia team grant (no. 177225) by the Swiss National Science Foundation. Half of the lipid dose comprises the oil of *Buglossiodes arvensis*, commonly termed corn gromwell. This oil marketed under the trade name "Ahiflower" by the Canada-based company Nature's Crops is rich in short-chain *n*−3 PUFAs (total 66% of fatty acids, FA), particularly high in α-linolenic acid (C18:3 *n*−3, 43%) and stearidonic acid (C18:4 *n*−3, 20%).[65,84–86] Ahiflower oil is inherently low in phytosterols, compared to soybean oil, and should thus pose less risk of promoting the development of IFALD.[82] Ahiflower oil was tolerated well by humans after ingestion[82,84] and elicited anti-inflammatory responses after oral supplementation.[87] The total percentage of saturated fatty acids (SFA) is only 5%. Most (95%) of the FAs in Ahiflower oil are C18 and longer carbon chains. To compensate for the lack of short- and medium chain triglycerides (MCT), which provide readily available energy, coconut oil with > 80% of FAs of 14 carbon atom chain length and shorter was added to the formula.[22,40,88] To provide essential *n*−9 FAs without disturbing the *n*−6 to *n*−3 balance, one quarter of olive oil was added. Due to the high PUFA content, the oil mixture was highly susceptible to oxidative degradation and counteracting excipients were needed.

Another influencing factor for IFALD is the infusion rate.[95–97] Excess infusion rates > 1.5 ml/kg body weight per day also promote the development of IFALD, but are in certain situations needed to meet the

energy requirements. In these situations, lipids are not uniformly distributed in the body to cover the energy expenditure, but rather deposited in the liver as fat storage, further promoting steatosis and worsening the effects on the liver. We thus also aim at developing formulations with a balanced tissue distribution. To confirm the tissue distribution, experiments with radioactively-labelled triglycerides were performed to check for the influence of the oil type on the distribution behavior.[332,333]

The goal of this part of the work was to develop a stable lipid emulsion for parenteral nutrition consisting of the lipid formula described above. The identified major challenges were the high content of PUFAs, which are highly susceptible to oxidation, and the intended long-term use of the emulsion. The excipients thus had to meet strict requirements. They should physically stabilize the emulsion, reduce PUFA oxidation, and at the same time be well tolerated by the organism under long-term use. The *in vivo* distribution of the final emulsion was studied in mice, in comparison with Intralipid. In this part, we focus on the choice and concentrations of the excipients, while the optimization of the manufacturing processes is described in Chapter 6, "Identification of Optimal Manufacturing Setup for the Production of Lipid Emulsions by High-Pressure Homogenization with Minimal Oxidation Products".

4.2 Methods

Production of the lipid emulsions

Lipid emulsions were produced by wetting 1.2% surfactant as indicated (shown in Tab. 4.1) in 20% of final volume purified water (NANOpure Diamond™ Barnstead, Thermo Scientific, Waltham MA, USA) and let to swell in a water bath at 45 °C for 2 hours. Surfactants in the concentration range indicated in Tab. 4.1 were either used alone or in combination to stabilize the oil-in-water emulsions. For the production of supply for *in vivo* studies in the final composition, certified endotoxin-free water was used (EMD Millipore, Billerica MA, USA or Cytiva HyPure™ Cell Culture Grade Water, HyClone™, Cytiva, HyClone Laboratories, Logan UT, USA). Use of commercial certified endotoxin-free water as starting material proved to be most effective to yield endotoxin-free emulsions. Technologies to remove endotoxins (GenScript ToxinEraser™ Endotoxin Removal Kit, Cat. No. L00338) based on filtration through a column with an active resin capturing endotoxins were inefficient in our pilot trials. Presence of endotoxins was thus best prevented by a "Quality by design" approach.

After the swelling, glycerol (99+%; Acros Organics, New Jersey, USA) was added at 2.2% final concentration as isotonicity agent. Chelator substances or buffer salts according to Tab. 4.1 were added to the aqueous phase pre-mix at this step. Chelator substances were included in the formulation to capture metal ions present in the formulation from contact with the machine. Metal ions could lower the activation energy required for the initiation step and thereby promote oxidative degradation of polyunsaturated fatty acids.[203,270,334]. Buffer components were included to stabilize the pH. Excipients were whenever possible chosen from the FDA inactive ingredients list to ensure regulatory compliance.

Tab. 4.1: Evaluated excipients

Type of excipient	Supplier	Purity/characteristics	Used concentration range
I. Surfactants			
a. Lecithins			
Egg phospholipids			
E 80	Lipoid GmbH, Ludwigshafen, Germany	80% egg phosphatidylcholine (PC)	0.6-2.5% (most typically 1.2%)
E 80 S	Lipoid	70% egg PC	1.2-2.5%
Lecithin from egg	Carl Roth GmbH, Karlsruhe, Germany	70% egg PC, for biochemistry	1.2%
Lecithin from egg	PanReac AppliChem, Darmstadt, Germany	60% egg PC	1.2%
Lecithin from eggs	Tokyo Chemical Industries, Tokyo, Japan	liquid	1.2%
Soybean phospholipids			
S 100-3	Lipoid	>94% soybean PC	1.2%
Soybean 90	PanReac	90% soybean PC	1.2%
Epikuron 200	Cargill, Minnetonka MN, USA	92% soybean PC	1.2%
Epikuron 145V	Cargill	PC-enriched fraction of soybean lecithin	1.2%
Other vegetable phospholipids			
H 100	Lipoid	>90% sunflower PC	19.6%
Canola Lecithin	IVOVITAL, Burgdorf, Germany	Rapeseed lecithin powder	5%
b. Phospholipids			
1,2-Distearoyl-sn-glycero-3-phospho-rac-glycerol, sodium salt (DSPG-Na)	Lipoid	100%, synthetic	0.66 mM
1,2-Dipalmitoyl-sn-glycero-3-phospho-rac-glycerol, sodium salt (DPPG-Na)	Lipoid	100%, synthetic	M
c. Sucrose Esters			
Tween 80	Sigma-Aldrich, Buchs, Switzerland		0.35%
Tween 80	Fisher Scientific, Waltham MA, USA		0.35%
Tween 20	Sigma-Aldrich		0.3%
Span 80	Sigma-Aldrich		0.35%
d. Free fatty acids			
Sodium Oleate B	Lipoid		0.03%

e. Other synthetic co-surfactants			
Kolliphor HS15	BASF, Ludwigshafen, Germany		5-25 mg/ml
f. Proteins			
Casein	Fluka, Buchs, Switzerland	from bovine milk	1.5%
Casein sodium salt	Sigma-Aldrich	From bovine milk	1.5%
II. Chelator substances			
Ethylenediaminetetraacetic acid (EDTA)	Carl Roth	disodium salt dihydrate, ≥99%	2.5-25 µM
Sodium citrate	Hänseler AG, Herisau, Switzerland	Ph. Eur.	5-50 µM
III. Buffer substances			
Tris-buffer	Sigma-Aldrich	≥99.9%	50 mM
Sodium hydrogen carbonate	Fluka	puriss. p.a.	0.83-3.3 mM
IV. Antioxidants a. Tocopherols			
α-tocopherol	Sigma-Aldrich	Type V	0.004-0.016% (v/v)
α-tocopherol	Tokyo Chemical Industries	>97.0%	0.016% (v/v)
γ-tocopherol	Sigma-Aldrich	≥96%	0.01% (v/v)
δ-tocopherol	Sigma-Aldrich	≥90%	0.0053-0.016% (v/v)
b. Other antioxidants			
Ascorbyl palmitate	Sigma-Aldrich	≥99%	1 mM
Dodecyl gallate	Tokyo Chemical Industries		

Next, 20% lipid phase ("Formula #3 oil mix") consisting of 50% Natures Crops Ahiflower oil (Natures Crops, Kensington PEI, Canada), 25% coconut oil (Bioriginal, Saskatoon SK, Canada) and 25% olive oil (LIPOID purified olive oil, Ph. Eur.; Lipoid AG, Steinhausen, Switzerland) was added. α-Tocopherol or other antioxidants were added to scavenge free radicals, thereby reducing lipid oxidation and also reducing harm to the body elicited from oxidative stress by oxidized lipids.[18,116,141,270] The evaluated antioxidants are shown in Table 1. They were added alone or in combination at a total final concentration of 0.016% (v/w). Purified water was added to reach the final volume (50 ml for pilot batches for excipient screening, 350 ml for *in vivo* studies). The coarse emulsion was processed by high-pressure homogenization on a ShearJet HL60 (Dyhydromatics, Maynard MA, USA) equipped with a 75.1T reaction chamber for 6 cycles at a set process pressure of 22 kpsi (1517 bar).

Cleaning of the HPH to prevent microbial contamination and lipid oxidation

Prior to processing the product, the HPH was washed with acetone, isopropanol and 0.5 M NaOH to mobilize and rinse out any microbial contamination. However, this cleaning protocol affected the

oxidative stability of lipids. We suspect a roughening of the stainless steel surface of the HPH through the strong organic solvents. As a consequence, divalent metal ions such as iron(II) get eluted from the surface into the product. In the emulsion, they can also act as radical initiators and further promote the oxidative degradation.[208,268,335] Thus, an additional cleaning step with a concentrated EDTA solution was introduced to ideally capture all mobilized metal ions into the EDTA solution. This again improved the situation. In preliminary experiments, a negative impact of residual organic solvent or base on the emulsion itself was ruled out. Simple pipetting together of either of them with a processed emulsion, without processing on the HPH, did not lead to increased oxidation. At excessive organic solvent levels though, the physical stability was impaired.

Sterilization of the emulsions and tests for microbial growth and endotoxins

The pH-value of the emulsion was adjusted to 8.5-9.5 with 1 M NaOH. Emulsions were filled in glass vials, the headspace was covered with inert gas (Argon 5.0, PanGas AG, Dagmersellen, Switzerland) and the vials were crimped. Emulsions were sterilized by autoclaving for 15 min at 121 °C at 2 bars (Systec DE-23, Systec GmbH, Linden, Germany). Absence of microbial growth (membrane-filtration method Ph Eur 2.6.1)[175] and endotoxins (< 0.1 IU/ml, Charles River, Dublin, Ireland, gel-clot method Ph Eur 2.6.14)[176] were confirmed at FDA-approved laboratory Bioexam AG, Lucerne, Switzerland. Because of the cost for this analysis and no suspected influence on other parameters (not affecting physical or chemical stability) relevant for the development of the formulation, this analysis was only performed on batches intended for *in vivo* experiments. For in-house determination of endotoxins, a commercial kit based on the gel-cloth method was utilized (GenScript ToxinSensor™ Single Test Kit, Cat. No. L00450).[336] Although the gel-clot assay is not the gold-standard for endotoxin-testing, use of the chromogenic assay was not possible due to the opacity of the emulsion.[177] This is a common issue in the quality control of lipid emulsions. Through the high lipid concentration (10-20%) and the droplet size > 100 nm, there is interference with the wavelength of natural sunlight, the light is diffracted at lipid droplets and the emulsion occurs white-opaque. This in turn renders all optical determination methods ineffective, as all light transmission is reduced, not just of a specific wavelength. Normally, in all injections, the absence of visible particles needs to be tested.[178] Due to the opacity, this cannot be tested here.

Haemolytic activity

Prior to *in vivo* experiments, the haemolytic potential of sterile and endotoxin-free batches of our emulsions intended for *in vivo* application was assessed by our project partners (group of Prof. Hersberger, University Children's Hospital, Zurich). Full human blood from donors was incubated with emulsions between 10 µM and 10 mM oil concentration for 24 and 96 hours and the absorbance was read at a wavelength of 544 nm. The reading was compared to 0.1% Triton as positive control. Occurrence of a turbid supernatant would be a positive signal, indicating that the emulsions lead to the rupture of red blood cells due to hyperosmolarity, toxicity of excipients or excessive degradation products from oxidation of unsaturated lipids. To further test for cytotoxicity, emulsions at oil concentrations between 0.1 mM and 5 mM were again incubated with $CD4^+$ T-cells isolated from peripheral blood mononuclear cells and after 18 and 48 hours incubation time, the cell viability was determined by flow cytometry. The incubation with live cells actively metabolizing the surrounding medium reflects the *in vivo* situation better and is thus more likely to show toxic effects.

Droplet size distribution

Droplet size was measured by dynamic light scattering (DLS, Malvern Zetasizer 3000 HS A, Malvern Instruments, Malvern, UK). DLS measurements are reliable for sizes up to 1000 nm.[169,187] To ensure compliance with the PFAT5 requirement set by the United States Pharmacopoeia, that the number of

droplets above 5 µm must not exceed 0.05%, scanning electron microscopy pictures and transmission electron micrographs were taken according to [192–194,337–340], showing the morphology of the emulsion with the final composition, intended for *in vivo* use.

Physical stability

To compare the stability of different formulations and get valuable information already upfront, emulsions were exposed to accelerated storage conditions. Emulsions were exposed to increased acceleration forces in a centrifuge-like setup. In a LUMiFuge (LUM GmbH, Berlin, Germany), a fusion of a centrifuge and a spectrometer, the distance-resolved transmission of a sample can be measured after every rotation.[193,194] An undiluted lipid emulsion sample with high lipid content is usually opaque (transmission near 0), but upon phase separation, the transmission of the aqueous phase increases. A measured increase in transmission thus indicates phase separation and by exposing different formulations to moderate stress conditions, the physical stability can be compared by observing phase separations that would not occur before 3-6 months under non-stressed conditions. Selected batches in the early phases of the development were exposed to accelerated conditions to observe influences of added excipients on the physical stability.

By increasing the temperature, degradation processes can be accelerated. According to Arrhenius law, the temperature determines the reaction rate.[295,341,342] Emulsions instead of being stored at 4 °C (prior to autoclaving, in glass without protecting gas atmosphere or plastic containers potentially permeable for atmospheric oxygen) or room temperature in the dark (after autoclaving, in sealed glass vials under argon protection atmosphere) were kept at 40 °C in a thermal cabinet to accelerate physical and oxidative degradation. Droplet size and degradation products from oxidative processes were monitored at several time points.

Quantification of primary and secondary oxidation products and free fatty acids

The primary oxidation products were quantified according to the mFOX assay, described in Chapter 2, “Quantification of Lipid Oxidation Products in Lipid Emulsions Requiring Minimal Sample Volume”.

Secondary oxidation products were quantified according to the TBARS assay, described in Chapter 2, “Quantification of Lipid Oxidation Products in Lipid Emulsions Requiring Minimal Sample Volume”.

Where no appropriate limits were available from pharmacopoeial standards, comparison and benchmarking to currently marketed formulations were performed. Intralipid is the most widely used intravenous lipid emulsion, consisting of 20% soybean oil. Omegaven is a 10% fish-oil based lipid emulsion, rich in $n-3$ PUFAs. Both formulations are marketed by Fresenius Kabi, Bad Homburg, Germany.

Total free fatty acids were quantified by fluorescence detection after labelling with a fluorophore and separation by high-pressure liquid chromatography, presented in Chapter 3, “Determination of Free Fatty Acids in Lipid Emulsions by Fluorescence-Detection Based High Performance Liquid Chromatography”.

Emulsion labelling with tritiated lipids

A Formula #3 oil-based emulsion and Intralipid as a commercial emulsion were spiked with tritiated lipids to follow their distribution *in vivo*. We first evaluated a simple spiking protocol with minimal instrument contamination. As simplest incorporation method, vortex mixing (30 sec) was evaluated. We assumed that the tritiated triglyceride, fatty acid or phospholipid molecule distribute spontaneously into the lipid phase of the emulsion to minimize energetic interactions.

Tracer incorporation was evaluated by size exclusion chromatography and equilibration shaking. For size exclusion chromatography, unlabeled emulsion, tritiated lipid in an ethanol-toluene mixture (1:1, for ^{3}H-triolein and ^{3}H-phosphatidylcholine) or pure ethanol (for ^{3}H-palmitic acid), or the tritiated lipid incorporated into the emulsion by vortex mixing for 30 seconds, was loaded onto a PD-10 (GE Healthcare, Chicago IL, USA) column and eluted with distilled water. Fractions were collected and mixed with scintillation liquid (Ultima Gold, Perkin Elmer, Waltham MA, USA) for radioactivity measurement in a Packard Tri-Carb 2250 CA liquid scintillation counter (Packard BioScience, Meriden CT, USA).

For *in vitro* distribution studies, trace amounts of tritiated lipids (^{3}H-triolein, ^{3}H-TO, 37 MBq/ml; ^{3}H-palmitic acid, ^{3}H-PA, 370 MBq/ml; ^{3}H-phosphatidylcholine, ^{3}H-PC, 37 MBq/ml; all from American Radiolabeled Chemicals, Saint Louis MO, USA) at a final concentration of 37 kBq (in 1 µl ethanol:toluene 1:1 for ^{3}H-TO and ^{3}H-PC or 0.1 µl ethanol for ^{3}H-PA) were added to 200 µl aliquots of lipid emulsions and vortex-mixed for 30 sec in glass vials. Labelled lipid emulsions were mixed in a 1:5 ratio with either phosphate buffered saline pH 7.4 (PBS, prepared from 10 mM sodium hydrogenphosphate [heptahydrate, p.a., ACS, 98-102%, Merck, Darmstadt, Germany], 1.8 mM potassium dihydrogenphosphate [purum p.a., ≥99.0%; Sigma-Aldrich], 0.137 M sodium chloride [puriss. p. a., ≥99.5%; Sigma-Aldrich] and 2.7 mM potassium chloride [puriss. p. a., ≥99.5%, Sigma-Aldrich,]) or PBS + 4% bovine serum albumin (cold ethanol fraction, ≥96%; Sigma-Aldrich). Mixtures were then constantly shaken at room temperature for 0, 10 or 60 minutes and phases were separated by centrifuging at 15'000 g for 15 min (Beckman GS-15R, Beckman Coulter). Separated phases were mixed with scintillation liquid (Ultima Gold, Perkin Elmer) in a 1:4 ratio and radioactivity was measured on a Packard Tri-Carb 2250 CA liquid scintillation counter (Packard BioScience, Meriden CT, USA).

In vivo distribution of the emulsions

The tissue distribution was studied for the lead Formula #3 lipid emulsion in comparison to commercial Intralipid (Lot 16NE4266, Fresenius Kabi). *In vivo* studies were performed in 10-12 weeks old male C57BL/6NCrl mice (Charles River, Sulzfeld, Germany) with a body weight between 22.0 and 27.9 g. The lead formulation with 0.016% α-tocopherol and 2.5 µM EDTA was vortex-mixed for 30 seconds with 37 kBq (in 1 µl ethanol:toluene 1:1 for ^{3}H-TO or 0.1 µl ethanol for ^{3}H-PA) of a tritiated lipid (^{3}H-TO, 37 MBq/ml or ^{3}H-PA, 370 MBq/ml; both from American Radiolabeled Chemicals) and either 50 or 100 µl (10 or 20 mg triglycerides) were administered intravenously by bolus injection to the tail vein. After 10 min and 60 min, respectively, animals were anesthetized with isoflurane and euthanized by decapitation under deep anesthesia. Organs were dissected and digested with SOLVABLE (Perkin Elmer) and decolorized according to the manufacturer's instructions. After complete tissue lysis and decoloration, scintillation liquid (Hionic-Fluor, Perkin Elmer) was added and radioactivity was measured on a Packard Tri-Carb 2250 CA liquid scintillation counter. Standardized uptake values (SUV) were calculated as the ratio between the injected activity per body weight (Bq/g) and the detected activity per tissue weight (Bq/g). All animal studies were approved by the cantonal authorities and carried out in accordance to national legislation (license ZH203/2019).

4.3 Results

Choice of surfactants and oil-to-surfactant ratio

In preliminary experiments, emulsions produced from soybean lecithin (characterized by >90% phosphatidylcholine, PC) yielded droplet sizes above 400 nm while egg-lecithin (60-80% PC) based emulsions lead to droplet sizes between 270 and 320 nm. Also other plant-derived lecithin sources

(sunflower, rapeseed) did not produce the desired droplet size of 250-300 nm. The total surfactant concentration and its ratio to the oil concentration had an effect on the droplet size. Droplet size increased with increasing oil-to-surfactant ratios. Use of co-surfactants (Tween, Span, Kolliphor) reduced the droplet sizes at constant homogenization energy (process pressure and cycle count). The oil type (or the combination with lecithin from a different source) influenced the droplet size as well, soybean oil-based emulsions led to droplet sizes > 350 nm, regardless if soybean or egg lecithin was used as surfactants. Ahiflower oil included in the Formula #3 oil mixture in combination with egg phospholipids with < 80% PC did not increase the droplet size beyond the desired range and it was possible to manufacture 20% lipid emulsions mimicking the 270-300 nm size range set by commercially available reference emulsions Intralipid and Omegaven. The fatty acid sodium oleate did not stabilize lipid droplets nor lead to reduced droplet size despite evidence from literature.[22,343] Kolliphor HS15 is a pegylated stearate, exploiting the effect of steric repulsion to stabilize emulsions apart from the fatty acid as emulsifier.[37,344–347] Use of Kolliphor HS15 stabilized the emulsion (longer induction time until the occurrence of phase separation), but its effect could be traced back to the increased total surfactant concentration and did not justify inclusion in the formulation at the cost of increased complexity. To avoid issues arising from toxicity induced by continuously infused high surfactant concentrations, it was decided to refrain from synthetic co-surfactant (Tween, Span) and limit the total surfactant concentration at 1.2% of the final volume. The egg phospholipids Lipoid E 80, E 80 S and products from other suppliers (Roth, PanReac) revealed stable emulsions of similar characteristics. The animal protein surfactant casein was not further evaluated due to the potential of eliciting allergic reactions when used in parenteral emulsions.

Emulsions stabilized with 1.2% egg phospholipids were physically stable at room temperature (after autoclaving, stored under protecting gas atmosphere in glass vials) for around 6 months, when first signs to creaming started to appear.

Excess infusion rates can promote the development of inflammatory adverse effects (see General Introduction). To meet the nutritional requirements and minimize infusion rate to also prevent harmful effects from fluid overload[124] (chronically increased blood pressure), higher lipid concentrations are preferred. We, therefore, fixed the oil concentration at 20% for future experiments.

Stabilization of the emulsions for autoclaving

Initial emulsions showed a declining pH-value over time, typically from around 5 (non-adjusted) to 3.5 within 30 days or 7.5-8 (adjusted) to 4 within 90 days. Addition of buffering substances (Tris-buffer, sodium hydrogen carbonate) increased droplet size and promoted physical instability (visual assessment as well as measurement by LUMiFuge). Autoclaving of the initial formulations resulted in phase separation. Addition of 0.66 mM phosphoglycerols DSPG and DPPG as net negatively charged phospholipids to the lecithin to modified the ζ-potential and thereby stabilize the emulsion did not prevent phase separation. Adjusting the pH-value with 1 M sodium hydroxide to 8.5-9.5 before autoclaving, a method frequently used to stabilize emulsions,[136,170] resulted in a decrease of the ζ-potential from between -10 and -20 mV to below -30 mV, ultimately leading to physically stable emulsions upon autoclaving. To alleviate negative effects from the thermal stress on the oxidations of polyunsaturated fatty acids, the head space was flushed with inert gas atmosphere prior to autoclaving. All autoclaved emulsions were sterile and if endotoxin-free water was used as starting material also tested negative (< 0.1 EU/ml) for endotoxins.

Protection against lipid oxidation

The Formula #3 was highly susceptible towards oxidative degradation, leading to increased oxidation values prior to the addition of excipients compared to commercial references. The chelators EDTA and sodium citrate were evaluated for their ability to reduce oxidation. Sodium citrate disturbed the pH-value of the formulation and impaired droplet size and physical stability. EDTA on the other hand effectively lowered the primary (assessed by mFOX-assay) and for higher concentrations also drastically the secondary (measured by TBARS-assay) oxidation products, as detailed in Fig. 4.1. To avoid interference with trace element homeostasis under daily parenteral nutrition therapy, the dose of EDTA was limited at 2.5 µM final concentration. Tocopherols (α-, γ- and δ-isoforms of vitamin E) were evaluated as possible lipid-soluble antioxidants. Although in literature different antioxidant potencies are reported[264,348,349], in preliminary studies we found similar efficiencies (also among manufacturers) and decided for cost reasons to work with α-tocopherol. In commercial formulations, α-tocopherol originates from the oil , is directly added or results from both.[62,350] We chose a similar approach and added α-tocopherol at similar amounts when standardized to the degree of unsaturated fatty acids present in our emulsions. As depicted in Fig. 4.1, the intermediary level proved to be the most beneficial to lower the degree of oxidation. The lipid soluble form of vitamin C, ascorbyl palmitate, however, interfered with the pH and emulsion stability; the plant-derived antioxidant dodecyl gallate besides only limited effect on lowering the oxidation products led to a dose-dependent increased in droplet size and thus was also not suitable for our purposes.

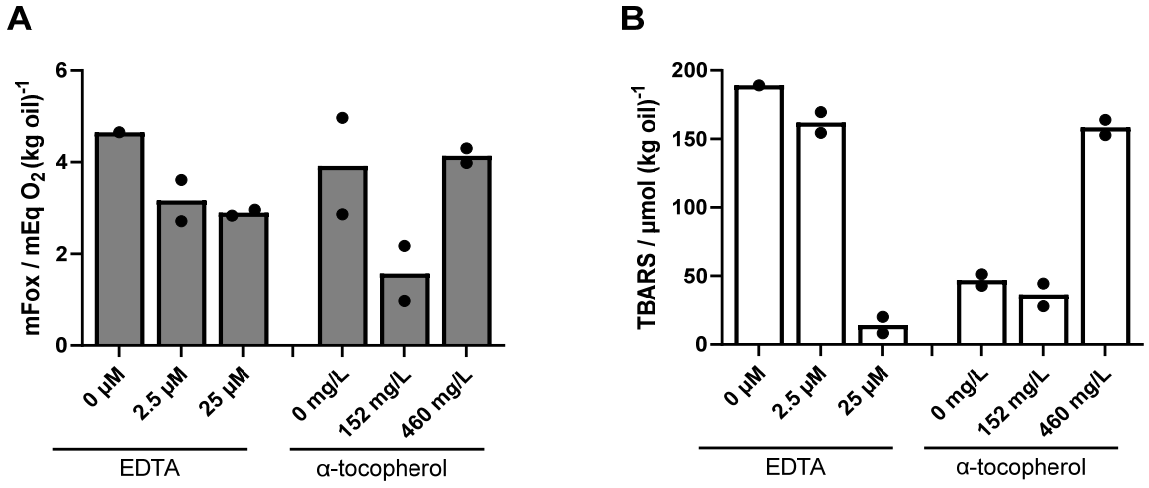

Fig. 4.1: Effect of chelating agent EDTA and antioxidant α-tocopherol at different dose levels on primary (A) and secondary (B) oxidation products. Bars, average of two emulsions (symbols: individual values).

Characteristics of the final emulsion

The characteristics of the lead formulation with 1.2% Lipoid E80, 2.5 µM EDTA, 0.016% (v/v; 152 mg/L) α-tocopherol and 20% Formula #3 oil mixture are summarized in Tab. 4.2 in comparison to marketed formulations Intralipid and Omegaven. In-house manufactured emulsions were characterized within 5 days after manufacturing, while the commercial formulations were characterized after obtaining them with unknown duration since the production, but all within the proposed shelf life. The droplet size could well be mimicked, the size distribution as measured by the polydispersity index (PDI) was below 0.1, indicating a narrow distribution. The pH-value complied with the requirements for intravenous infusion. Primary oxidation products as assessed by the mFOX-assay were above the level of Intralipid, but below the values of Omegaven, which in terms of degree of unsaturation represents our

Formula #3 emulsion better. The secondary oxidation products were higher than in Intralipid but in the range of Omegaven, while the free fatty acids (FFA) were substantially lower than in the reference emulsions. No haemolysis or reduced cell viability were observed *in vitro*.

Tab. 4.2: Physical and chemical characteristics of lead Formula #3 oil emulsion (n=9, ± standard deviation, SD) in comparison to commercially available references Intralipid and Omegaven (data from n=1 batch).

	Intralipid	Omegaven	Formula #3 (n=9, mean ± SD)
droplet size / nm	285.6	247.8	286 ± 2
PDI	0.018	0.0672	0.04 ± 0.02
pH	5.31	6.29	7.43 ± 0.14
mFOX (1° oxidation products) / mEq O_2 (kg oil)$^{-1}$	0.67	5.13	1.30 ± 0.24
TBARS (2° oxidation products) / µmol (kg oil)$^{-1}$	0.99	35.51	43.2 ± 8.0
total FFA / mmol (kg oil)$^{-1}$	15.6	70.4	4.16 ± 0.57

Droplet-size distribution

The average droplet size was below 500 nm and complied with the requirements set by the USP.[169] In the representative scanning electron micrographs in Fig. 4.2 and Fig. 4.3, the dynamic light scattering measurements was confirmed and the absence of particles > 5 µm was demonstrated. Some artifacts from the freeze-fracture sample preparation process were visible, indicated with yellow arrows, and some smaller than the average droplets (possibly phospholipid-only liposomes, red arrows) while only one droplet > 800 nm was found in 30 pictures (highlighted with a blue arrow in Fig. 4.3). A transmission electron micrograph showing a single multilamellar vesicle is shown in the Appendix (Fig. A2). Representative micrographs of Intralipid and Omegaven are given as references in Fig. A3-Fig. A6 in the Appendix. Also there, a similar distribution was found and DLS measurements could be verified.

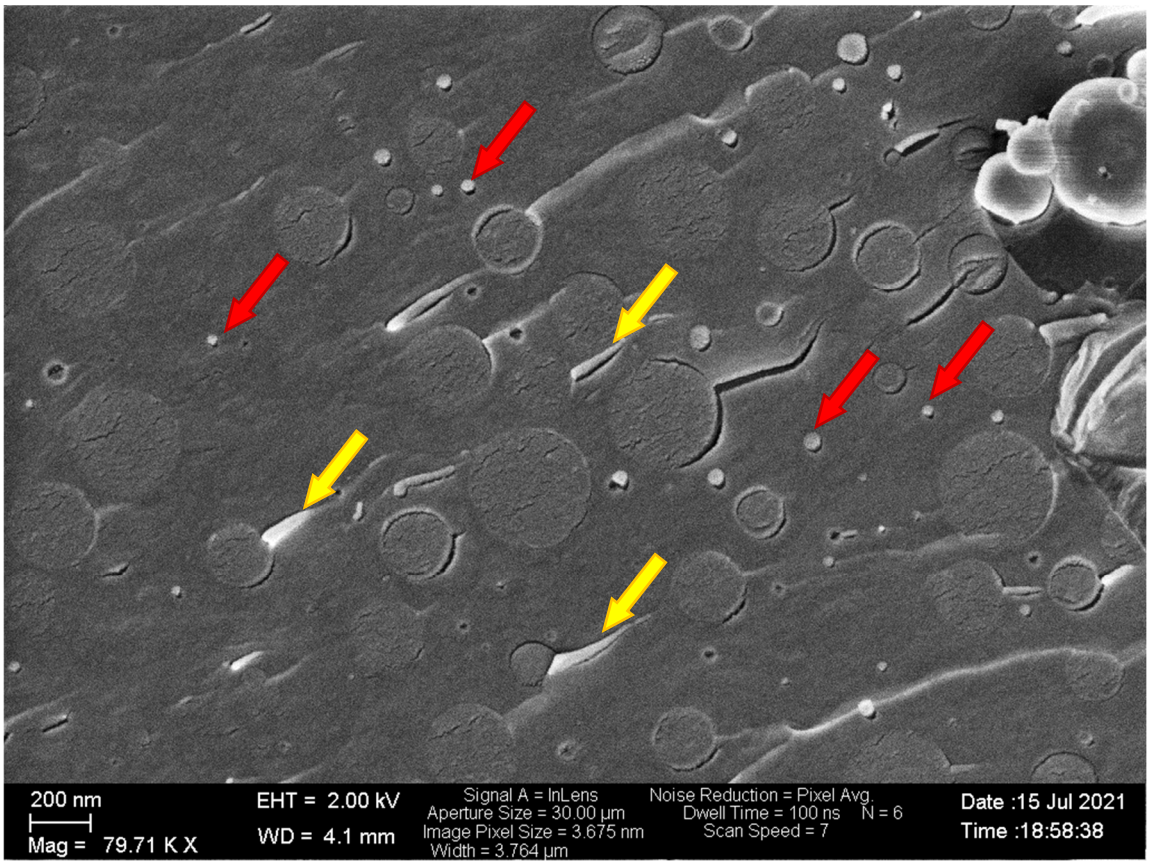

Fig. 4.2: High-magnification scanning electron microscopy picture of standard-sized Formula #3 emulsion with marked very small droplets (red arrows) and artifacts from the sample preparation (yellow arrows).

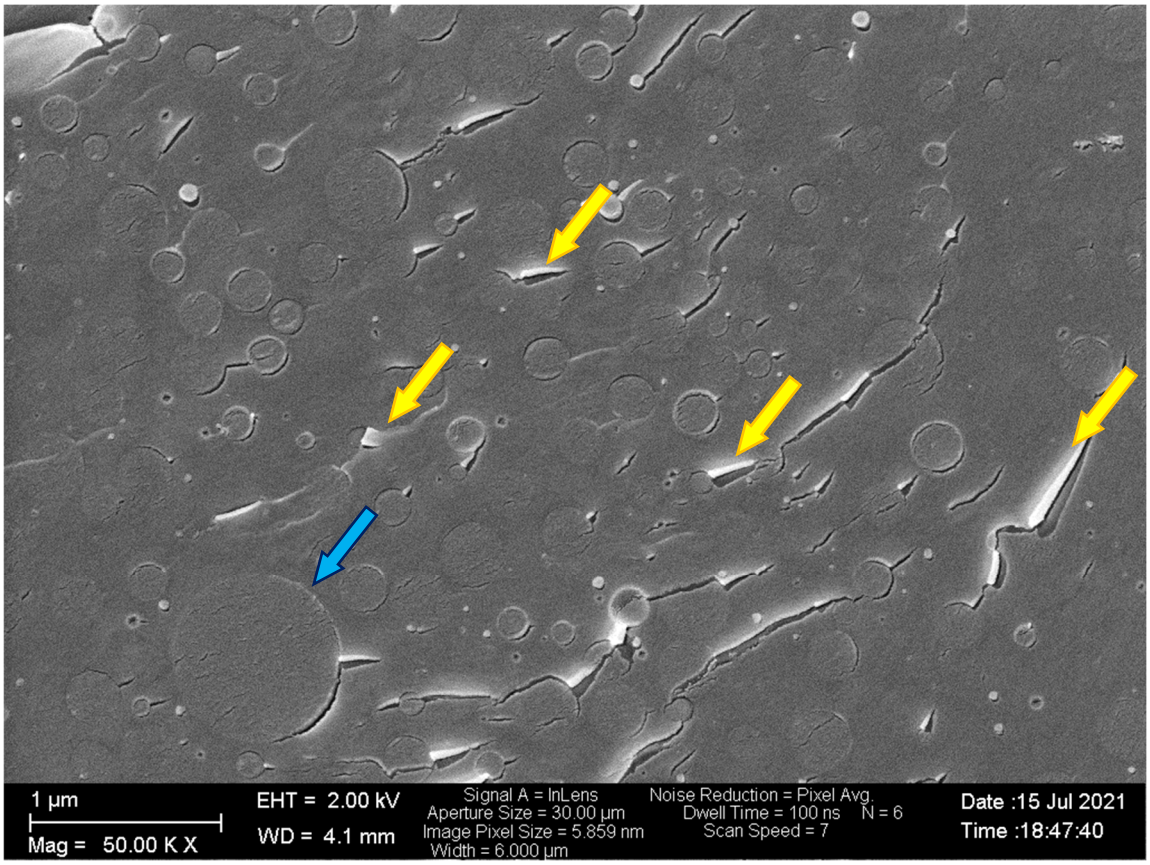

Fig. 4.3 Low-magnification scanning electron microscopy picture to show regulatory compliance with PFAT5 requirement: Only a single lipid droplet in the range of 800 nm (blue arrow) is visible.

No differences in the subjective, qualitative observation of the viscosity of the manufactured lipid emulsions with the one of the commercial references have been found as long as the lipid part was not increased above 30% or the phospholipid content above 10%.

Incorporation of tritiated lipids into the emulsions

Vortex-mixing of the final emulsions with the triglyceride tracer (^{3}H-TO) efficiently incorporated the tracer into the lipid phase as evaluated by the equilibrium shaking method and shown in Fig. 4.4. The fatty acid tracer ^{3}H-PA distributed to ~ 60% to the lipid phase when tested against PBS. In the presence of BSA, the fraction found in the lipid phase was reduced to 20%, in agreement with the binding of FFAs to albumin. Because of the presence of albumin in plasma, this tracer is not a valid molecule to reliably follow the distribution of the lipid phase upon *in vivo* administration of the emulsions. The phospholipid tracer ^{3}H-PC did not show binding to albumin and on average 50% of the activity was found in the lipid phase when tested against PBS or BSA/PBS. This was not considered sufficient for following the emulsion droplets *in vivo*. Size-exclusion chromatography comparing the elution times of the tracers with or without incorporation into the emulsions, depicted in Fig. A7 in the Appendix, confirmed these findings.

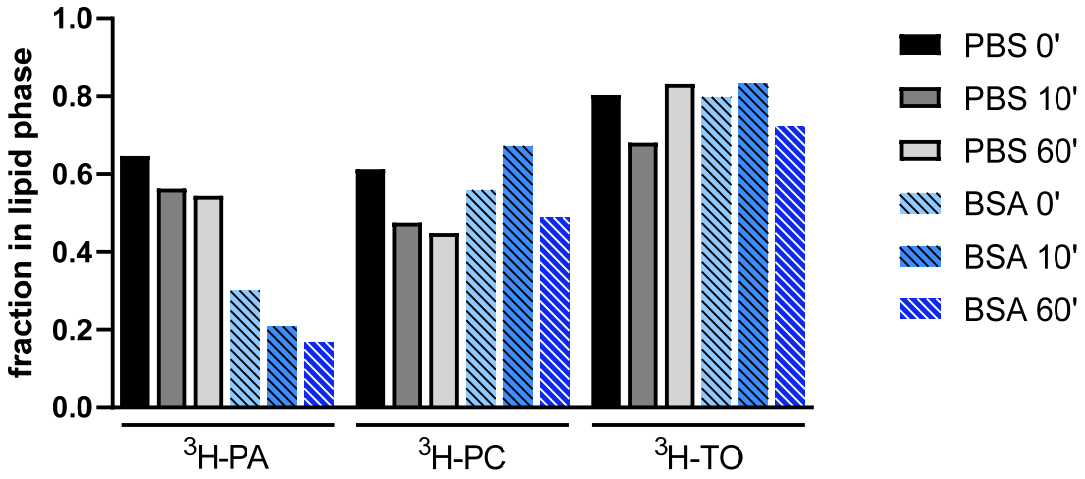

Fig. 4.4: Distribution of tritiated lipids between the lipid phase of Formula #3 lipid emulsions and an aqueous phase. Fraction of recovered activity in the lipid phase at different time points (0', 10' or 60', as indicated) after shaking the lipid phase containing the tracer with PBS (PBS) or PBS containing 4% BSA (BSA). ^{3}H-PA, ^{3}H-palmitic acid; ^{3}H-PC, ^{3}H-phosphatidylcholine; ^{3}H-TO, ^{3}H-triolein.

In vivo distribution of the emulsions in mice

Formula #3 lipid emulsion and Intralipid were spiked with ^{3}H-TO and injected intravenously in mice. Doses were 50 and 100 µl each of non-diluted emulsion. Mice were euthanized under anesthesia at 10 or 60 min after injection and dissected. These were pilot experiments; each condition was only studied in one mouse each. The results are shown in Fig. 4.5 and Fig. 4.6. The following trends were observed: Formula #3 lipid emulsion cleared faster from blood/plasma than Intralipid. This was also seen from the milky appearance of plasma at 10 min after injection of 100 µl Intralipid but not of Formula #3. The SUV was highest in lung for both emulsions with higher lung uptake for Formula #3 than Intralipid. Lung uptake was higher at the lower dose for both emulsions, pointing to a potentially saturable uptake mechanism in lung. Pre-administration of 50 µl unlabeled emulsion prior to administration of equal volume of labelled emulsion (Fig. A8) reduced the accumulation of Formula #3 in lung as compared to

the 50 µl dose without pre-administration (Fig. 4.6). The distribution of the two emulsions was similar for the remaining tissues (i.e., no striking trend was seen with these pilot experiments). A homogeneous distribution in the body would result in SUV = 1. Spleen, liver, kidney, heart and brown adipose tissue had SUVs > 1 while white adipose tissue and muscle showed the lowest uptake besides brain. A small fraction of ^{3}H was accumulated in bile.

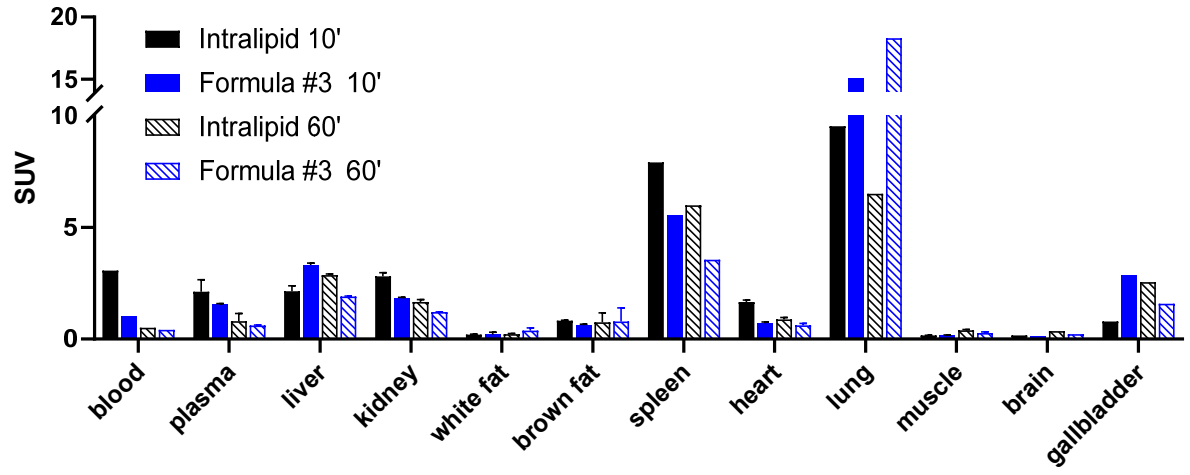

Fig. 4.5: Standardized uptake values (SUV) of selected tissues after administration of 37 kBq ^{3}H-triolein in 100 µl either Formula #3 (blue bars) or commercial Intralipid (black bars) lipid emulsion. Results are 10 min post-injection (p.i.) for filled bars and 60 min p.i. for diagonal down striped bars. Bars, means or individual values; error bars, standard deviations if more than one tissue sample of the same mouse was analyzed (n=1 animal per timepoint).

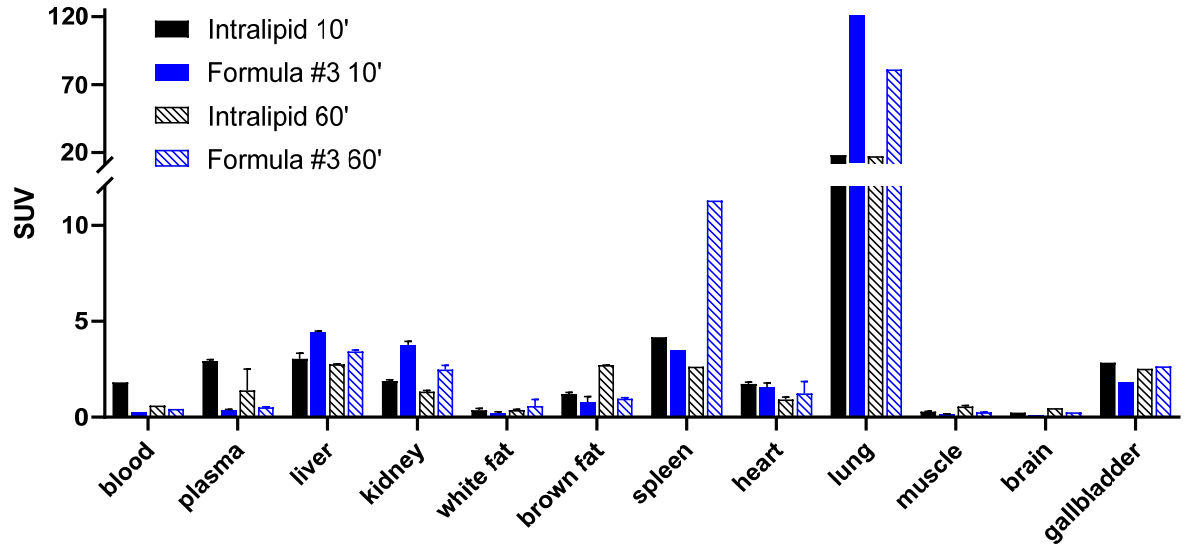

Fig. 4.6: Standardized uptake values (SUV) of different tissues after 10 minutes (filled bars) or 60 minutes (diagonal down striped bars) after administration of 37 kBq ^{3}H-triolein in 50 µl Intralipid (black bars) or Formula #3 (blue bars) lipid emulsion. Bars, means or individual values; error bars, standard deviations if more than one tissue sample of the same mouse was analyzed (n=1 animal per timepoint).

Fig. 4.7 shows the distribution of ^{3}H-PA after its incorporation into the emulsions. The distribution pattern is completely different from those described in Fig. 4.5 and Fig. 4.6 with ^{3}H-TO. This is in agreement with the competition between lipid phase distribution and binding to BSA *in vitro*. With the label ^{3}H-PA, the radioactivity distribution most probably does not reflect the distribution of the oil droplets but rather the distribution of ^{3}H-PA itself.

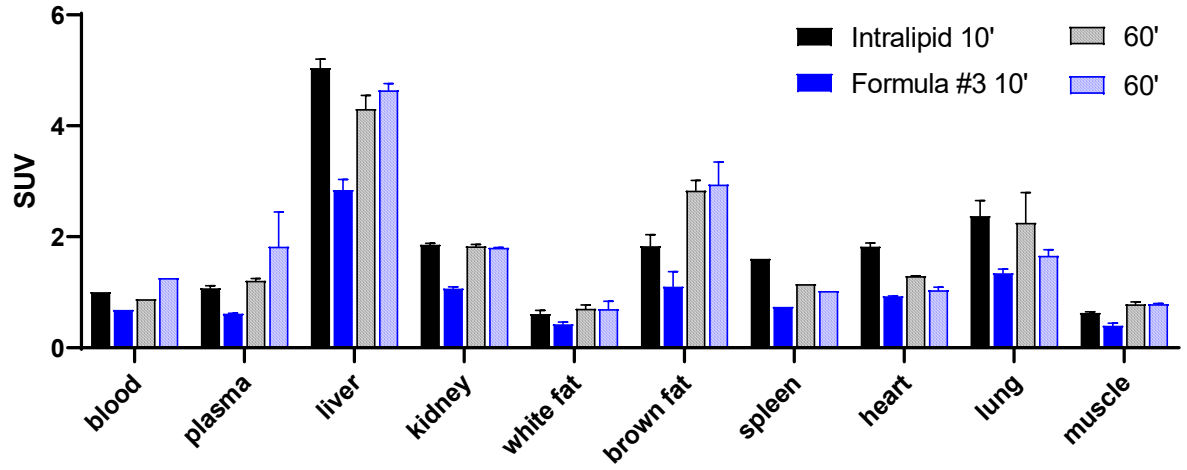

Fig. 4.7: Standardized uptake values (SUV) for different tissues after administration of 37 kBq ^{3}H-palmitic acid in 50 µl Intralipid (black bars) or Formula #3 emulsion (blue bars) after pre-injection of 50 µl unlabeled emulsion. Filled bars: 10 minutes incubation time, diagonal down filled bars: 60 minutes after injection. Bars, means or individual values; error bars, standard deviations if more than one tissue sample of the same mouse was analyzed (n=1 animal per timepoint).

4.4 Discussion

Identification of suitable excipients proved to be cumbersome. Initial formulations mimicking the composition of commercially available reference emulsions failed to yield the same low oxidation levels and thus excipients were needed to limit the degree of lipid oxidation. From a regulatory perspective the formulation is preferred as simple as possible to avoid adverse effects induced by substances where little experience exists.[136,219] To avoid toxicity from daily administered excipients, doses should be chosen as low as possible. But still, the desired stabilizing effect needs to be elicited. Many of the tested excipients counteracted their positive effect of reducing oxidation by increasing the droplet size and impairing the physical stability of the emulsion. This is thought to be mainly mediated by disturbing the pH or ζ-potential of the emulsion, thus interfering with the stabilizing repulsive forces.[188] α-Tocopherol is already endogenously contained in many oils, especially in fish oil, and thus also in Omegaven as marketed formulation, and to a lesser extent also in Intralipid (there, γ-tocopherol prevails).[22,62,350,351] As a vitamin with known tolerated daily doses, it is an ideal excipient for parenteral emulsions. Apart from the intended antioxidative effect for the protection of the PUFAs, there is evidence that it helps to prevent IFALD from occurring by scavenging radicals that would harm the liver[9,116,352], although also contradicting reports exist.[353] At elevated concentrations, α-tocopherol is known to exert pro-oxidant effects.[354–357] EDTA as chelating agent has been described before to reduce lipid oxidation, primarily in food emulsions[126,239,294], but was also found to be safe in repeated intravenous infusion.[358]

Currently observed inflammatory adverse effects seen with the use of marketed lipid emulsions for parenteral nutrition are closely related to the liver. The high uptake into the liver reported in literature

(> 40% injected activity)[333,359–361] is thought to be responsible for eliciting these inflammatory adverse effect. In our *in vivo* distribution experiments, both Formula #3 and Intralipid reached SUV between 1.8 and 5 in liver. This corresponds to 9 to 25% injected activity in liver, assuming a relative liver weight of 5%[362] of body weight. Further experiments are planned to compare the kinetics of liver uptake in more detail.

The uptake in the lungs was noticeably high. The corresponding % injected activity in lung would correspond to ~0.75-fold the SUV (assuming a relative lung weight of 0.75%[363]). After tail-vein injection, the lung is the first organ encountered where the vasculature diameter is getting narrower again.[364,365] After tail vein injection the emulsion droplets firstly travel to the heart and from there to the lungs and the first capillary system. The concentration in blood is still high as the droplets did not distribute yet in the complete vascular system. The lung is thus exposed to much higher lipid concentrations during this first passage than any other tissue. This may explain the high uptake in comparison to other tissues. There seems to also be a contributing factor from the oil type. This has also been found before where *n*−3 PUFA rich lipid emulsions showed higher lung uptake.[332,366] Our data indicate that the mechanism of lung uptake is saturable. The infusion rate during parenteral nutrition could, therefore, have an influence on the relative uptake in lung. The rationale for the choice of the reduced administration volume of 50 µl was based on the administered dose in the continuous setting over 7 days by our project partners, where 250-330 µl of fully compounded parenteral nutrition mixture are infused per hour, corresponding to 30-40 µl of lipid.

The tissues where accumulation was highest in our experiments – liver, spleen, lungs – all belong to the reticulo-endothelial system with high presence of macrophages.[367,368] Increased uptake there has already been observed from early on after the introduction of lipid emulsions to the clinics[73] and confirmed later.[124,369] Still, the time frame remains questionable, despite some reports 60 minutes incubation time might be challenging for uptake in macrophages.[370] Pronounced trapping has been seen for formulations exceeding the PFAT5 requirement due to physical instability and lipid aggregation[130,163] while in our studies the compliance has been demonstrated by scanning electron microscopy.

In other studies, the distribution was affected by heparin pre-administration[333,360] and fasting of the animals[332], parameters that have not been addressed yet in our studies. By fasting, it is assumed that the uptake in heart and skeletal muscle tissue could be promoted. In the current setting, animals had access to chow before and after the injection of the emulsion, from where the energy expenditure can be covered as well. Interestingly, they are on the other hand not directly deposited as fat storages in adipose tissue. This could be enhanced by pre-administration of heparin, inducing lipoprotein lipase to promote lipid digestion.[371] Heparin is used in long-term infusion of lipid emulsions to prevent clogging of the infusion line through coagulation of the blood. Also prolonging the incubation period could shift the picture and could allow to follow metabolism. The ^{3}H-TO tracer is radioactively labelled on the esterified fatty acids. Hydrolysis to free the fatty acids would still allow to follow the molecule, but then not as valid proxy for the distribution of triglycerides anymore. A clearly distinct distribution profile is visible compared between the injection of a triglyceride tracer and direct injection of a free fatty acid tracer, indicating that the ^{3}H-TO was not completely hydrolyzed during the 60 min distribution period. But this limitation that is globally valid: The stability of the tracer was verified *in vitro* and it was ensured that it would remain to a good portion in the lipid phase. However, activity measurements by scintillation just yield the distribution of the label, and not necessarily the intact labelled molecule. The label can get lost through metabolism *in vivo*, a process difficult to mimic *in vitro* through a multitude of different cleaving enzymes and thus not practically controllable.

Despite standardizing to the amount of activity injected, the organ weight and also the weight of the individual animal and calculating results as SUV, not always the same relative amount of activity was recovered. This gives a hint that there are tissues where activity was trapped that were not evaluated. In a search for such potential sinks the excreting organs were mainly of interest. No considerable amount of activity was found in the kidney or urine, exhaling of ^{3}H is in contrast to radioactive carbon molecules ($[^{11}C]CO_2$ or $[^{14}C]CO_2$) not possible, and also in the stomach or intestines no increased activity was found. Also gallbladder and brain showed only marginal uptake. Bone does not seem reasonable because of the short incubation time; maximal 60 min post injection would not allow for considerable uptake in the bones. Also activity receding at the site of injection due to the stickiness is a known issue. However, analysis of the tail showed no increased activity.

All animal experiments are only single experiments with one animal each per timepoint and thus merely act as hypothesis generating findings. After promising findings in pilot experiments, confirmatory studies with higher statistical power can be performed. As time points of interest 10 minutes and 60 minutes were chosen to study the rapid distribution immediately after administration, but also the equilibrium conditions later on. Longer durations of 2-6 hours might also be of interest.

4.5 Conclusion

A novel parenteral lipid emulsion formulation has been engineered based on a composite oil mixture with oils rich in $n-3$ PUFAs complying with all pharmacopoeial requirements. The novel oil mixture was highly susceptible to oxidative degradation and thus EDTA as metal chelator and α-tocopherol antioxidant were included at minimal concentrations to meet the benchmark thresholds in terms of lipid oxidation set by commercial reference products. Distinct tissue distributions were found for commercial Intralipid and novel Formula #3 lipid emulsion based on the type of oil used and the emulsion dose. The uptake was highest in lung tissue. Distribution studies need to be repeated with higher sample number for statistically sound conclusions, but trends were identified. A manuscript showing the beneficial effect of Formula #3 lipid emulsion when continuously infused for 7 days on immune markers in mice is in preparation, in collaboration with our project partners.

4.6 Acknowledgment

The authors thank Stephan Handschin of ScopeM (ETH Zurich) for acquiring the cryoSEM and TEM pictures. Claudia Keller (Center for Radiopharmaceutical Sciences, ETH Zurich) is acknowledged for help with the injections during animal experimentation. Nazek Noureddine, Paulina Wawrzyniak and Claudio Gemperle (University Children's Hospital, Zurich) are thanked for conducting the haemolysis and cell viability experiments. Eliana Lucchinetti conceptualized the novel Formula #3 oil mixture. Lipoid E 80 S, H 100, DSPG, DPPG, Sodium Oleate B and Purified Soybean Oil 700 (Ph Eur, USP) were all kindly provided by Lipoid GmbH, Ludwigshafen, Germany.

5 Engineering of Lipid Nanoemulsions at Low Surfactant Concentrations Stabilized by High Contents of Glucose

Gregory Holtzhauer and Stefanie D. Krämer

Biopharmacy / Center for Radiopharmaceutical Sciences, Institute of Pharmaceutical Sciences, ETH Zurich

Scientific contributions:

Gregory Holtzhauer conceptualized, executed and analysed all experiments, and wrote the chapter. Stefanie D. Krämer performed the mixed effects modelling and supervised the work.

5.1 Introduction

Mixtures of oils in water are as such immiscible.[127] With the help of amphiphilic surfactant molecules lowering the surface tension, it is possible to formulate lipid droplets as emulsions in a continuous aqueous phase.[129] When administered parenterally as lipid and calorie source in parenteral nutrition or as carrier vehicle in drug therapy, the size of the emulsion droplets affects their behaviour in the body and their effects at the cellular and molecular level. Lipid droplets of excess size can elicit harmful adverse effects such as lipid embolism and are thus limited by the pharmacopoeia.[70] The number of particles above 5 µm in a lipid injectable is limited to 0.05% and the average droplet size needs to be below 500 nm.[169]

Currently available lipid emulsions have an average droplet diameter of 250-300 nm.[187,372] Prolonged use of parenteral lipid emulsions can lead to inflammatory adverse effects.[96,97,100] Some of these adverse effects of current therapies are thought to be linked to the droplet size. The adverse effects originate from the liver where a high uptake of the administered lipids is seen.[332,360,366,373] Apart from fine-tuning the $n-6$ to $n-3$ PUFA profile[18,45,49] as discussed in Chapter 4, "Excipient Screening for the Development of Lipid Emulsions based on Vegetable Oils Rich in $n-3$ Polyunsaturated Fatty Acids", and surface modifications (PEGylation)[374], the uptake in the liver can also be influenced by the choice of the lipid droplet size.[124,375–377] Rensen and colleagues were able to reduce the hepatic uptake 2.7-fold by decreasing the lipid droplet size from 150 nm to 50 nm.[36] Seki *et al.* confirmed this trend and lowered the liver uptake 18-fold by creating lipid emulsions with droplet sizes of 25-50 nm compared to former 200-300 nm sized emulsions.[369]

For terminology, we will further refer to the standard 20% lipid emulsions including the commercially available Intralipid and Omegaven at droplet sizes of 250-300 nm as conventional lipid emulsions. Emulsions with droplet sizes below 200 nm (radius < 100 nm) in contrast will be referred to as lipid nanoemulsions. Regarding the terminology, there is conflicting convention in literature where some authors refer to nanoemulsions as having droplet sizes 200-1000 nm and < 100 nm as microemulsions instead.[129,162,190] In contrast to conventional lipid emulsions, nanoemulsions are a thermodynamically stable system and thus physically stable for longer duration[125,137,149], while conventional emulsions may phase separate at some point, depending on the viscosity and electrostatic interaction forces between droplets.

Lipid nanoemulsions can be created by either modifying the compositions or increasing the process energy or both.[147] Working at a higher process pressure or increasing the number of homogenization cycles allows to increase the process energy. Increasing the process energy too much can lead to over-processing, a process where phase separation occurs as a consequence of excess energy input.[126,156,378] Droplet size reductions from increasing the process energy are often transient and the system reverts back to the energetically most favourable state mainly governed by the composition. The rate of this return can be influenced among others by the viscosity of the product. When varying the composition, decreasing the oil-to-surfactant ratio (increasing the surfactant concentration and/or lowering the oil content)[379] or increasing the viscosity and ionic pressure[129] helps to produce smaller droplet sizes. For energetic reasons, there is a certain minimal surfactant concentration necessary to maintain the organization as lipid droplets over phase separation into a bi-phasic system with a single lipid layer and all the surfactant molecules oriented at the interface. At constant oil volume, smaller droplet diameters create a larger relative (with regard to the oil volume) surface area. This area needs to be covered with surfactant molecules as the lipid molecules themselves do not mix with water. Increasing the surfactant

concentration leads to a reduction of the droplet size as a larger relative surface (at constant oil volume) can be covered. This can also be achieved by lowering the relative oil volume while keeping the surfactant concentration constant, thereby also changing the oil-to-surfactant ratio in a favourable way. Increasing the viscosity of the continuous (aqueous) phase by mixing with glucose is also known to stabilize emulsions with smaller droplet sizes.[133,172,380]

Lipid emulsions and high glucose containing solutions are routinely mixed during compounding of total parenteral nutrition admixtures.[25,130,163,381] In these cases, the two components are mixed after homogenization of the lipid emulsion. Combining the two components before homogenization allows to exploit the viscosity-increasing effect of the glucose. We hypothesized that this increase in viscosity and thus shear forces would result in smaller lipid droplets than in the absence of glucose.

The aim of this study was to develop a formulation with reduced droplet size to lower the lipid uptake in the liver while maintaining compliance with the requirements of the pharmacopoeia for parenteral administration, i.e., maintaining the high caloric load of the emulsion, keeping surfactant concentrations similar to conventional emulsions and meeting the threshold levels set by commercial reference emulsions for the formation of lipid degradation products.

5.2 Methods

Preparation of the lipid emulsions

Lipid nanoemulsions with a final batch size of 50 ml were manufactured by wetting Lipoid E80 (Lipoid GmbH, Ludwigshafen, Germany) in < 5 ml purified water (NANOpure Diamond™ Barnstead, Thermo Scientific, Waltham MA, USA). Experiments were carried out at either 0.25% (oil-to-surfactant mass ratio of 16.7), 0.5% (oil-to-surfactant mass ratio of 8.3) or 1.2% (oil-to-surfactant mass ratio of 3.5) final concentration of lecithin. Lecithin premixes were let to swell for 2 hours in a water bath at 45 °C. Ethylenediaminetetraacetic acid (EDTA; disodium salt dihydrate, ≥99%; Carl Roth GmbH + Co. KG, Karlsruhe, Germany) predissolved in water was added at a final concentration between 0.53-11.875 µM to maintain a constant chelator-to-oil ratio (µM/g) of either 0.25 or 4.75-fold higher at 1.1875 ("4.75-fold EDTA"). Concentrated (70%) glucose solution was prepared by stepwise dissolution of either D(+)-glucose anhydrous (from Fluka, Buchs, Switzerland; Acros Organics, New Jersey, USA; Scharlau, Barcelona, Spain; or neoFroxx, Einhausen, Germany) or D(+)-glucose monohydrate (from Hänseler, Herisau, Switzerland; or neoFroxx) under constant stirring at a temperature of > 60 °C in purified water. The glucose solution was added to the aqueous phase to reach a final concentration of 0%, 33%, 45%, 52% or 55% glucose in the final formulation. Either the preblended Formula #3 oil mixture (Chapter 4) consisting of 50% Natures Crops Ahiflower oil (Natures Crops, Kensington PEI, Canada), 25% coconut oil (Bioriginal, Saskatoon SK, Canada) and 25% olive oil (LIPOID purified olive oil, Ph. Eur.; Lipoid AG, Steinhausen, Switzerland), or soybean oil (Lipoid Purified Soybean Oil 700, Ph. Eur., USP; Lipoid GmbH) or fish oil (Bioriginal, Saskatoon SK, Canada) was added to reach a final oil content of 20 mass-%, 10.5%, 7%, 5.3% or 4.2% at the correspondingly increasing glucose concentrations. α-Tocopherol (Type V, ~1000 IU/g, Sigma-Aldrich) was added at concentrations between 0.016% (v/v) and 0.0034% to the oil phase to maintain a constant ratio of antioxidant-to-oil of 0.8 (µl/g). Lastly, purified water was added to reach the final volume of 50 ml. Coarse premixes were kept on a rocking shaker before processing for 6 cycles at a process pressure of 22'000-23'000 psi (1517-1586 bar) on a ShearJet HL60 (Dyhdromatics, Maynard MA, USA) equipped with a 75.1 T reaction chamber (Chapter 4).

After manufacturing, the pH (typically in the range of 4-5) was adjusted to 7.4 using 1 M NaOH. The pH-adjusted nanoemulsion was sterile-filtered through a 0.2 µm filter (Acrodisc® 25 mm, hydrophilic

polyethersulfone membrane, PALL, Port Washington NY, USA) into autoclaved 5 ml glass vials (Müller+Krempel, Bülach, Switzerland) and the headspace was covered with argon (PanGas AG, Dagmersellen, Switzerland). Absence of microbial endotoxins was ensured by using GenScript ToxinSensor™ Single Test Kit (0.125 EU/ml, Cat. No. L00450, GenScript, Piscataway NJ, USA) according to the manufacturer's instructions.[336]

Characterization of the droplet size by dynamic light scattering and electron microscopy

Droplet size was measured routinely by dynamic light scattering (Zetasizer 3000 HS A, Malvern Instruments, Malvern, UK) and for selected representative batches by scanning electron microscopy[192–194] (carried out by ScopeM microscopy service, ETH Zurich). Transmission electron micrographs[337–340] (TEM) were also taken by ScopeM microscopy service at ETH of nanoemulsions where glucose had been removed by 8 times washing with purified water and centrifuging for 40 minutes each at 1200 g (Beckman GS-15R, Beckman Coulter, Brea CA, USA) in 15 ml dialysis tubes (Vivaspin 6, MWCO 30'000 Da, polyethersulfone membrane; Vivascience, Hannover, Germany). TEM pictures with nanoemulsions directly failed, due to the high glucose content samples could not be shock frozen which is required to break them apart for proper imaging. Absence of glucose was qualitatively ensured by incubating 0.5 ml retained sample with 1 ml of 0.33 M copper(II) acetate monohydrate (puriss. p. a., ≥ 99.0%; Fluka, Steinheim, Germany) in 1% acetic acid (puriss. p. a., ACS, Ph Eur, ≥99.8%; Sigma-Aldrich), also known as Barfoed's reagent[382–385], at 95 °C for 3 minutes and letting cool down to room temperature again. Successful removal of glucose was confirmed by absence of formation of a red precipitate.

Quantification of primary and secondary oxidation products and of free fatty acids

Primary and secondary oxidation products were quantified using the modified ferrous oxidation-xylenol orange assay (mFOX)[253] and thiobarbituric acid reactive substances assay (TBARS)[288], respectively, described in detail in Chapter 2, "Quantification of Lipid Oxidation Products in Lipid Emulsions Requiring Minimal Sample Volume". For valid comparison between formulations, values were standardized to the oil content. Free fatty acids were quantified by HPLC after fluorescence-labelling[317], described in Chapter 3, "Determination of Free Fatty Acids in Lipid Emulsions by Fluorescence-Detection Based High Performance Liquid Chromatography". For comparison in the respective data evaluation, the 20% lipid emulsion at 1.2% lecithin (oil-to-surfactant ratio of 16.7) without glucose, but with 2.2% glycerol, previously described in detail in Chapter 4, is added to the plots.

Additional emulsions were prepared to study the underlying cause for the increased oxidation of glucose-containing nanoemulsions. Emulsions with Formula #3 oil mix and oil-to-surfactant ratio of 8.3 were prepared as described above, at various glucose concentrations to achieve different droplet sizes. After homogenization, each sample was split and varying amounts of 70% glucose or water were added to yield combinations of 5 different droplet sizes and 4 different glucose concentrations (total 20 emulsions). These samples were exposed to "stress" storage conditions at 40 °C for 6 days under ambient air. After incubation, the droplet size as well as the primary and secondary oxidation products were determined as described above.

Labelling of the emulsion with tritiated lipids for in vivo studies

Prior to *in vivo* tissue distribution studies with a nanoemulsion spiked with a tritiated lipid, proper incorporation of the tritiated lipids into the oil droplets was studied similar to the previous procedure with 250-300 nm-sized emulsions in Chapter 4. For these purposes, an intermediary formulation with 45% glucose and 7% Formula #3 oil-mixture was used. Radioactive molecules ^{3}H-triolein or ^{3}H-

phosphatidylcholine (both 37 MBq/ml; from American Radiolabeled Chemicals, Saint Louis MO, USA) corresponding to 37 kBq were added to 500 µl aliquots of lipid emulsion and vortex-mixed for 30 sec in glass vials. Labelled lipid emulsions were mixed in a 1:1 ratio with either phosphate buffered saline pH 7.4 (PBS), prepared from 10 mM sodium hydrogenphosphate (heptahydrate, p.a., ACS, 98-102%, Merck, Darmstadt, Germany), 1.8 mM potassium dihydrogenphosphate (purum p.a., ≥99.0%; Sigma-Aldrich), 0.137 M sodium chloride (puriss. p. a., ≥99.5%; Sigma-Aldrich) and 2.7 mM potassium chloride (puriss. p. a., ≥99.5%, Sigma-Aldrich) or PBS + 4% bovine serum albumin (cold ethanol fraction, ≥96%; Sigma-Aldrich). Mixtures were then constantly shaken at room temperature for 0, 10 or 60 minutes and phases were separated by centrifuging at 15'000 g for 15 min at 25 °C (Beckman GS-15R, Beckman Coulter). Separated phases were mixed with scintillation liquid (Ultima Gold, Perkin Elmer, Waltham MA, USA) in a 1:4 ratio and radioactivity was measured on a Tri-Carb 2250 CA liquid scintillation counter (Packard BioScience, Meriden CT, USA).

In vivo tissue distribution studies in mice

The tissue distribution was studied for the same lead emulsion (45% glucose, 7% Formula #3 oil mixture) in comparison to a nanoemulsion based on soybean oil (45% glucose, 7% soybean oil). *In vivo* studies with the ^{3}H-triolein tracer were performed in 10-12 weeks old male C57BL/6NCrl mice (Charles River, Sulzfeld, Germany) with a weight between 24.1 and 25.1 g. Lipid emulsions were vortex-mixed for 30 seconds with 37 kBq of ^{3}H-triolein per 100 µl (37 MBq/ml, 2.22 TBq/mmol; American Radiolabeled Chemicals) and 100 µl were administered intravenously by bolus injection to the tail vein. After fixed incubation times of 10 min and 60 min, animals were anesthetized with isoflurane and euthanized by decapitation under deep anesthesia. Organs were dissected and digested with SOLVABLE (Perkin Elmer) according to the manufacturer's instructions. After complete tissue lysis and decoloration with H_2O_2, scintillation liquid (Hionic-Fluor, Perkin Elmer) was added and radioactivity was measured on a Tri-Carb 2250 CA liquid scintillation counter. All animal studies were approved by the cantonal authorities and carried out in accordance to national legislation (license ZH203/2019). For comparison for data evaluation, experiments performed with corresponding oil types, but conventional droplet size (270-300 nm), described before in Chapter 4 are plotted as well.

Statistical analysis

Results of the stress test were analysed by mixed-effects modelling in R (R-project, v 4.0.4) with the function lme of the package nlme (v 3.1-152). Tested effects were size, glucose concentration and their interaction. For TBARS values, mFOX was tested as an additional effect, with interactions with glucose, size or both. Data were grouped according to the individual homogenization batches (n=5). Effects were considered significant at p values < 0.05.

5.3 Results

Effect of glucose on the droplet size of Formula #3 nanoemulsions

Incorporation of glucose at increasing concentrations for the preparation of Formula #3 nanoemulsions led to a glucose-concentration dependent decrease in the measured droplet size. Smallest droplets with a hydrodynamic diameter of 98.7 nm resulted from manufacturing at increased relative surfactant concentrations (oil-to-surfactant ratio of 3.5, see Fig. 5.1). The use of less lecithin (0.25% and 0.51% instead of 1.2%) led a minimal droplet size of 182.4 nm and 139.4 nm, respectively, at 55% glucose. Due to the increased lecithin-concentration also the droplet sizes of formulations produced without glucose (dark green bars at 3.5 and 8.3 oil-to-surfactant ratio) were markedly smaller than the corresponding reference

sample depicted in red. Note that emulsions to study the influence of glucose (added for processing) on droplet size, oxidation products and total free fatty acid levels were produced and tested once each.

Influence of glucose and/or droplet size on lipid oxidation and hydrolysis

The primary and secondary oxidation products depicted in Fig. 5.2 and Fig. 5.3 increased with increasing glucose concentration used in the formulation and decreasing droplet size. Formation of primary and secondary oxidation products is interlinked (Chapter 1, General Introduction). In our study, primary oxidation products increased with the reduction of the oil-to-surfactant ratio (corresponding to a reduction in droplet size), while secondary oxidation products behaved opposite or were ratio and size-independent in the absence of glucose. In general, mFOX-values (primary oxidation products) were drastically higher than in the reference emulsion without glucose (stabilized with 2.2% glycerol instead; red bar). TBARS-values of nanoemulsions produced without or only low glucose were similar to the value of the reference solution. It should be noted, that each condition was studied once. Total free fatty acids in general (Fig. 5.4) show less clear dependency on the glucose concentration and lecithin concentration. The total free fatty acids were in general not higher in the glucose-containing than the reference emulsion. As each condition was analysed once and trends are not as obvious as for the oxidation products, individual bars of Fig. 5.4 are not discussed.

The effect of EDTA on lipid oxidation

To tackle the increased formation of oxidation products, formulations at 4.75-fold increased chelator levels and intermediary lecithin concentration (oil-to-surfactant ratio 8.3) were manufactured for comparison. Increasing the EDTA-concentration did only minimally affect the droplet size, as shown in Fig. 5.5, and the dependency on the glucose concentration was maintained. The increased EDTA concentration had no influence on the levels of the primary oxidation products (Fig. 5.6). However, secondary oxidation products were effectively reduced compared to the formulation with 1-fold EDTA. At intermediate glucose concentrations (33%, 45%) secondary oxidation products were completely diminished at the increased chelator concentration. When standardized to the lower relative oil content, TBARS values in Fig. 5.7 were measured even lower than for the reference emulsion without glucose, but with glycerol. The increased EDTA concentration had no obvious effect on the total free fatty acid concentration (Fig. 5.8).

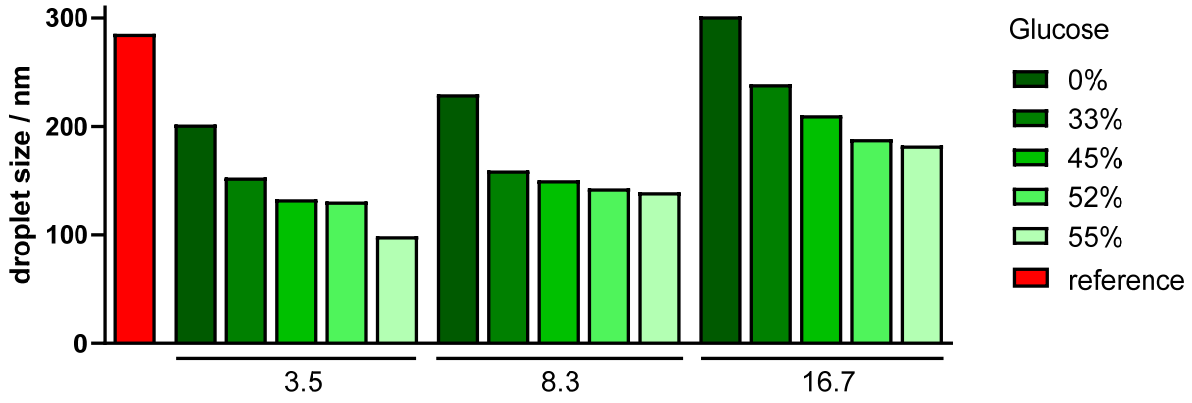

Fig. 5.1: Droplet size of Formula #3 nanoemulsions with increasing concentrations of glucose (green shading, as indicated) added at three different oil-to-surfactant ratios; 3.5, 8.3 and 16.7 (n=1). Note that these emulsions did not contain glycerol. The droplet size of the reference emulsion (conventional Formula #3 emulsion, Chapter 4) with an oil-to-surfactant ratio of 16.7 without glucose is indicated with a red bar.

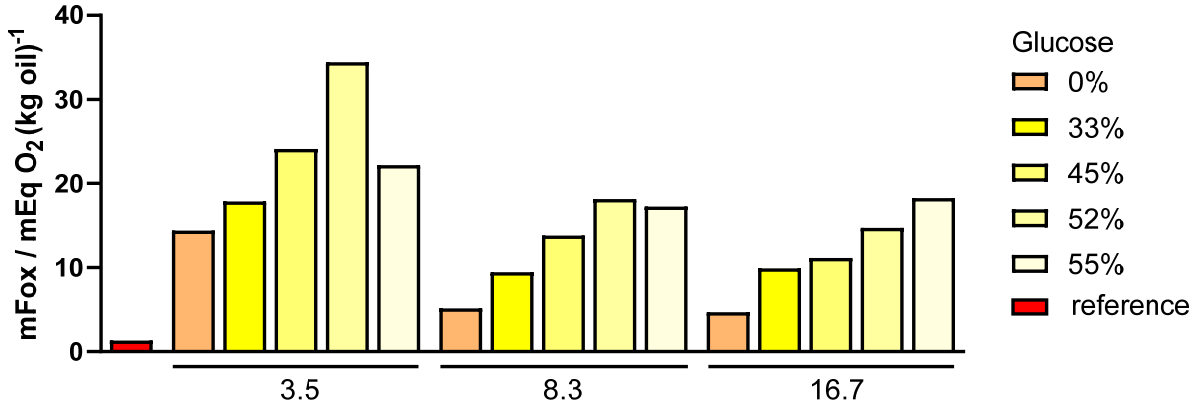

Fig. 5.2: Primary oxidations products as measured by mFOX assay of various nanoemulsions manufactured at increasing glucose concentrations (fading yellow bar color) and at three different oil-to-surfactant ratios of 3.5, 8.3 and 16.7 (n=1). The value of the reference emulsion produced without glucose at an oil-to-surfactant ratio of 16.7 is plotted with a red bar for comparison. Note that this emulsion was the only one in the figure containing glycerol.

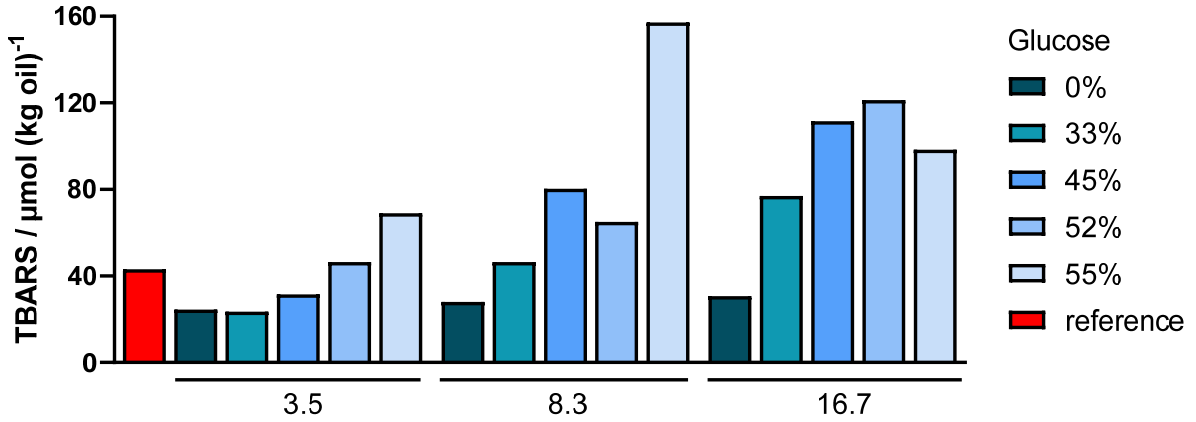

Fig. 5.3: Thiobarbituric acid reactive substances of lipid nanoemulsions produced at increasing glucose concentrations (from left to right within a sample subset, fading turquoise/blue bar color) at an oil-to-surfactant ratio of either 3.5, 8.3 or 16.7 (n=1). A reference value obtained from an emulsion produced without glucose (but with glycerol) at an oil-to-surfactant ratio of 16.7 is shown with a red bar.

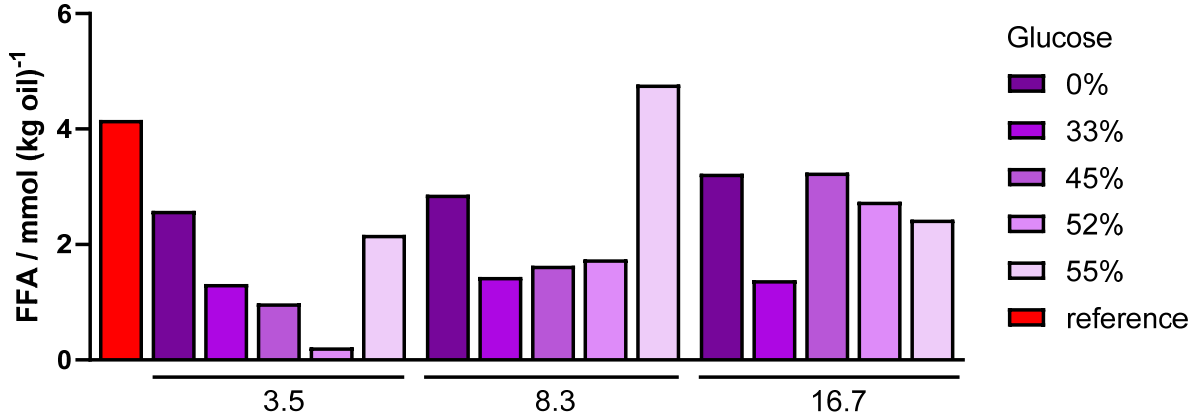

Fig. 5.4: Total free fatty acids as measured by HPLC after fluorescence labelling, standardized to the respective oil content of nanoemulsions manufactured at increasing glucose concentrations (fading bar color) for either 3.5, 8.3 or 16.7 oil-to-surfactant ratio (n=1). In red, the value of an emulsion produced at an oil-to-surfactant ratio of 16.7, without glucose (but with glycerol) is shown for reference.

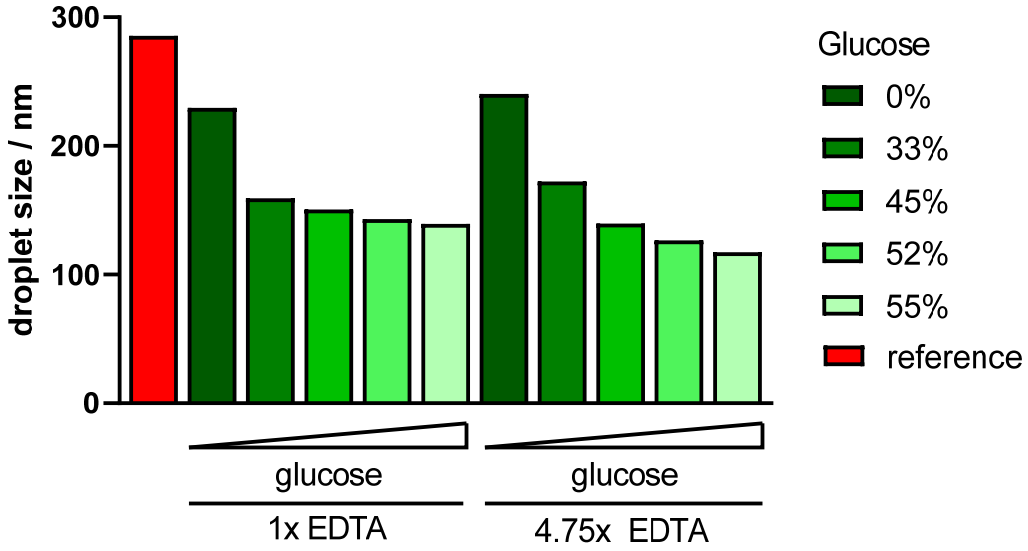

Fig. 5.5: Droplet size of formulations produced with glucose ranging from 0%-55% at an oil-to-surfactant ratio of 8.3 and at two different EDTA concentrations (for 1x EDTA same data as in Fig. 5.1, n=1). For comparison, the droplet size of a reference emulsion without glucose (containing glycerol) at 1x EDTA and an oil-to-surfactant ratio of 16.7 is shown as red bar.

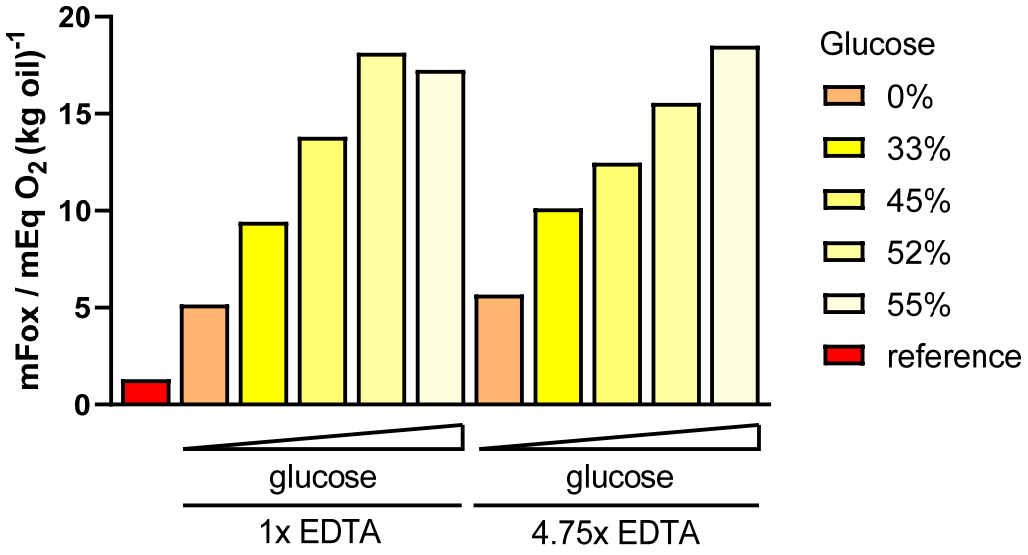

Fig. 5.6: Comparison of two different EDTA-levels, 1x and 4.75x, on primary oxidation products of lipid nanoemulsions produced at increasing glucose concentrations (fading bar color, indicated below with inclining ramp) and an oil-to-surfactant ratio of 8.3 (1x EDTA data same as in Fig. 5.2, n=1). The same reference as in Fig. 5.2 is also plotted here for comparison.

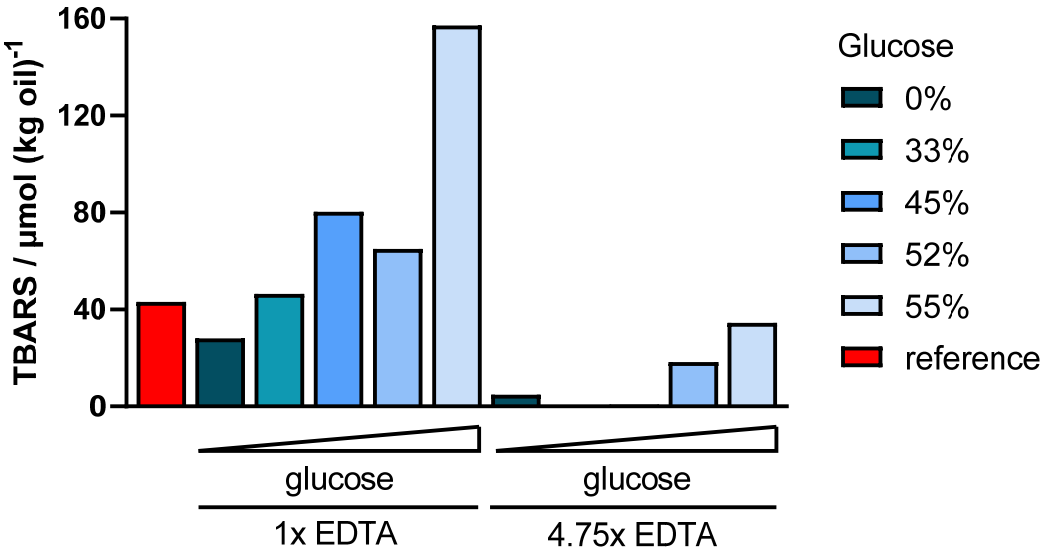

Fig. 5.7: Secondary oxidation products of lipid emulsions with increasing glucose concentration manufactured at an oil-to-surfactant ratio of 8.3 depending on the EDTA-level (1x same data as in Fig. 5.3Fig. 5.4 n=1). A reference value of an emulsion without glucose, produced at an oil-to-surfactant ratio of 16.7 and with glycerol is marked as red bar. Values for 4.75x EDTA at 33% and 45% glucose not visible in the figure were 0.47 µmol (kg oil)$^{-1}$ and 0.71 µmol (kg oil)$^{-1}$, respectively

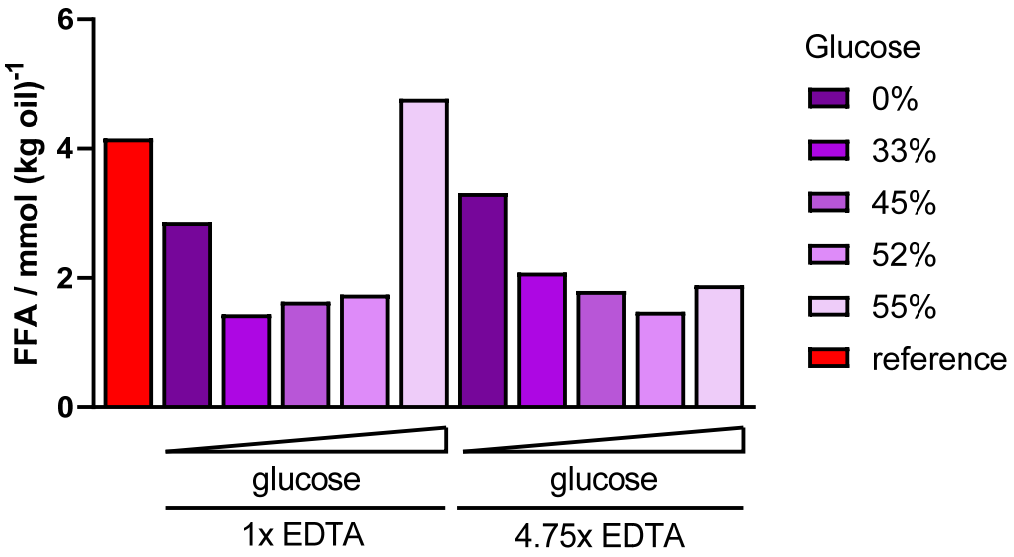

Fig. 5.8: Total free fatty acids of lipid nanoemulsions produced at increasing glucose concentration (fading color of bars) and a constant oil-to-surfactant ratio of 8.3 compared to same corresponding formulations with 4.75-fold increased ETDA levels (1x EDTA data same as in Fig. 5.4, n=1). The reference value from the previous lead formulation (16.7 oil-to-surfactant ratio, no glucose, 2.2% glycerol) is shown in red.

Effects of emulsion droplet size and glucose level on lipid oxidation

Primary and secondary oxidation products of samples kept at 40°C for 6 days in ambient air were one to two magnitudes higher than in the non-stressed emulsions in Fig. 5.2 and Fig. 5.3. The individual values for the formulations with combinations of varying glucose concentration and varying droplet size are shown in Fig. 5.9. Plotting mFOX and TBARS values against droplet size (Fig. 5.9 A and B) did not show an unambiguous effect of droplet size on the levels of the oxidation products. mFOX levels were higher at smaller size by trend though. Plotting the levels of the oxidation products against the glucose

concentration showed a possible negative effect of glucose on mFOX values and a parabolic relationship between levels of secondary oxidation products and glucose.

In mixed effects modelling, the effects of droplet size and glucose levels on mFOX values were not significant. Values of *p* were 0.17 and 0.19, respectively, for the two parameters analyzed as individual effects. The effect sizes may suggest, though not at the significance level, that reducing the size increases primary oxidation products but increasing the glucose concentration rather reduces primary oxidation products (both as also suggested from Fig. 5.9 A and C).

The parabolic relationship between the TBARS values and the glucose levels was confirmed with a model including a positive effect of the glucose concentration ($p = 0.015$) and a negative effect of glucose concentration to the power of 1.1 ($p = 0.015$). The power term was not optimised in this model but was chosen from visual inspection. Significance was furthermore reached in a simple model with mFOX levels as the predictor of TBARS values ($p = 0.037$), however, this simple model would ignore the bell-shaped relationships between TBARS and glucose levels (comparing Fig. 5.9 C with D).

In summary, primary oxidation products may depend on both size and glucose concentration, both with negative effect on the level of primary oxidation products (significance levels not reached). The secondary oxidation products depend significantly on the glucose concentration in a bell-shaped function with highest TBARS at intermediate glucose levels.

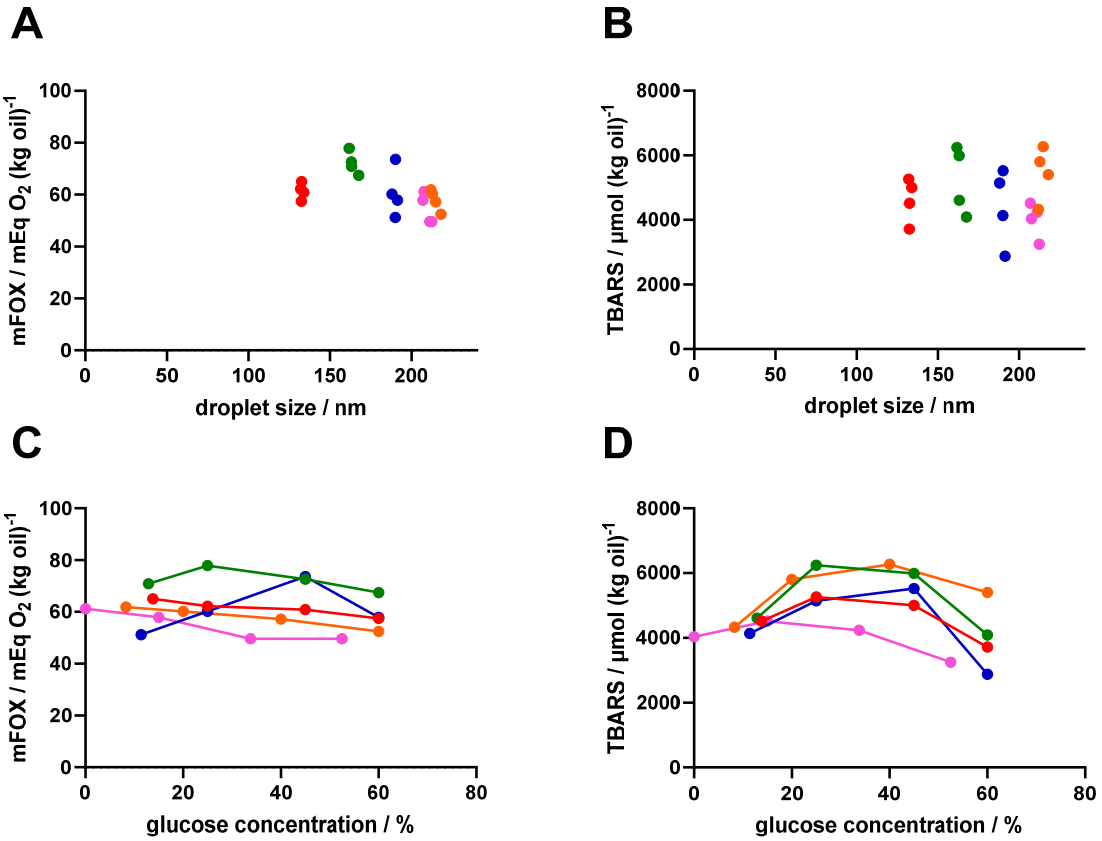

Fig. 5.9: Evaluation of stress test of lipid nanoemulsions stored for 6 days at 40 °C. Primary (A and C) and secondary (B and D) oxidation products of lipid nanoemulsions at different droplet sizes (A and B) and various glucose concentrations (C and D, same data as in A and B) added either prior of after homogenization. Emulsions with the same color were prepared in the same homogenization process. Oil-to-surfactant ratios were 8.3.

Labelling and further characterization of the Formula #3 nanoemulsion for in vivo experiments

As a compromise between droplet size and levels of oxidation products, we chose 45% glucose at an oil content of 7% and an oil-to-surfactant ratio of 8.3 for the further evaluation *in vivo*. Prior to *in vivo* tissue distribution studies, the suitability of ^{3}H-phosphatidylcholine and ^{3}H-triolein to label nanoemulsions was checked by the method used before with 280 nm-sized emulsions (Chapter 4, "Excipient Screening for the Development of Lipid Emulsions based on Vegetable Oils Rich in *n*−3 Polyunsaturated Fatty Acids"). On average, 40% of the recovered activity of the phospholipid tracer was found in the lipid phase of the nanoemulsion while > 85% of the triglyceride tracer was found for corresponding samples. BSA in the aqueous phase had no substantial effect. The findings previously seen for a 280 nm-sized emulsion could be confirmed also for lipid nanoemulsions with droplet sizes < 200 nm. The phospholipid tracer was not considered a valid tracer while the triglyceride tracer was further utilized in *in vivo* tissue distribution studies.

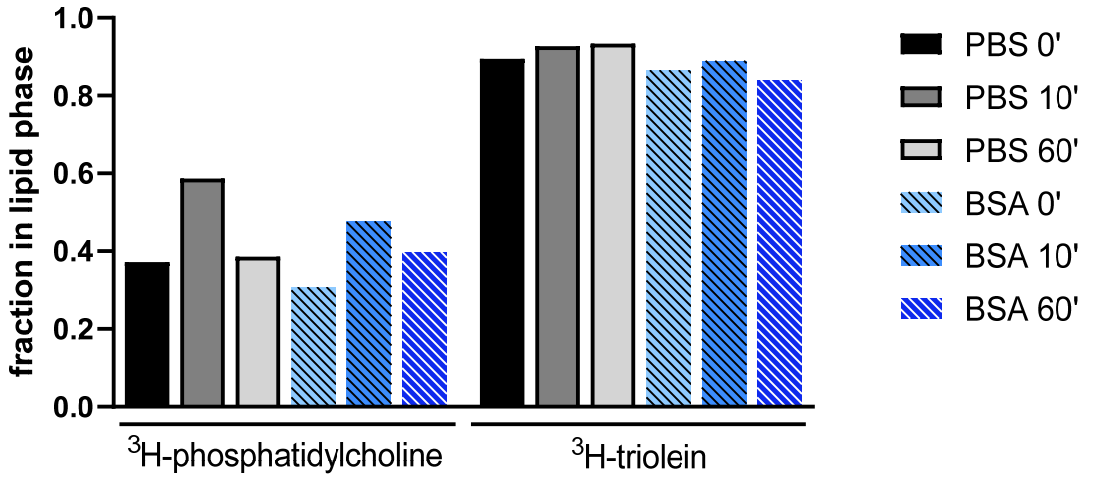

Fig. 5.10: In vitro *distribution of two radioactively labelled molecules, ^{3}H-phosphatidylcholine and ^{3}H-triolein. Fraction recovered from the lipid phase when mixed with lipid nanoemulsion (Formula #3 oil mix, oil-to-surfactant ratio 8.3, 45% glucose) in presence of either phosphate-buffered saline (PBS, black bars) or PBS + 4% bovine serum albumin (BSA, blue bars).*

The droplet size uniformity and validation of DLS measurements of the nanoemulsions for *in vivo* experiments were carried out by imaging with scanning electron microscopy. In representative images of nanoemulsions manufactured from either Formula #3 oil mixture (Fig. 5.11) or soybean oil (Fig. 5.12) did not reveal droplets markedly larger than the average determined by DLS of 160-170 nm. No droplets above the pharmacopoeial limit of 5 µm[168,169] were observed. The same was true for fish oil nanoemulsions (see Appendix Fig. A9). Only in few selected micrographs single droplets between 350-570 nm were found (see Appendix Fig. A10, Fig. A11 and Fig. A12), but all formulations still complied with the PFAT5 requirement. Also transmission electron micrographs showed the sphericity of the particles (Fig. A13 and Fig. A14 in the Appendix). Minimal particle size maturation though the repeated centrifugation for glucose removal from 161 nm to 180 nm was found by DLS. An individual TEM picture (Fig. A13) out of thirteen pictures taken showed also larger particles in the area of 500 nm. Most droplets were oil-filled, only few oil-free (phospholipid-only) structures (transparent fill), and only few liposomes (red arrows) and multilamellar droplets (green arrows) were found.

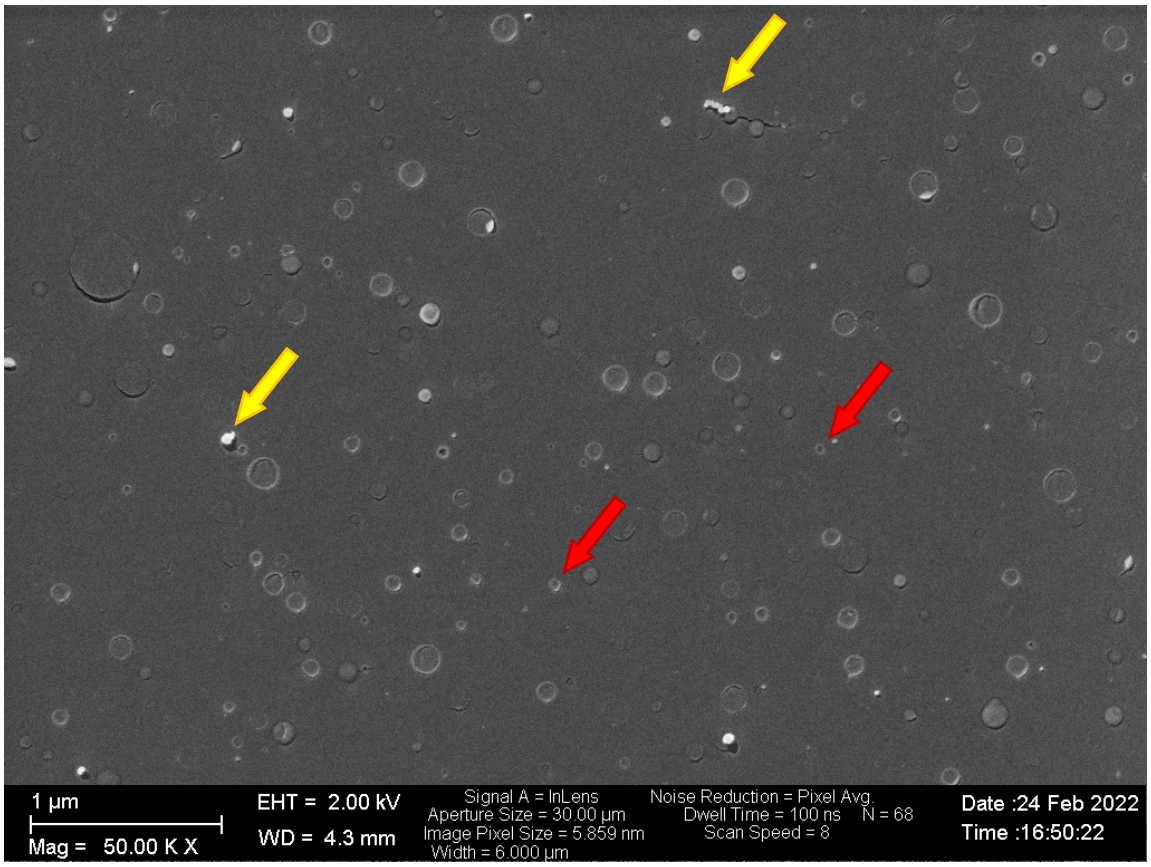

Fig. 5.11: Scanning electron micrograph of lipid nanoemulsion consisting of 7% n−3 PUFA-rich plant-based oil mixture, 45% glucose and manufactured at an oil-to-surfactant ratio of 8.3. Artifacts from the sample preparation process are indicated with yellow arrows, selected smaller-than-average lipid droplets with a red arrow.

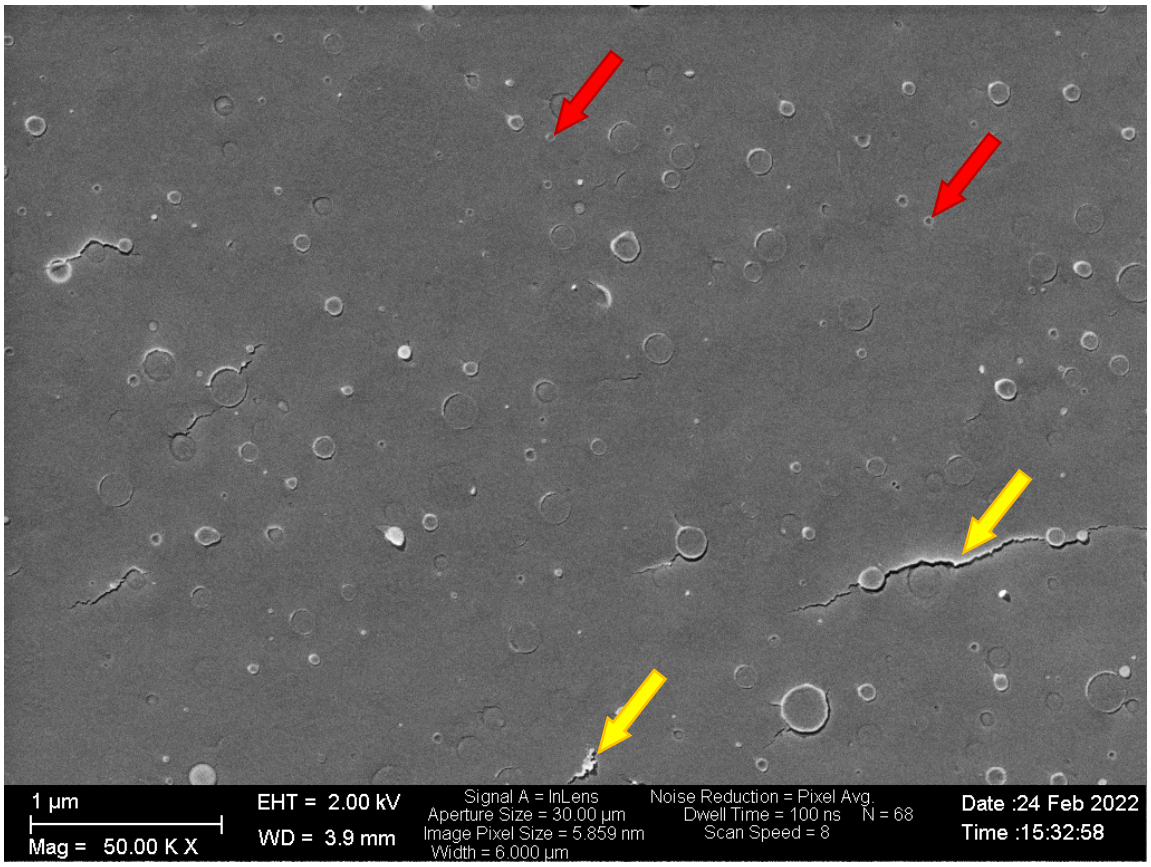

Fig. 5.12: Representative scanning electron micrograph of 7% soybean oil nanoemulsion stabilized with 45% glucose (oil-to-surfactant ratio of 8.3, same composition as used in in vivo experiments in Fig. 5.14). Artifacts from freeze-fracture are marked with yellow arrows, remarkably small lipid droplets are highlighted with red arrows.

In vivo tissue distribution of Formula #3 and soybean oil nanoemulsions

The *in vivo* tissue distribution was determined for nanoemulsions containing 7% oil, which was either Formula #3 oil mix or soybean oil, an oil-to-surfactant ratio of 8.3 and 45% glucose. The droplet sizes were 161.0 nm and 166.9 nm, respectively. The results of the tissue distribution study with Formula #3 oil mixture are shown in Fig. 5.13. For unknown reasons, radioactivity recovery was unexpectedly low in this experiment and data needs to be evaluated with care. Assuming that recovery was proportionally reduced equally in all tissues, the pattern of tissue distribution was similar to the previous results with 280 nm-sized emulsions (Chapter 4, "Excipient Screening for the Development of Lipid Emulsions based on Vegetable Oils Rich in *n*−3 Polyunsaturated Fatty Acids", Fig. 4.6). The highest uptake was found in lung tissue, with less pronounced differences to other tissues than observed for the 280 nm-sized equivalent emulsion. The liver, brown fat and spleen as tissue with second most uptake show values corresponding to around half the uptake in the lungs. This ratio is low compared to the experiments with 280 nm-sized emulsions where the uptake in the lung exceeded the uptake in any other tissue more than 10-fold.

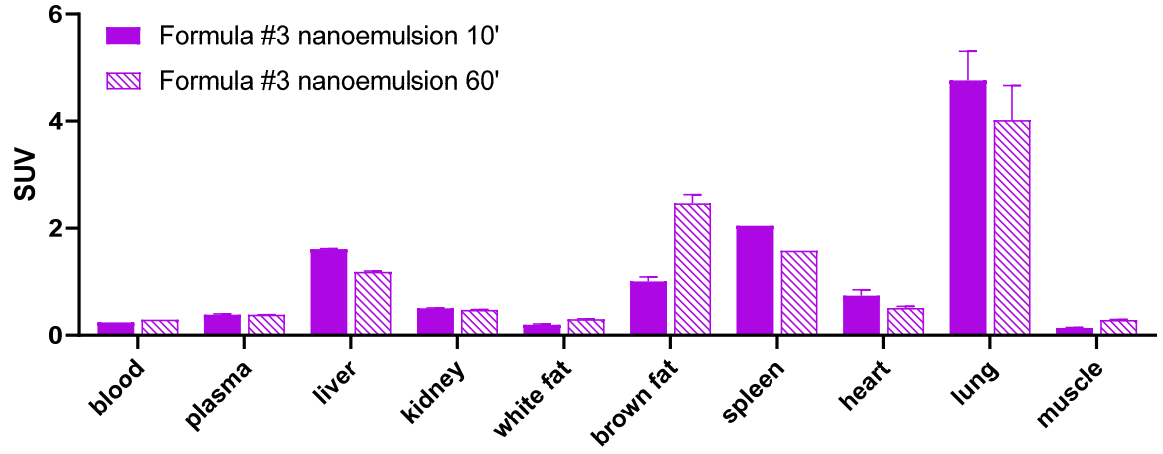

Fig. 5.13: Standardized uptake values in different tissues after administration of 100 µl nanoemulsion with 7% Formula #3 oil mixture, oil-to-surfactant ratio 8.3, 45% glucose and 161 nm mean droplet size. Time points after injection as indicated (n=1 animal per time point; bars, individual values or means and standard deviation if more than one tissue sample of the same mouse was analyzed). The recovered radioactivity was unexpectedly low in these experiments, resulting in the low SUV values as compared to other in vivo *experiments.*

The reduced uptake in the lung compared to previous experiments with larger oil droplets was also found in the experiment with a lipid nanoemulsion produced from soybean oil. Uptake in lung tissue was still highest, but only 1.5-fold of the uptake in the spleen after 10 minutes and 3-fold than the liver and brown adipose tissue as areas with next highest uptake. The uptake in white adipose tissue from different locations or in muscle on the other hand remained low (maximal SUV 2.4 and 0.5, respectively). We analyzed additional samples in this experiment (urine, gallbladder, intestines, tail as site of injection). They all did not show SUV > 1.

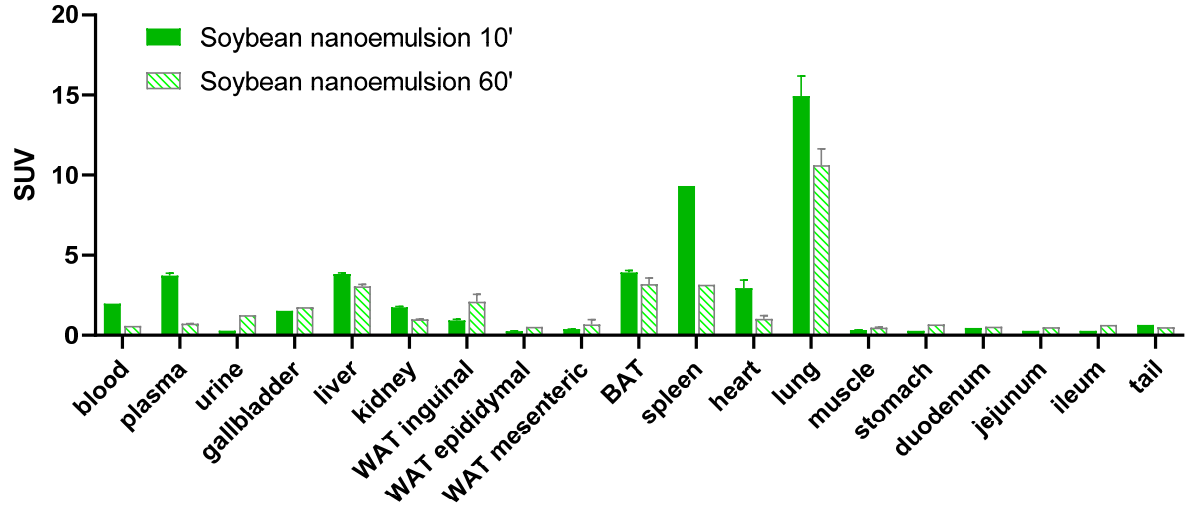

Fig. 5.14: Standardized uptake value SUV in different tissues of 37 kBq ^{3}H-triolein dispersed in 100 µl of 7% soybean oil nanoemulsion stabilized with 45% glucose, resulting in 224.7 cal administered. The droplet size of the nanoemulsion was 167 nm. The incubation times of 10 minutes (filled bars) and 60 minutes (diagonal down) are plotted differently (n=1 animal per time point; bars, individual values or means and standard deviation if more than one tissue sample of the same mouse was analyzed). Abbreviations: white adipose tissue (WAT) and brown adipose tissue (BAT).

Comparison with the 280 nm-sized Intralipid, also based on soybean oil (visualized in Fig. 5.15), revealed a similar uptake pattern between the two formulations despite the size difference. This hints to the oil type rather than the droplet size being the main driver for the tissue distribution. The corresponding comparison of 280 nm- and 161 nm-sized Formula #3 oil mixture (Fig. A15) or of the two nanoemulsions manufactured from different oil sources (Fig. A16) are more challenging due to the reduced total activity recovered in the case of the Formula #3-based nanoemulsion.

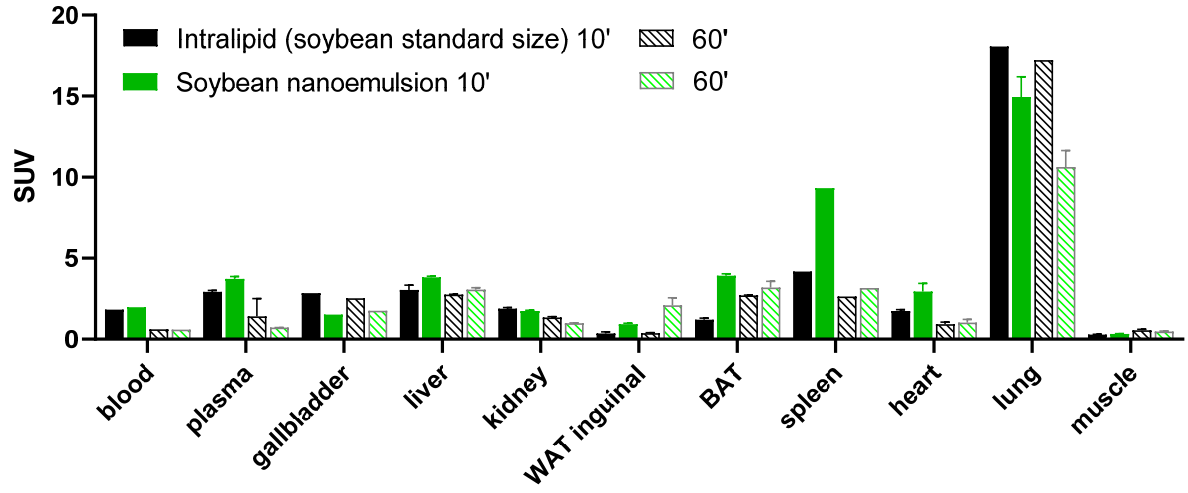

Fig. 5.15: Comparison of tissue distribution of Intralipid (20% soybean oil emulsion with a droplet size of 288.7 nm, black bars) and soybean nanoemulsion (7% oil stabilized with 45% glucose, 166.9 nm droplet size, green bars, same data as in Fig. 5.14) 10 minutes (filled bars) and 60 minutes (diagonal down filled bars) after injection (n=1 animal per time point; bars, individual values or means and standard deviation if more than one tissue sample of the same mouse was analyzed). Intralipid was administered at 50 µl, corresponding to 10 µl oil and 20 cal, while the nanoemulsion was administered at 100 µl, resulting in 7 µl oil and 224.7 cal.

5.4 Discussion

The novel approach here is that the glucose usually added after homogenization during the compounding step is added already before, thereby exploiting the dilution and viscosity-increasing effect[172,380], resulting in a droplet size reduction and stabilizing effect. For the preparation of the final mixture for total parenteral nutrition (TPN) during compounding, 3.75 equivalents of 70% glucose are added to one equivalent of lipid emulsion[386], leading to a dilution factor of 4.75 frequently encountered in the further rationale for the preparation of subsequent formulations in this work. Original experiments were carried out at an oil-to-surfactant ratio of 3.5 to reach a final lecithin-concentration of 1.2%, but were then downscaled to an oil-to-surfactant ratio of first 16.7 (mimicking the previous ratio, and also the one of commercially available Intralipid[387,388]) for concerns of unknown effects from excess phospholipids. Although later dismissed[154], excess phospholipids could, based on their structure, incorporate into biological membranes and interfere with their function. Since the droplet size reduction was then considered sufficient to observe differences *in vivo*, the final composition experiments were carried out with an oil-to-surfactant ratio of 8.3, corresponding to the ratio also seen in commercial Omegaven.[62,388]

During the final compounding for TPN, varying residual amounts of glucose need to be added to the formulations produced in this project, to reach a final glucose concentration of 55% in all formulations. No glucose needs to be added to the ones already containing 55% glucose (the highest glucose concentration studied), and lots of glucose still needs to be added to the 0%-formulations.

The EDTA-concentration became diluted up to 4.75-fold to 0.53 µM in the most extreme case (in formulations containing 55% glucose), but was still corresponding to the original 2.5 µM when only the oil and water from the original lipid emulsion portion was considered. Doses were chosen to always maintain a chelator-to-oil ratio of 0.25. This results in constant EDTA daily doses at isocaloric dosing of the emulsions. When measured oxidation values were unsatisfactory and exceeded previously seen values manifold, the EDTA concentration was increased 4.75-fold, to reach a global 2.5 µM in the finally adjusted glucose-lipid emulsion mixture (after adding all the residual glucose amount still missing). In the formulations not at maximal glucose concentration yet and still requiring glucose addition, this resulted in 11.9 µM EDTA before final compounding. The content of α-tocopherol as antioxidant resulted in a constant ratio of antioxidant-to-oil of 0.8 (µl/g), similar to the original Formula #3 formulation (see Chapter 4). In previous studies described in Chapter 4, further increasing the antioxidant concentration did not reduce the formation of lipid oxidation products.

For further *in vivo* evaluation, an intermediate glucose concentration of 45% was chosen. The oil-to-surfactant ratio was identified as primary driver determining the droplet size and not the maximally possible glucose concentration of 55% was needed to yield the target droplet size of < 200 nm. Lowering the glucose concentration allowed to considerably reduce the immediate formation of lipid oxidation products at a minimal cost of increased droplet size compared to the highest glucose concentration. In subsequent stability studies under accelerated storage conditions, the choice of 45% glucose for our lead formulation seems to be unfortunate. The data measured hint to maximal secondary oxidation product formation at glucose concentrations between 20-40% and a relative minimization in turn at 55% glucose. How these reduced relative oxidation products at 55% glucose compared to 20-40% relate to the increased oxidation products measured at 55% glucose (compared to at 33-45% glucose) immediately after manufacturing remains to be elucidated.

Obtaining smaller droplet sizes provides the benefit of allowing the lipid nanoemulsions to be sterile-filtered, thereby effectively circumventing the thermal stress from autoclaving for sterilization. Moreover, manufacturing combined glucose-lipid emulsions simplifies the compounding process, at least if working with the formulation already containing all the needed glucose. The compounding process has been identified as potential source of errors.[389–391] Thereby simplifying this process helps to increase patient safety. However, by combining the glucose and lipid emulsion already, no personalized compounding respecting the individual's needs is possible anymore as it is unlikely that a high-pressure homogenizer is available on site. Moreover, the middle-term stability required to demonstrate practical use in clinics has not been thoroughly investigated yet, neither in terms of droplet size stability (though glucose has a physically stabilizing effect from the increased viscosity[172], and also nanoemulsions should be thermodynamically stable[144,158,190,392]), nor for the increased formation of oxidation products. Storage in the fridge at 4 °C in an attempt to slow down degradation (Arrhenius law[295,341,342]) was not possible as glucose crystalized. Therefore, proper exclusion of oxygen by covering the headspace with argon and tight sealing is crucial.

The results of the stress test at 40 °C for 6 days indicate that a reduction in droplet size may increase the levels of primary oxidation products, however, the effect was not significant. Such an effect could result from the increased interface area between oil and water at the reduced droplet size. Glucose levels had a significant bell-shaped effect on the levels of secondary oxidation products. The latter furthermore correlated significantly with mFOX values. These results would agree with a model where size reduction induces lipid oxidation resulting in primary oxidation products and where glucose promotes the further reaction of primary to secondary oxidation products (reducing primary and increasing secondary

oxidation products) and furthermore from secondary to tertiary oxidation products (bell-shaped relationship between secondary oxidation products and glucose levels). However, this is only one of several possible models and would need to be corroborated by further investigations.

Increasing the EDTA levels 4.75-fold in the Formula #3 nanoemulsion was considered justified in an attempt to reduce the secondary oxidation products that are potentially harmful as well.[195,196] Also at an increased level, doses are still below what has been used in clinical trials before (once per week administration instead of continuous application).[358]

Tissue distribution studies showed highest uptake in the lung for both Formula #3 and soybean oil nanoemulsions. The difference to the tissues with next highest uptake was less pronounced than with the respective emulsions with > 260 nm droplet size. This could be a result of the droplet size but also of the glucose present in the nanoemulsions, but not in the conventional emulsions.

All the tissues showing high uptake – liver, lungs and spleen – belong to the reticuloendothelial system (RES) with high presence of macrophages.[128] Pronounced uptake of lipid emulsions in these tissues has already been found from the very beginning of parenteral nutrition[73] and repeatedly been confirmed.[33,102,361] Particles with droplet sizes above 1000 nm arising from instable formulations promote uptake in organs of the RES.[130,163]

At reduced droplet size, previous reports have found a prolonged plasma residence (slower extraction)[37,124,369,377,393] and a reduced hepatic uptake.[36,347] The limit of optimal size is debated, while a droplet size below 100 nm is necessary for less unspecific uptake in the RES[147], Litzinger *et al.* found in 1994 an intermediate droplet size between 150 and 200 nm to yield the longest circulation time.[375] Based on these evidences, a reduced uptake of the nanoformulations in the liver, but also spleen and lung would have been expected. In turn, a higher remaining activity in plasma was expected that was not found in our experiments. Also the uptake in the spleen contradicts these expectations.

Because of the reduced total activity recovery in the case of the Formula #3 oil-mix based nanoemulsion, the data need to be interpreted with caution. The results obtained with the soybean oil-based nanoemulsion on the other hand showed a similar pattern as the 280 nm-sized Intralipid also based on soybean oil (but from a different supplier). This hints to the oil type being the main driver for the tissue distribution rather than the size. Similar findings that the oil type influences the distribution behaviour have already been reported before.[332,366] Qi and co-workers found in 2003 that the oil type was more important for the tissue distribution for larger particles, while for smaller droplets almost no influence of the oil type was found anymore.[394]

When comparing the distribution of glucose-stabilized nanoemulsions with the conventional sized emulsions, it is important to keep in mind that the oil amount was attempted to be mimicked as much as possible (7 µl oil vs. 10 µl for nano- and conventionally sized emulsions respectively, but not individually adjusted for the weight for the animal). More importantly, because of the addition of glucose, the amount of administered calories varied by a factor of 11, *i.e.,* 224.7 cal vs. 20 cal for the nanoemulsions and the conventionally-sized emulsions, respectively. The presence of glucose as energy source could furthermore affect the lipid uptake in the tissues. For a proper control of this confounder, conventionally-sized emulsions could be mixed with glucose after homogenizing and then prepared in the same way to administer equal amounts of calories, but at different lipid droplet sizes. The transferability of the findings to the long-term *in vivo* setting is not optimal, as in this case glucose and amino acids are co-administered with the lipid emulsion.

Overall, the same restrictions apply as already discussed in the previous chapter on the tissue distribution of 280 nm-sized lipid emulsions. Fasting of the animals would presumably increase the uptake in heart and peripheral skeletal muscle, co- or pre-administration of heparin could also affect the uptake as reported in literature.[333,360] For lipid nanoemulsions stabilized with glucose, a reduced lipid uptake in muscle is expected, as the muscles would preferentially metabolize the rapidly available energy provided from the glucose. Glucose uptake would however not be reflected in the distribution pattern assessed with a triglyceride tracer, as glucose comprises the outer continuous phase of the nanoemulsion while the tracer is distributed to the lipid droplet core and thus does not reflect the distribution (and possible metabolism) of the outer continuous phase.

Finally, these experiments are seen as pilot experiments providing hints for the identification of optimized experimental setups. For statistically sound conclusions on the biodistribution, repetitions of the *in vivo* experiments need to be conducted with larger group sizes.

5.5 Conclusion

Adding high concentrations of glucose to coarse lipid emulsions prior to homogenization led to a considerable reduction of the obtained droplet size below 200 nm while maintaining the oil-to-surfactant ratio and process energy. The incorporation of glucose and reduction in droplet size in turn led to an increase in the formation of lipid oxidation products that could be offset by increasing the EDTA chelator concentration in the case of secondary oxidation products. Preliminary tissue distribution studies carried out in mice showed a reduced – compared to previous studies with 280 nm-sized emulsions – but still highest uptake in lung tissue.

5.6 Acknowledgment

The authors thank Stephan Handschin of ScopeM (ETH Zurich) for acquiring the cryoSEM and TEM pictures. Claudia Keller (Center for Radiopharmaceutical Sciences, ETH Zurich) is acknowledged for help with the injections during animal experimentation.

6 IDENTIFICATION OF OPTIMAL MANUFACTURING SETUP FOR THE PRODUCTION OF LIPID EMULSIONS BY HIGH-PRESSURE HOMOGENIZATION WITH MINIMAL OXIDATION PRODUCTS

Gregory Holtzhauer and Stefanie D. Krämer

Biopharmacy / Center for Radiopharmaceutical Sciences, Institute of Pharmaceutical Sciences, ETH Zurich

Scientific contributions:

Gregory Holtzhauer conceptualized, executed and analysed all experiments, and wrote the chapter. Stefanie D. Krämer supervised the work.

6.1 Introduction

Intravenous lipid emulsions intended for clinical application must comply with high regulatory standards.[70] Patients already weakened from a primary disease needing parenteral nutrition should not be burdened with low-quality therapeutics further worsening their condition. Highly unsaturated lipids are inherently susceptible to oxidative degradation.[395] Oxidized lipids on the one hand do not fulfill their intended purpose as supply of essential fatty acids anymore and on the other hand can further exert severe health effects by impairing the structure and as a consequence also the function of cell membranes, proteins and DNA.[396] It is thus crucial to diligently test lipid emulsions prior to administration. To increase confidence of compliance with the limits and reduce rejects from non-compliant batches, the manufacturing process should be designed to reliably deliver high quality products.

Lipid oxidation products can either be limited by introducing counteracting excipients[397] into the formulation or by setting up the process[346] in such a way that oxidation is reduced or even prevented. From the perspective of the regulatory bodies, a formulation should be as simple as possible and contain only few selected excipients.[219] In single applications such as once-only injections, higher doses of excipients are tolerated. In potentially repeatedly administered infusions with higher volumes, less amounts of excipients are tolerated to avoid chronic toxicity.[153] Through the continuous administration, also low doses can easily accumulate and harm the patient. From a scientific perspective it is better to control the process and prevent the occurrence rather than counteract the avoidable effects with excipients. In this chapter, the influence of the manufacturing protocol on the emulsions' characteristics was studied with the aim of identifying optimal process parameters to limit the lipid oxidation.

When producing lipid emulsions by high-pressure homogenization, several process parameters can be varied, including the batch size, the number of homogenization cycles, the process pressure and the cooling temperature. Varying these parameters can have an influence on the physical (droplet size, pH) and chemical (oxidation products, hydrolysis) stability of the produced emulsion. A higher process pressure can mean that a higher stress is encountered, but that the total number to cycles necessary to reach the target droplet size is reduced[136], so that overall the total oxidative stress is reduced. Efficient premixing reduces the number of required cycles and thus also minimizes total oxidative stress.

The number of homogenization cycles should be carefully chosen to be as low as possible, but as many cycles as are needed to yield formulations stable for the intended usage period of at least three months. After exposure of the high process pressure within the reaction chamber, the pressure is rapidly released when the product is back to atmospheric pressure at the outlet. This rapid pressure drop can have a negative impact on the product and thus ways to mitigate the harsh release are studied. Feed through a stainless steel cooling coil where the walls cannot expand and thus provide support, helps to alleviate the pressure drop. The longer the cooling coil, the longer the distance for the pressure to drop and thus the flatter the gradient. Using a shorter or no cooling unit at all can be insufficient. The introduction of a backpressure module can be a valid alternative in this situation.[145,147] The function of a backpressure module is similar to the confined walls of the cooling coil. By keeping the product inside a narrow path that only gradually widens, the pressure drop can be modulated. Apart from the introduction of a backpressure module, also its position up- or downstream of the reaction chamber can be varied.

To account for the heat of compression, the product can be cooled after homogenization.[144,150,398] This happens by circulating the product in a cooling coil (also termed heat exchanger), submerged in a cooling medium, without the two fluids touching. The cooling efficiency can be influenced by the duration of this interaction (via the length of the cooling coil), but also by choosing the temperature of the cooling

medium. At increased temperature the viscosity is decreased and thereby size reduction is more efficient, again potentially requiring less homogenization cycles. Thus, also complete omission of the cooling option and instead collection of the product right after the high-pressure reaction chamber is an option evaluated. The batch size can be flexibly varied from a minimal batch size of 10 ml onwards. In preliminary studies, an effect of the batch size on the oxidation parameters was found.

Another point of manipulation of the process is the determination how the emulsion is fed into the system. The default setup at the time of acquiring is an open funnel-shaped reservoir. This reservoir is available either in glass or stainless steel. For the reservoir, interaction with the environment is possible. This on the one hand allows to continuously mix the coarse emulsion in the feeder to improve the homogenization efficiency and lower de-mixing stress on the oil phase, but on the other hand bears the risk of product contamination with endotoxins, microbes or prolonged exposure of the highly susceptible poly-unsaturated fatty acids to atmospheric oxygen. Alternatively, adapters with luer-connectors for fitting syringes are available. The luer adapters allow the system to work with syringes where the product is fed in with a syringe. For that no action by the operator is required, same as for the open reservoir the underpressure created by the pump automatically feeds in the coarse emulsion. After passing the reaction chamber and the optional cooling unit the product is fed into a second syringe. For a subsequent homogenization cycle, simply the positioning of the two syringes (empty and filled) can be exchanged and the machine is run another time. The motivation to use syringes is that they protect the emulsion from the surrounding environment, reducing environmental contamination as well as exposure to atmospheric oxygen. Moreover, no contact with the product is possible anymore, especially favourable for working with radioactive material (as planned for *in vivo* biodistribution studies) so that no contamination of the operator is possible.

The choice of the manufacturing parameters can heavily affect the obtained product characteristics. Compared to commercial reference emulsions, the oxidation parameters of in-house manufactured emulsions are increased. Therefore, possible modifications of the process parameters were studied in search of identifying those leading to the lowest formation of oxidative degradation products.

6.2 Methods

Lipid emulsions were produced by wetting 1.2% Lipoid E80 (Lipoid GmbH, Ludwigshafen, Germany) in 5-10 ml purified water (NANOpure Diamond™ Barnstead, Thermo Scientific, Waltham MA, USA) and let to swell in a water bath at 45 °C for 2 hours. Ethylenediaminetetraacetic acid (EDTA; disodium salt dihydrate, ≥99%; Carl Roth GmbH + Co. KG, Karlsruhe, Germany) in water was added at a final concentration of 2.5 µM followed by 2.2% glycerol (99+%; Acros Organics, New Jersey, USA) as isotonicity agent. Next, either 20% soybean oil (Lipoid Purified Soybean Oil 700, Ph. Eur., USP; Lipoid GmbH), 10% fish oil (Bioriginal, Saskatoon SK, Canada), 20% SMOF oil mix (consisting of 30% Lipoid soybean oil, 30% Bioriginal coconut oil, 25% Lipoid Purified olive oil and 15% Bioriginal fish oil) or 20% Formula#3 oil mix (consisting of 50% Natures' Crop Ahiflower oil [Natures' Crops, Kensington PEI, Canada], 25% coconut oil [Bioriginal] and 25% olive oil [LIPOID purified olive oil, Ph. Eur., Lipoid AG, Steinhausen, Switzerland]) was added as oil phase. α-Tocopherol (Type V, ~1000 IU/g; Sigma-Aldrich, St. Louis MO, USA) was supplemented at a final concentration of 0.016% and purified water was added to reach the final volume of 50 ml. The coarse emulsion was processed by high-pressure homogenization on a ShearJet HL60 (Dyhydromatics, Maynard MA, USA) equipped with a 75.1T reaction chamber for 6 cycles at a set process pressure of 22 kpsi (1517 bar). The manufacturing process was varied for the used cooling unit, the insertion of a backpressure module and type of feeder. Variable

parameters are displayed in Tab. 6.1. The 200.2 L backpressure module and the long heat exchanger were taken from the ShearJet PL300, where previous emulsions had been manufactured on.

Tab. 6.1: Variable process parameters evaluated for the identification of an optimal manufacturing setup

Variable Parameter	Different levels studied		
Cooling unit	short (5 cm length, 4 cm diameter, 7 coil windings)	long (21 cm length, 7 cm diameter, 27 coil windings)	none
Backpressure module	none	downstream of reaction chamber	upstream of reaction chamber
Type of feeder	stainless steel reservoir	plastic syringe	

Emulsions were characterized before and after autoclaving. For autoclaving, pH was adjusted to 8.5-9.5 with 1 M NaOH. Emulsions were filled in glass vials, the headspace was covered with inert gas (Argon 5.0, PanGas AG, Dagmersellen, Switzerland) and the vial was crimped. Emulsions were sterilized by autoclaving for 15 min at 121 °C at 2 bars (Systec DE-23, Systec GmbH, Linden, Germany). Droplet size was measured by dynamic light scattering (Malvern Zetasizer 3000 HS A, Malvern Instruments, Malvern, UK). The primary oxidation products were quantified according to the method described in Chapter 2, "Quantification of Lipid Oxidation Products in Lipid Emulsions Requiring Minimal Sample Volume", using the mFOX assay. Secondary oxidation products were quantified according to the TBARS assay, detailed in Chapter 2. Total free fatty acids were quantified by fluorescence detection after labelling with a fluorophore and separation by high-pressure liquid chromatography, as described in Chapter 3, "Determination of Free Fatty Acids in Lipid Emulsions by Fluorescence-Detection Based High Performance Liquid Chromatography".

6.3 Results

A total number of 48 emulsions with different oil types were produced in the course of this study, considering the autoclaving step gave rise to 96 data points per parameter. The thermal stress from autoclaving did only have a minor impact on the emulsions' characteristics. The composition within one subset for each oil type remained constant to allow meaningful comparison. All emulsions were produced at a constant batch size of 50 ml and a set process pressure of 22 kpsi (1517 bar). With regard to formation of oxidative degradation products, an ideal batch size of 50 ml and process pressure of 22 kpsi was identified in preliminary experiments (data not shown). The batch size is to be chosen as low as possible to minimize resource consumption, but also had an influence on the obtained oxidation parameters. Below as well as above 50-100 ml, increased oxidation levels were encountered. Further studies did not reveal the reason for this phenomenon. Formulations with the minimal batch size possible for the machine, 10 ml, were paused in between cycles to mimic the time required for processing a higher batch size, but still yielded increased oxidation values. Also batch-processing higher volumes in smaller steps and subsequent pooling counter-intuitively lead to increased values, excluding exposure time as a major influence factor. The stainless steel reservoir has a volume of 100 ml, when working with volumes above this threshold level, two containers need to be used for the manufacturing while otherwise the product can be cycled back into the original container, possibly leading to more efficient homogenization. The increased values of smaller batch sizes could be explained by a smaller dilution factor of the oxidative stress of the initial acceleration at the beginning of each cycle until the machine is running.

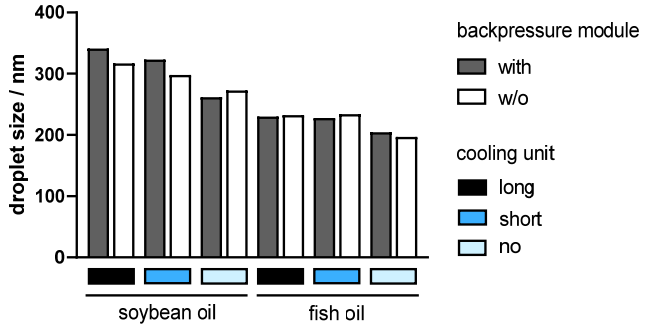

Fig. 6.1: Comparison of droplet sizes of autoclaved emulsions manufactured using the backpressure module inserted downstream of the reaction chamber and without it (n=1). Use of the backpressure module is indicated with grey bars, while direct transfer from the reaction chamber to the outlet is indicated with white bars.

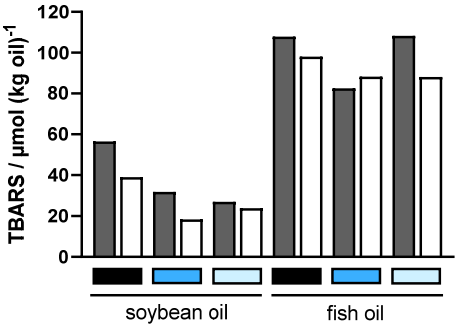

Fig. 6.2: Secondary oxidation products of autoclaved emulsions to investigate the effect of the back-pressure module on oxidation (n=1). The values of untreated oils are 0 µmol/ kg oil for soybean oil and 3.6 µmol/kg oil for fish oil. Color codes, see Fig. 6.1.

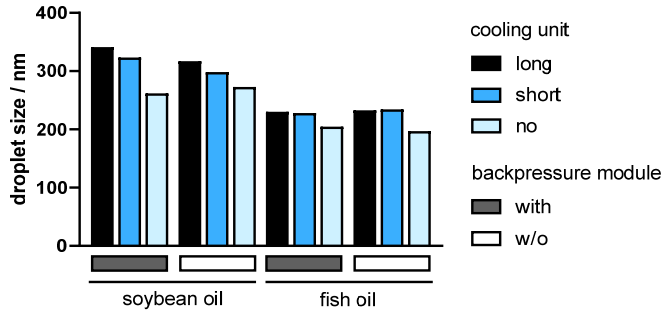

Fig. 6.3: Droplet size of non-autoclaved emulsions (same emulsions as in Fig. 6.1) depending on the cooling system (n=1). The long cooling unit is shown as black bars, the short cooling unit in blue and omission of cooling with light blue bars.

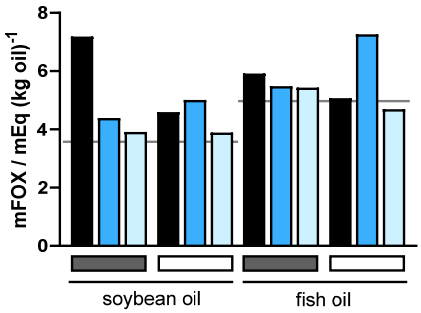

Fig. 6.4: Influence of the cooling system on primary oxidation products of emulsions right after manufacturing (n=1). Reference values of untreated oils are indicated with grey horizontal lines. Color codes, see Fig. 6.3.

On average, a yield of 95-98% of the starting volume was achieved when using the open reservoir compared to values between 80-90% when using the plastic syringes, depending on the number of cycles homogenized. The yield of emulsions prepared using plastic syringes to feed the material was not optimal as the feeding syringe could not be emptied as much as the open reservoir. Instead, a resistant pressure built up from the outlet side, and as soon as the receiving syringe at the outlet was removed (and thus the resistance removed), the pressure was released and some product squirted out. Use of the backpressure module installed downstream of the reaction chamber resulted only in a minimal effect on the droplet size, as shown exemplary for autoclaved emulsions in Fig. 6.1 and Fig. 6.5. The largest difference is seen for soybean oil-based emulsions where use of the backpressure module lead to minimally larger droplet sizes. Upstream insertion of the backpressure module also did not lead to considerable changes in the droplet size. Comparing the obtained droplet sizes, the strongest influence can be attributed to the used oil type: droplets of fish oil emulsions were smaller than droplets of emulsions with soybean oil, SMOF or Formula #3. This distribution also corresponds to the used oil-to-lecithin ratio, which was 8.3 for the fish oil emulsions and 16.7 for the other three compositions. The used cooling unit also had an effect on the obtained droplet size, this time shown for the emulsions prior to autoclaving in Fig. 6.3 and Fig. 6.7. While the measured difference between the droplet size of emulsions produced using the long and the short cooling unit remained below 10%, complete omission of the cooling decreased the obtained droplet size by more than 15% with a maximum difference of 30.4% again seen for soybean oil. The same trend is seen when manufacturing emulsions using the syringe

setup (data in Appendix, see Fig. A17-Fig. A19), where also smaller droplet sizes result from omitting the cooling. Using syringes instead of the open stainless steel feeder generally led to smaller droplet sizes. Nevertheless, through the sealing in syringes, the coarse pre-mix was not accessible from outside and no constant mixing of the unprocessed emulsion in the feeding syringe was possible. This led to a rapid de-mixing and then isolated homogenization of the two phases, occasionally requiring more homogenization cycles to homogenize until no isolated lipid droplets floating on top were visible anymore. Especially in situations of insufficient premixing or de-mixing because of the inaccessibility of the system, cooling was sensitive. Excessive cooling in these cases led to solidification of the isolated oil phase. Solidification of isolated oil under excessive cooling also bore the risk of clogging the instrument.

The influence of the manufacturing parameters on the primary oxidation products is shown in Fig. 6.4 and Fig. 6.6, this time shown as representative example the non-autoclaved emulsions produced with soybean oil and fish oil and autoclaved emulsions with SMOFlipid and Formula #3 oil mixture. Highest values were measured when using the backpressure module, irrespective of the insertion position. The situation with regard to the influence of the cooling system is inconclusive, for soybean oil the highest value is obtained when using the long cooling unit, while for the other oil types highest values are obtained while using the short cooling unit. Again, clustering based on the used oil type can be observed, emulsions prepared from soybean oil yielded the lowest values of primary oxidation products overall. The influence of the homogenization process itself is visualized in Fig. 6.4, the increase compared to reference values of unprocessed oils is marginal.

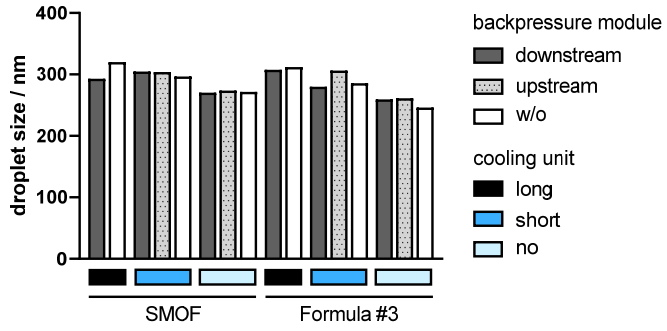

Fig. 6.5: Droplet sizes of autoclaved SMOFlipid and Formula #3-based emulsions manufactured using the backpressure module and without it (n=1). Meanings of colors, as indicated.

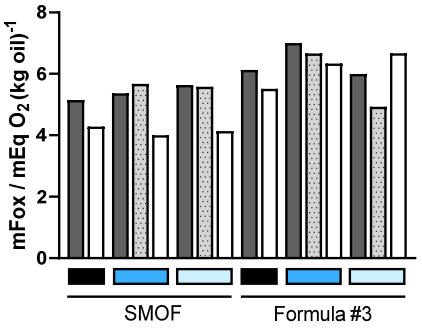

Fig. 6.6: Primary oxidation products of autoclaved emulsions depending on the use of the back-pressure module (n=1). Color codes, see Fig. 6.5.

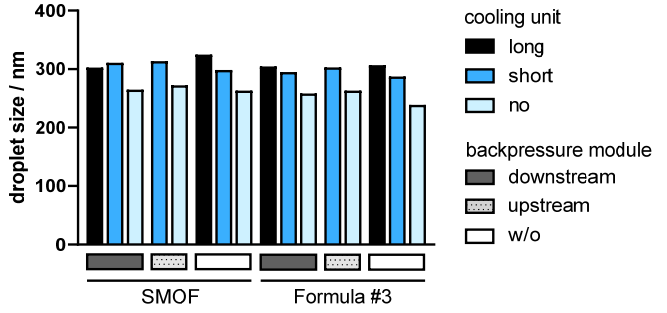

Fig. 6.7: Droplet sizes of non-autoclaved SMOFlipid and Formula #3-based emulsions (same emulsions as in Fig. 6.5) manufactured using different cooling setups (n=1). Color codes, as indicated.

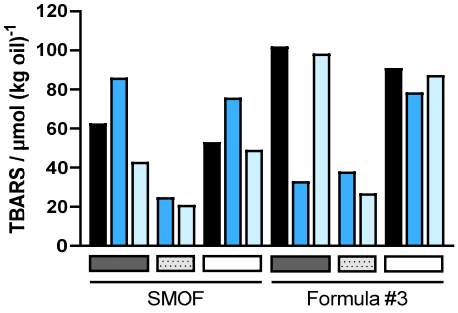

Fig. 6.8: TBARS of autoclaved emulsions and influence of the cooling system (n=1). Colour codes, see Fig. 6.7.

For the secondary oxidation products, the main contributor was the homogenization process itself. The increase compared to reference values from unprocessed oil was up to 30-fold. Same as for the primary oxidation products, a trend based on the used oil type can be observed, especially pronounced when comparing soybean and fish oil-based emulsions in Fig. 6.2. When omitting the backpressure module, lower or equal values were obtained, with the exception of Formula #3 in Fig. 6.8 for the short cooling unit. This is the only case where the insertion of the backpressure module upstream of the reaction chamber resulted in a reduction of the oxidation parameters. The influence of the choice of the cooling setup on the product characteristics is less conclusive. Also, the relative difference between the corresponding samples produced with the same oil type and backpressure setup is – again with the exception of the short cooling unit for Formula #3 and the long cooling unit where the relative difference was > 50% – much smaller. For soybean and SMOF-oil based emulsions, no cooling led to the lowest values, while for the other two oil types use of the short cooling unit gave rise to the lowest values.

Meanwhile, no influence of the manufacturing setup could be found on the hydrolysis products by measuring the free fatty acids (data not shown). The values were generally lower than the corresponding commercial references. For soybean oil emulsions, an average of 30% of the value of Intralipid was found, for fish oil emulsions similar values were obtained, equaling to only 6% of the reference value obtained for Omegaven.

6.4 Discussion

The short cooling coil, no backpressure module and a stainless steel reservoir represent the standard setup of the ShearJet HL60. Use of plastic syringes did not prove beneficial for practical reasons. On the one hand, the yield was reduced through product loss while exchanging syringes in between cycles. For possible working with radioactive material later on to study the biodistribution, this is not acceptable as there is the risk of contamination. The syringe adapters are only compatible with the small cooling unit, not the long heat exchanger, therefore this combination could not be studied. The oxidation products formed in emulsions prepared using syringes to feed were increased on average compared to formulations produced with the open reservoir and the physical stability was reduced. The hypothesis was established that the orifice of the syringe adapter is smaller than the one for the reservoir, leading to a turbulent instead of a laminar flow. If air is entrapped inside the lipid droplets, this negatively impacts the physical stability as well as promotes oxidative degradation. It could also be that the fittings were not as tight as for the reservoir and that air was sucked in at the connections, although additional sealing with Teflon band and/or parafilm did not improve the situation. Inclusion of air bubbles inside lipid droplets will diminish all efforts of packing under protecting atmosphere, if the oxygen is already trapped inside the formulation. This is suspected to happen when working with the syringe setup. Moreover, entrapped air will also markedly lower the physical stability.[132] Eventually, any gasses incorporated will be gassing out and rise to the surface, thereby also promoting phase separation. Without the input of additional energy after gassing out (i.e. re-working after some days) spontaneous re-emulsification is very unlikely. It is then energetically more favourable for the phases to separate and to form two individual layers.

The size of the syringe and the material can be freely chosen, although in our case only 10, 20, and 50 ml plastic syringes were evaluated. The same is true for the open reservoir, in this project only two 100 ml cylinders made from either glass or stainless steel were studied. From the short interaction time no influence of the material on the product is expected. Glass should be inert anyways, and the other surfaces the product later on comes into contact with (reaction chamber, cooling coil) are made from stainless

steel, so contact with this material cannot be avoided anyways. With the glass reservoir, emptying can be visually observed better as the machine should never run dry. This is on the one hand to prevent collapsing of the narrow paths in the reaction chamber and thereby permanent damage to the costly reaction chamber but also intentional incorporation of air into the product that would negatively impact the chemical and physical stability. With the stainless steel reservoir on the other hand, it is possible to insert an inline-thermometer to monitor the product temperature.

The oxidation values of initial emulsions produced on the ShearJet HL60 were elevated compared to previous experience from working on the ShearJet PL300. To check for a possible benefit, extension of the cooling by installing the heat exchanger of the ShearJet PL300 on the ShearJet HL60 was examined. Intuitively, the colder and longer the cooling, the better for the product to minimize the extent of oxidative degradation (under the assumption that – according to the Arrhenius law – at increased temperature also degradation reactions occur faster). However, excessive cooling is also to be avoided, as triglycerides may solidify at a higher temperature than water. The melting temperature of triglycerides depends on the degree of unsaturation and how densely they can be packed.[399] The higher the degree of unsaturation, the lower the melting point. Fish oil with a high number of unsaturated bonds remains liquid in the fridge, while coconut oil, the almost fully saturated and rather short-chained FAs (according to Tab. 1.2, General Introduction, 80% C14 and shorter fully saturated FAs, 91.5% total SFA) melt only above 30 °C. This can become an issue in too harsh cooling. We observed that if the temperature dropped below 15 °C (in a mixture the melting point is lowered), the lipid phase started to solidify, was separated from the rest of the formulation and this was thought to further increase the stress of the separated lipid phase. Inside an emulsion on the other hand, the lipids are better protected from stress, and thus also proper pre-mixing should reduce the oxidative degradation. Efficient pre-mixing experimentally also reduced the number of required cycles and thus also lowered total oxidative stress.

In summary, the cooling parameters can have a considerable influence on the products' characteristics and determining the right cooling temperature and duration is important to minimize oxidative degradation. Some phenomena counteract each other, so it is not automatically the colder the better, but one or several local optima may exist. In our studies, no striking benefit of extending the cooling unit at the cost of the increased minimal batch size was detected. The data rather hint towards complete omission of any cooling, although the product temperature then reached levels of up to 75 °C and it remains questionable how such a thermal stress is not reflected in the measurement of the oxidative degradation products. One explanation could be that all the oxidation products have been oxidized further to subsequent degradation products not captured with our current assays. For this hesitation, it was decided to continue working with the standard short cooling unit. Although the omission of the cooling unit led to smaller droplet sizes, all produced emulsions met the target droplet size < 350 nm.

Some commercially available machines (Microfluidizer M-110Y, Dyhydromatics ShearJet PL300, see Chapter 1, General Introduction) are equipped with a backpressure module by default, and thus also a potential benefit for the Dyhydromatics ShearJet HL60 was studied by inserting a backpressure module downstream of the reaction chamber. When using the Microfluidizer M-110Y with the H30Z (Z-type) interaction chamber, the manufacturer recommends introducing the backpressure module upstream of the interaction chamber. Instead of modulating the pressure drop it then acts to pre-mix the unprocessed mixture prior to the Z-type interaction chamber with less efficient homogenization properties than the Y-type interaction chamber. For this reason, also runs with the backpressure module introduced upstream of the reaction chamber were conducted and evaluated in an attempt to identify the optimal manufacturing setup. Also here, deviation from the standard process did not result in a reward. The droplet

size was increased and the oxidation parameters were not lowered. Study of a single oxidation parameter alone is meaningless, only both parameters combined allow the drawing of reasonable conclusions. As the generation of oxidation products are interlinked, a reduction of the primary oxidation products may in turn lead to an increase in the secondary oxidation products. Based on our results, the strongest contribution was attributed to the used oil type and – for the secondary oxidation products – the homogenization process itself.

The free fatty acids were only minimally affected by the manufacturing setup. All values remained well below the thresholds levels of commercial references and were thus not considered as indicative for identifying an optimal manufacturing setup. All emulsions are only n=1 and we should not draw too many conclusions from these results yet. However, these studies conducted either identified trends in terms of avoiding the generation of oxidative degradation products or revealed practical limitations of deviating from the standard manufacturing protocol.

6.5 Conclusion

For practical reasons, use of syringes to feed the product was abandoned and not studied further. The introduction of a backpressure module either up- or downstream of the reaction chamber only had a marginal effect on the droplet size and no consistent benefit on the measured degradation products. The same is true for extending the cooling unit where increased levels of degradation products were found when using the elongated cooling unit. Omitting the cooling at all led to a smaller droplet size with inconclusive impact on the oxidation products. No studied alteration from the standard process setup proved consistently superior regarding lipid oxidation in all four studied formulations. Changes to the manufacturing process seem to be less suited as means to lower the degradation products. Instead, further studies of incorporating excipients into the formulation to reduce oxidation are indicated. For routine production of our emulsions, we will use the standard setup with the installed open feeder, no backpressure module and the standard short cooling unit, resulting in a product outlet temperature around 15 °C.

7 FINAL DISCUSSION AND FUTURE PERSPECTIVES

Need for innovation

In particular in preterm infants, timely use of PN is critical to ensure proper supply of nutrients and avoid deficiencies.[21,400] Due to transient gut immaturity, preterm infants do not tolerate enteral nutrition yet and most preterm infants receive PN for at least the first few days of their life.[8,401] Lipid emulsions are important constituents of PN; studies in preterm infants showed that biochemical signs of essential fatty acid deficiencies can develop within already 72 hours[402,403] of insufficient provision with essential fatty acids and after 7 days also clinical signs are apparent.[404]

Intralipid as most commonly used parenteral lipid emulsions is based on soybean oil rich in *n*−6 PUFAs, but lacks adequate levels of *n*−3 PUFAs.[28,62] In recent years, strong evidence has emerged on the health benefits of *n*−3 PUFAs in the diet for the prevention of cardiovascular diseases[405,406], maintenance of neurological function[407] and healthier aging[408], inflammatory conditions[406,409]. These findings have also been extended to PN.[410] Particularly for use in preterm infants, sufficient supply with *n*−3 PUFAs is required to ensure proper neurological development.[411,412] For this reason, further use of Intralipid in preterm infants is not adequate anymore.[413] Growth or developmental delays can affect patients' health and wellbeing for the rest of their lives and thus need to be prevented as much as possible.[401]

In this work we described the manufacturing of a lipid emulsion formulation based on a composite plant-derived oil component rich in shorter *n*−3 PUFA. We started by evaluating different modes of manufacturing and decided to acquire an electrically-powered high-pressure homogenizer to overcome the shortcomings of insufficient stable supply of high-pressure air supply in our laboratories. We then demonstrated that it is possible to reproducibly manufacture lipid emulsions on the new machine with consistent physical characteristics. Replacing the oil type did not alter the obtained physical product properties and the droplet sizes of the commercial references could successfully be mimicked. Processing the coarse emulsions on a Dyhydromatics ShearJet HL60 at a process pressure of 1500-1600 bar yielded the desired characteristics in six cycles. Using two different techniques, dynamic light scattering[187,188] and scanning electron microscopy[191–194], a narrow droplet size distribution of our formulations was shown and regulatory compliance with the mean droplet size and PFAT5 requirement[130,163,169] for the prevention of lipid embolisms set by the United States Pharmacopoeia was proven.

The Formula #3 oil mixture was invented by Dr. Eliana Lucchinetti, the residual composition of the lipid emulsion (i.e., isotonicity agent, antioxidant, phospholipid concentration) was inspired from the composition of currently existing formulations.[28,79] Egg phospholipids[153] proved to be most effective for the production of physically stable lipid emulsions with narrow droplet size distributions. While guidelines exist for the physical parameters, no equivalent requirements are set for the chemical stability. Unsaturated fatty acids, while essential for ensuring normal functioning of the body[28], are susceptible to lipid oxidation and thus detrimental to product quality.[198–200] Moreover, patients weakened from a primary condition requiring the use of parenteral nutrition should be spared from further harm from oxidized lipids impairing cardiovascular health and promoting oxidative stress.[18,296–298]

Implementation of assays for the quantification of the degree of lipid oxidation built the essential cornerstone for the successful development of lipid emulsions suitable for clinical use. The successful development of two spectrophotometric assays for the quantification of lipid oxidation products using minimal sample volume in a 96-well plate allowed to timely characterize the manufactured emulsions and optimize the composition accordingly. Due to the lack of pharmacopoeial limits for lipid oxidation

products, the values determined from commercial references were used as benchmarks. The newly introduced plant-based composite oil mixture rich in *n*−3 PUFA was highly susceptible to oxidative degradation, primarily due to the newly introduced Ahiflower oil with > 92% of mono- and polyunsaturated FAs. EDTA[126,239,294] was added at a final concentration of 2.5 µM as metal chelator to scavenge divalent metal ions stemming from the equipment surface that could act as prooxidants for the generation of secondary oxidation products while α-tocopherol[18,116,141,270] was added at 152 mg per liter of emulsion (760 mg (kg oil)$^{-1}$) as potent antioxidant also endogenously present in certain oil sources. For considerations of accumulation in a therapy setting where lipid emulsions are continuously administered over longer periods (> 14 days), the EDTA concentration was chosen as low as possible to still reach levels of secondary oxidation products similar to those found in commercial lipid emulsions for PN. Concentrations of α-tocopherol were chosen similar to the levels found in commercial lipid emulsions. While EDTA is neither present in Intralipid nor Omegaven, both formulations also contain α-tocopherol.[28] Intralipid contains only little α-tocopherol, but primarily the isoform γ-tocopherol. Total tocopherol contents in both formulations range around 190 mg (L emulsion)$^{-1}$ (950 mg (kg oil)$^{-1}$) and 150-300 mg (L emulsion)$^{-1}$ (1.5-3 g (kg oil)$^{-1}$) in Intralipid and Omegaven, respectively. Through the incorporation of these excipients, the primary oxidation products were reduced to 1.95-fold the level of Intralipid and 0.25-fold the level of Omegaven. The secondary oxidation products were measured at 43.6-fold and 1.22-fold the levels of Intralipid and Omegaven, respectively. Further screening for suitable excipients to lower the secondary oxidation products may be needed, although no toxic effects were observed from the increased (mainly secondary) oxidation products in the *in vitro* cell viability experiments as well as after 7 days infusion for total parenteral nutrition in mice by our collaborators. The total FFAs complied with the limits stated by the United States Pharmacopoeia[168] and were measured at 27% and 6% of the corresponding levels of Intralipid and Omegaven. FFAs are again crucial to be limited particularly for the use of lipid emulsions in preterm infants: Excess FFAs may bind to albumin and compete with bilirubin. Increased bilirubin levels in infants in turn may lead to jaundice with possible progression up to severe neurotoxicity.[305–309]

Reduced droplet size

Following evidence from literature that smaller lipid droplets are extracted slower and accumulate less in the liver[36,369,376], a formulation with < 200 nm droplet size has been developed. The droplet size reduction was achieved by adding high amounts of glucose to the formulation prior to homogenization, but otherwise maintaining the process parameters (homogenization cycle number, process pressure) and by keeping the oil-to-surfactant ratio at the same level as Omegaven. With this, a droplet size reduction down to 35% of the initial value was achieved. An intermediary formulation at 56% of the original droplet size (161 nm) was chosen as starting point for further improvements. Through the reduced droplet size and the high glucose concentration, the oxidation products were increased. By increasing the EDTA concentrations 4.75-fold, the elevation of secondary oxidation products was successfully reverted back to the original range. The primary oxidation products were still increased at 8-fold of the original level. Further innovation is needed to identify a way – either by adding suitable excipients or by modifying the manufacturing process – to lower the primary oxidation products.

Optimizations of the manufacturing process and scale-up

Changes to the manufacturing process to alleviate the pressure drop from the high process pressure to atmospheric conditions potentially harming the lipids as well as improving the cooling of the product to spare from the heat of compression did not reduce the formation of oxidative degradation products.

However, for a future transition to a clinical setting, scale-up and transfer to a good manufacturing practice (GMP)-compliant environment is needed.[346,390,414] By chance, this holds the potential of further reducing the lipid oxidation. In an enclosed space in an insulator, and by flushing with inert gas (*e.g.,* nitrogen), atmospheric oxygen can be prevented from coming into contact with the products. This was not available in the current academic setting so far.

The current product output of the machine is limited at 7-10 ml processed emulsion per minute.[415] For supply of clinical trials with larger quantities required, the switch from the current pilot-scale to an industry-scale homogenizer is likely needed. Dyhydromatics also offers large-scale homogenizers with the promise that process parameters can easily be transferred from the pilot scale instrument. Large-scale homogenizers also work with two complementary pumps, so that the high pressure is always maintained and stress from the rapid acceleration is effectively diminished. Efforts to scale-up may therefore incidentally lead to a reduction of the oxidation parameters.

Further insights are needed for the determination of an appropriate shelf-life.[295] Up to now, oxidation was the limiting factor defining for how long the emulsions could be used in *in vivo* experiments. However, these findings were compromised from oxygen entering through multiply pierced rubber stoppers. If left alone and not repeatedly sampled the physical stability becomes the limiting factor with signs of creaming around 6 months after manufacturing. In the current setting, it was feasible to have a fresh production every 3 months. However, for future applications further insights into the degradation pathways are needed to define appropriate shelf-lives and also take preventive measures for an effective improvement of the duration a product can still be used.

Tissue distribution

In our biodistribution studies in mice, a consistently high uptake in the lung was found (> SUV 15) for both *n*−6 PUFA rich soybean oil and *n*−3 PUFA-rich plant oil-based emulsions. This pattern was reproduced for both formulations also at a reduced droplet size, although the effect was less pronounced. *n*−3 PUFA-rich formulations cleared faster from blood and plasma than soybean oil-based formulations. This is in agreement with Qi *et al.*'s report from 2002[332], however, in a different report[366], slower blood clearance was found for pure fish oil-based emulsions. Addition of medium-chain triglycerides and *n*−6 long chain triglycerides to fish oil again accelerated the blood clearance, making it even faster than MCT/*n*−6 long chain PUFA alone.[333,366] For an accelerated blood clearance of *n*−3 rich oils thus the addition of MCT seems crucial. This condition is fulfilled in our case where apart from the *n*−3 PUFA rich Ahiflower oil also coconut oil rich in MCT is injected. Qi *et al.* in 2003 further confirmed the effect of fish oil addition leading to a more rapid blood clearance, with a size-dependent effect size, which was more pronounced for larger lipid droplet sizes.[394] In our experiment, no difference in the blood clearance between 170 nm and 285 nm sized soybean emulsions was found.

Pure fish oil-based formulations have not been studied yet in our experiments. To confirm the lipid type as driver for the blood clearance, formulations based on *n*−3 PUFA-rich fish oil or addition of alternative oil sources to the Formula #3 oil mixture could be prepared as in the example of commercial SMOFlipid and studied accordingly. Also different mixing ratios of *n*−6 rich soybean oil and *n*−3 rich Formula #3 within the same formulations might reveal a dose-dependent shift in blood clearance. Similar considerations can also be done for the droplet size. Further droplet size levels could be prepared to determine a size-dependent effect, then also with a control sample for the increased glucose administration.

Tissue distribution studies to identify optimal experimental parameters (injection volume/lipid dose, organs of interest, incubation times, administration mode) have been conducted in a pilot setup style to

reduce unnecessary animal experiments, but need to be confirmed for the optimal conditions at higher replicate numbers for consolidated, statistically sound statements. With all these further requests for animal studies, animal welfare considerations need not be forgotten to only perform animal studies if the information cannot be obtained by other means and all experimental designs need to be carefully set up.

For easier handling, commercial availability and a long physical (decay) half-life, biodistribution studies have so far been conducted with the long-lived isotope ^{3}H.[416] They come with the drawback of low tissue penetration of the emitted radiation and thus the need for tissue dissection, solubilization and discoloration for analysis. Efforts will continue to develop a ^{11}C-radiolabelled triglyceride radiotracer to study the time-resolved tissue distribution of lipid emulsions by positron emission tomography.[417–419] This then allows the analysis of multiple time points per animal. This may even allow to follow the *in vivo* metabolism of triglycerides after administration, by identifying and quantifying the radiometabolites by HPLC with radiodetection or trapping in a cartridge for ^{11}C-carbonate. Our center (Radiopharmaceutical Science at the ETH) is currently establishing a method for FA and triglyceride labelling, under the supervision of Dr. Linjing Mu in our research group.

Obtaining formulations with a balanced tissue distribution, *i.e.* less uptake in the liver, is the outcome we can assess with our available techniques. What we ultimately aim for, however, is achieving a reduced inflammatory, potentially even anti-inflammatory action, and this is only confirmed in a long-term *in vivo* setting. These are the clinically relevant conditions and it may well be that this is also achieved independent of lower liver uptake. Uptake in the liver alone may not be harmful, if the formulation is rich in *n*−3 and the anti-inflammatory action of *n*−3 is strong in the liver, high uptake does not necessarily lead to promoted inflammation. In parallel, our 285 nm-sized formulation with the *n*−3 PUFA rich plant-based oil source was evaluated in a continuous infusion setting over 7 days in mice by our project partners Prof. Michael Zaugg (University of Alberta, Edmonton, Canada) and Dr. Eliana Lucchinetti (University of Alberta, Edmonton, Canada).[386] Compared to the two reference emulsions Intralipid and Omegaven, our emulsion lead to more beneficial biological effects (see joint manuscript). A patent has been filed to the European Patent Office and is still under embargo.

Before we can also translate the formulations with the reduced droplet size to the 7 day-*in vivo* setup, toxicity from elevated (mainly primary) oxidation products needs to be excluded. For 285 nm sized emulsions in a long-term setting over 7 days, no toxic effects were found due to increased – for the 285 nm-sized formulations compared to Omegaven secondary – oxidation products. However, we do not know how these elevated levels can act as confounders for the tissue distribution – or worst case – the inflammatory reactions in the body. Although we did not see acute toxicity in our tissue distribution studies with maximally 60 minutes observation period after injection, this is not guaranteed that these effects also directly translate to the 7-day infusion setting and reproduce the anti-inflammatory effects seen with 285-nm-sized Formula #3 lipid emulsion.

Conclusion

A novel lipid emulsion suitable for parenteral nutrition with the potential to change paradigms in clinical use was successfully developed. Exchanging the oil source from a *n*−6 PUFA rich soybean oil to a plant-based *n*−3 PUFA rich oil source with lower phytosterol levels and increased supplemented α-tocopherol levels showed promising effects on immune markers *in vivo*, as concluded by our project partners. The clinical benefits need to be confirmed in subsequent studies. Upcoming activities including attempts towards the time resolved imaging of the tissue distribution and scale-up of the production to support the further development towards clinical translation are the challenges awaiting us next.

8 REFERENCES

1. Compher, C.; Bingham, A. L.; McCall, M.; Patel, J.; Rice, T. W.; Braunschweig, C.; McKeever, L. Guidelines for the Provision of Nutrition Support Therapy in the Adult Critically Ill Patient: The American Society for Parenteral and Enteral Nutrition. *J. Parenter. Enter. Nutr.* **2022**, *46* (1), 12–41.
2. Pironi, L.; Boeykens, K.; Bozzetti, F.; Joly, F.; Klek, S.; Lal, S.; Lichota, M.; Mühlebach, S.; Van Gossum, A.; Wanten, G.; et al. ESPEN Guideline on Home Parenteral Nutrition. *Clin. Nutr.* **2020**, *39* (6), 1645–1666.
3. Bischoff, S. C.; Austin, P.; Boeykens, K.; Chourdakis, M.; Cuerda, C.; Jonkers-Schuitema, C.; Lichota, M.; Nyulasi, I.; Schneider, S. M.; Stanga, Z.; et al. ESPEN Practical Guideline: Home Enteral Nutrition. *Clin. Nutr.* **2022**, *41* (2), 468–488.
4. Bischoff, S. C.; Escher, J.; Hébuterne, X.; Kłęk, S.; Krznaric, Z.; Schneider, S.; Shamir, R.; Stardelova, K.; Wierdsma, N.; Wiskin, A. E.; et al. ESPEN Practical Guideline: Clinical Nutrition in Inflammatory Bowel Disease. *Clin. Nutr.* **2020**, *39* (3), 632–653.
5. Cuerda, C.; Pironi, L.; Arends, J.; Bozzetti, F.; Gillanders, L.; Jeppesen, P. B.; Joly, F.; Kelly, D.; Lal, S.; Staun, M.; et al. ESPEN Practical Guideline: Clinical Nutrition in Chronic Intestinal Failure. *Clin. Nutr.* **2021**, *40* (9), 5196–5220.
6. Muscaritoli, M.; Arends, J.; Bachmann, P.; Baracos, V.; Barthelemy, N.; Bertz, H.; Bozzetti, F.; Hütterer, E.; Isenring, E.; Kaasa, S.; et al. ESPEN Practical Guideline: Clinical Nutrition in Cancer. *Clin. Nutr.* **2021**, *40* (5), 2898–2913.
7. Bozzetti, F.; Caccialanza, R.; Cotogni, P.; Finocchiaro, C.; Pironi, L.; Santarpia, L.; Zanetti, M. SINPE Position Paper on the Use of Home Parenteral Nutrition in Cancer Patients. *Nutrition* **2022**, *95*, 111578.
8. Bronsky, J.; Moltu, S. J.; Puntis, J.; Szitanyi, P.; Fidler Mis, N.; Lapillonne, A.; Cai, W.; Mihályi, K.; Prell, C.; Koletzko, B.; et al. ESPGHAN/ESPEN/ESPR/CSPEN Guidelines on Pediatric Parenteral Nutrition: Lipids. *Clin. Nutr.* **2018**, *37* (6), 2324–2336.
9. Rochling, F. A. Intravenous Lipid Emulsions in the Prevention and Treatment of Liver Disease in Intestinal Failure. *Nutrients* **2021**, *13* (3), 895.
10. Alja'nini, Z.; Merlino-Barr, S.; Brumfiel, A.; McNelis, K.; Viswanathan, S.; Collin, M.; Groh-Wargo, S. Effect of Parenteral Nutrition Duration on Patterns of Growth and Body Composition in Very Low-birth-weight Premature Infants. *J. Parenter. Enter. Nutr.* **2021**, *45* (8), 1673–1682.
11. Wanden-Berghe, C.; Virgili Casas, N.; Cuerda Compés, C.; Ramos Boluda, E.; Pereira Cunill, J. L.; Maíz Jiménez, M. I.; Burgos Peláez, R.; Gómez Candela, C.; Penacho Lázaro, M. Á.; Sánchez Martos, E. Á.; et al. Home and Ambulatory Artificial Nutrition (NADYA) Group Report: Home Parenteral Nutrition in Spain, 2019. *Nutr. Hosp.* **2021**, *38* (6), 1304–1309.
12. Pironi, L.; Candusso, M.; Biondo, A.; Bosco, A.; Castaldi, P.; Contaldo, F.; Finocchiaro, E.; Giannoni, A.; Mazzuoli, S.; Orlandoni, P.; et al. Prevalence of Home Artificial Nutrition in Italy in 2005: A Survey by the Italian Society for Parenteral and Enteral Nutrition (SINPE). *Clin. Nutr.* **2007**, *26* (1), 123–132.
13. Goulet, O.; Breton, A.; Coste, M.-E.; Dubern, B.; Ecochard-Dugelay, E.; Guimber, D.; Loras-Duclaux, I.; Abi Nader, E.; Marinier, E.; Peretti, N.; et al. Pediatric Home Parenteral Nutrition in France: A Six Years National Survey. *Clin. Nutr.* **2021**, *40* (10), 5278–5287.
14. Folwarski, M.; Kłęk, S.; Szlagatys-Sidorkiewicz, A.; Wyszomirski, A.; Brzeziński, M.; Skotnicka, M. Trend Observations in Home Parenteral Nutrition. Prevalence, Hospitalizations and Costs: Results from a Nationwide Analysis of Health Care Provider Data. *Nutrients* **2021**, *13* (10), 1–11.
15. Storck, L. J.; Ruehlin, M.; Wagener, N.; Moeltgen, C.; Genton, L.; Ballmer, P. E. Results from an Epidemiological Follow-Up Survey on Home Artificial Nutrition in Switzerland from 2010 to 2015. *Ann. Nutr. Metab.* **2020**, *76* (5), 345–353.
16. Arhip, L.; García-Peris, P.; Romero, R. M.; Frías, L.; Bretón, I.; Camblor, M.; Motilla, M.; Velasco, C.; Morales, A.; Carrascal, M. L.; et al. Direct Costs of a Home Parenteral Nutrition Programme. *Clin. Nutr.* **2019**, *38* (4), 1945–1951.
17. Mundi, M. S.; Pattinson, A.; McMahon, M. T.; Davidson, J.; Hurt, R. T. Prevalence of Home Parenteral and Enteral Nutrition in the United States. *Nutr. Clin. Pract.* **2017**, *32* (6), 799–805.
18. Mundi, M. S.; Klek, S.; Martindale, R. G. Use of Lipids in Adult Patients Requiring Parenteral Nutrition in the Home Setting. *J. Parenter. Enter. Nutr.* **2020**, *44* (S1), S39–S44.
19. Arhip, L.; Serrano-Moreno, C.; Romero, I.; Camblor, M.; Cuerda, C. The Economic Costs of Home Parenteral Nutrition: Systematic Review of Partial and Full Economic Evaluations. *Clin. Nutr.* **2021**, *40* (2), 339–349.

20. Eglseer, D.; Huppertz, V.; Kammer, L.; Saka, B.; Schols, J.; Everink, I. The Quality of Nutritional Care in Hospitals: A Comparison between Austria, Switzerland and Turkey. *Nutrition* **2020**, *80*, 110990.
21. Joosten, K.; Embleton, N.; Yan, W.; Senterre, T.; Braegger, C.; Bronsky, J.; Cai, W.; Campoy, C.; Carnielli, V.; Darmaun, D.; et al. ESPGHAN/ESPEN/ESPR/CSPEN Guidelines on Pediatric Parenteral Nutrition: Energy. *Clin. Nutr.* **2018**, *37* (6), 2309–2314.
22. Fell, G. L.; Nandivada, P.; Gura, K. M.; Puder, M. Intravenous Lipid Emulsions in Parenteral Nutrition. *Adv. Nutr.* **2015**, *6* (5), 600–610.
23. Scheurer, D.; Kirkland, L. L. Parenteral Nutrition in the Hospitalized Patient. *Hosp. Med. Clin.* **2012**, *1* (3), e404–e415.
24. Boullata, J. I.; Mirtallo, J. M.; Sacks, G. S.; Salman, G.; Gura, K.; Canada, T.; Maguire, A. Parenteral Nutrition Compatibility and Stability: A Comprehensive Review. *J. Parenter. Enter. Nutr.* **2022**, *46* (2), 273–299.
25. Boullata, J. I.; Berlana, D.; Pietka, M.; Klek, S.; Martindale, R. Use of Intravenous Lipid Emulsions With Parenteral Nutrition: Practical Handling Aspects. *J. Parenter. Enter. Nutr.* **2020**, *44* (S1), S74–S81.
26. Cogle, S. V.; Martindale, R. G.; Ramos, M.; Roberti, G. J.; Roberts, P. R.; Taylor, K.; Sacks, G. S. Multicenter Prospective Evaluation of Parenteral Nutrition Preparation Time and Resource Utilization: 3-Chamber Bags Compared With Hospital Pharmacy–Compounded Bags. *J. Parenter. Enter. Nutr.* **2021**, *45* (7), 1552–1558.
27. Waitzberg, D. L.; Torrinhas, R. S. Fish Oil Lipid Emulsions and Immune Response: What Clinicians Need to Know. *Nutr. Clin. Pract.* **2009**, *24* (4), 487–499.
28. Mundi, M. S.; Salonen, B. R.; Bonnes, S. Home Parenteral Nutrition. *Nutr. Clin. Pract.* **2016**, *31* (5), 629–641.
29. Burdge, G. C.; Calder, P. C. Introduction to Fatty Acids and Lipids. *World Rev. Nutr. Diet.* **2015**, *112*, 1–16.
30. West, A. L.; Miles, E. A.; Lillycrop, K. A.; Napier, J. A.; Calder, P. C.; Burdge, G. C. Genetically Modified Plants Are an Alternative to Oily Fish for Providing n -3 Polyunsaturated Fatty Acids in the Human Diet: A Summary of the Findings of a Biotechnology and Biological Sciences Research Council Funded Project. *Nutr. Bull.* **2021**, *46* (1), 60–68.
31. Molina, T. L.; Stoll, B.; Mohammad, M.; Mohila, C. A.; Call, L.; Cui, L.; Guthrie, G.; Kunichoff, D.; Lin, S.; Welch-Jernigan, R.; et al. New Generation Lipid Emulsions Increase Brain DHA and Improve Body Composition, but Not Short-Term Neurodevelopment in Parenterally-Fed Preterm Piglets. *Brain. Behav. Immun.* **2020**, *85*, 46–56.
32. Chen, I.-L.; Hung, C.-H.; Huang, H.-C. Smoflipid Is Better Than Lipofundin for Long-Term Neurodevelopmental Outcomes in Preterm Infants. *Nutrients* **2021**, *13* (8), 2548.
33. Sadu Singh, B. K.; Narayanan, S. S.; Khor, B. H.; Sahathevan, S.; Abdul Gafor, A. H.; Fiaccadori, E.; Sundram, K.; Karupaiah, T. Composition and Functionality of Lipid Emulsions in Parenteral Nutrition: Examining Evidence in Clinical Applications. *Front. Pharmacol.* **2020**, *11* (April), 506.
34. Mashek, D. G.; Bertics, S. J.; Grummer, R. R. Effects of Intravenous Triacylglycerol Emulsions on Hepatic Metabolism and Blood Metabolites in Fasted Dairy Cows. *J. Dairy Sci.* **2005**, *88* (1), 100–109.
35. Reddy, L. H. V.; Murthy, R. S. R. Lymphatic Transport of Orally Administered Drugs. *Indian J. Exp. Biol.* **2002**, *40* (10), 1097–1109.
36. Rensen, P. C.; Herijgers, N.; Netscher, M. H.; Meskers, S. C.; van Eck, M.; van Berkel, T. J. Particle Size Determines the Specificity of Apolipoprotein E-Containing Triglyceride-Rich Emulsions for the LDL Receptor versus Hepatic Remnant Receptor in Vivo. *J. Lipid Res.* **1997**, *38* (6), 1070–1084.
37. Tamilvanan, S. Oil-in-Water Lipid Emulsions: Implications for Parenteral and Ocular Delivering Systems. *Prog. Lipid Res.* **2004**, *43* (6), 489–533.
38. Handa, T. Lipid Emulsions: Formation, Stability, and Metabolism. In *Encyclopedia of Surface and Colloid Science*; Somasundaran, P. P., Deo, N., Farinato, R., Grassian, V., Lu, M., Malmsten, M., Mittal, K. L., Nagarajan, R., Partha, P., Sukhorukov, G., Wasan, D., Eds.; CRC Press: Boca Raton, 2015; pp 3782–3791.
39. Fahy, E.; Cotter, D.; Sud, M.; Subramaniam, S. Lipid Classification, Structures and Tools. *Biochim. Biophys. Acta - Mol. Cell Biol. Lipids* **2011**, *1811* (11), 637–647.
40. Wanten, G. J.; Calder, P. C. Immune Modulation by Parenteral Lipid Emulsions. *Am J Clin Nutr* **2007**, *85*, 1171–1184.
41. Valenzuela, C. A.; Baker, E. J.; Miles, E. A.; Calder, P. C. Eighteen-carbon Trans Fatty Acids and Inflammation in the Context of Atherosclerosis. *Prog. Lipid Res.* **2019**, *76*, 101009.
42. Ratnayake, W. M. N.; Galli, C. Fat and Fatty Acid Terminology, Methods of Analysis and Fat Digestion and Metabolism: A Background Review Paper. *Ann. Nutr. Metab.* **2009**, *55* (1–3), 8–43.

43. Murray, A. J.; Knight, N. S.; Little, S. E.; Cochlin, L. E.; Clements, M.; Clarke, K. Dietary Long-Chain, but Not Medium-Chain, Triglycerides Impair Exercise Performance and Uncouple Cardiac Mitochondria in Rats. *Nutr. Metab. (Lond).* **2011**, *8* (1), 55.
44. Miles, E. A.; Childs, C. E.; Calder, P. C. Long-Chain Polyunsaturated Fatty Acids (LCPUFAs) and the Developing Immune System: A Narrative Review. *Nutrients* **2021**, *13* (1), 247.
45. Mundi, M. S.; Martindale, R. G.; Hurt, R. T. Emergence of Mixed-Oil Fat Emulsions for Use in Parenteral Nutrition. *J. Parenter. Enter. Nutr.* **2017**, *41* (Suppl 1), 3S-13S.
46. Calder, P. C. Marine Omega-3 Fatty Acids and Inflammatory Processes: Effects, Mechanisms and Clinical Relevance. *Biochim. Biophys. Acta - Mol. Cell Biol. Lipids* **2015**, *1851* (4), 469–484.
47. Miles, E. A.; Calder, P. C. Fatty Acids, Lipid Emulsions and the Immune and Inflammatory Systems. *World Rev. Nutr. Diet.* **2015**, *112*, 17–30.
48. Notz, Q.; Lee, Z.-Y.; Menger, J.; Elke, G.; Hill, A.; Kranke, P.; Roeder, D.; Lotz, C.; Meybohm, P.; Heyland, D. K.; et al. Omega-6 Sparing Effects of Parenteral Lipid Emulsions—an Updated Systematic Review and Meta-Analysis on Clinical Outcomes in Critically Ill Patients. *Crit. Care* **2022**, *26* (1), 23.
49. Wichman, B. E.; Nilson, J.; Govindan, S.; Chen, A.; Jain, A.; Arun, V.; Derdoy, J.; Krebs, J.; Jain, A. K. Beyond Lipids: Novel Mechanisms for Parenteral Nutrition–Associated Liver Disease. *Nutr. Clin. Pract.* **2022**, *37* (2), 265–273.
50. Mundi, M. S.; Bonnes, S. L.; Salonen, B. R.; McMahon, M. M.; Martindale, R.; Hurt, R. T. Clinical Application of Fish-oil Intravenous Lipid Emulsion in Adult Home Parenteral Nutrition Patients. *Nutr. Clin. Pract.* **2021**, *36* (4), 839–852.
51. Goulet, O. J.; Cai, W.; Seo, J. Lipid Emulsion Use in Pediatric Patients Requiring Long-Term Parenteral Nutrition. *J. Parenter. Enter. Nutr.* **2020**, *44* (S1), S55–S67.
52. Miles, E. A.; Calder, P. C. Influence of Marine n -3 Polyunsaturated Fatty Acids on Immune Function and a Systematic Review of Their Effects on Clinical Outcomes in Rheumatoid Arthritis. *Br. J. Nutr.* **2012**, *107* (S2), S171–S184.
53. Schwanke, R. C.; Marcon, R.; Bento, A. F.; Calixto, J. B. EPA- and DHA-Derived Resolvins' Actions in Inflammatory Bowel Disease. *Eur. J. Pharmacol.* **2016**, *785*, 156–164.
54. Duvall, M. G.; Levy, B. D. DHA- and EPA-Derived Resolvins, Protectins, and Maresins in Airway Inflammation. *Eur. J. Pharmacol.* **2016**, *785*, 144–155.
55. Serhan, C. N. Pro-Resolving Lipid Mediators Are Leads for Resolution Physiology. *Nature* **2014**, *510* (7503), 92–101.
56. Patterson, E.; Wall, R.; Fitzgerald, G. F.; Ross, R. P.; Stanton, C. Health Implications of High Dietary Omega-6 Polyunsaturated Fatty Acids. *J. Nutr. Metab.* **2012**, 539426.
57. Balić, A.; Vlašić, D.; Žužul, K.; Marinović, B.; Bukvić Mokos, Z. Omega-3 Versus Omega-6 Polyunsaturated Fatty Acids in the Prevention and Treatment of Inflammatory Skin Diseases. *Int. J. Mol. Sci.* **2020**, *21* (3), 741.
58. Chilton-Lopez, T.; Surette, M. E.; Swan, D. D.; Fonteh, A. N.; Johnson, M. M.; Chilton, F. H. Metabolism of Gammalinolenic Acid in Human Neutrophils. *J. Immunol.* **1996**, *156* (8), 2941–2947.
59. Calder, P. C. N−3 Polyunsaturated Fatty Acids, Inflammation, and Inflammatory Diseases. *Am. J. Clin. Nutr.* **2006**, *83* (6), 1505S-1519S.
60. Calder, P. C.; Waitzberg, D. L.; Klek, S.; Martindale, R. G. Lipids in Parenteral Nutrition: Biological Aspects. *J. Parenter. Enter. Nutr.* **2020**, *44* (S1), S21–S27.
61. Tabor, E. The Complex Pathway to United States Food and Drug Administration Approval of Smoflipid. *J. Parenter. Enter. Nutr.* **2022**, *46* (4), 748–751.
62. Mostad, I. L.; Bjerve, K. S.; Basu, S.; Sutton, P.; Frayn, K. N.; Grill, V. Addition of N-3 Fatty Acids to a 4-Hour Lipid Infusion Does Not Affect Insulin Sensitivity, Insulin Secretion, or Markers of Oxidative Stress in Subjects with Type 2 Diabetes Mellitus. *Metabolism.* **2009**, *58* (12), 1753–1761.
63. Nash, S. M. B.; Schlabach, M.; Nichols, P. D. A Nutritional-Toxicological Assessment of Antarctic Krill Oil versus Fish Oil Dietary Supplements. *Nutrients* **2014**, *6* (9), 3382–3402.
64. Surette, M. E. Dietary Omega-3 PUFA and Health: Stearidonic Acid-Containing Seed Oils as Effective and Sustainable Alternatives to Traditional Marine Oils. *Mol. Nutr. Food Res.* **2013**, *57* (5), 748–759.
65. Saini, R. K.; Prasad, P.; Sreedhar, R. V.; Akhilender Naidu, K.; Shang, X.; Keum, Y.-S. Omega−3 Polyunsaturated Fatty Acids (PUFAs): Emerging Plant and Microbial Sources, Oxidative Stability, Bioavailability, and Health Benefits—A Review. *Antioxidants* **2021**, *10* (10), 1627.

66. Miguel, G. A.; Jacobsen, C.; Prieto, C.; Kempen, P. J.; Lagaron, J. M.; Chronakis, I. S.; García-Moreno, P. J. Oxidative Stability and Physical Properties of Mayonnaise Fortified with Zein Electrosprayed Capsules Loaded with Fish Oil. *J. Food Eng.* **2019**, *263*, 348–358.
67. Kitessa, S. M.; Abeywardena, M.; Wijesundera, C.; Nichols, P. D. DHA-Containing Oilseed: A Timely Solution for the Sustainability Issues Surrounding Fish Oil Sources of the Health-Benefitting Long-Chain Omega-3 Oils. *Nutrients* **2014**, *6* (5), 2035–2058.
68. Singh, K. K.; Mridula, D.; Rehal, J.; Barnwal, P. Flaxseed: A Potential Source of Food, Feed and Fiber. *Crit. Rev. Food Sci. Nutr.* **2011**, *51* (3), 210–222.
69. Gura, K. M. The Power of Networking and Lessons Learned from Omegaven. *J. Pediatr. Pharmacol. Ther.* **2020**, *25* (8), 663–674.
70. Driscoll, D. F. Pharmaceutical and Clinical Aspects of Lipid Injectable Emulsions. *J. Parenter. Enter. Nutr.* **2017**, *41* (1), 125–134.
71. Crocker, K. S.; Noga, R.; Filibeck, D. J.; Krey, S. H.; Markovic, M.; Steffee, W. P. Microbial Growth Comparisons of Five Commercial Parenteral Lipid Emulsions. *J. Parenter. Enter. Nutr.* **1984**, *8* (4), 391–395.
72. Hainsworth, J. G.; Hershenson, H.; Pool, W. O. Fat Emulsion and Process of Producing Same. Patent US 3.004.892, 1961.
73. Edgren, B.; Wretlind, A. The Theoretical Background of the Intravenous Nutrition with Fat Emulsions. *Nutr. Dieta. Eur. Rev. Nutr. Diet.* **1963**, *5* (3–4), 364–386.
74. Benda, G. I. M.; Babson, S. G. Peripheral Intravenous Alimentation of the Small Premature Infant. *J. Pediatr.* **1971**, *79* (3), 494–498.
75. Wilmore, D. W.; Groff, D. B.; Bishop, H. C.; Dudrick, S. J. Total Parenteral Nutrition in Infants with Catastrophic Gastrointestinal Anomalies. *J. Pediatr. Surg.* **1969**, *4* (2), 181–189.
76. Bang, H. O.; Dyerberg, J.; Nielsen, A. B. Plasma Lipid and Lipoprotein Pattern in Greenlandic West-Coast Eskimos. *Lancet* **1971**, *297* (7710), 1143–1146.
77. Fleming, C.; Remington, M. Intestinal Failure. In *Nutrition and the Surgical Patient*; Hill, G., Ed.; Churchill Livingstone: New York, 1981; pp 219–235.
78. Washington, C.; Davis, S. S. The Production of Parenteral Feeding Emulsions by Microfluidizer. *Int. J. Pharm.* **1988**, *44* (1–3), 169–176.
79. Gramlich, L.; Ireton-Jones, C.; Miles, J. M.; Morrison, M.; Pontes-Arruda, A. Essential Fatty Acid Requirements and Intravenous Lipid Emulsions. *J. Parenter. Enter. Nutr.* **2019**, *43* (6), 697–707.
80. Wang, X.; Yu, K.; Cheng, C.; Peng, D.; Yu, X.; Chen, H.; Chen, Y.; Julian McClements, D.; Deng, Q. Effect of Sesamol on the Physical and Chemical Stability of Plant-Based Flaxseed Oil-in-Water Emulsions Stabilized by Proteins or Phospholipids. *Food Funct.* **2021**, *12* (5), 2090–2101.
81. Hong, M. Y.; Lumibao, J.; Mistry, P.; Saleh, R.; Hoh, E. Fish Oil Contaminated with Persistent Organic Pollutants Reduces Antioxidant Capacity and Induces Oxidative Stress without Affecting Its Capacity to Lower Lipid Concentrations and Systemic Inflammation in Rats. *J. Nutr.* **2015**, *145* (5), 939–944.
82. EFSA Panel on Dietetic Products Nutrition and Allergies. Scientific Opinion on the Safety of Refined Buglossoides Oil as a Novel Food Ingredient. *EFSA J.* **2015**, *13* (2), 1–21.
83. Prasad, P.; Savyasachi, S.; Reddy, L. P. A.; Sreedhar, R. V. Physico-Chemical Characterization, Profiling of Total Lipids and Triacylglycerol Molecular Species of Omega-3 Fatty Acid Rich *B. Arvensis* Seed Oil from India. *J. Oleo Sci.* **2019**, *68* (3), 209–223.
84. Lefort, N.; LeBlanc, R.; Giroux, M.-A.; Surette, M. E. Consumption of Buglossoides Arvensis Seed Oil Is Safe and Increases Tissue Long-Chain n -3 Fatty Acid Content More than Flax Seed Oil – Results of a Phase I Randomised Clinical Trial. *J. Nutr. Sci.* **2016**, *5*, e2.
85. Fickler, A.; Staats, S.; Hasler, M.; Rimbach, G.; Schulz, C. Dietary Buglossoides Arvensis Oil as a Potential Candidate to Substitute Fish Oil in Rainbow Trout Diets. *Lipids* **2018**, *53* (8), 809–823.
86. Murru, E.; Lopes, P. A.; Carta, G.; Manca, C.; Abolghasemi, A.; Guil-Guerrero, J. L.; Prates, J. A. M.; Banni, S. Different Dietary N-3 Polyunsaturated Fatty Acid Formulations Distinctively Modify Tissue Fatty Acid and N-Acylethanolamine Profiles. *Nutrients* **2021**, *13* (2), 625.
87. Lefort, N.; LeBlanc, R.; Surette, M. Dietary Buglossoides Arvensis Oil Increases Circulating N-3 Polyunsaturated Fatty Acids in a Dose-Dependent Manner and Enhances Lipopolysaccharide-Stimulated Whole Blood Interleukin-10—A Randomized Placebo-Controlled Trial. *Nutrients* **2017**, *9* (3), 261.

88. Tesser, A.; Torrinhas, R. S. M. M.; Garla, P. C.; Oliveira-Filho, R. S.; Aprobato, F. G. G.; Tamanaha, E. M.; Antunes, M. S.; Sampaio, G. R.; Torres, E.; Calder, P. C.; et al. Is There an Advantage in Enriching Parenteral Lipid Emulsions Containing Fatty Acids From Fish Oil With Medium-Chain Triglycerides? A Study on Body Pool Concentrations of Ω-3 Fatty Acids in Lewis Rats. *J. Parenter. Enter. Nutr.* **2021**, *45* (7), 1581–1590.

89. Broadwater, M. H.; Seaborn, G. T.; Schwacke, J. H. Forensic Identification of Seal Oils Using Lipid Profiles and Statistical Models. *J. Forensic Sci.* **2013**, *58* (2), 336–343.

90. Heyland, D. K. Parenteral Nutrition in the Critically-Ill Patient: More Harm than Good? In *Proceedings of the Nutrition Society*; 2000; Vol. 59, pp 457–466.

91. Lee, W. S.; Chew, K. S.; Ng, R. T.; Kasmi, K. El; Sokol, R. J. Intestinal Failure-Associated Liver Disease (IFALD): Insights into Pathogenesis and Advances in Management. *Hepatol. Int.* **2020**, *14* (3), 305–316.

92. Christensen, R. D.; Henry, E.; Wiedmeier, S. E.; Burnett, J.; Lambert, D. K. Identifying Patients, on the First Day of Life, at High-Risk of Developing Parenteral Nutrition-Associated Liver Disease. *J. Perinatol.* **2007**, *27* (5), 284–290.

93. Yang, X.; Liu, G.; Yi, B. Mdr3 Gene Mutation in Preterm Infants with Parenteral Nutrition-associated Cholestasis. *Mol. Genet. Genomic Med.* **2022**, *10* (3), 1–8.

94. El Kasmi, K. C.; Anderson, A. L.; Devereaux, M. W.; Balasubramaniyan, N.; Suchy, F. J.; Orlicky, D. J.; Shearn, C. T.; Sokol, R. J. Interrupting Tumor Necrosis Factor–Alpha Signaling Prevents Parenteral Nutrition–Associated Cholestasis in Mice. *J. Parenter. Enter. Nutr.* **2022**, *46* (5), 1096–1106.

95. Gupta, K.; Wang, H.; Amin, S. B. Soybean-Oil Lipid Minimization for Prevention of Intestinal Failure–Associated Liver Disease in Late-Preterm and Term Infants With Gastrointestinal Surgical Disorders. *J. Parenter. Enter. Nutr.* **2021**, *45* (6), 1239–1248.

96. Wanten, G. J. A. Parenteral Lipids: Safety Aspects and Toxicity. *World Rev. Nutr. Diet.* **2015**, *112*, 63–70.

97. Wanten, G. J. A. Parenteral Lipid Tolerance and Adverse Effects. *J. Parenter. Enter. Nutr.* **2015**, *39* (Suppl 1), 33S-38S.

98. Fukushima, K.; Omura, K.; Goshi, S.; Okada, A.; Tanaka, M.; Tsujimoto, T.; Iriyama, K.; Sugioka, N. Individualization of the Infusion Rate of a Soybean Oil–Based Intravenous Lipid Emulsion for Inpatients, Based on Baseline Triglyceride Concentrations: A Population Pharmacokinetic Approach. *J. Parenter. Enter. Nutr.* **2022**, *46* (1), 104–113.

99. Machigashira, S.; Kaji, T.; Onishi, S.; Yano, K.; Harumatsu, T.; Yamada, K.; Yamada, W.; Matsukubo, M.; Muto, M.; Ieiri, S. What Is the Optimal Lipid Emulsion for Preventing Intestinal Failure-Associated Liver Disease Following Parenteral Feeding in a Rat Model of Short-Bowel Syndrome? *Pediatr. Surg. Int.* **2021**, *37* (2), 247–256.

100. Melendez, M.; Yeh, D. D. Exploring the Long-term Risk Factors Associated with Intestinal Failure–Associated Liver Disease in Pediatric and Adult Patients: The Role of Lipid Injectable Emulsions in the Development of Liver Disease. *Nutr. Clin. Pract.* **2022**, https://doi.org/10.1002/ncp.10824.

101. Guthrie, G.; Stoll, B.; Chacko, S.; Mohammad, M.; Style, C.; Verla, M.; Olutoye, O.; Schady, D.; Lauridsen, C.; Tataryn, N.; et al. Depletion and Enrichment of Phytosterols in Soybean Oil Lipid Emulsions Directly Associate with Serum Markers of Cholestasis in Preterm Parenteral Nutrition–Fed Pigs. *J. Parenter. Enter. Nutr.* **2022**, *46* (1), 160–171.

102. Hojsak, I.; Colomb, V.; Braegger, C.; Bronsky, J.; Campoy, C.; Domellöf, M.; Embleton, N.; Fidler Mis, N.; Hulst, J. M.; Indrio, F.; et al. ESPGHAN Committee on Nutrition Position Paper. Intravenous Lipid Emulsions and Risk of Hepatotoxicity in Infants and Children: A Systematic Review and Meta-Analysis. *J. Pediatr. Gastroenterol. Nutr.* **2016**, *62* (5), 776–792.

103. Andersen, S.; Staudacher, H.; Weber, N.; Kennedy, G.; Varelias, A.; Banks, M.; Bauer, J. Pilot Study Investigating the Effect of Enteral and Parenteral Nutrition on the Gastrointestinal Microbiome Post-allogeneic Transplantation. *Br. J. Haematol.* **2020**, *188* (4), 570–581.

104. Demehri, F. R.; Barrett, M.; Teitelbaum, D. H. Changes to the Intestinal Microbiome With Parenteral Nutrition. *Nutr. Clin. Pract.* **2015**, *30* (6), 798–806.

105. Andersen, S.; Banks, M.; Bauer, J. Nutrition Support and the Gastrointestinal Microbiome- a Narrative Systematic Review. *Clin. Nutr. ESPEN* **2020**, *35*, 212.

106. Harris, J. K.; El Kasmi, K. C.; Anderson, A. L.; Devereaux, M. W.; Fillon, S. A.; Robertson, C. E.; Wagner, B. D.; Stevens, M. J.; Pace, N. R.; Sokol, R. J. Specific Microbiome Changes in a Mouse Model of Parenteral Nutrition Associated Liver Injury and Intestinal Inflammation. *PLoS One* **2014**, *9* (10), e110396.

107. Cahova, M.; Bratova, M.; Wohl, P. Parenteral Nutrition-Associated Liver Disease: The Role of the Gut Microbiota. *Nutrients* **2017**, *9* (9), 987.

108. Wang, N.; Wang, J.; Zhang, T.; Huang, L.; Yan, W.; Lu, L.; Jia, J.; Tao, Y.; Cai, W.; Wang, Y. Alterations of Gut Microbiota and Serum Bile Acids Are Associated with Parenteral Nutrition-Associated Liver Disease. *J. Pediatr. Surg.* **2021**, *56* (4), 738–744.

109. Liu, T.; Wang, C.; Wang, Y.; Wang, L.; Ojo, O.; Feng, Q.; Jiang, X.; Wang, X. Effect of Dietary Fiber on Gut Barrier Function, Gut Microbiota, Short-chain Fatty Acids, Inflammation, and Clinical Outcomes in Critically Ill Patients: A Systematic Review and Meta-analysis. *J. Parenter. Enter. Nutr.* **2022**, *46* (5), 997–1010.

110. Alomari, M.; Al Momani, L.; Sarmini, M. T.; El Kurdi, B.; Khazaaleh, S.; Nehme, F.; Young, M.; Romero-Marrero, C. Effects of Probiotics on Intestinal Failure-Associated Liver Disease in Adult Patients Receiving Prolonged Parenteral Support: A Tertiary Care Center Experience. *Am. J. Gastroenterol.* **2019**, *114* (Supplement), S552.

111. Neelis, E. G.; Koning, B. A. E.; Hulst, J. M.; Papadopoulou, R.; Kerbiriou, C.; Rings, E. H. H. M.; Wijnen, R. M. H.; Nichols, B.; Gerasimidis, K. Gut Microbiota and Its Diet-related Activity in Children with Intestinal Failure Receiving Long-term Parenteral Nutrition. *J. Parenter. Enter. Nutr.* **2022**, *46* (3), 693–708.

112. Chen, S.; Xiao, Y.; Liu, Y.; Tian, X.; Wang, W.; Jiang, L.; Wu, W.; Zhang, T.; Cai, W.; Wang, Y. Fish Oil–Based Lipid Emulsion Alleviates Parenteral Nutrition–Associated Liver Diseases and Intestinal Injury in Piglets. *J. Parenter. Enter. Nutr.* **2022**, *46* (3), 709–720.

113. Gura, K. M.; Calkins, K. L.; Premkumar, M. H.; Puder, M. Use of Intravenous Soybean and Fish Oil Emulsions in Pediatric Intestinal Failure-Associated Liver Disease: A Multicenter Integrated Analysis Report on Extrahepatic Adverse Events. *J. Pediatr.* **2022**, *241*, 173-180.e1.

114. Zhang, T.; Li, G.; Duan, M.; Lv, T.; Feng, D.; Lu, N.; Zhou, Y.; Gu, L.; Zhu, W.; Gong, J. Perioperative Parenteral Fish Oil Supplementation Improves Postoperative Coagulation Function and Outcomes in Patients Undergoing Colectomy for Ulcerative Colitis. *J. Parenter. Enter. Nutr.* **2022**, *46* (4), 878–886.

115. Ng, K.; Stoll, B.; Chacko, S.; Saenz De Pipaon, M.; Lauridsen, C.; Gray, M.; Squires, E. J.; Marini, J.; Zamora, I. J.; Olutoye, O. O.; et al. Vitamin E in New-Generation Lipid Emulsions Protects against Parenteral Nutrition-Associated Liver Disease in Parenteral Nutrition-Fed Preterm Pigs. *J. Parenter. Enter. Nutr.* **2016**, *40* (5), 656–671.

116. Burrin, D. G.; Ng, K.; Stoll, B.; De Pipaón, M. S. Impact of New-Generation Lipid Emulsions on Cellular Mechanisms of Parenteral Nutrition–Associated Liver Disease. *Adv. Nutr.* **2014**, *5* (1), 82–91.

117. Stramara, L.; Hernandez, L.; Bloom, B. T.; Durham, C. Development of Parenteral Nutrition–Associated Liver Disease and Other Adverse Effects in Neonates Receiving SMOFlipid or Intralipid. *J. Parenter. Enter. Nutr.* **2020**, *44* (8), 1530–1534.

118. Belza, C.; Wales, J. C.; Courtney-Martin, G.; Silva, N.; Avitzur, Y.; Wales, P. W. An Observational Study of Smoflipid vs Intralipid on the Evolution of Intestinal Failure–Associated Liver Disease in Infants With Intestinal Failure. *J. Parenter. Enter. Nutr.* **2020**, *44* (4), 688–696.

119. Mundi, M. S.; Kuchkuntla, A. R.; Salonen, B. R.; Bonnes, S.; Hurt, R. T. Long-Term Use of Mixed-Oil Lipid Emulsion in Soybean Oil–Intolerant Home Parenteral Nutrition Patients. *J. Parenter. Enter. Nutr.* **2020**, *44* (2), 301–307.

120. Pradelli, L.; Klek, S.; Mayer, K.; Omar Alsaleh, A. J.; Rosenthal, M. D.; Heller, A. R.; Muscaritoli, M. Omega-3 Fatty Acid-Containing Parenteral Nutrition in ICU Patients: Systematic Review with Meta-Analysis and Cost-Effectiveness Analysis. *Crit. Care* **2020**, *24* (1), 634.

121. Pradelli, L.; Muscaritoli, M.; Klek, S.; Martindale, R. G. Pharmacoeconomics of Parenteral Nutrition with ω-3 Fatty Acids in Hospitalized Adults. *JPEN. J. Parenter. Enteral Nutr.* **2020**, *44*, S68–S73.

122. Pradelli, L.; Klek, S.; Mayer, K.; Omar Alsaleh, A. J.; Rosenthal, M. D.; Heller, A. R.; Muscaritoli, M. Cost-Effectiveness of Parenteral Nutrition Containing Ω-3 Fatty Acids in Hospitalized Adult Patients From 5 European Countries and the US. *J. Parenter. Enter. Nutr.* **2021**, *45* (5), 999–1008.

123. Rumore, S.; McGrath, K.; Scott, A.; Sexton, E.; Wong, T. Fat Soluble Vitamin Status in Children on Home Parenteral Nutrition in a Tertiary Paediatric Intestinal Rehabilitation Unit. *Clin. Nutr. ESPEN* **2021**, *46*, 240–245.

124. Lutz, O.; Meraihi, Z.; Mura, J. L.; Frey, A.; Riess, G. H.; Bach, A. C. Fat Emulsion Particle Size: Influence on the Clearance Rate and the Tissue Lipolytic Activity. *Am. J. Clin. Nutr.* **1989**, *50* (6), 1370–1381.

125. McClements, D. J. Critical Review of Techniques and Methodologies for Characterization of Emulsion Stability. *Crit. Rev. Food Sci. Nutr.* **2007**, *47* (7), 611–649.

126. McClements, D. J. *Food Emulsions: Principles, Practices, and Techniques*, 3rd ed.; CRC Press: Boca Raton, 2015.

127. Driscoll, D. F. Commercial Lipid Emulsions and All-in-One Mixtures for Intravenous Infusion - Composition and Physicochemical Properties. *World Rev. Nutr. Diet.* **2015**, *112*, 48–56.

128. Mirtallo, J. M.; Ayers, P.; Boullata, J.; Gura, K. M.; Plogsted, S.; Anderson, C. R.; Worthington, P.; Seres, D. S.; Nicolai, E.; Alsharhan, M.; et al. ASPEN Lipid Injectable Emulsion Safety Recommendations, Part 1: Background and Adult Considerations. *Nutr. Clin. Pract.* **2020**, *35* (5), 769–782.
129. McClements, D. J. Edible Nanoemulsions: Fabrication, Properties, and Functional Performance. *Soft Matter* **2011**, *7* (6), 2297–2316.
130. Klang, M. G. PFAT5 and the Evolution of Lipid Admixture Stability. *J. Parenter. Enter. Nutr.* **2015**, *39* (Suppl 1), 67S-71S.
131. Washington, C. Stability of Lipid Emulsions for Drug Delivery. *Adv. Drug Deliv. Rev.* **1996**, *20* (2–3), 131–145.
132. Leal-Calderon, F.; Bibette, J.; Schmitt, V. *Emulsion Science: Basic Principles*, 2nd ed.; Leal-Calderon, F., Bibette, J., Schmitt, V., Eds.; Springer, 2007.
133. Arii, K.; Fukuta, Y.; Kai, T.; Kokuba, Y. Preparation of Fine Emulsified Fat Particles without Glycerol for Intravenous Nutrition. *Eur. J. Pharm. Sci.* **1999**, *9* (1), 67–73.
134. Collins-Gold, L. C.; Lyons, R. T.; Bartholow, L. C. Parenteral Emulsions for Drug Delivery. *Adv. Drug Deliv. Rev.* **1990**, *5* (3), 189–208.
135. Gupta, A. *Nanoemulsions*; Elsevier Inc., 2020.
136. Deng, Y.; Zhong, G.; Wang, Y.; Wang, N.; Yu, Q.; Yu, X. Quality by Design Approach for the Preparation of Fat-Soluble Vitamins Lipid Injectable Emulsion. *Int. J. Pharm.* **2019**, *571*, 118717.
137. Khalil, R. M.; Basha, M.; Kamel, R. Nanoemulsions as Parenteral Drug Delivery Systems for a New Anticancer Benzimidazole Derivative: Formulation and in-Vitro Evaluation. *Egypt. Pharm. J.* **2015**, *14* (3), 166.
138. Da Silva, G. B. R. F.; Scarpa, M. V.; Carlos, I. Z.; Quilles, M. B.; Lia, R. C. C.; Do Egito, E. S. T.; De Oliveira, A. G. Oil-in-Water Biocompatible Microemulsion as a Carrier for the Antitumor Drug Compound Methyl Dihydrojasmonate. *Int. J. Nanomedicine* **2015**, *10*, 585–594.
139. Smejkal, G. B.; Ting, E. Y.; Nambi Arul Nambi, K.; Schumacher, R. T.; Lazarev, A. V. Characterization of Astaxanthin Nanoemulsions Produced by Intense Fluid Shear through a Self-Throttling Nanometer Range Annular Orifice Valve-Based High-Pressure Homogenizer. *Molecules* **2021**, *26* (10), 2856.
140. Mirkovic, D.; Ibric, S. Investigation of Short-Term Stability of Parenteral Nutrition Nanoemulsions Prepared under Laboratory Conditions. *Vojnosanit. Pregl. Med. Pharm. J. Serbia* **2020**, *77* (7), 688–696.
141. Amran, M. H. H.; Zulfakar, M. H.; Danik, M. F.; Abdullah, M. S. P.; Shamsuddin, A. F. A New Alternative for Intravenous Lipid Emulsion 20% w/w from Superolein Oil and Its Effect on Lipid and Liver Profiles in an Animal Model. *DARU J. Pharm. Sci.* **2019**, *27* (1), 191–201.
142. Johl, H.-J. High-Pressure Homogenization. *World Pumps* **2019**, *2019* (10), 26–28.
143. Microfluidics. Compressors for Microfluidizer Air Machines (LM10). **2018**.
144. Singh, Y.; Meher, J. G.; Raval, K.; Khan, F. A.; Chaurasia, M.; Jain, N. K.; Chourasia, M. K. Nanoemulsion: Concepts, Development and Applications in Drug Delivery. *J. Control. Release* **2017**, *252*, 28–49.
145. Microfluidics. Microfluidizer Processor User Guide. **2014**.
146. Choi, S. J.; McClements, D. J. Nanoemulsions as Delivery Systems for Lipophilic Nutraceuticals: Strategies for Improving Their Formulation, Stability, Functionality and Bioavailability. *Food Sci. Biotechnol.* **2020**, *29* (2), 149–168.
147. Saheki, A.; Seki, J.; Nakanishi, T.; Tamai, I. Effect of Back Pressure on Emulsification of Lipid Nanodispersions in a High-Pressure Homogenizer. *Int. J. Pharm.* **2012**, *422* (1–2), 489–494.
148. Rueckl, H.; Scheffczik, H. Arranging Interaction and Back Pressure Chambers for Microfluidization. Patent US 9.700.616 B2, 2017.
149. Jain, J.; Fernandes, C.; Patravale, V. Formulation Development of Parenteral Phospholipid-Based Microemulsion of Etoposide. *AAPS PharmSciTech* **2010**, *11* (2), 826–831.
150. Velderrain-Rodríguez, G. R.; Salvia-Trujillo, L.; González-Aguilar, G. A.; Martín-Belloso, O. Interfacial Activity of Phenolic-Rich Extracts from Avocado Fruit Waste: Influence on the Colloidal and Oxidative Stability of Emulsions and Nanoemulsions. *Innov. Food Sci. Emerg. Technol.* **2021**, *69*, 102665.
151. Bin Sintang, M. D.; Danthine, S.; Patel, A. R.; Rimaux, T.; Van De Walle, D.; Dewettinck, K. Mixed Surfactant Systems of Sucrose Esters and Lecithin as a Synergistic Approach for Oil Structuring. *J. Colloid Interface Sci.* **2017**, *504*, 387–396.
152. Zheng, Y.; Zheng, M.; Ma, Z.; Xin, B.; Guo, R.; Xu, X. *Sugar Fatty Acid Esters*; AOCS Press, 2015.
153. van Hoogevest, P.; Wendel, A. The Use of Natural and Synthetic Phospholipids as Pharmaceutical Excipients. *Eur. J. Lipid Sci. Technol.* **2014**, *116* (9), 1088–1107.

154. Drescher, S.; van Hoogevest, P. The Phospholipid Research Center: Current Research in Phospholipids and Their Use in Drug Delivery. *Pharmaceutics* **2020**, *12* (12), 1235.
155. Wang, J.; Han, L.; Wang, D.; Sun, Y.; Huang, J.; Shahidi, F. Stability and Stabilization of Omega-3 Oils: A Review. *Trends Food Sci. Technol.* **2021**, *118*, 17–35.
156. Barbosa-Canovas, G. V. *Nano-Food Engineering*; Hebbar, U., Ranjan, S., Dasgupta, N., Mishra, R. K., Eds.; Springer Nature Switzerland AG, 2020.
157. Docena, G. H.; Fernandez, R.; Chirdo, F. G.; Fossati, C. A. Identification of Casein as the Major Allergenic and Antigenic Protein of Cow's Milk. *Allergy Eur. J. Allergy Clin. Immunol.* **1996**, *51* (6), 412–416.
158. Anton, N.; Benoit, J. P.; Saulnier, P. Design and Production of Nanoparticles Formulated from Nano-Emulsion Templates-A Review. *J. Control. Release* **2008**, *128* (3), 185–199.
159. Otto, F.; van Hoogevest, P.; Syrowatka, F.; Heinl, V.; Neubert, R. H. H. Assessment of the Applicability of HLB Values for Natural Phospholipid Emulsifiers for Preparation of Stable Emulsions. *Pharmazie* **2020**, *75* (8), 365–370.
160. Miller, R. *Emulsifiers: Types and Uses*, 1st ed.; Elsevier Ltd., 2015.
161. Ng, N.; Rogers, M. A. Surfactants. *Encycl. Food Chem.* **2018**, *1*, 276–282.
162. Genot, C.; Kabri, T.-H.; Meynier, A. Stabilization of Omega-3 Oils and Enriched Foods Using Emulsifiers. In *Food Enrichment with Omega-3 Fatty Acids*; Elsevier, 2013; pp 150–193.
163. Driscoll, D. F. Lipid Injectable Emulsions: Pharmacopeial and Safety Issues. *Pharm. Res.* **2006**, *23* (9), 1959–1969.
164. Brown, R.; Burke, D. The Hidden Cost of Catheter Related Blood Stream Infections in Patients on Parenteral Nutrition. *Clin. Nutr. ESPEN* **2020**, *36*, 146–149.
165. Salonen, B. R.; Mundi, M. S.; Hurt, R. T.; Bonnes, S. L. The Role of Parenteral Nutrition for Incurable Cancer: Bridging Expectations and Reality. *Curr. Nutr. Rep.* **2021**, *10* (3), 226–231.
166. Brandt, C. F.; Tribler, S.; Hvistendahl, M.; Naimi, R. M.; Brøbech, P.; Staun, M.; Jeppesen, P. B. Home Parenteral Nutrition in Adult Patients With Chronic Intestinal Failure. *J. Parenter. Enter. Nutr.* **2016**, *42* (1), 95–103.
167. Eriksson, J. Instruction for Use - Intralipid ® 20%. **2001**.
168. United States Pharmacopoeia. Lipid Injectable Emulsion. *USP-NF*. The United States Pharmacopeial Convention: Rockville, MD 2022.
169. United States Pharmacopoeia. ⟨729⟩ Globule Size Distribution in Lipid Injectable Emulsions. *USP-NF*. The United States Pharmacopeial Convention: Rockville, MD 2022.
170. Chansiri, G.; Lyons, R. T.; Patel, M. V.; Hem, S. L. Effect of Surface Charge on the Stability of Oil/Water Emulsions during Steam Sterilization. *J. Pharm. Sci.* **1999**, *88* (4), 454–458.
171. Zhang, T.; Li, M.; Yang, R.; Zhang, D.; Guan, J.; Yu, J.; Yang, B.; Zhang, H.; Zhang, S.; Liu, D.; et al. Therapeutic Efficacy of Lipid Emulsions of Docetaxel-Linoleic Acid Conjugate in Breast Cancer. *Int. J. Pharm.* **2018**, *546*, 61–69.
172. Washington, C.; Athersuch, A.; Kynoch, D. J. The Electrokinetic Properties of Phospholipid Stabilized Fat Emulsions. IV. The Effect of Glucose and of PH. *Int. J. Pharm.* **1990**, *64* (2–3), 217–222.
173. Bischoff, S. C.; Bernal, W.; Dasarathy, S.; Merli, M.; Plank, L. D.; Schütz, T.; Plauth, M. ESPEN Practical Guideline: Clinical Nutrition in Liver Disease. *Clin. Nutr.* **2020**, *39* (12), 3533–3562.
174. Hansrani, P. K.; Davis, S. S.; Groves, M. J. The Preparation and Properties of Sterile Intravenous Emulsions. *J. Parenter. Sci. Technol.* **1983**, *37* (4), 145–150.
175. Council of Europe. 2.6.1 Sterility. *European Pharmacopoeia*. 2011, pp 191–194.
176. Council of Europe. 2.6.14 Bacterial Endotoxins. *European Pharmacopoeia*. 2018, pp 209–213.
177. Jimenez, L.; Rana, N.; Travers, K.; Tolomanoska, V.; Walker, K. Evaluation of the Endosafe® Portable Testing System™ for the Rapid Analysis of Biopharmaceutical Samples. *PDA J. Pharm. Sci. Technol.* **2010**, *64* (3), 211–221.
178. United States Pharmacopeial Convention. <1> Injections. *USP*. Rockville, MD 2012, pp 33–37.
179. Hörmann, K.; Zimmer, A. Drug Delivery and Drug Targeting with Parenteral Lipid Nanoemulsions — A Review. *J. Control. Release* **2016**, *223*, 85–98.
180. Rasouli, M. Basic Concepts and Practical Equations on Osmolality: Biochemical Approach. *Clin. Biochem.* **2016**, *49* (12), 936–941.
181. Ferencz, N. I.10: Concentrations of Solutes and Osmolarity. In *Learning and Mastering Pharmaceutical Calculations*; Ferencz, N., Ed.; American Society of Health-System Pharmacists: Bethesda, 2018; pp 99–110.

182. Kroy, K.; Capron, I.; Djabourov, M. On the Viscosity of Emulsions. *Trans. Faraday Soc.* **1999**, *26*, 233.
183. Pernin, A.; Bosc, V.; Soto, P.; Le Roux, E.; Maillard, M. Lipid Oxidation in Oil-in-Water Emulsions Rich in Omega-3: Effect of Aqueous Phase Viscosity, Emulsifiers, and Antioxidants. *Eur. J. Lipid Sci. Technol.* **2019**, *121* (9), 1800462.
184. Yesiltas, B.; Sørensen, A.-D. M.; García-Moreno, P. J.; Anankanbil, S.; Guo, Z.; Jacobsen, C. Combination of Sodium Caseinate and Succinylated Alginate Improved Stability of High Fat Fish Oil-in-Water Emulsions. *Food Chem.* **2018**, *255*, 290–299.
185. Driscoll, D. F. Lipid Injectable Emulsions: 2006. *Nutr. Clin. Pract.* **2006**, *21* (4), 381–386.
186. Driscoll, D. F.; Ling, P. R.; Bistrian, B. R. Pharmacopeial Compliance of Fish Oil-Containing Parenteral Lipid Emulsion Mixtures: Globule Size Distribution (GSD) and Fatty Acid Analyses. *Int. J. Pharm.* **2009**, *379* (1–2), 125–130.
187. Driscoll, D. F.; Etzler, F.; Barber, T. A.; Nehne, J.; Niemann, W.; Bistrian, B. R. Physicochemical Assessments of Parenteral Lipid Emulsions: Light Obscuration versus Laser Diffraction. *Int. J. Pharm.* **2001**, *219* (1–2), 21–37.
188. Bhattacharjee, S. DLS and Zeta Potential – What They Are and What They Are Not? *J. Control. Release* **2016**, *235*, 337–351.
189. Malvern Instruments. A Basic Guide to Particle Characterization. 2015, pp 1–24.
190. McClements, D. J. Nanoemulsions versus Microemulsions: Terminology, Differences, and Similarities. *Soft Matter* **2012**, *8* (6), 1719–1729.
191. Klang, V.; Matsko, N. B. Electron Microscopy of Pharmaceutical Systems. *Adv. Imaging Electron Phys.* **2014**, *181*, 125–208.
192. Fujimoto, T.; Ohsaki, Y.; Suzuki, M.; Cheng, J. Imaging Lipid Droplets by Electron Microscopy. In *Methods in Cell Biology*; Elsevier Inc., 2013; Vol. 116, pp 227–251.
193. Sedaghat Doost, A.; Afghari, N.; Abbasi, H.; Nikbakht Nasrabadi, M.; Dewettinck, K.; Van der Meeren, P. Nano-Lipid Carriers Stabilized by Hydrophobically Modified Starch or Sucrose Stearate for the Delivery of Lutein as a Nutraceutical Beverage Model. *Colloids Surfaces A Physicochem. Eng. Asp.* **2020**, *605*, 125349.
194. Guo, X.; McClements, D. J.; Chen, J.; He, X.; Liu, W.; Dai, T.; Liu, C. The Nutritional and Physicochemical Properties of Whole Corn Slurry Prepared by a Novel Industry-Scale Microfluidizer System. *LWT* **2021**, *144*, 111096.
195. Lise Halvorsen, B.; Blomhoff, R. Determination of Lipid Oxidation Products in Vegetable Oils and Marine Omega-3 Supplements. *Food Nutr. Res.* **2011**, *55* (1), 5792.
196. Zeb, A. Chemistry and Liquid Chromatography Methods for the Analyses of Primary Oxidation Products of Triacylglycerols. *Free Radic. Res.* **2015**, *49* (5), 549–564.
197. Grotto, D.; Maria, L. S.; Valentini, J.; Paniz, C.; Schmitt, G.; Garcia, S. C.; Pomblum, V. J.; Rocha, J. B. T.; Farina, M. Importance of the Lipid Peroxidation Biomarkers and Methodological Aspects FOR Malondialdehyde Quantification. *Quim. Nova* **2009**, *32* (1), 169–174.
198. Anthonymuthu, T. S.; Kenny, E. M.; Bayır, H. Therapies Targeting Lipid Peroxidation in Traumatic Brain Injury. *Brain Res.* **2016**, *1640*, 57–76.
199. Ayala, A.; Muñoz, M. F.; Argüelles, S. Lipid Peroxidation: Production, Metabolism, and Signaling Mechanisms of Malondialdehyde and 4-Hydroxy-2-Nonenal. *Oxid. Med. Cell. Longev.* **2014**, *2014*, 360438.
200. Bravo-Díaz, C. Advances in the Control of Lipid Peroxidation in Oil-in-Water Emulsions: Kinetic Approaches. *Crit. Rev. Food Sci. Nutr.* **2022**, https://doi.org/10.1080/10408398.2022.2029827.
201. Costa, M.; Losada-Barreiro, S.; Paiva-Martins, F.; Bravo-Díaz, C. Polyphenolic Antioxidants in Lipid Emulsions: Partitioning Effects and Interfacial Phenomena. *Foods* **2021**, *10* (3), 539.
202. Mitrus, O.; Zuraw, M.; Losada-Barreiro, S.; Bravo-Díaz, C.; Paiva-Martins, F.; Paiva-Martins, T. Targeting Antioxidants to Interfaces: Control of the Oxidative Stability of Lipid-Based Emulsions. *J. Agric. Food Chem.* **2019**, *67* (11), 3266–3274.
203. Choe, E.; Min, D. B. Mechanisms and Factors for Edible Oil Oxidation. *Compr. Rev. Food Sci. Food Saf.* **2006**, *5* (4), 169–186.
204. Loveday, S. M.; Okubanjo, S. S.; Ye, A. M.; Singh, H.; Wilde, P. J. Droplet-Stabilized Oil-in-Water Emulsions Protect Unsaturated Lipids from Oxidation. *J. Agric. Food Chem.* **2019**, *67*, 2626–2636.
205. Daoud, S.; Bou-maroun, E.; Dujourdy, L.; Waschatko, G.; Billecke, N.; Cayot, P. Fast and Direct Analysis of Oxidation Levels of Oil-in-Water Emulsions Using ATR-FTIR. *Food Chem.* **2019**, *293*, 307–314.
206. Boléa, G.; Ginies, C.; Vallier, M. J.; Dufour, C. Lipid Protection by Polyphenol-Rich Apple Matrices Is Modulated by PH and Pepsin in in Vitro Gastric Digestion. *Food Funct.* **2019**, *10* (7), 3942–3954.

207. Viau, M.; Genot, C.; Ribourg, L.; Meynier, A. Amounts of the Reactive Aldehydes, Malonaldehyde, 4-hydroxy-2-hexenal, and 4-hydroxy-2-nonenal in Fresh and Oxidized Edible Oils Do Not Necessary Reflect Their Peroxide and Anisidine Values. *Eur. J. Lipid Sci. Technol.* **2016**, *118* (3), 435–444.
208. Daoud, S.; Bou-Maroun, E.; Waschatko, G.; Cayot, P. Lipid Oxidation in Oil-in-Water Emulsions: Iron Complexation by Buffer Ions and Transfer on the Interface as a Possible Mechanism. *Food Chem.* **2021**, *342* (September), 128273.
209. Lethuaut, L.; Métro, F.; Genot, C. Effect of Droplet Size on Lipid Oxidation Rates of Oil-in-Water Emulsions Stabilized by Protein. *JAOCS, J. Am. Oil Chem. Soc.* **2002**, *79* (5), 425–430.
210. Farooq, S.; Abdullah; Zhang, H.; Weiss, J. A Comprehensive Review on Polarity, Partitioning, and Interactions of Phenolic Antioxidants at Oil–Water Interface of Food Emulsions. *Compr. Rev. Food Sci. Food Saf.* **2021**, *20* (5), 4250–4277.
211. Schröder, A.; Sprakel, J.; Boerkamp, W.; Schroën, K.; Berton-Carabin, C. C. Can We Prevent Lipid Oxidation in Emulsions by Using Fat-Based Pickering Particles? *Food Res. Int.* **2019**, *120*, 352–363.
212. Yang, S.; Verhoeff, A. A.; Merkx, D. W. H.; van Duynhoven, J. P. M.; Hohlbein, J. Quantitative Spatiotemporal Mapping of Lipid and Protein Oxidation in Mayonnaise. *Antioxidants* **2020**, *9* (12), 1–13.
213. Li, P.; McClements, D. J.; Decker, E. A. Application of Flow Cytometry As Novel Technology in Studying the Effect of Droplet Size on Lipid Oxidation in Oil-in-Water Emulsions. *J. Agric. Food Chem.* **2020**, *68*, 567–573.
214. Yalçinöz, Ş.; Erçelebi, E. Effect of Surfactant Type and Droplet Size on Lipid Oxidation in Oil-in-Water Nano-Emulsions. *Qual. Assur. Saf. Crop. Foods* **2020**, *12* (2), 1–11.
215. Gebicki, J. M.; Nauser, T. Initiation and Prevention of Biological Damage by Radiation-Generated Protein Radicals. *Int. J. Mol. Sci.* **2021**, *23* (1), 396.
216. Singer, P.; Blaser, A. R.; Berger, M. M.; Alhazzani, W.; Calder, P. C.; Casaer, M. P.; Hiesmayr, M.; Mayer, K.; Montejo, J. C.; Pichard, C.; et al. ESPEN Guideline on Clinical Nutrition in the Intensive Care Unit. *Clin. Nutr.* **2019**, *38* (1), 48–79.
217. Singer, P. Preserving the Quality of Life: Nutrition in the ICU. *Crit. Care* **2019**, *23* (S1), 139.
218. Gostyńska, A.; Stawny, M.; Dettlaff, K.; Jelińska, A. Clinical Nutrition of Critically Ill Patients in the Context of the Latest ESPEN Guidelines. *Medicina (B. Aires).* **2019**, *55* (12), 770.
219. Tabor, E. Tutorial on How the US Food and Drug Administration Regulates Parenteral Nutrition Products. *J. Parenter. Enter. Nutr.* **2020**, *44* (2), 174–181.
220. Desai, S. N.; Farris, F. F.; Ray, S. D. *Lipid Peroxidation*, Third Edit.; Elsevier, 2014; Vol. 3.
221. Fuchs, P.; Perez-Pinzon, M. A.; Dave, K. R. Cerebral Ischemia in Diabetics and Oxidative Stress. In *Diabetes: Oxidative Stress and Dietary Antioxidants*; Preedy, V. R., Ed.; Elsevier: London, 2014; pp 15–23.
222. Saxena, R. Arthritis as a Disease of Aging and Changes in Antioxidant Status. In *Aging: Oxidative Stress and Dietary Antioxidants*; Preedy, V. R., Ed.; Elsevier: Oxford, 2014; pp 49–59.
223. Kumar, S.; Krishna Chaitanya, R.; Preedy, V. R. Assessment of Antioxidant Potential of Dietary Components. In *HIV/AIDS: Oxidative Stress and Dietary Antioxidants*; Preedy, V. R., Ed.; Elsevier Inc.: London, 2018; pp 239–25.
224. Borza, C.; Muntean, D.; Dehelean, C.; Savoiu, G.; Serban, C.; Simu, G.; Andoni, M.; Butur, M.; Drag, S. Oxidative Stress and Lipid Peroxidation – A Lipid Metabolism Dysfunction. In *Lipid Metabolism*; InTech, 2013.
225. Council of Europe. 2.5.4 Iodine Value. *European Pharmacopoeia*. 2016, pp 167–168.
226. United States Pharmacopeia. ⟨401⟩ Fats and Fixed Oils. *USP-NF*. The United States Pharmacopeial Convention: Rockville, MD 2022.
227. Council of Europe. 2.5.5 Peroxide Value. *European Pharmacopoeia*. 2016, pp 168–169.
228. Merkx, D. W. H.; Swager, A.; van Velzen, E. J. J.; van Duynhoven, J. P. M.; Hennebelle, M. Quantitative and Predictive Modelling of Lipid Oxidation in Mayonnaise. *Antioxidants* **2021**, *10* (2), 287.
229. American Oil Chemists' Society. AOCS Official Method Cd 8-53. 2003, pp 1–2.
230. Metrohm. Analysis of Edible Oils and Fats. *Appl. Bull. 141/5e* **2019**, *141/5*, 1–20.
231. Crowe, T. D.; White, P. J. Adaptation of the AOCS Official Method for Measuring Hydroperoxides from Small-Scale Oil Samples. *JAOCS, J. Am. Oil Chem. Soc.* **2001**, *78* (12), 1267–1269.
232. LeBel, C. P.; Ischiropoulos, H.; Bondy, S. C. Evaluation of the Probe 2',7'-Dichlorofluorescin as an Indicator of Reactive Oxygen Species Formation and Oxidative Stress. *Chem. Res. Toxicol.* **1992**, *5* (2), 227–231.

233. Sharma, R.; Roychoudhury, S.; Singh, N. Methods to Measure Reactive Oxygen Species (ROS) and Total Antioxidant Capacity (TAC) in the Reproductive System. In *Oxidative Stress in Human Reproduction*; Agarwal, A., Sharma, R., Gupta, S., Harlev, A., Ahmad, G., du Plessis, S. S., Esteves, S. C., Wang, S. M., Durairajanayagam, D., Eds.; Springer, 2017; pp 17–46.
234. Silva, H. D.; Beldíková, E.; Poejo, J.; Abrunhosa, L.; Serra, A. T.; Duarte, C. M. M.; Brányik, T.; Cerqueira, M. A.; Pinheiro, A. C.; Vicente, A. A. Evaluating the Effect of Chitosan Layer on Bioaccessibility and Cellular Uptake of Curcumin Nanoemulsions. *J. Food Eng.* **2019**, *243*, 89–100.
235. Zhong, L.; Ma, N.; Wu, Y.; Zhao, L.; Ma, G.; Pei, F.; Hu, Q. Gastrointestinal Fate and Antioxidation of β-Carotene Emulsion Prepared by Oat Protein Isolate-Pleurotus Ostreatus β-Glucan Conjugate. *Carbohydr. Polym.* **2019**, *221*, 10–20.
236. Van Kuijk, F. J. G. M.; Thomas, D. W.; Stephens, R. J.; Dratz, E. A. Gas Chromatography-Mass Spectrometry Assays for Lipid Peroxides. In *Methods in Enzymology*; Packer, L., Glazer, A. N., Eds.; 1990; Vol. 186, pp 388–398.
237. Patrignani, M.; Conforti, P. A.; Lupano, C. E. Lipid Oxidation in Biscuits: Comparison of Different Lipid Extraction Methods. *J. Food Meas. Charact.* **2015**, *9* (1), 104–109.
238. Charuwat, P.; Boardman, G.; Bott, C.; Novak, J. T. Thermal Degradation of Long Chain Fatty Acids. *Water Environ. Res.* **2018**, *90* (3), 278–287.
239. Celus, M.; Kyomugasho, C.; Keunen, J.; Van Loey, A. M.; Grauwet, T.; Hendrickx, M. E. Simultaneous Use of Low Methylesterified Citrus Pectin and EDTA as Antioxidants in Linseed/Sunflower Oil-in-Water Emulsions. *Food Hydrocoll.* **2020**, *100*, 105386.
240. King, H. M.; Cosslett, A. G.; Thomas, C. P.; Price-Davies, R. A HPLC Method to Monitor the Occurrence of Lipid Peroxidation in Intravenous Lipid Emulsions Used in Parenteral Nutrition Using In-Line UV and Charged Aerosol Detection. *Clin. Nutr. ESPEN* **2018**, *28*, 96–102.
241. Matthäus, B.; Wiezorek, C.; Eichner, K. Fast Chemiluminescence Method for Detection of Oxidized Lipids. *Lipid / Fett* **1994**, *96* (3), 95–99.
242. Barriuso, B.; Astiasarán, I.; Ansorena, D. A Review of Analytical Methods Measuring Lipid Oxidation Status in Foods: A Challenging Task. *Eur. Food Res. Technol.* **2013**, *236* (1), 1–15.
243. Uy, B.; McGlashan, S. R.; Shaikh, S. B. Measurement of Reactive Oxygen Species in the Culture Media Using Acridan Lumigen PS-3 Assay. *J. Biomol. Tech.* **2011**, *22* (3), 95–107.
244. Szterk, A.; Lewicki, P. P. A New Chemiluminescence Method for Detecting Lipid Peroxides in Vegetable Oils. *J. Am. Oil Chem. Soc.* **2010**, *87* (4), 361–367.
245. Wada, M.; Yamaguchi, A.; Ogawa, A.; Kido, H.; Nakamura, S.; Takada, M.; Kawakami, S.; Kuroda, N.; Nakashima, K. Luminol Chemiluminescence Profile of O/W Emulsions during Thermal Oxidation. *Anal. Sci.* **2017**, *33* (February), 249–252.
246. Rolewski, P.; Siger, A.; Nogala-Kałucka, M.; Polewski, K. Chemiluminescent Assay of Lipid Hydroperoxides Quantification in Emulsions of Fatty Acids and Oils. *Food Res. Int.* **2009**, *42* (1), 165–170.
247. Uluata, S.; Durmaz, G.; Julian McClements, D.; Decker, E. A. Comparing DPPP Fluorescence and UV Based Methods to Assess Oxidation Degree of Krill Oil-in-Water Emulsions. *Food Chem.* **2021**, *339*, 127898.
248. Gotoh, N.; Miyake, S.; Takei, H.; Sasaki, K.; Okuda, S.; Ishinaga, M.; Wada, S. Simple Method for Measuring the Peroxide Value in a Colored Lipid. *Food Anal. Methods* **2011**, *4* (4), 525–530.
249. Okimoto, Y.; Watanabe, A.; Niki, E.; Yamashita, T.; Noguchi, N. A Novel Fluorescent Probe Diphenyl-1-Pyrenylphosphine to Follow Lipid Peroxidation in Cell Membranes. *FEBS Lett.* **2000**, *474* (2–3), 137–140.
250. Li, P.; McClements, D. J.; Decker, E. A. Application of Flow Cytometry as Novel Technology in Studying Lipid Oxidation and Mass Transport Phenomena in Oil-in-Water Emulsions. *Food Chem.* **2020**, *315*, 126225.
251. Qiu, B.; Simon, M. BODIPY 493/503 Staining of Neutral Lipid Droplets for Microscopy and Quantification by Flow Cytometry. *Bio-Protocol* **2016**, *6* (17), 1–6.
252. Ye, L.; Pham-Mondala, A.; Li, J.; Joseph, P.; Nahas, R.; Michel-Salaun, F. Using Confocal Microscopy to Estimate the Distribution of Natural Antioxidants in Poultry Meal and Extruded Kibbles. *Eur. J. Lipid Sci. Technol.* **2019**, *121* (9), 1800374.
253. Shantha, N. C.; Decker, E. A. Rapid, Sensitive, Iron-Based Spectrophotometric Methods for Determination of Peroxide Values of Food Lipids. *J. AOAC Int.* **1994**, *77* (2), 421–424.
254. Dermiş, S.; Can, S.; Doru, B. Determination of Peroxide Values of Some Fixed Oils by Using the MFOX Method. *Spectrosc. Lett.* **2012**, *45* (5), 359–363.
255. Bou, R.; Codony, R.; Tres, A.; Decker, E. A.; Guardiola, F. Determination of Hydroperoxides in Foods and Biological Samples by the Ferrous Oxidation-Xylenol Orange Method: A Review of the Factors That Influence the Method's Performance. *Anal. Biochem.* **2008**, *377*, 1–15.

256. DeLong, J. M.; Prange, R. K.; Hodges, D. M.; Forney, C. F.; Bishop, M. C.; Quilliam, M. Using a Modified Ferrous Oxidation−Xylenol Orange (FOX) Assay for Detection of Lipid Hydroperoxides in Plant Tissue. *J. Agric. Food Chem.* **2002**, *50* (2), 248–254.
257. Balet, A.; Cardona, D.; Jané, S.; Molins-Pujol, A. M.; Sánchez Quesada, J. L.; Gich, I.; Mangues, M. A. Effects of Multilayered Bags vs Ethylvinyl-Acetate Bags on Oxidation of Parenteral Nutrition. *J. Parenter. Enter. Nutr.* **2004**, *28* (2), 85–91.
258. Erel, O. A New Automated Colorimetric Method for Measuring Total Oxidant Status. *Clin. Biochem.* **2005**, *38* (12), 1103–1111.
259. Mihaljević, B.; Katušin-Ražem, B.; Ražem, D. The Reevaluation of the Ferric Thiocyanate Assay for Lipid Hydroperoxides with Special Considerations of the Mechanistic Aspects of the Response. *Free Radic. Biol. Med.* **1996**, *21* (1), 53–63.
260. Young, C. A.; Vogt, R. R.; Nieuwland, J. A. Colorimetric Estimation of Peroxides in Unsaturated Compounds. *Ind. Eng. Chem. Anal. Ed.* **1936**, *8* (3), 198–199.
261. Mackay, K. I. Studies on Methods for the Determination of Peroxides in Fats and Oils, McGill University, 1947.
262. Chapman, R. A.; Mackay, K. The Estimation of Peroxides in Fats and Oils by the Ferric Thiocyanate Method. *J. Am. Oil Chem. Soc.* **1949**, *26* (7), 360–363.
263. Nielsen, N. S.; Timm-Heinrich, M.; Jacobsen, C. Comparison of Wet-Chemical Methods for Determination of Lipid Hydroperoxides. *J. Food Lipids* **2003**, *10* (1), 35–50.
264. Samdani, G. K.; McClements, D. J.; Decker, E. A. Impact of Phospholipids and Tocopherols on the Oxidative Stability of Soybean Oil-in-Water Emulsions. *J. Agric. Food Chem.* **2018**, *66* (15), 3939–3948.
265. Sun, L.; Wang, H.; Li, X.; Lan, S.; Wang, J.; Yu, D. Ultrasonic-Assisted Preparation of α-Tocopherol/Casein Nanoparticles and Application in Grape Seed Oil Emulsion. *Ultrason. Sonochem.* **2021**, *80*, 105810.
266. Hornero-Méndez, D.; Pérez-Gálvez, A.; Mínguez-Mosquera, M. I. A Rapid Spectrophotometric Method for the Determination of Peroxide Value in Food Lipids with High Carotenoid Content. *J. Am. Oil Chem. Soc.* **2001**, *78* (11), 1151–1155.
267. American Oil Chemists' Society. AOCS Official Method Cd 18-90. 2017.
268. Cengiz, A.; Schroën, K.; Berton-Carabin, C. Towards Oxidatively Stable Emulsions Containing Iron-Loaded Liposomes: The Key Role of Phospholipid-to-Iron Ratio. *Foods* **2021**, *10* (6), 1293.
269. Chotimarkorn, C.; Silalai, N.; Chaitanawisuit, N. Changes and Deterioration of Lipid in Farmed Spotted Babylon Snail (Babylonia Areolat a) Muscle during Iced Storage. *Food Sci. Technol. Int.* **2009**, *15* (5), 427–433.
270. Feng, J.; Schroën, K.; Fogliano, V.; Berton-Carabin, C. Antioxidant Potential of Non-Modified and Glycated Soy Proteins in the Continuous Phase of Oil-in-Water Emulsions. *Food Hydrocoll.* **2021**, *114*, 106564.
271. Espín, S.; Sánchez-Virosta, P.; García-Fernández, A. J.; Eeva, T. A Microplate Adaptation of the Thiobarbituric Acid Reactive Substances Assay to Determine Lipid Peroxidation Fluorometrically in Small Sample Volumes. *Rev. Toxicol.* **2017**, *34* (2), 94–98.
272. Papastergiadis, A.; Mubiru, E.; Van Langenhove, H.; De Meulenaer, B. Malondialdehyde Measurement in Oxidized Foods: Evaluation of the Spectrophotometric Thiobarbituric Acid Reactive Substances (TBARS) Test in Various Foods. *J. Agric. Food Chem.* **2012**, *60* (38), 9589–9594.
273. Hu, J.-N.; Zheng, H.; Chen, X.-X.; Li, X.; Xu, Y.; Xu, M.-F. Synergetic Effects of Whey Protein Isolate and Naringin on Physical and Oxidative Stability of Oil-in-Water Emulsions. *Food Hydrocoll.* **2020**, *101*, 105517.
274. Shen, Y.; Hu, R.; Li, Y. Antioxidant and Emulsifying Activities of Corn Gluten Meal Hydrolysates in Oil-in-Water Emulsions. *J. Am. Oil Chem. Soc.* **2020**, *97* (2), 175–185.
275. Dahle, L. K.; Hill, E. G.; Holman, R. T. The Thiobarbituric Acid Reaction and the Autoxidations of Polyunsaturated Fatty Acid Methyl Esters. *Arch. Biochem. Biophys.* **1962**, *98* (2), 253–261.
276. Brownley, C. A.; Lachman, L. Use of 2-thiobarbituric Acid—Malonaldehyde Reaction as a Measure of Antioxidant Effectiveness in Pharmaceutical Oils. *J. Pharm. Sci.* **1965**, *54* (10), 1480–1487.
277. Ghani, M. A.; Barril, C.; Bedgood, D. R.; Prenzler, P. D. Substrate and TBARS Variability in a Multi-Phase Oxidation System. *Eur. J. Lipid Sci. Technol.* **2017**, *119* (4), 1500500.
278. Ling, Z.; Ai, M.; Zhou, Q.; Guo, S.; Zhou, L.; Fan, H.; Cao, Y.; Jiang, A. Fabrication Egg White Gel Hydrolysates-Stabilized Oil-in-Water Emulsion and Characterization of Its Stability and Digestibility. *Food Hydrocoll.* **2020**, *102*, 105621.
279. Yu, T. C.; Sinnhuber, R. O. An Improved 2-Thiobarbituric Acid (TBA) Procedure for the Measurement of Autoxidation in Fish Oils. *J. Am. Oil Chem. Soc.* **1967**, *44* (4), 256–258.

280. Phonsatta, N.; Luangpituksa, P.; Figueroa-Espinoza, M. C.; Lecomte, J.; Durand, E.; Villeneuve, P.; Visessanguan, W.; Deetae, P.; Uawisetwathana, U.; Pongprayoon, W.; et al. Conjugated Autoxidizable Triene-Based (CAT and ApoCAT) Assays: Their Practical Application for Screening of Crude Plant Extracts with Antioxidant Functions in Relevant to Oil-in-Water Emulsions. *Eur. J. Lipid Sci. Technol.* **2019**, *121* (1), 1800239.

281. Wang, L. L.; Xiong, Y. L. Inhibition of Lipid Oxidation in Cooked Beef Patties by Hydrolyzed Potato Protein Is Related to Its Reducing and Radical Scavenging Ability. *J. Agric. Food Chem.* **2005**, *53* (23), 9186–9192.

282. Nikoo, M.; Benjakul, S.; Yasemi, M.; Ahmadi Gavlighi, H.; Xu, X. Hydrolysates from Rainbow Trout (Oncorhynchus Mykiss) Processing by-Product with Different Pretreatments: Antioxidant Activity and Their Effect on Lipid and Protein Oxidation of Raw Fish Emulsion. *LWT* **2019**, *108*, 120–128.

283. Zhu, S.; Meng, N.; Li, Y.; Chen, S.; Xia, Y. Antioxidant Activities of Lipophilic (−)-Epigallocatechin Gallate Derivatives in Vitro and in Lipid-Based Food Systems. *Food Biosci.* **2021**, *42*, 101055.

284. Hyatt, J. R.; Zhang, S.; Akoh, C. C. Comparison of Antioxidant Activities of Selected Phenolic Compounds in O/W Emulsions and Bulk Oil. *Food Chem.* **2021**, *349*, 129037.

285. Ilyasov, I. R.; Beloborodov, V. L.; Selivanova, I. A.; Terekhov, R. P. ABTS/PP Decolorization Assay of Antioxidant Capacity Reaction Pathways. *Int. J. Mol. Sci.* **2020**, *21* (3), 1131.

286. Shimamura, T.; Sumikura, Y.; Yamazaki, T.; Tada, A.; Kashiwagi, T.; Ishikawa, H.; Matsui, T.; Sugimoto, N.; Akiyama, H.; Ukeda, H. Applicability of the DPPH Assay for Evaluating the Antioxidant Capacity of Food Additives - Inter-Laboratory Evaluation Study. *Anal. Sci.* **2014**, *30* (7), 717–721.

287. Li, J.; Shen, Y.; Zhai, J.; Su, Y.; Gu, L.; Chang, C.; Yang, Y. Enhancing the Oxidative Stability of Algal Oil Powders Stabilized by Egg Yolk Granules/Lecithin Composites. *Food Chem.* **2021**, *345*, 128782.

288. Moon, J.-K.; Shibamoto, T. Antioxidant Assays for Plant and Food Components. *J Agric Food Chem* **2009**, *57*, 1655–1666.

289. Nourooz-Zadeh, J.; Tajaddini-Sarmadi, J.; Wolff, S. P.; Birlouez-Aragon, I. Measurement of Hydroperoxides in Edible Oils Using the Ferrous Oxidation in Xylenol Orange Assay. *J. Agric. Food Chem.* **1995**, *43* (1), 17–21.

290. Jiang, Z.-Y.; Hunt, J. V; Wolff, S. P. Ferrous Ion Oxidation in the Presence of Xylenol Orange for Detection of Lipid Hydroperoxide in Low Density Lipoprotein. *Anal. Biochem.* **1992**, *202* (2), 384–389.

291. Meisner, P.; Gebicki, J. L. Determination of Hydroperoxides in Aqueous Solutions Containing Surfactants by the Ferrous Oxidation-Xylenol Orange Method. *Acta Biochim. Pol.* **2009**, *56* (3), 523–527.

292. Hermes-Lima, M.; Willmore, W. G.; Storey, K. B. Quantification of Lipid Peroxidation in Tissue Extracts Based on Fe(III)Xylenol Orange Complex Formation. *Free Radic. Biol. Med.* **1995**, *19* (3), 271–280.

293. Fukuzawa, K.; Fujisaki, A.; Akai, K.; Tokumura, A.; Terao, J.; Gebicki, J. M. Measurement of Phosphatidylcholine Hydroperoxides in Solution and in Intact Membranes by the Ferric-Xylenol Orange Assay. *Anal. Biochem.* **2006**, *359* (1), 18–25.

294. Alamed, J.; McClements, D. J.; Decker, E. A. Influence of Heat Processing and Calcium Ions on the Ability of EDTA to Inhibit Lipid Oxidation in Oil-in-Water Emulsions Containing Omega-3 Fatty Acids. *Food Chem.* **2006**, *95* (4), 585–590.

295. Allen Zhang, J.; Pawelchak, J. Effect of PH, Ionic Strength and Oxygen Burden on the Chemical Stability of EPC/Cholesterol Liposomes under Accelerated Conditions. *Eur. J. Pharm. Biopharm.* **2000**, *50* (3), 357–364.

296. Belfort, R.; Mandarino, L.; Kashyap, S.; Wirfel, K.; Pratipanawatr, T.; Berria, R.; Defronzo, R. A.; Cusi, K. Dose-Response Effect of Elevated Plasma Free Fatty Acid on Insulin Signaling. *Diabetes* **2005**, *54* (6), 1640–1648.

297. Ebbert, J. O.; Jensen, M. D. Fat Depots, Free Fatty Acids, and Dyslipidemia. *Nutrients* **2013**, *5* (2), 495–508.

298. Henderson, G. C. Plasma Free Fatty Acid Concentration as a Modifiable Risk Factor for Metabolic Disease. *Nutrients* **2021**, *13* (8), 2590.

299. Ngaosuwan, K.; Lotero, E.; Suwannakarn, K.; Goodwin, J. G.; Praserthdam, P. Hydrolysis of Triglycerides Using Solid Acid Catalysts. *Ind. Eng. Chem. Res.* **2009**, *48* (10), 4757–4767.

300. Elke, G.; Hartl, W. H.; Kreymann, K. G.; Adolph, M.; Felbinger, T. W.; Graf, T.; de Heer, G.; Heller, A. R.; Kampa, U.; Mayer, K.; et al. Clinical Nutrition in Critical Care Medicine – Guideline of the German Society for Nutritional Medicine (DGEM). *Clin. Nutr. ESPEN* **2019**, *33*, 220–275.

301. Mayer, K.; Klek, S.; García-de-Lorenzo, A.; Rosenthal, M. D.; Li, A.; Evans, D. C.; Muscaritoli, M.; Martindale, R. G. Lipid Use in Hospitalized Adults Requiring Parenteral Nutrition. *J. Parenter. Enter. Nutr.* **2020**, *44* (S1), S28–S38.

302. Koletzko, B.; Goulet, O.; Hunt, J.; Krohn, K.; Shamir, R. ESPGHAN and ESPEN Guidelines Paediatric Parenteral Nutrition - Annex: List of Products. *J. Pediatr. Gastroenterol. Nutr.* **2005**, *41* (Supplement 2), S85–S87.

303. Odell, G. B.; Cukier, J. O.; Ostrea, E. M.; Maglalang, A. C.; Poland, R. L. The Influence of Fatty Acids on the Binding of Bilirubin to Albumin. *J. Lab. Clin. Med.* **1977**, *89* (2), 295–307.

304. Amin, S. B. Effect of Free Fatty Acids on Bilirubin–Albumin Binding Affinity and Unbound Bilirubin in Premature Infants. *J. Parenter. Enter. Nutr.* **2010**, *34* (4), 414–420.

305. Cowan, R. E.; Thompson, R. P. H. Fatty Acids and the Control of Bilirubin Levels in Blood. *Med. Hypotheses* **1983**, *11* (3), 343–351.

306. Uhari, M.; Alkku, A.; Nikkari, T.; Timonen, E. Neonatal Jaundice and Fatty Acid Composition of the Maternal Diet. *Acta Pædiatrica* **1985**, *74* (6), 867–873.

307. Hegyi, T.; Kleinfeld, A.; Huber, A.; Weinberger, B.; Memon, N.; Shih, W. J.; Carayannopoulos, M.; Oh, W. Effects of Soybean Lipid Infusion on Unbound Free Fatty Acids and Unbound Bilirubin in Preterm Infants. *J. Pediatr.* **2017**, *184*, 45–50.

308. Amin, S. B.; Maisels, M. J.; Watchko, J. F. Early Lipid Infusions and Unbound Bilirubin in Preterm Neonates: A Cause for Concern? *J. Pediatr.* **2017**, *184*, 6–7.

309. Satar, M.; Şimşek, H.; Özlü, F.; Tuli, A.; Alparslan, M. M.; Mert, M. K.; Yıldızdaş, H. Y. The Effect of Different Intravenous Lipids on Free Bilirubin Levels in Premature Infants. *Eur. J. Clin. Nutr.* **2022**, *76* (6), 879–882.

310. Kim, H.; Salem, N. Separation of Lipid Classes by Solid Phase Extraction. *J. Lipid Res.* **1990**, *31* (3), 2285–2289.

311. Suzuki, E.; Sano, A.; Kuriki, T.; Miki, T. Improved Separation and Determination of Phospholipids in Animal Tissues Emplyoing Solid Phase Extraction. *Biol Pharm Bull* **1997**, *20* (4), 299–303.

312. Flurkey, W. H. Use of Solid Phase Extraction in the Biochemistry Laboratory to Separate Different Lipids. *Biochem. Mol. Biol. Educ.* **2005**, *33* (5), 357–360.

313. Pérez-Palacios, T.; Ruiz, J.; Antequera, T. Improvement of a Solid Phase Extraction Method for Separation of Animal Muscle Phospholipid Classes. *Food Chem.* **2007**, *102* (3), 875–879.

314. Mills, C. T.; Goldhaber, M. B. On Silica-Based Solid Phase Extraction Techniques for Isolating Microbial Membrane Phospholipids: Ensuring Quantitative Recovery of Phosphatidylcholine-Derived Fatty Acids. *Soil Biol. Biochem.* **2010**, *42* (7), 1179–1182.

315. Toyo'oka, T.; Ishibashi, M.; Takeda, Y.; Nakashima, K.; Akiyama, S.; Uzu, S.; Imai, K. Precolumn Fluorescence Tagging Reagent for Carboxylic Acids in High-Performance Liquid Chromatography: 4-Substituted-7-Aminoalkylamino-2,1,3-Benzoxadiazoles. *J. Chromatogr. A* **1991**, *588* (1–2), 61–71.

316. Uzu, S.; Imai, K.; Nakashima, K.; Akiyama, S. 4-(N,N-Dimethylaminosulphonyl)-7-Fluoro-2,1,3-Benzoxadiazole as Chemilumigenic Reagent for High Performance Liquid Chromatographic Peroxyoxalate Chemiluminescence Detection. *Biomed. Chromatogr.* **1991**, *5* (4), 184–185.

317. Ueno, Y.; Matsunaga, H.; Umemoto, K.; Nishijima, K. Determination of Free Fatty Acids in o/w Injectable Emulsions by HPLC with Fluorescence Detection Using 4-(N,N-Dimethylaminosulfonyl)-7-N- Piperazino-2,1,3-Benzoxadiazole. *Chem. Pharm. Bull.* **1999**, *47* (10), 1375–1379.

318. Amran, M. H. H.; Danik, M. F.; Abdullah, M. S. P.; Zulfakar, M. H.; Shamsuddin, A. F. Superolein Based Intravenous Lipid Emulsion 20% w/w Physicochemical Characterization, Stability and Its Effect on Liver Status. *Sains Malaysiana* **2019**, *48* (5), 1043–1054.

319. Liu, L.; Pan, Y.; Zhang, X.; Zhang, Y.; Li, X. Effect of Particle Size and Interface Composition on the Lipid Digestion of Droplets Covered with Membrane Phospholipids. *J. Agric. Food Chem.* **2021**, *69* (1), 159–169.

320. Wabaidur, S. M.; AlAmmari, A.; Aqel, A.; AL-Tamrah, S. A.; Alothman, Z. A.; Ahmed, A. Y. B. H. Determination of Free Fatty Acids in Olive Oils by UPHLC–MS. *J. Chromatogr. B Anal. Technol. Biomed. Life Sci.* **2016**, *1031*, 109–115.

321. Miksa, I. R.; Buckley, C. L.; Poppenga, R. H. Detection of Nonesterified (Free) Fatty Acids in Bovine Serum: Comparative Evaluation of Two Methods. *J. Vet. Diagnostic Investig.* **2004**, *16* (2), 139–144.

322. Matsubara, C.; Nishikawa, Y.; Yoshida, Y.; Takamura, K. A Spectrophotometric Method for the Determination of Free Fatty Acid in Serum Using Acyl-Coenzyme A Synthetase and Acyl-Coenzyme A Oxidase. *Anal. Biochem.* **1983**, *130* (1), 128–133.

323. Skořepa, P.; Fortunato, J.; Sobotka, O.; Tichá, A.; Bláha, V.; Sobotka, L.; Horáček, J. M. The Influence of Total Parenteral Nutrition on the Metabolism of Non-Esterified Fatty Acids in Critically Ill Patients: Ongoing Data from a Prospective Randomized Study. *Mil. Med. Sci. Lett.* **2019**, *88* (4), 150–158.

324. Mahesar, S. A.; Sherazi, S. T. H.; Khaskheli, A. R.; Kandhro, A. A.; Uddin, S. Analytical Approaches for the Assessment of Free Fatty Acids in Oils and Fats. *Anal. Methods* **2014**, *6* (14), 4956–4963.
325. Lv, S.; Gu, J.; Zhang, R.; Zhang, Y.; Tan, H.; McClements, D. J. Vitamin E Encapsulation in Plant-Based Nanoemulsions Fabricated Using Dual-Channel Microfluidization: Formation, Stability, and Bioaccessibility. *J. Agric. Food Chem.* **2018**, *66* (40), 10532–10542.
326. Scheuble, N.; Schaffner, J.; Schumacher, M.; Windhab, E. J.; Liu, D.; Parker, H.; Steingoetter, A.; Fischer, P. Tailoring Emulsions for Controlled Lipid Release: Establishing in Vitro–in Vivo Correlation for Digestion of Lipids. *ACS Appl. Mater. Interfaces* **2018**, *10* (21), 17571–17581.
327. Wang, S.-Z.; Dai, H.-Q.; Chen, K.-X.; Li, J.; Chen, Z.-X. Synergistic Interaction between Exogenous and Endogenous Emulsifiers and Its Impact on in Vitro Digestion of Lipid in Crowded Medium. *Food Chem.* **2019**, *299*, 125164.
328. Marefati, A.; Wiege, B.; Abdul Hadi, N.; Dejmek, P.; Rayner, M. In Vitro Intestinal Lipolysis of Emulsions Based on Starch Granule Pickering Stabilization. *Food Hydrocoll.* **2019**, *95*, 468–475.
329. Ma, L.; Zou, L.; McClements, D. J.; Liu, W. One-Step Preparation of High Internal Phase Emulsions Using Natural Edible Pickering Stabilizers: Gliadin Nanoparticles/Gum Arabic. *Food Hydrocoll.* **2020**, *100*, 105381.
330. Kawasaki, A.; Yasuda, M.; Mawatari, K. ichi; Fukuuchi, T.; Yamaoka, N.; Kaneko, K.; Iijima, R.; Yui, S.; Satoh, M.; Nakagomi, K. Sensitive Analysis of Sialic Acid and Related Compound by Hydrophilic Interaction Liquid Chromatography Using Fluorescence Detection after Derivatization with DBD-PZ. *Anal. Sci.* **2018**, *34* (7), 841–844.
331. El Kasmi, K. C.; Anderson, A. L.; Devereaux, M. W.; Vue, P. M.; Zhang, W.; Setchell, K. D. R.; Karpen, S. J.; Sokol, R. J. Phytosterols Promote Liver Injury and Kupffer Cell Activation in Parenteral Nutrition–Associated Liver Disease. *Sci. Transl. Med.* **2013**, *5* (206), 206ra137.
332. Qi, K.; Seo, T.; Al-Haideri, M.; Worgall, T. S.; Vogel, T.; Carpentier, Y. A.; Deckelbaum, R. J. Omega-3 Triglycerides Modify Blood Clearance and Tissue Targeting Pathways of Lipid Emulsions. *Biochemistry* **2002**, *41* (9), 3119–3127.
333. Qi, K.; Seo, T.; Jiang, Z.; Carpentier, Y. A.; Deckelbaum, R. J. Triglycerides in Fish Oil Affect the Blood Clearance of Lipid Emulsions Containing Long- and Medium-Chain Triglycerides in Mice. *J. Nutr.* **2006**, *136* (11), 2766–2772.
334. Fruehwirth, S.; Egger, S.; Kurzbach, D.; Windisch, J.; Jirsa, F.; Flecker, T.; Ressler, M.; Reiner, A. T.; Firat, N.; Pignitter, M. Ingredient-Dependent Extent of Lipid Oxidation in Margarine. *Antioxidants* **2021**, *10* (1), 105.
335. Kim, J.; Choe, E. Interaction Effect of Tocopherol Homologs with Peppermint Extract on the Iron-Catalyzed Oxidation of Soybean Oil-in-Water Emulsion. *Food Sci. Biotechnol.* **2019**, *28* (6), 1679–1685.
336. Genscript. ToxinSensor Single Test Kit Technical Manual. *No. TM0639* **2015**.
337. Fatouros, D. G.; Bergenstahl, B.; Mullertz, A. Morphological Observations on a Lipid-Based Drug Delivery System during in Vitro Digestion. *Eur. J. Pharm. Sci.* **2007**, *31* (2), 85–94.
338. Helvig, S.; Azmi, I. D. M.; Moghimi, S. M.; Yaghmur, A. Recent Advances in Cryo-TEM Imaging of Soft Lipid Nanoparticles. *AIMS Biophys.* **2015**, *2* (2), 116–130.
339. Meister, A.; Blume, A. (Cryo)Transmission Electron Microscopy of Phospholipid Model Membranes Interacting with Amphiphilic and Polyphilic Molecules. *Polymers (Basel).* **2017**, *9* (12), 521.
340. Dianzani, C.; Monge, C.; Miglio, G.; Serpe, L.; Martina, K.; Cangemi, L.; Ferraris, C.; Mioletti, S.; Osella, S.; Gigliotti, C. L.; et al. Nanoemulsions as Delivery Systems for Poly-Chemotherapy Aiming at Melanoma Treatment. *Cancers (Basel).* **2020**, *12* (5), 1–18.
341. Tonnesen, H. H. *Photostability of Drugs and Drug Formulations*, 2nd ed.; CRC Press: Boca Raton, 2004.
342. Crapiste H., G.; Brevedan I.V., M.; Carelli A., A. Oxidation of Sunflower Oil During Storage. *JAOCS* **1999**, *76* (12), 1437–1443.
343. Raman, M.; Almutairdi, A.; Mulesa, L.; Alberda, C.; Beattie, C.; Gramlich, L. Parenteral Nutrition and Lipids. *Nutrients* **2017**, *9* (4), 388.
344. Busmann, E. F.; Martínez, D. G.; Lucas, H.; Mäder, K. Phase Inversion-Based Nanoemulsions of Medium Chain Triglyceride as Potential Drug Delivery System for Parenteral Applications. *Beilstein J. Nanotechnol.* **2020**, *11*, 213–224.
345. Ali, S.; Kolter, K. Kolliphor® HS 15 - An Enabler for Parenteral and Oral Formulations. *Am. Pharm. Rev.* **2019**, *22* (1).
346. Hippalgaonkar, K.; Majumdar, S.; Kansara, V. Injectable Lipid Emulsions—Advancements, Opportunities and Challenges. *AAPS PharmSciTech* **2010**, *11* (4), 1526–1540.

347. Fan, W.; Yu, Z.; Peng, H.; He, H.; Lu, Y.; Qi, J.; Dong, X.; Zhao, W.; Wu, W. Effect of Particle Size on the Pharmacokinetics and Biodistribution of Parenteral Nanoemulsions. *Int. J. Pharm.* **2020**, *586*, 119551.

348. Burton, G. W.; Ingold, K. U. Autoxidation of Biological Molecules. 1. Antioxidant Activity of Vitamin E and Related Chain-Breaking Phenolic Antioxidants in Vitro. *J. Am. Chem. Soc.* **1981**, *103* (21), 6472–6477.

349. Barouh, N.; Bourlieu-Lacanal, C.; Figueroa-Espinoza, M. C.; Durand, E.; Villeneuve, P. Tocopherols as Antioxidants in Lipid-based Systems: The Combination of Chemical and Physicochemical Interactions Determines Their Efficiency. *Compr. Rev. Food Sci. Food Saf.* **2022**, *21* (1), 642–688.

350. Xu, Z.; Harvey, K. A.; Pavlina, T. M.; Zaloga, G. P.; Siddiqui, R. A. Tocopherol and Tocotrienol Homologs in Parenteral Lipid Emulsions. *Eur. J. Lipid Sci. Technol.* **2015**, *117* (1), 15–22.

351. Schwartz, H.; Ollilainen, V.; Piironen, V.; Lampi, A.-M. Tocopherol, Tocotrienol and Plant Sterol Contents of Vegetable Oils and Industrial Fats. *J. Food Compos. Anal.* **2008**, *21*, 152–161.

352. Baker, M. A.; Cho, B. S.; Anez-Bustillos, L.; Dao, D. T.; Pan, A.; O'Loughlin, A. A.; Lans, Z. M.; Mitchell, P. D.; Nosé, V.; Gura, K. M.; et al. Fish Oil–Based Injectable Lipid Emulsions Containing Medium-Chain Triglycerides or Added α-Tocopherol Offer Anti-Inflammatory Benefits in a Murine Model of Parenteral Nutrition–Induced Liver Injury. *Am. J. Clin. Nutr.* **2018**, *109* (4), 1038–1050.

353. Guthrie, G.; Stoll, B.; Chacko, S.; Lauridsen, C.; Plat, J.; Burrin, D. G. Rifampicin, Not Vitamin E, Suppresses Parenteral Nutrition Associated Liver Disease Development through Pregnane X Receptor Pathway in Piglets. *Am. J. Physiol. Liver Physiol.* **2019**, *4* (42), 41–52.

354. Martin-Rubio, A. S.; Sopelana, P.; Ibargoitia, M. L.; Guillén, M. D. Prooxidant Effect of α-Tocopherol on Soybean Oil. Global Monitoring of Its Oxidation Process under Accelerated Storage Conditions by 1H Nuclear Magnetic Resonance. *Food Chem.* **2018**, *245*, 312–323.

355. Kim, H. J.; Lee, H. O.; Min, D. B. Effects and Prooxidant Mechanisms of Oxidized α-Tocopherol on the Oxidative Stability of Soybean Oil. *J. Food Sci.* **2007**, *72* (4), C223–C230.

356. Bakir, T.; Yildoğan Beker, B.; Sönmezoğlu, I.; Imer, F.; Apak, R. Antioxidant and Prooxidant Effects of α-Tocopherol in a Linoleic Acid-Copper(II)-Ascorbate System. *Eur. J. Lipid Sci. Technol.* **2013**, *115* (3), 372–376.

357. Carr, A. C.; Zhu, B. Z.; Frei, B. Potential Antiatherogenic Mechanisms of Ascorbate (Vitamin C) and α-Tocopherol (Vitamin E). *Circ. Res.* **2000**, *87* (5), 349–354.

358. Lamas, G. A.; Goertz, C.; Boineau, R.; Mark, D. B.; Rozema, T.; Nahin, R. L.; Lindblad, L.; Lewis, E. F.; Drisko, J.; Lee, K. L. Effect of Disodium EDTA Chelation Regimen. *JAMA* **2013**, *309* (12), 1241–1250.

359. Xu, X.-T.; Huang, H.; Tian, M.-X.; Hu, R.-C.; Dai, Z.; Jin, X. A Four-Oil Intravenous Lipid Emulsion Improves Markers of Liver Function, Triglyceride Levels and Shortens Length of Hospital Stay in Adults: A Systematic Review and Meta-Analysis. *Nutr. Res.* **2021**, *92*, 1–11.

360. Van Bennekum, A. M.; Kako, Y.; Weinstock, P. H.; Harrison, E. H.; Deckelbaum, R. J.; Goldberg, I. J.; Blaner, W. S. Lipoprotein Lipase Expression Level Influences Tissue Clearance of Chylomicron Retinyl Ester. *J. Lipid Res.* **1999**, *40* (3), 565–574.

361. Nagachinta, S.; Becker, G.; Dammicco, S.; Serrano, M. E.; Leroi, N.; Bahri, M. A.; Plenevaux, A.; Lemaire, C.; Lopez, R.; Luxen, A.; et al. Radiolabelling of Lipid-Based Nanocarriers with Fluorine-18 for in Vivo Tracking by PET. *Colloids Surfaces B Biointerfaces* **2020**, *188*, 110793.

362. Bradford, B. U.; Lock, E. F.; Kosyk, O.; Kim, S.; Uehara, T.; Harbourt, D.; DeSimone, M.; Threadgill, D. W.; Tryndyak, V.; Pogribny, I. P.; et al. Interstrain Differences in the Liver Effects of Trichloroethylene in a Multistrain Panel of Inbred Mice. *Toxicol. Sci.* **2011**, *120* (1), 206–217.

363. Leist, S. R.; Pilzner, C.; van den Brand, J. M. A.; Dengler, L.; Geffers, R.; Kuiken, T.; Balling, R.; Kollmus, H.; Schughart, K. Influenza H3N2 Infection of the Collaborative Cross Founder Strains Reveals Highly Divergent Host Responses and Identifies a Unique Phenotype in CAST/EiJ Mice. *BMC Genomics* **2016**, *17* (1), 1–30.

364. Gomez-Cuadrado, L.; Tracey, N.; Ma, R.; Qian, B.; Brunton, V. G. Mouse Models of Metastasis: Progress and Prospects. *DMM Dis. Model. Mech.* **2017**, *10* (9), 1061–1074.

365. Labelle, M.; Begum, S.; Hynes, R. O. Platelets Guide the Formation of Early Metastatic Niches. *Proc. Natl. Acad. Sci. U. S. A.* **2014**, *111* (30), E3053–E3061.

366. Treskova, E.; Carpentier, Y. A.; Ramakrishnan, R.; Al-Haideri, M.; Seo, T.; Deckelbaum, R. J. Blood Clearance and Tissue Uptake of Intravenous Lipid Emulsions Containing Long-Chain and Medium-Chain Triglycerides and Fish Oil in a Mouse Model. *J. Parenter. Enter. Nutr.* **1999**, *23* (5), 253–259.

367. Epelman, S.; Lavine, K. J.; Randolph, G. J. Origin and Functions of Tissue Macrophages. *Immunity* **2014**, *41* (1), 21–35.

368. Gordon, S.; Plüddemann, A. Tissue Macrophages: Heterogeneity and Functions. *BMC Biol.* **2017**, *15* (1), 1–18.
369. Seki, J.; Sonoke, S.; Saheki, A.; Fukui, H.; Sasaki, H.; Mayumi, T. A Nanometer Lipid Emulsion, Lipid Nano-Sphere (LNS®), as a Parenteral Drug Carrier for Passive Drug Targeting. *Int. J. Pharm.* **2004**, *273* (1–2), 75–83.
370. Kapellos, T. S.; Taylor, L.; Lee, H.; Cowley, S. A.; James, W. S.; Iqbal, A. J.; Greaves, D. R. A Novel Real Time Imaging Platform to Quantify Macrophage Phagocytosis. *Biochem. Pharmacol.* **2016**, *116*, 107–119.
371. Persson, E. Lipoprotein Lipase, Hepatic Lipase and Plasma Lipolytic Activity. Effects of Heparin and a Low Molecular Weight Heparin Fragment (Fragmin). *Acta Med. Scand. Suppl.* **1988**, *724*, 1–56.
372. Gallegos, C.; Partal, P.; Franco, J. M. Droplet-Size Distribution and Stability of Lipid Injectable Emulsions. *Am. J. Heal. Pharm.* **2009**, *66* (2), 162–166.
373. Hu, C.; Ding, H.; Zhuang, Q.; Llanos, P.; Pillay, T.; Hernandez, C.; Carpentier, Y. A.; Deckelbaum, R. J.; Chang, C. L. Blood Clearance Kinetics and Organ Delivery of Medium-Chain Triglyceride and Fish Oil-Containing Lipid Emulsions: Comparing Different Animal Species. *Clin. Nutr.* **2021**, *40* (3), 987–996.
374. Fang, C.-L.; A. Al-Suwayeh, S.; Fang, J.-Y. Nanostructured Lipid Carriers (NLCs) for Drug Delivery and Targeting. *Recent Pat. Nanotechnol.* **2012**, *7* (1), 41–55.
375. Litzinger, D. C.; Buiting, A. M. J.; van Rooijen, N.; Huang, L. Effect of Liposome Size on the Circulation Time and Intraorgan Distribution of Amphipathic Poly(Ethylene Glycol)-Containing Liposomes. *Biochim. Biophys. Acta - Biomembr.* **1994**, *1190* (1), 99–107.
376. Martins, I. J.; Mortimer, B. C.; Miller, J.; Redgrave, T. G. Effects of Particle Size and Number on the Plasma Clearance of Chylomicrons and Remnants. *J. Lipid Res.* **1996**, *37* (12), 2696–2705.
377. Fukui, H.; Koike, T.; Saheki, A.; Sonoke, S.; Seki, J. A Novel Delivery System for Amphotericin B with Lipid Nano-Sphere (LNS ®). *Int. J. Pharm.* **2003**, *265*, 37–45.
378. Li, Y.; Wu, C.-L.; Liu, J.; Zhu, Y.; Zhang, X.-Y.; Jiang, L.-Z.; Qi, B.-K.; Zhang, X.-N.; Wang, Z.-J.; Teng, F. Soy Protein Isolate-Phosphatidylcholine Nanoemulsions Prepared Using High-Pressure Homogenization. *Nanomaterials* **2018**, *8* (5), 307.
379. Aguiar, A. C.; Paula, J. T.; Mundo, J. L. M.; Martínez, J.; McClements, D. J. Influence of Type of Natural Emulsifier and Microfluidization Conditions on Capsicum Oleoresin Nanoemulsions Properties and Stability. *J. Food Process Eng.* **2021**, *44* (4), 1–13.
380. Télessy, I. G.; Balogh, J.; Turmezei, J.; Dredán, J.; Zelkó, R. Stability Assessment of o/w Parenteral Nutrition Emulsions in the Presence of High Glucose and Calcium Concentrations. *J. Pharm. Biomed. Anal.* **2011**, *56* (2), 159–164.
381. Gao, S.; Fan, J.; Jia, X.; Li, B.; Li, X.; Li, Z.; Li, J. PFAT5 Stability Assessment of Lipovenoes MCT in Total Nutrient Admixtures. *Ann. Palliat. Med.* **2021**, *10* (12), 12244–12250.
382. Hinkel, F. C.; Sherman, H. C. Experiments upon Barfoed's Acid Cupric Acetate Solution as a Means of Distinguishing Glucose from Maltose, Lactose and Sucrose. *J. Am. Chem. Soc.* **1907**, *29* (12), 1744–1747.
383. Welker, W. H. A Disturbing Factor in Barfoed's Test. *J. Am. Chem. Soc.* **1915**, *37* (9), 2227–2230.
384. Jones, E. Qualitative Analysis—Carbohydrates. In *Manual of Practical Medical Biochemistry*; Jones, E., Ed.; Jaypee Brothers Medical Publishers (P) Ltd.: New Delhi, 2011; pp 1–119.
385. Elzagheid, M. I. Laboratory Activities to Introduce Carbohydrates Qualitative Analysis to College Students. *World J. Chem. Educ.* **2018**, *6* (2), 82–86.
386. Lou, P. H.; Lucchinetti, E.; Wawrzyniak, P.; Morsy, Y.; Wawrzyniak, M.; Scharl, M.; Krämer, S. D.; Rogler, G.; Hersberger, M.; Zaugg, M. Choice of Lipid Emulsion Determines Inflammation of the Gut-Liver Axis, Incretin Profile, and Insulin Signaling in a Murine Model of Total Parenteral Nutrition. *Mol. Nutr. Food Res.* **2021**, *65* (5), 1–15.
387. Pichot, R.; Watson, R.; Norton, I. Phospholipids at the Interface: Current Trends and Challenges. *Int. J. Mol. Sci.* **2013**, *14* (6), 11767–11794.
388. Biesboer, A. N.; Stoehr, N. A. A Product Review of Alternative Oil-Based Intravenous Fat Emulsions. *Nutr. Clin. Pract.* **2016**, *31* (5), 610–618.
389. Sommer, I.; Palmero, D.; Fischer Fumeaux, C. J.; Bonnabry, P.; Bouchoud, L.; Sadeghipour, F. Parenteral Nutrition Process Management for Newborn and Preterm Infants – A Preliminary Risk Analysis. *Ther. Clin. Risk Manag.* **2021**, *17* (May), 497–506.
390. Reber, E.; Messerli, M.; Stanga, Z.; Mühlebach, S. Pharmaceutical Aspects of Artificial Nutrition. *J. Clin. Med.* **2019**, *8* (11), 1–21.
391. Mistry, P.; Smith, R. H.; Fox, A. Patient Safety Incidents Related to the Use of Parenteral Nutrition in All Patient Groups: A Systematic Scoping Review. *Drug Saf.* **2022**, *45* (1), 1–18.

392. Wang, X.; Collot, M.; Omran, Z.; Vandamme, T. F.; Klymchenko, A.; Anton, N. Further Insights into Release Mechanisms from Nano-Emulsions, Assessed by a Simple Fluorescence-Based Method. *J. Colloid Interface Sci.* **2020**, *578*, 768–778.

393. Seki, J.; Sonoke, S.; Saheki, A.; Koike, T.; Fukui, H.; Doi, M.; Mayumi, T. Lipid Transfer Protein Transports Compounds from Lipid Nanoparticles to Plasma Lipoproteins. *Int. J. Pharm.* **2004**, *275*, 239–248.

394. Qi, K.; Al-Haideri, M.; Seo, T.; Carpentier, Y. A.; Deckelbaum, R. J. Effects of Particle Size on Blood Clearance and Tissue Uptake of Lipid Emulsions with Different Triglyceride Compositions. *J. Parenter. Enter. Nutr.* **2003**, *27* (1), 58–64.

395. Zaloga, G. P. Narrative Review of N-3 Polyunsaturated Fatty Acid Supplementation upon Immune Functions, Resolution Molecules and Lipid Peroxidation. *Nutrients* **2021**, *13* (2), 1–30.

396. Gaschler, M. M.; Stockwell, B. R. Lipid Peroxidation in Cell Death. *Biochem. Biophys. Res. Commun.* **2017**, *482* (3), 419–425.

397. Liu, J.; Guo, Y. S.; Si, T. L.; Li, X. Z.; McClements, D. J.; Ma, C. G. Effects of Chelating Agents and Salts on Interfacial Properties and Lipid Oxidation in Oil-in-Water Emulsions. *J. Agric. Food Chem.* **2019**, *67* (49), 13718–13727.

398. Lane, K. E.; Zhou, Q.; Robinson, S.; Li, W. The Composition and Oxidative Stability of Vegetarian Omega-3 Algal Oil Nanoemulsions Suitable for Functional Food Enrichment. *J. Sci. Food Agric.* **2020**, *100* (2), 695–704.

399. Zhu, Y.; McClements, D. J.; Zhou, W.; Peng, S.; Zhou, L.; Zou, L.; Liu, W. Influence of Ionic Strength and Thermal Pretreatment on the Freeze-Thaw Stability of Pickering Emulsion Gels. *Food Chem.* **2020**, *303*, 125401.

400. Kapoor, V.; Malviya, M. N.; Soll, R. Lipid Emulsions for Parenterally Fed Preterm Infants. *Cochrane Database Syst. Rev.* **2019**, No. 6.

401. Darmaun, D.; Lapillonne, A.; Simeoni, U.; Picaud, J. C.; Rozé, J. C.; Saliba, E.; Bocquet, A.; Chouraqui, J. P.; Dupont, C.; Feillet, F.; et al. Parenteral Nutrition for Preterm Infants: Issues and Strategy. *Arch. Pediatr.* **2018**, *25* (4), 286–294.

402. Gutcher, G. R.; Farrell, P. M. Intravenous Infusion of Lipid for the Prevention of Essential Fatty Acid Deficiency in Premature Infants. *Am. J. Clin. Nutr.* **1991**, *54* (6), 1024–1028.

403. Velaphi, S. Nutritional Requirements and Parenteral Nutrition in Preterm Infants. *South African J. Clin. Nutr.* **2011**, *24* (3 SUPPL. 1), 27–31.

404. Riskin, A.; Hartman, C.; Shamir, R. Parenteral Nutrition in Very Low Birth Weight Preterm Infants. *Isr. Med. Assoc. J.* **2015**, *17* (5), 310–315.

405. Mozaffarian, D.; Rimm, E. B. Fish Intake, Contaminants, and Human Health. *JAMA* **2006**, *296* (15), 1885.

406. Ruxton, C. H. S.; Reed, S. C.; Simpson, M. J. A.; Millington, K. J. The Health Benefits of Omega-3 Polyunsaturated Fatty Acids: A Review of the Evidence. *J. Hum. Nutr. Diet.* **2004**, *17* (5), 449–459.

407. Innis, S. M. Dietary (n-3) Fatty Acids and Brain Development. *J. Nutr.* **2007**, *137* (4), 855–859.

408. Swanson, D.; Block, R.; Mousa, S. A. Omega-3 Fatty Acids EPA and DHA: Health Benefits Throughout Life. *Adv. Nutr.* **2012**, *3* (1), 1–7.

409. Siriwardhana, N.; Kalupahana, N. S.; Moustaid-Moussa, N. Health Benefits of N-3 Polyunsaturated Fatty Acids. In *Advances in Food and Nutrition Research*; Kim, S.-K., Ed.; Elsevier Inc.: Waltham MA, 2012; Vol. 65, pp 211–222.

410. Heller, A. R.; Stengel, S.; Stehr, S. N.; Gama de Abreu, M.; Koch, R.; Koch, T. Impact of the Ratio of Intravenous Omega-3 vs. Omega-6 Polyunsaturated Fatty Acids in Postoperative and in Septic Patients-A Post Hoc Database Analysis. *e-SPEN* **2007**, *2* (5).

411. Leyrolle, Q.; Decoeur, F.; Dejean, C.; Brière, G.; Leon, S.; Bakoyiannis, I.; Baroux, E.; Sterley, T. L.; Bosch-Bouju, C.; Morel, L.; et al. N-3 PUFA Deficiency Disrupts Oligodendrocyte Maturation and Myelin Integrity during Brain Development. *Glia* **2022**, *70* (1), 50–70.

412. Decoeur, F.; Picard, K.; St-Pierre, M.-K.; Greenhalgh, A. D.; Delpech, J.-C.; Sere, A.; Layé, S.; Tremblay, M.-E.; Nadjar, A. N-3 PUFA Deficiency Affects the Ultrastructural Organization and Density of White Matter Microglia in the Developing Brain of Male Mice. *Front. Cell. Neurosci.* **2022**, *16* (February), 1–11.

413. Senterre, T.; Terrin, G.; Curtis, M. De; Rigo, J. Parenteral Nutrition in Premature Infants. In *Textbook of Pediatric Gastroenterology, Hepatology and Nutrition*; Guandalini, S., Dhawan, A., Branski, D., Eds.; Springer International Publishing: Cham, 2016; pp 73–85.

414. Lin, X.; Ma, L.; Racette, S. B.; Swaney, W. P.; Ostlund, R. E. Preparation of Intravenous Cholesterol Tracer Using Current Good Manufacturing Practices. *J. Lipid Res.* **2015**, *56* (12), 2393–2398.

415. Dyhydromatics. Solutions for High Pressure Homogenizization Combining Science and Engineering: Equipment, Process Development and Service from One Source. 2018.
416. Cook, G. T.; Passo, C. J.; Carter, B. Environmental Liquid Scintillation Analysis. In *Handbook of Radioactivity Analysis*; L'Annunziata, M. F., Ed.; Elsevier: San Diego, 2003; pp 537–607.
417. Bailey, D. L.; Karp, J. S.; Surti, S. Physics and Instrumentation in PET. In *Positron Emission Tomography*; Bailey, D. L., Townsend, D. W., Valk, P. E., Maisey, M. N., Eds.; Springer-Verlag: London, 2005; pp 13–39.
418. Pekošak, A.; Bulc, J.; Korat, Š.; Schuit, R. C.; Kooijman, E.; Vos, R.; Rongen, M.; Verlaan, M.; Takkenkamp, K.; Beaino, W.; et al. Synthesis and Preclinical Evaluation of the First Carbon-11 Labeled PET Tracers Targeting Substance P1-7. *Mol. Pharm.* **2018**, *15* (11), 4872–4883.
419. Goud, N. S.; Bhattacharya, A.; Joshi, R. K.; Nagaraj, C.; Bharath, R. D.; Kumar, P. Carbon-11: Radiochemistry and Target-Based PET Molecular Imaging Applications in Oncology, Cardiology, and Neurology. *J. Med. Chem.* **2021**, *64* (3), 1223–1259.

9 APPENDIX

Tab. A1: Supplier and purity of commercially obtained fatty acid standards used to establish calibration curves for quantification.

Fatty acid standard	Provider	Purity
C8:0, caprylic acid (octanoic)	Fluorochem	99%
C10:0, capric acid (decanoic)	Roth	≥98%
C12:0, lauric acid	Fluka	98%
C20:5, eicosapentaenoic acid	Cayman Chemical	>98%
C13:0, tridecanoic acid	Sigma-Aldrich	≥98%
C18:3 *n*−3, α-linolenic acid	Fluorochem	70%
C18:3 *n*−6, γ-linolenic acid	Cayman Chemical	>98%
C22:6, docosahexaenoic acid	Cayman Chemical	>98%
C14:0, myristic acid	Acros Organics	99%
C20:4, arachidonic acid	Cayman Chemical	>98%
C18:2 *n*−6, linoleic acid	Sigma-Aldrich	≥99%
C15:0, pentadecanoic acid	Acros Organics	99%
C16:0, palmitic acid	Sigma-Aldrich	99%
C18:1, oleic acid	Fluorochem	99%
C17:0, heptadecanoic acid	Tokyo Chemical Industries	>98.0%
C18:0, stearic acid	Hänseler	Ph. Eur.

Tab. A2: Quantification matrix for establishing calibration curves with a typical composition of Intralipid. Pure standards are mixed at different concentrations to yield similar (22.5-25 µM) total spiked FAs.

Fatty acid standard	Mix 4	Mix 5	Mix 6	Ctrl
C18:3 *n−6*	+2.5 µM	+5 µM	+10 µM	
C14:0	+10 µM	+2.5 µM	+5 µM	
C18:2	+2.5 µM	+10 µM	+5 µM	
C15:0	+10 µM	+10 µM	+10 µM	+10 µM
C17:0	+10 µM	+10 µM	+10 µM	+10 µM
C18:0	+10 µM	+5 µM	+2.5 µM	

Tab. A3: Composition of a spiking matrix for establishing calibration curves for quantification of FFA levels in Omegaven.

Fatty acid standard	Mix 7	Mix 8	Mix 9	Ctrl
C20:5	+2.5 µM	+10 µM	+5 µM	
C22:6	+10 µM	+2.5 µM	+5 µM	
C20:4	+10 µM	+5 µM	+2.5 µM	
C18:2	+2.5 µM	+10 µM	+5 µM	
C15:0	+10 µM	+10 µM	+10 µM	+10 µM
C17:0	+10 µM	+10 µM	+10 µM	+10 µM
C18:0	+5 µM	+2.5 µM	+10 µM	

Tab. A4: Matrix for establishing calibration curves for the quantification of FFA-levels in SMOFlipid emulsions. Quantities are chosen to achieve similar total spiked FAs (30-32.5 µM) in all four standard mixes.

Fatty acid standard	Mix 10	Mix 11	Mix 12	Mix 13	Ctrl
C20:5	+10 µM	+5 µM	+2.5 µM		
C22:6		+10 µM	+5 µM	+2.5 µM	
C18:2	+2.5 µM		+10 µM	+5 µM	
C15:0	+10 µM	+10 µM	+10 µM	+10 µM	+10 µM
C16:0	+10 µM	+5 µM	+2.5 µM		
C17:0	+10 µM	+10 µM	+10 µM	+10 µM	+10 µM
C18:0	+5 µM	+2.5 µM		+10 µM	

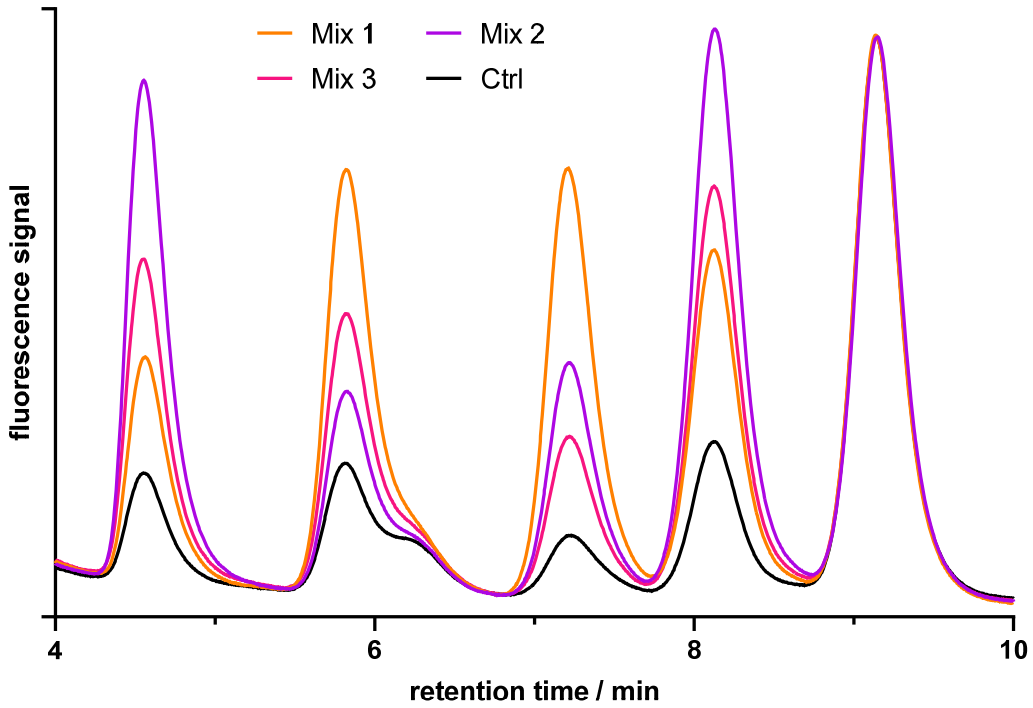

Fig. A1: Chromatograms of calibration mixes 1-3 spiked with different amounts of selected pure standards according to Tab. 3.1 in comparison to an unspiked control sample ("Ctrl"), all standardized to the internal standard C15:0 at a retention time of 9.2 min.

Tab. A5: Experimentally determined relative free fatty acid profiles of commercially available Intralipid and Omegaven as well as Formula #3 lipid emulsion compared to theoretical composition of total (esterified and free) fatty acids, calculated from literature values[62] and CoAs of oil components.

Intralipid	experimental	literature / CoA
C14:0	4.7%	0-0.1%
C16:0, C18:1	62.4%	32-35%
C18:0	18.7%	4%
C18:2	11.7%	53-56%
C18:3 *n*−6	2.5%	7.8-8.1%
Omegaven	experimental	literature / CoA
C14:0	-	4%
C16:0, C18:1	71.8%	32-35.4%
C18:0	16.4%	1.25-2.1%
C18:2	3.6%	3.4-4%
C18:3 *n*−3	-	4%
C20:4	3.9%	2.5-2.8%
C20:5	1.1%	20.3-24%
C22:6	3.2%	17.5-24%
Others	-	7%
Formula #3	experimental	literature / CoA
C12:0	4.5%	12%
C14:0	2.1%	4.5%
C16:0, C18:1	78.5%	32.3%
C18:0	13.4%	0.9%
C18:2	1%	9.1%
C18:3 *n*−3	0.5%	31.6%
others	-	9.6%

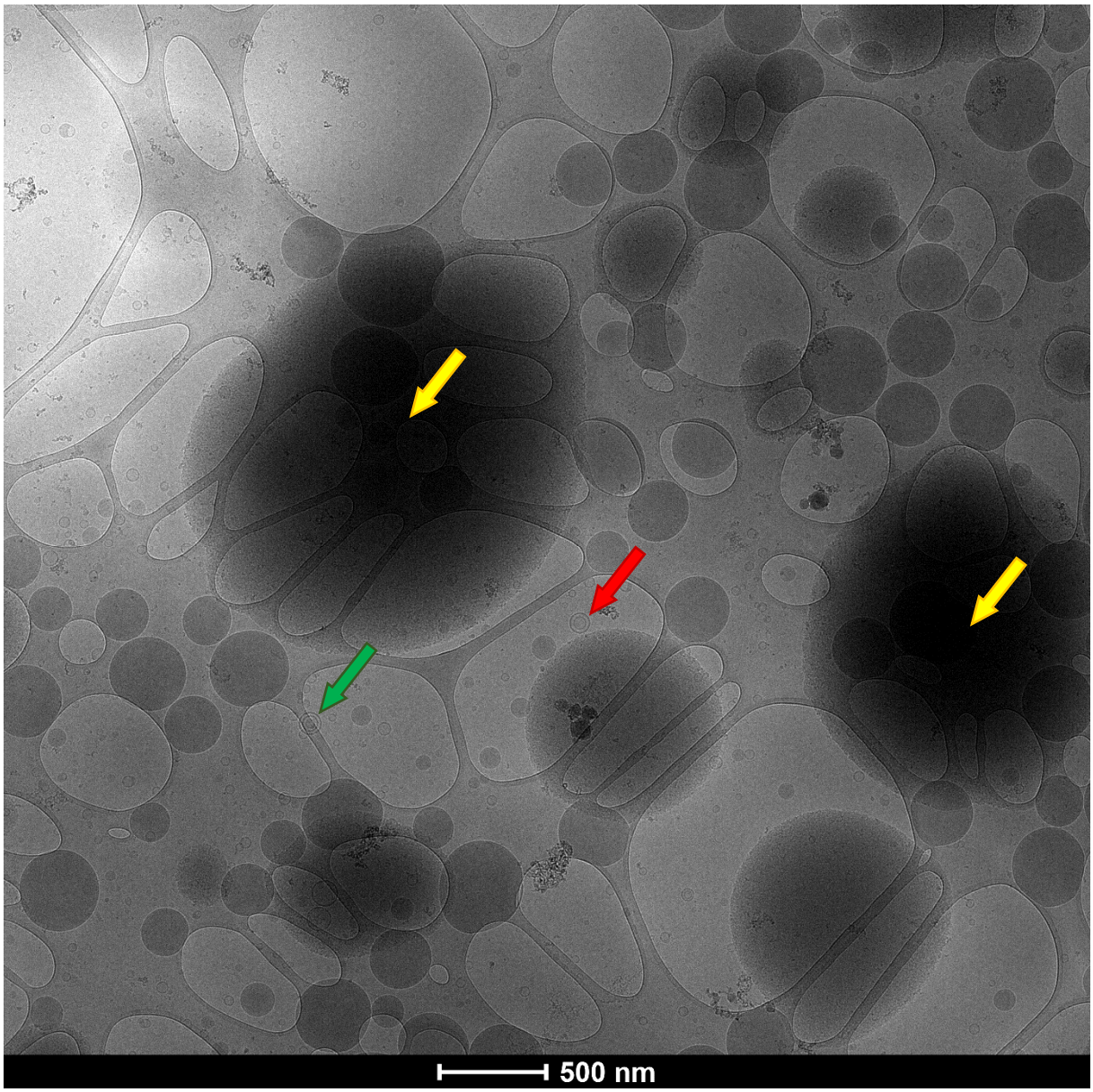

Fig. A2: Transmission electron micrograph of Formula #3 lipid emulsion showing very few (smaller) liposomes (diameter around 80-100 nm, red arrow), and a single multilamellar vesicle (green arrow). Dark shades correspond to imaging artifacts and are indicated with yellow arrows.

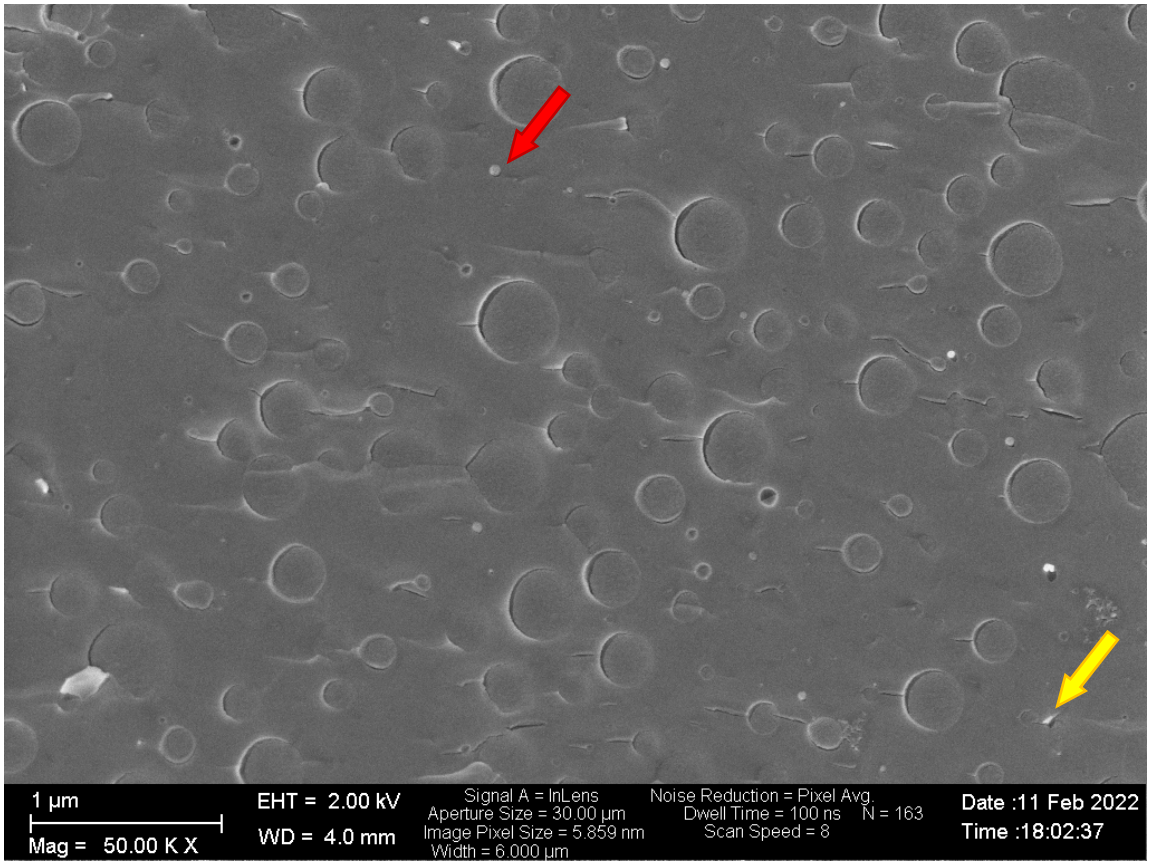

Fig. A3: Representative cryoSEM picture of commercial Intralipid for comparison. Small particles are marked with a red arrow, artifacts from the sample preparation process with a yellow arrow.

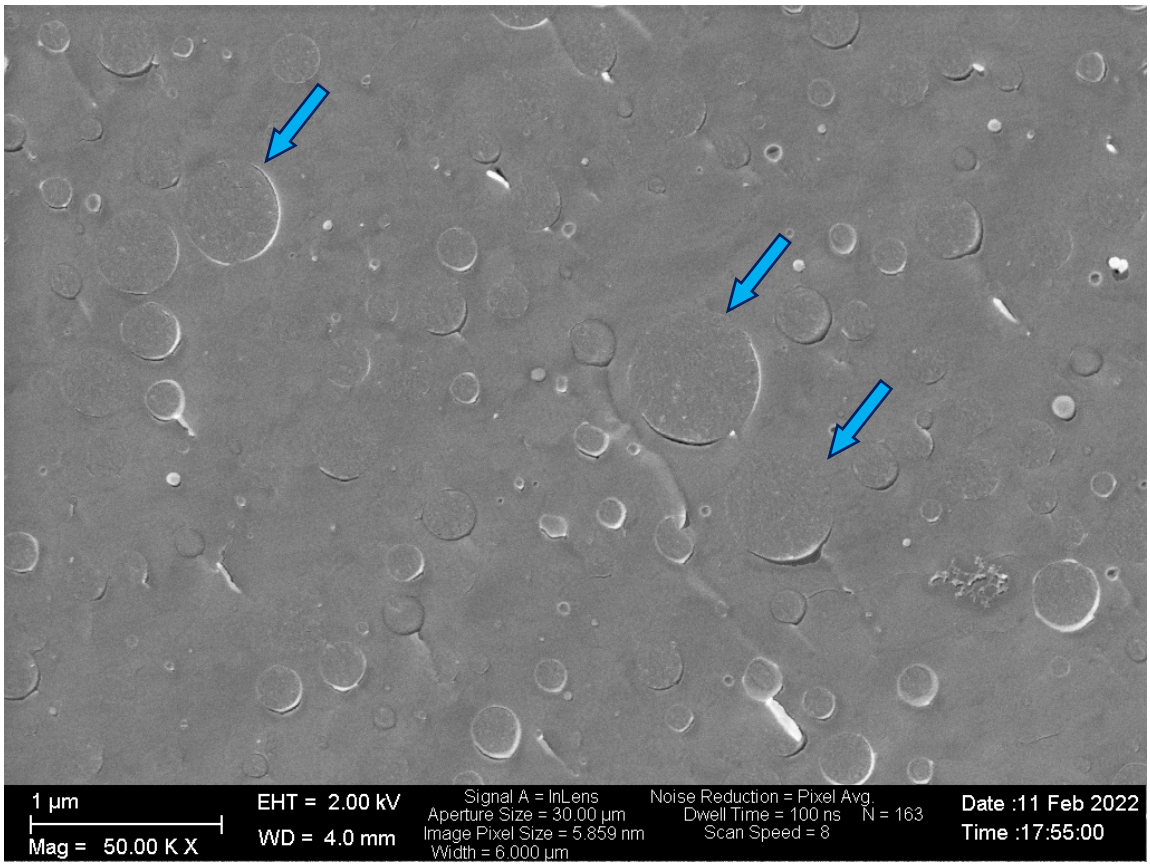

Fig. A4: Selected cryoSEM view of commercial Intralipid showing enlarged lipid droplets marked up to a diameter of 800 nm, marked with blue arrows.

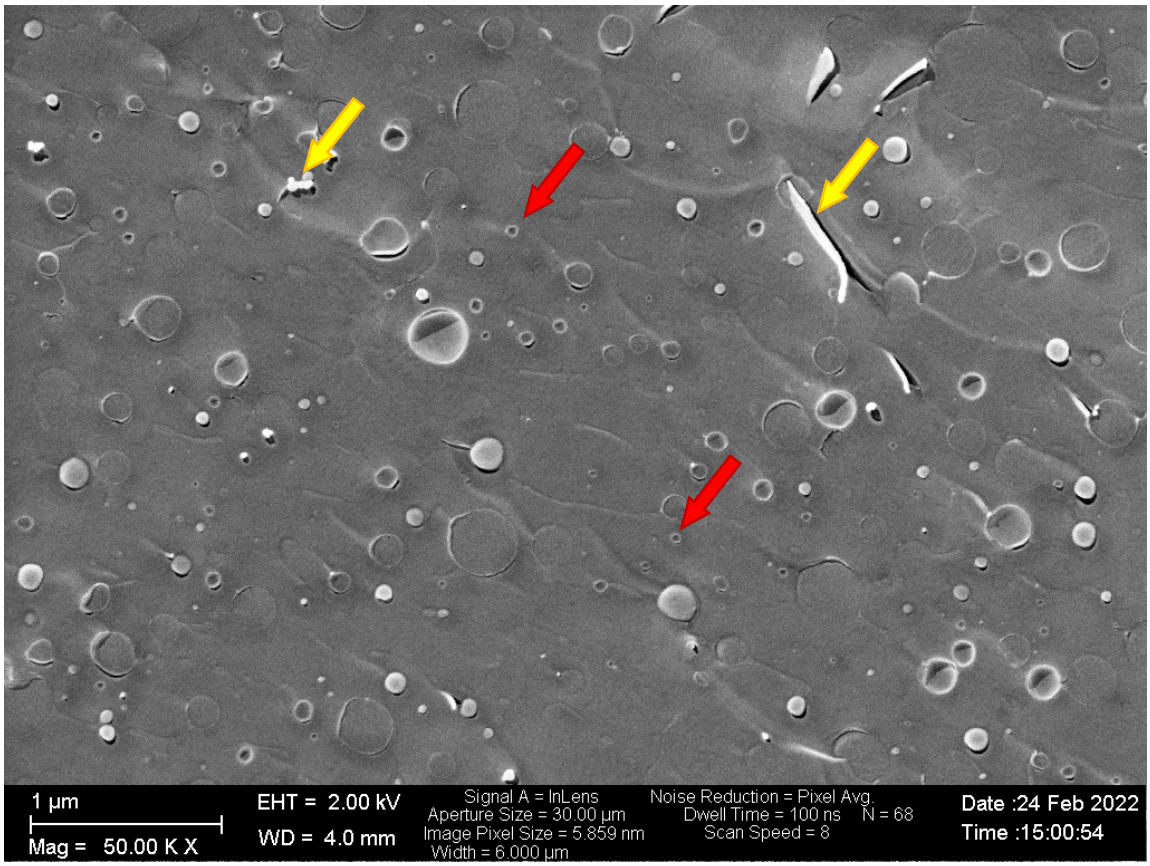

Fig. A5: Representative cryoSEM picture of commercial Omegaven. Extraordinary small particles are marked with red arrows, artifacts from the sample preparation (ice crystals from freezing, cracks) with yellow arrows.

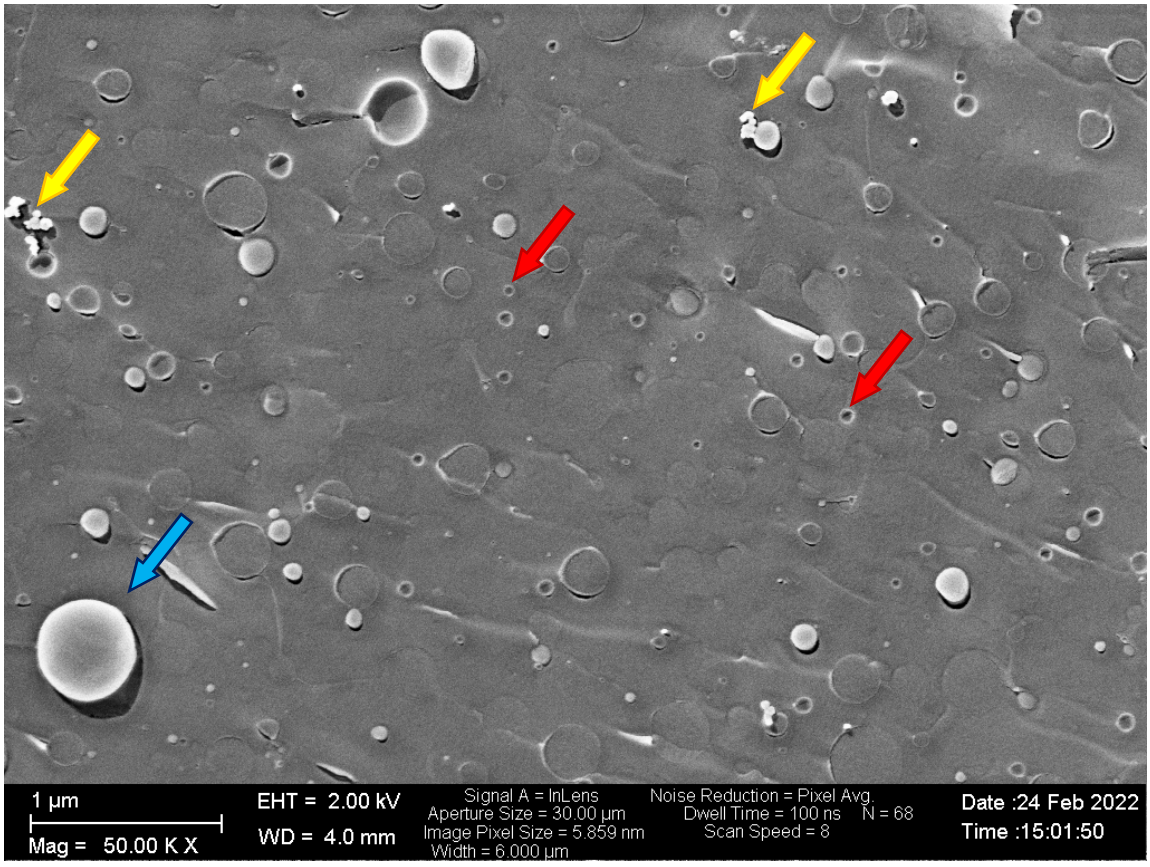

Fig. A6: Selected excerpt of cryoSEM of commercial Omegaven showing a single droplet at 500 nm (blue arrow), all other droplets are smaller. Many much smaller droplets are marked with a red arrow, artifacts from the sample preparation process are highlighted with yellow arrows.

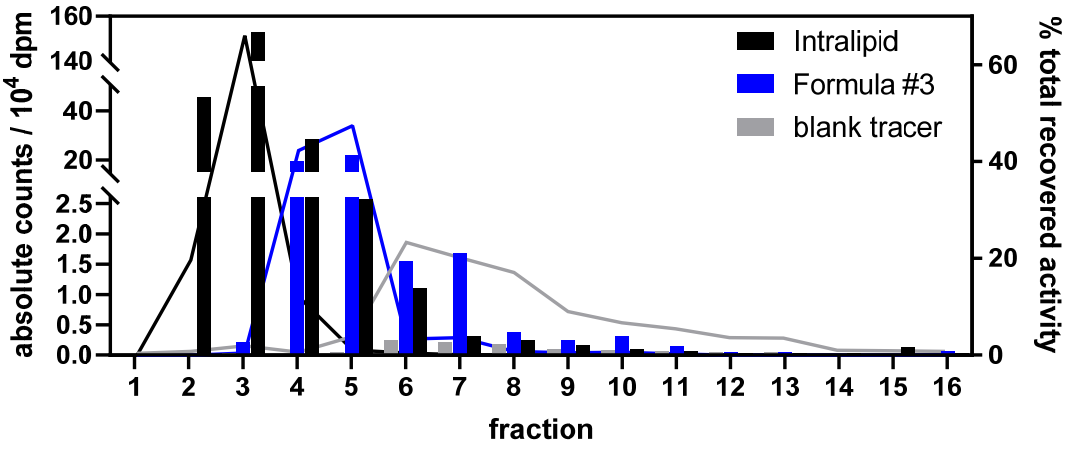

Fig. A7: Absolute (bars, left axis) and relative (connected line, right axis) activity of consecutively collected fractions of ^{3}H-triolein tracer incorporated into commercial Intralipid (black), Formula #3 (blue) or blank (grey) after separation by size exclusion chromatography.

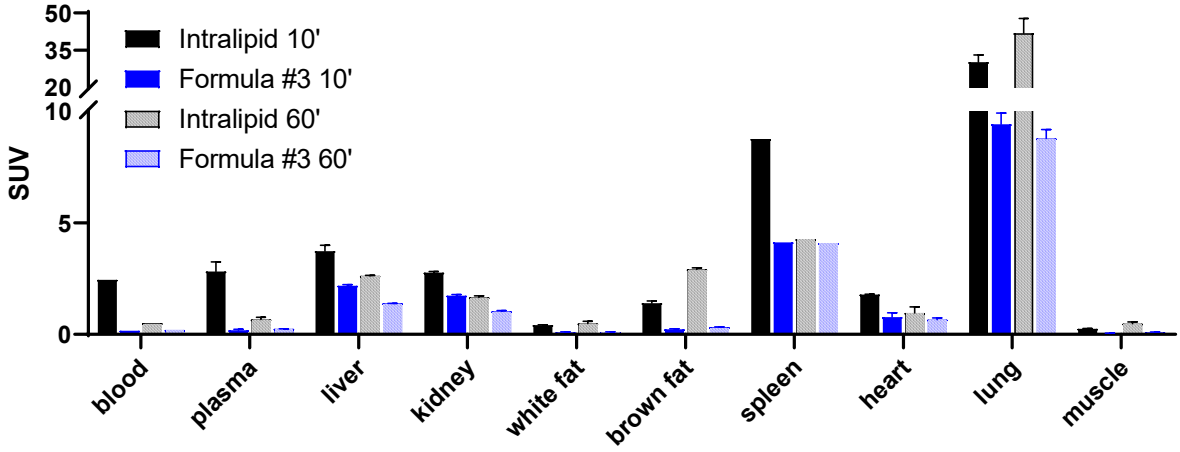

Fig. A8: Standardized uptake values (SUV) of different tissues after administration of 37 kBq ^{3}H-triolein in 50 µl emulsion (Intralipid, black bars or Formula #3, blue bars) after pre-injection of 50 µl of corresponding unlabeled emulsion, 10 minutes (filled bars) or 60 minutes (diagonal down striped bars) after injection (n=1 animal per time point; bars, individual values or means and standard deviation if more tissues of the same animal were analysed).

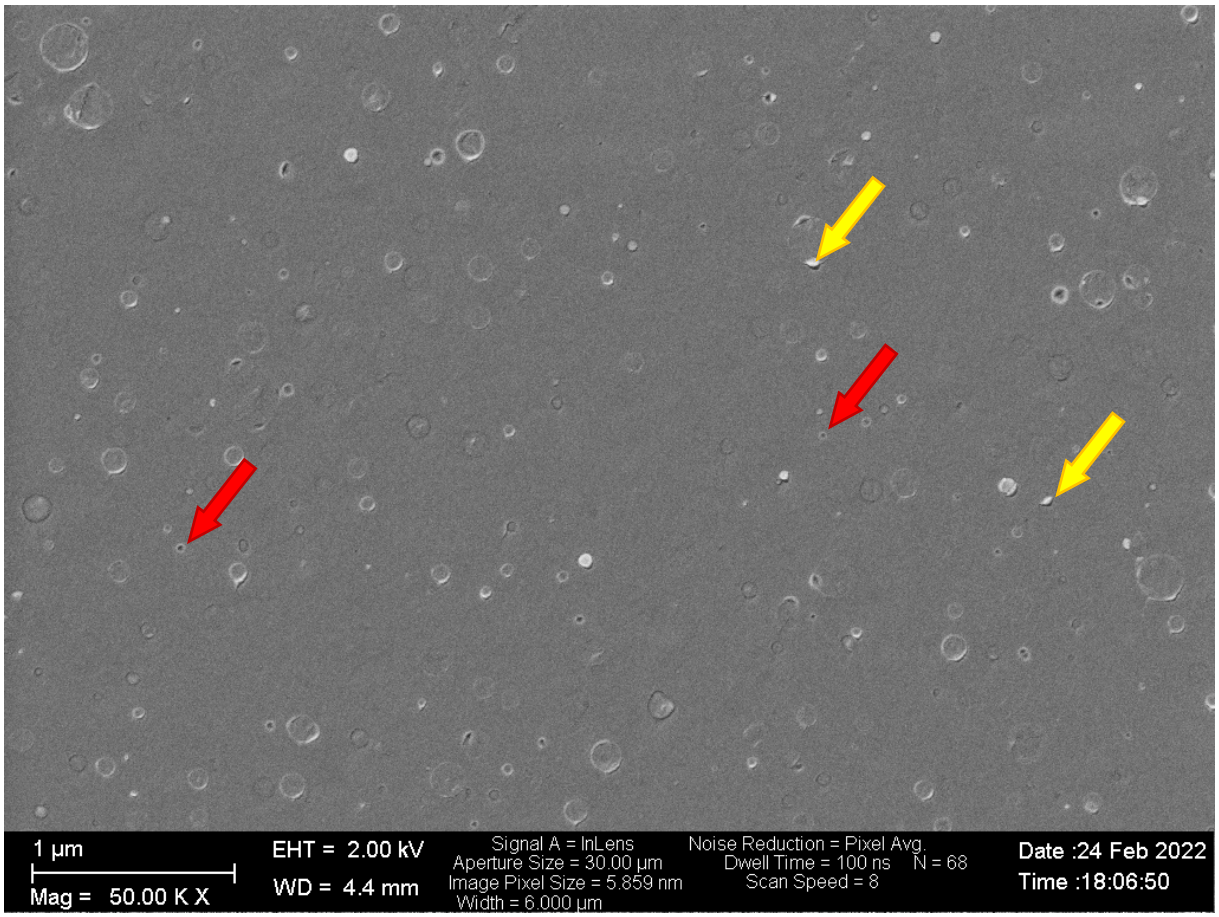

Fig. A9: Representative scanning electron micrograph of a 7% fish oil nanoemulsion stabilized with 45% glucose. Red arrows indicate selected markedly smaller than average droplets while yellow arrows highlight artifacts from the sample preparation process.

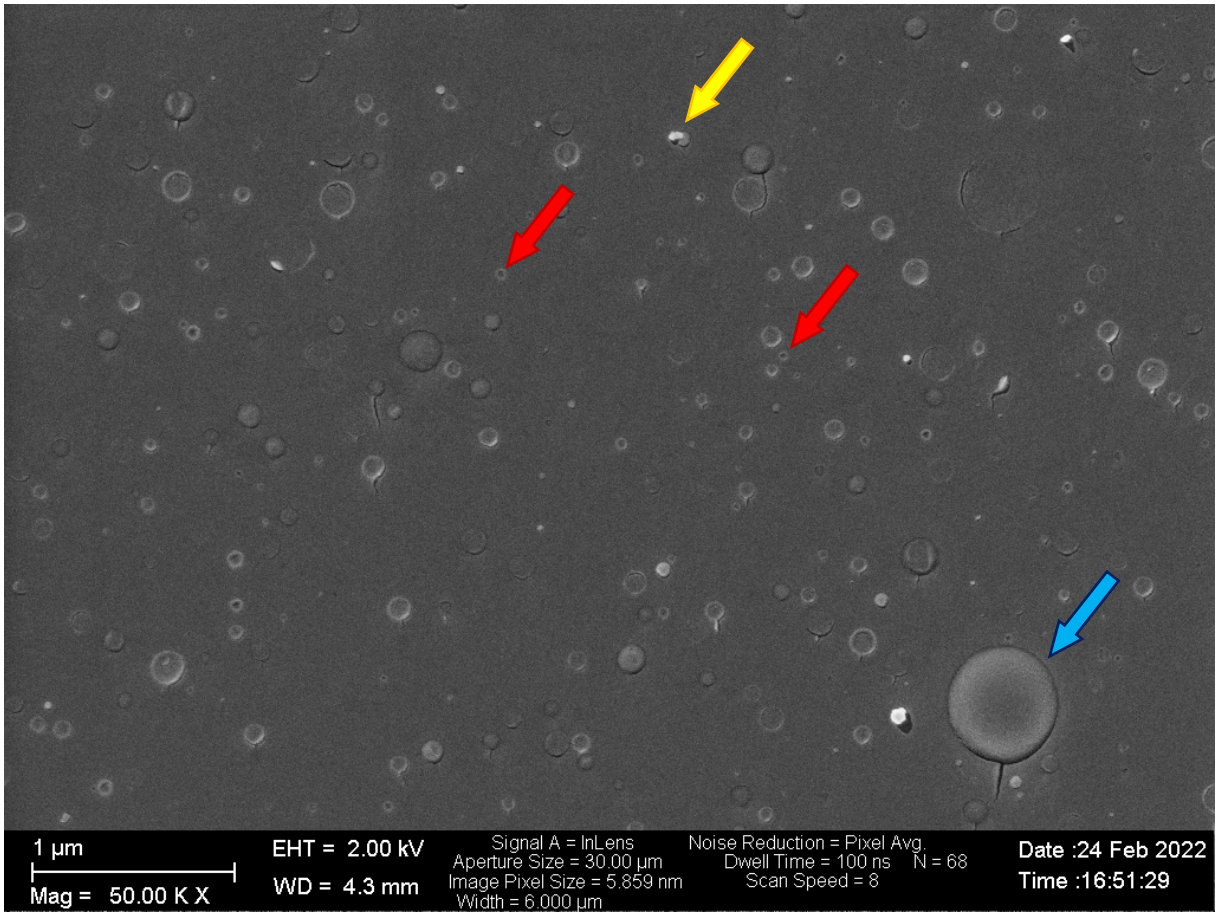

Fig. A10: Selected scanning electron micrograph of identical formulation as in Fig. 5.11, with additional single lipid droplet with a diameter of 570 nm, marked in blue. Artifacts are marked with a yellow arrow, especially small droplets with red arrows.

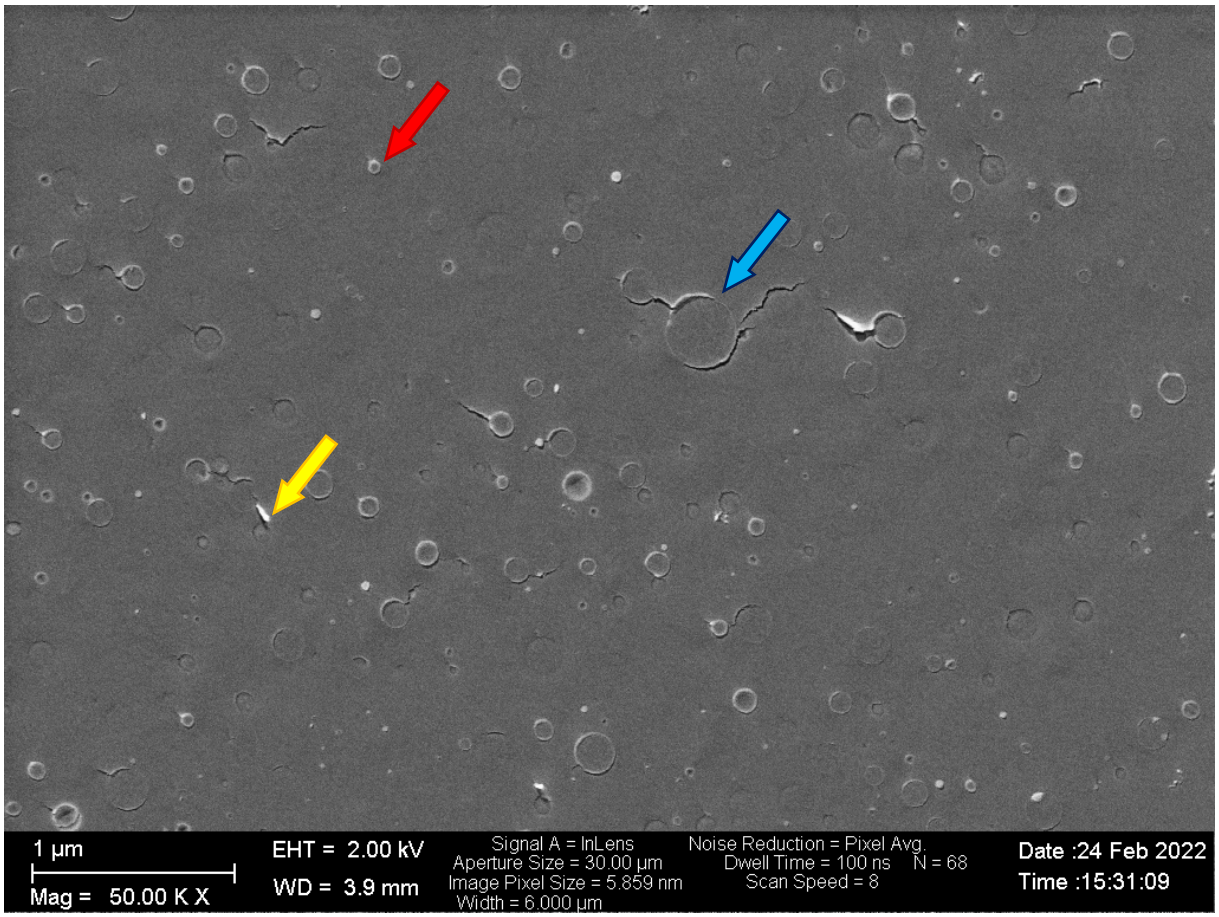

Fig. A11: Selected scanning electron microscopy picture of 7% soybean emulsion with 45% glucose, showing a single lipid droplet at increased size of 360 nm (marked with a blue arrow). Imaging artifacts are again highlighted with a yellow arrow, a selected small droplet with a red arrow.

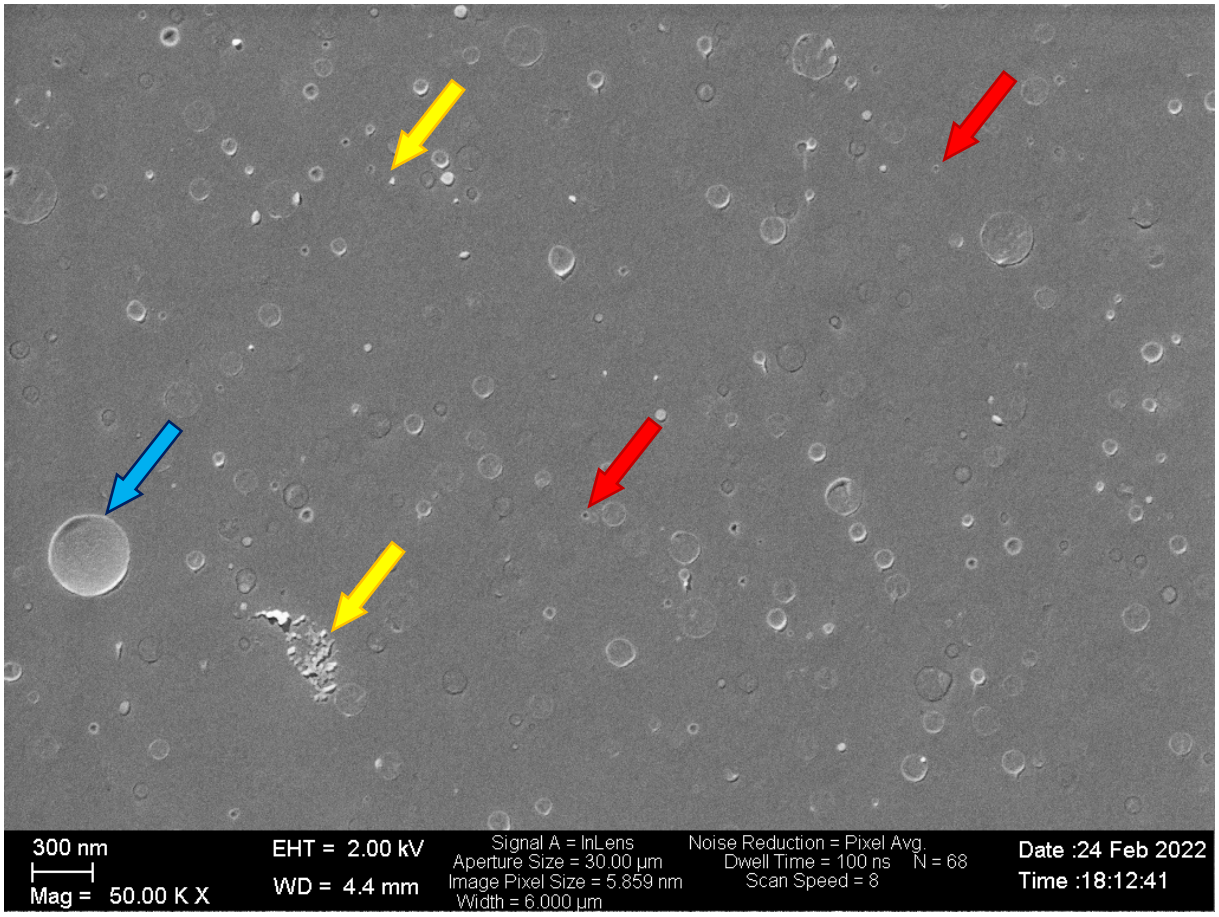

Fig. A12: Selected scanning electron micrograph of a 7% fish oil nanoemulsion stabilized with 45% glucose. Smaller-than-average droplets are marked with red arrows, artifacts from the sample preparation process with yellow arrows, and a single lipid droplet at an increased size of 405 nm is highlighted with a blue arrow.

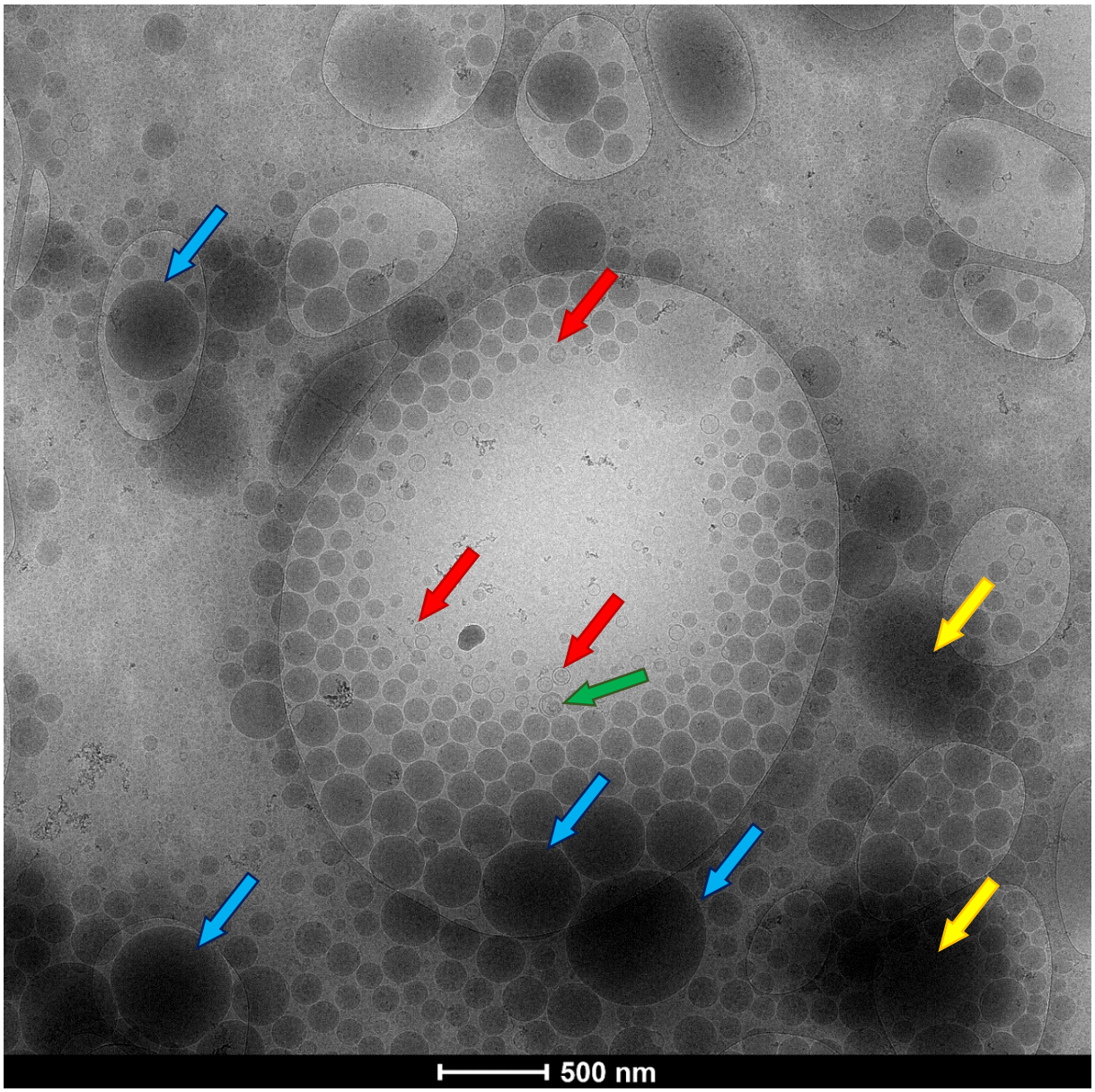

Fig. A13: Transmission electron micrograph of n−3 PUFA-rich plant-based lipid nanoemulsion after removal of glucose. Few particles maturated from the repeated centrifugation are marked with blue arrows, liposomes with red arrows and a single multilamellar vesicle with a green arrow. Black shades indicated with yellow arrows correspond to artifacts from the imaging process.

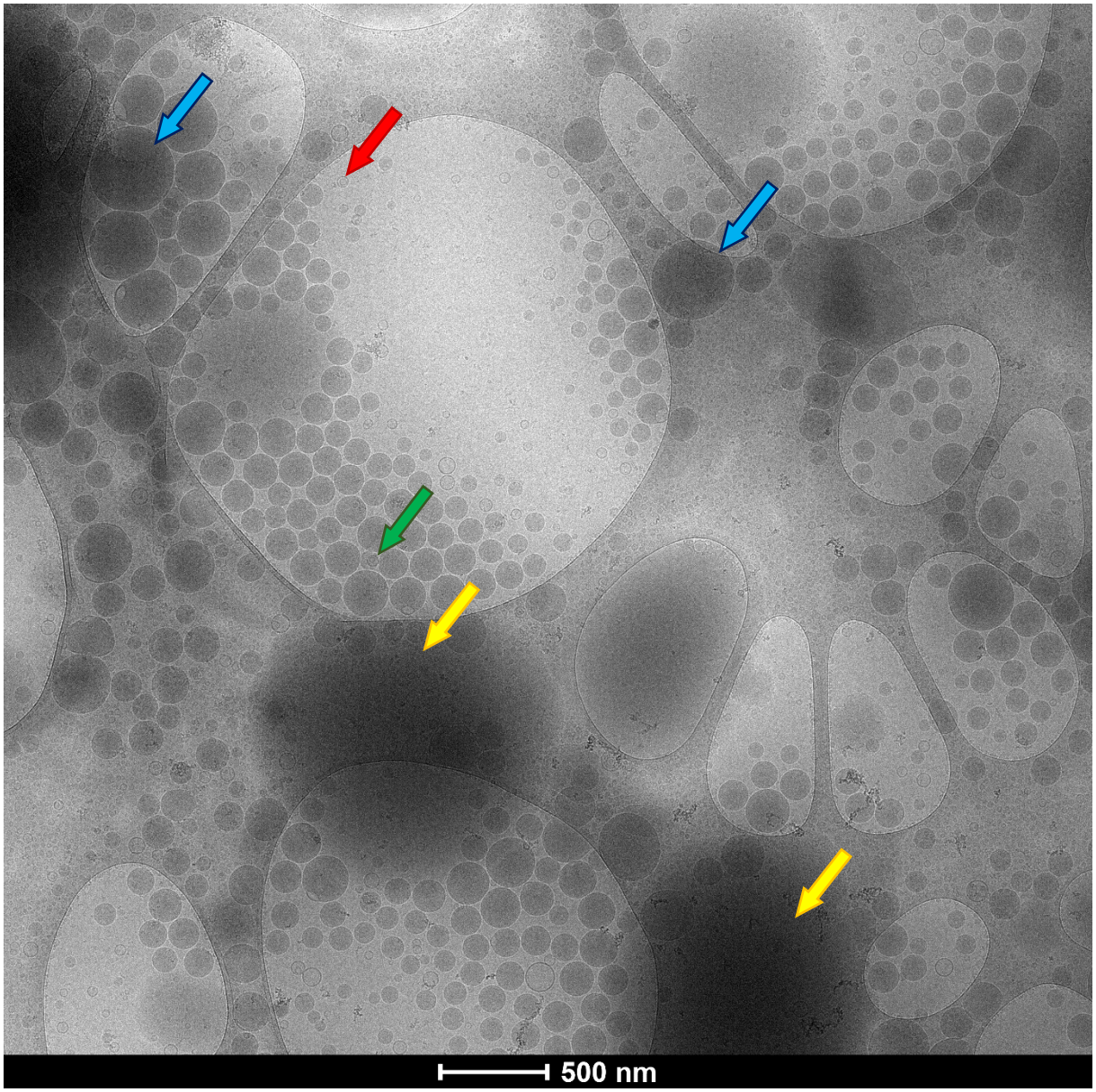

Fig. A14: Representative transmission electron micrograph of n−3 PUFA-rich plant-based lipid nanoemulsion after removal of glucose by repeated centrifugation. Matured particles from the centrifugation stress wider than the average droplets are highlighted with blue arrows, liposomes with a red arrow and a multilamellar vesicle with a green arrow. Yellow arrows represent artifacts from the imaging process.

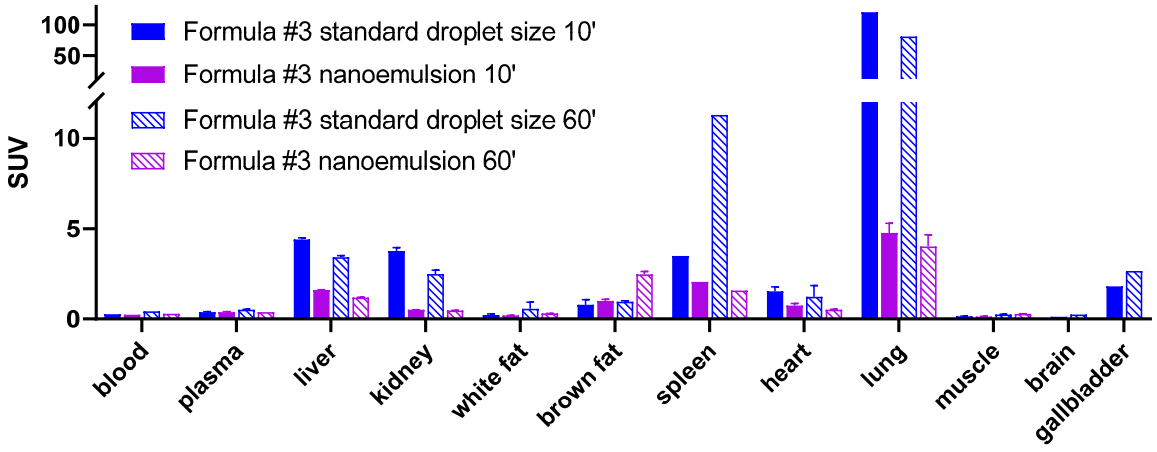

Fig. A15: Standardized uptake value in different tissues 10 minutes (filled bars) and 60 minutes (diagonal down striped bars) after administration of 50 µl 20% lipid emulsion (blue bars, droplet size 272.4 nm, equivalent to 20 cal) in comparison to 100 µl 7% lipid nanoemulsion (purple bars, droplet size 161.0 nm, same data as in Fig. 5.13) stabilized with 45% glucose (total calories administered 224.7 cal, n=1 animal per time point; bars, individual values or means and standard deviation if more tissues of the same animal were analysed)). Both formulations share the same Formula #3 oil source, but in different relative portions.

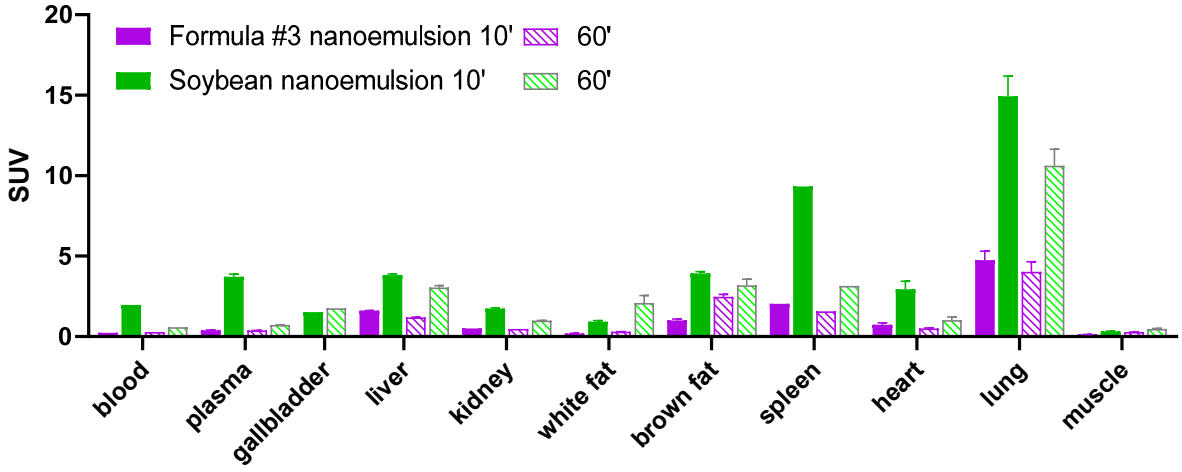

Fig. A16: Comparison of standardized uptake values (SUV) of 100 µl soybean oil- (green bars, 166.9 nm droplet size, same data as in Fig. 5.14) and n−3 PUFA-rich plant-based oil (Formula #3, purple bars, 161.0 nm droplet size, same data as in Fig. 5.13) nanoemulsions 10 minutes (filled bars) and 60 minutes (diagonal down striped bars) after injection (n=1 animal per time point; bars, individual values or means and standard deviation if more tissues of the same animal were analysed). Apart from the oil type, both formulations share the same composition.

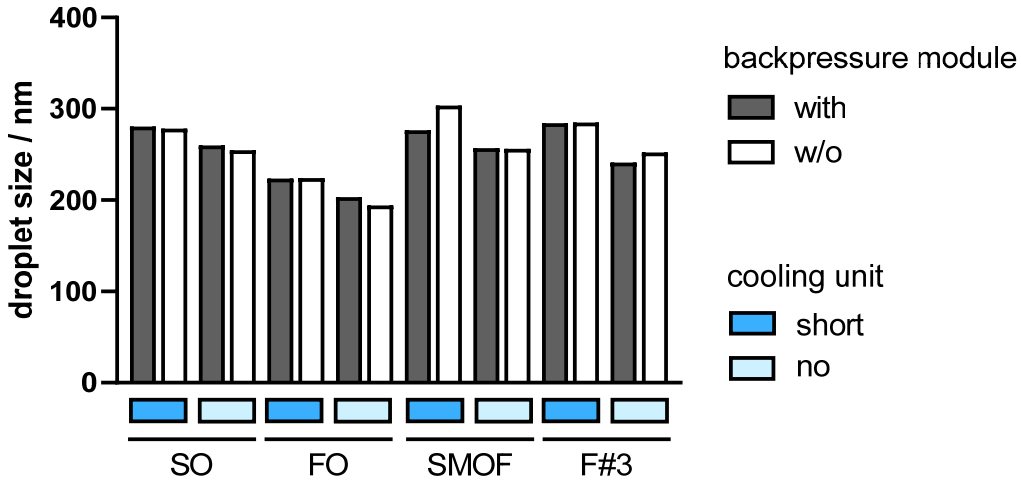

Fig. A17: Droplet sizes of emulsions prepared using plastic syringes, prior to autoclaving (n=1).

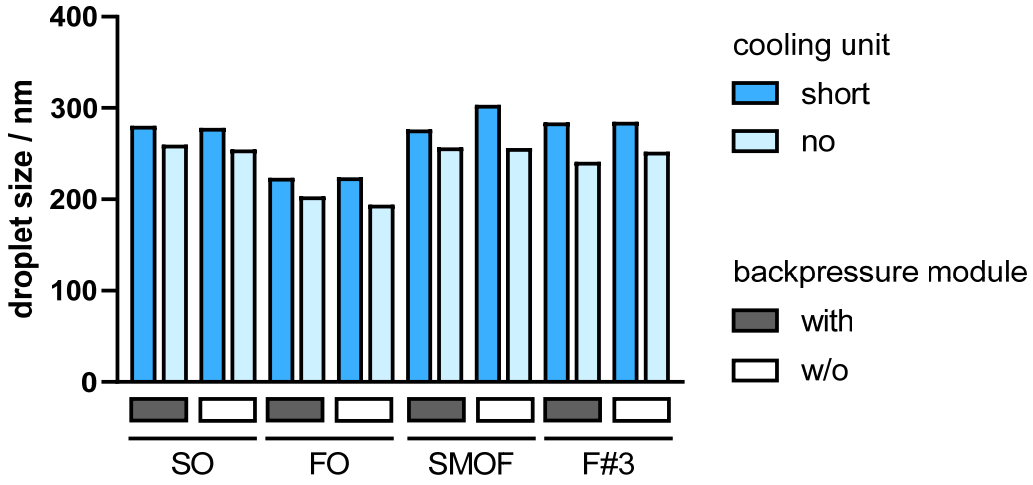

Fig. A18: Droplet sizes of emulsions manufactured using plastic syringes, as a function of the used cooling system. Data prior to autoclaving, same data as in Fig. A17 (n=1).

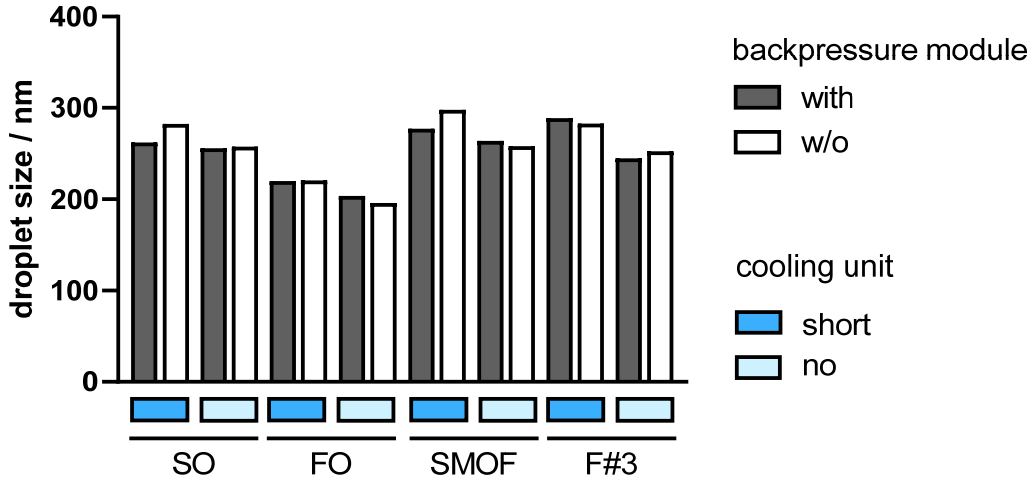

Fig. A19: Droplet sizes of autoclaved emulsions prepared using plastic syringes (n=1). Same emulsions as in Fig. A17 and Fig. A18.